Development of Tools and Technologies for the Characterisation of Novel Drug Delivery Systems

Thesis submitted for the degree of Doctor of Philosophy (Ph.D.)

by

Pamela Johanna Riester

Cardiff School of Biosciences

Cardiff University

2017

Acknowledgements

I would like to thank my supervisor Peter Watson for his invaluable support and guidance throughout this project. Thank you Pete for all your advice, patience and for always motivating me and challenging me to improve my scientific skills. I also wish to thank my second supervisor Arwyn Jones for his help and advice throughout this project. Thanks to the IMI and the EFPIA for funding the COMPACT consortium and enabling the possibility for partners in academia and industry to work towards a joint aim to improve macromolecular delivery to their cellular targets. Thanks to all the COMPACT consortium partners, it has been an invaluable experience to collaborate with you and to be a part of this consortium.

I would also like to thank all the students who have worked on this project as part of an Erasmus placement or their final year dissertation. Thank you, Alex, Josh, Connor, Mayowa, Scott, Felix and Jack. Furthermore I would like to thank the Data Clinic for all the help and support with the statistics. Thanks to Arwyn Jone's group for giving me help and advice in lab meetings.

A special thanks to the third floor east group in Biosciences. It was great to work with you and to solve lunch time cross words. Thank you Anika for being my friend and your endless scientific advice. A special thanks goes out to the one and only Josie, my time in Cardiff would have not been the same without you!

Furthermore I would like to thank my familiy for supporting me with a special note to my mum. Liebe Mama, ich kann dir nicht genug danken. Du hast mir in den letzten Jahren immer mit Rat und Tat beiseitegestanden und mich in all meinen Vorhaben unterstützt. Danke! Finally, Alex, I cannot thank you enough for your love and support during this challenging period of my life. Thank you for making me a happy person!

Abstract

Biological macromolecules such as peptides have a great potential to act as therapeutic agents to cure disease. However, they are unable to translocate biological membranes and require drug delivery systems (DDSs) for intracellular delivery. In order to evaluate the ability of novel DDSs to deliver peptide cargo, it is crucial that we are able to assess the functional delivery of the peptide to its intracellular target.

In this study a technique based on split green fluorescent protein (GFP) has been developed to address this. Split GFP consists of two non-fluorescent fragments, GFP1-10 and a small peptide fragment called M3. In the presented assay, GFP1-10 acts as a cytosolic target protein expressed in HeLa cells and M3 mimics the peptide cargo that is delivered by a DDS. Upon functional delivery of the M3 peptide by a DDS to the cytosol, M3 and GFP1-10 complement to form full length GFP and GFP fluorescence is rescued. In this thesis, the development of this split GFP based method is described. Furthermore, a stable cell line expressing GFP1-10 was generated and we were able to show that our model DDS, the cell penetrating peptide octaarginine (R8), functionally delivers M3 to its cytosolic GFP1-10 target in a concentration dependent manner. The addition of two Phenylalanine residues to R8-M3 (FFR8-M3) significantly increases M3 delivery. Furthermore it is shown that M3 delivery can be investigated in real time using a widefield microscope. Moreover, the split GFP complementation assay not only shows if and when the M3 peptide cargo is delivered to its intracellular target but also where it localises in the cell. It is demonstrated that the subcellular localisation of complemented GFP is dependent on the DDS utilised to deliver M3. A second system has been developed within this project where the fluorescent protein mCherry acts as an expression marker of GFP1-10 expression. This system has the potential to correlate complemented GFP fluorescence with the amount of expressed GFP1-10 in order to gain information how much M3 peptide has been delivered to the cytosol.

Table of Contents

List of Figures

List of Tables

Abbreviations

°C	Degree Celcius
2D	Two-dimensional
3D	Three-dimensional
ASO	Antisense oligonucleotide
BSA	Bovine serum albumin
C. elegans	Caenorhabditis elegans
CALM	Complementation activated light microscopy
CFP	cyan fluorescent protein
CME	Clathrin mediated endocytosis
CMV	Cytomegalovirus
CPP	Cell penetrating peptide
CTCF	Corrected total cell fluorescence
DDS	Drug delivery System
DMSO	Dimethyl sulfoxyide
DNA	Desoxyribonucleic acid
E.Coli	*Escherichia coli*
EDTA	Ethylenediaminetetraacetic acid
EDTA	Ethylenediaminetetraacetic acid
EED	Endosomal escape domain
EGF	Epidermal growth factor
EGFP	Enhanced green fluorescent protein
F	Phenylalanine
FACS	Fluorescence activated cell sorting
FAD	Flavin adenine dinuclotide
FITC	Fluorescein isothiocyanate
FSC	Forward scatter

G	Glycine
G418	Geneticin
GFP	Green fluoresccent protein
GLP-1	Glucagon-like peptide 1
GNRH	Gonadotropin-Releasing-Hormone
GPCR	G protein coupled receptor
h	Hour
H6	Histidine x6
HIV	Human immunodefficiency virus
kb	Kilo base
kDa	Kilo Dalton
L	Linker
MAb	Monoclonal antibody
mCherry	monomeric Cherry
mCherrySCL51	mCherry split cell line 51
MEM	Minimum essential media
min	Minute
mRNA	Messenger ribonucleic acid
NADH	Nicotinamide adenine dinucleotide
PA	Photoactivation
PA-GFP	Photo activatable green fluorescent protein
PBS	Phosphate buffered saline
PCR	Polymerase chain reaction
PDT	Protein transduction domain
PEG	Polyethynelglycol
PFA	Paraformaldehyde
PI	Propidium Iodide

PS	Photoswitching
PS CFP	Photoswitchable cyan fluorescent protein
R8	Octaarginine
RFU	Relative fluorescent units
Rh	Rhodamine
RNA	Ribonucleic acid
ROI	Region of interest
RPMI	Roswell Park Memorial Institute
SCL1	Split cell line 1
SD	Standard deviation
SEM	Standard error of the mean
siRNA	Small interfering
SSC	Sideward scatter
TNF alpha	Tumor necrosis factor alpha
TR	Transferrin receptor
YFP	Yellow fluorescent protein

1   Introduction

1.1   The importance of biologics to cure disease

Biologics include vaccines, therapeutic peptides and proteins, monoclonal antibodies and nucleic acids based therapeutics. They are therapeutic substances that are manufactured in living systems or are produced using biotechnology which makes use of biological processes, organisms, cells or cellular components in order to develop new technologies to treat disease. In contrast, traditional pharmaceuticals like small molecule drugs are chemically manufactured. Biologics are of growing importance for the pharmaceutical industry to act as novel therapeutics to cure disease and their development has revolutionized the pharmaceutical industry (Stockwin and Holmes 2003; Vlieghe *et al.* 2010; Lundin *et al.* 2015).

In the year 2000, the main reasons for attrition of drugs in the clinic was lack of clinical safety and toxicology as well as a lack of efficiency of drugs (Kola and Landis 2004). A study between the years 1991 to 2000 that investigated the top 10 drug companies' success and failure rates from across different therapeutic areas showed that attrition mainly occurs in Phase II and Phase III clinical trials (Kola and Landis 2004). Biologics brought a big change into the pharmaceutical industry with the prospect to cure disease with higher specificity and less side effects compared to small molecule drugs. In fact, it can be shown that the likelihood of moving from Phase I clinical trial to launch has been higher for biologics compared to small molecules from 1996 to 2014 (Figure 1-1 a). Between 2012 and 2014 it was even twice as likely for biologics (18%) to move from Phase I clinical trial to launch compared to small molecules (9%). Furthermore it was shown that the success rate was increased for biologics to move to the next phase of clinical trials between 2012 and 2014 (Figure 1-1 b) (Smietana *et al.* 2016). Thus, biologics have been shown to be more successful to act as therapeutics than small molecules.

The impact of biologics to act as therapeutics is also reflected in an overview of best-selling drugs in 2016 where top-selling drugs were ranked based on sales or revenue reported for 2016 by biopharma companies in press announcements, annual reports, investor materials, and/or conference calls. Eight of the ten best selling drugs were biologics (genengnews.com).
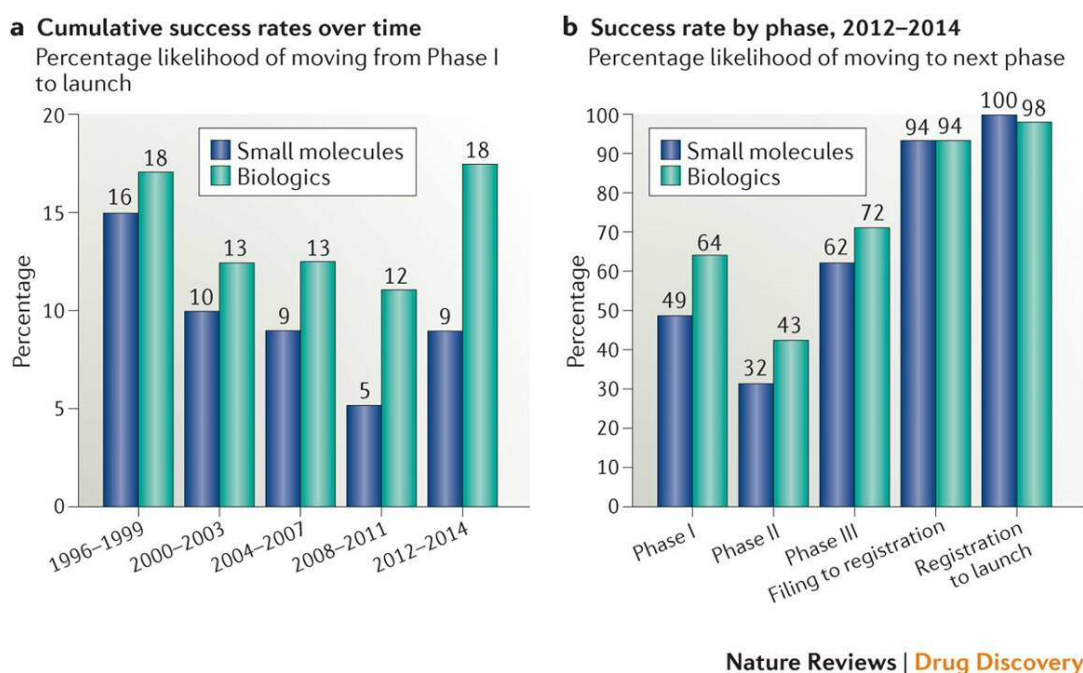
Figure 1-1 Comparison of success rates of small molecules and biologics in clinical trials.
(a) Comparison of the cumulative success rates of small molecules and biologics to move from Phase I clinical trial to launch 1996-2014. (b) Success of small molecules and biologics to move to the next phase 2012-2014. Figure obtained from (Smietana *et al.* 2016). Permission for reprint: license number 4270770091808.

1.1.1 Extracellular targets of biologics

Thus far biologics have been successful to act as therapeutics to target extracellular receptors that trigger an intracellular response or extracellular factors such as antigens or cytokines.

The top-selling drug shown in the overview of best-selling drugs in 2016 is Humira (AbbVie) (genengnews.com). Humira is a therapeutic monoclonal antibody (MAb) that targets the extracellular soluble cytokine TNF alpha in order to treat the autoimmune disease rheumatoid arthritis. MAb are complex macromolecules that are highly specific to their antigens and bind these with high specificity and high affinity. In 2015, 47 approved MAb products were on the market. All targeting strategies of these products to treat disease involved the targeting of extracellular factors such as cell surface antigens, cytokines and extracellular receptors with the most successful strategies for marketed MAb products being cytokine binding to treat autoimmune diseases and extracellular receptor binding in order to treat cancer (Doig Alfred 2015).

Monoclonal antibodies are just one example of approved biologics that have extracellular targets. A second type of biologics are therapeutic peptides. Peptide therapeutics are macromolecules of a size of up 50 amino acids. The majority of therapeutic peptides on the market act as receptor agonists to trigger an intracellular response (Vlieghe *et al.* 2010; Kaspar and Reichert 2013). One class of receptors that are a popular target for peptide therapeutics are G protein coupled receptors (GPCRs). In 2003 peptides targeting GPCRs accounted for the biggest class of therapeutic peptides on the market (almost 50%) (Pichereau 2005). One example is the Gonadotropin-Releasing-Hormone (GNRH) agonists Leuprolide (Lupron1; Abbott Laboratories) which is used to treat prostate cancer. It achieved global sales of over US$2 billion in 2011: the second best-selling peptide therapeutic drug between 2009 and 2011 out of 25 US-approved products (Kaspar and Reichert 2013). Another peptide therapeutic which targets a GPCR is the glucagon-like peptide 1 (GLP-1) receptor agonist for the treatment of type 2 diabetes. The glucagon-like peptide

1(GLP-1) receptor presented the biggest class of G-protein coupled receptor targets of peptides in clinical studies in 2012 (Kaspar and Reichert 2013).

1.1.2 Intracellular targets of biologics

Extracellular targets are the low hanging fruits in the development of biologic therapeutics as these targets do not require the macromolecules to pass the plasma membrane. A new promising area for biologic drugs is to carry out their function at intracellular targets. Intracellular targets include cytoplasmic (e.g. kinases and other enzymes), mitochondrial (e.g. pro or anti-apoptotic factors) or nuclear targets (e.g. transcription factors) (Mitragotri *et al.* 2014).

One major therapeutic area that requires the access of therapeutics to intracellular targets is gene therapy. Nucleic acid based therapeutics can be utilised for gene therapy that allows the specific targeting of genes that are responsible for causing disease and control their expression. Popular approaches in order to achieve this are antisense oligonucleotides (ASOs) or small interfering RNAs (siRNA). Both of these strategies are induce targeted downregulation of gene expression post transcriptional through Watson-Crick base pairing with the complementary mRNA. ASOs are single stranded and inhibit gene expression by binding to mRNA thereby blocking access of ribosomes the mRNA, modulate splicing or recruit cleaving enzymes to the complex. In contrast, siRNA is double stranded consisting of a passenger and a guide strand. While the passenger strand is released in the process of gene silencing, the guide strand ensures the recruitment of degrading protein complexes to the complementary mRNA strand (reviewed in (Watts and Corey 2012)). Nucleic acid based therapeutics are especially promising therapeutics for cancer therapy where cells undergo numerous genetic changes which lead to tumour cell growth (reviewed in (Devi 2006; Young *et al.* 2016).

Antibodies have been shown to be successful therapeutic agents to act at extracellular targets. They are also believed to have a great potential to act intracellularly in order to target protein-protein interactions, protein-nucleic acid interactions or even relocation of their antigens to subcellular locations (reviewed in (Lobato and Rabbitts 2003)).

Another group of therapeutics promising to target intracellular protein-protein interactions are therapeutic peptides (Nevola and Giralt 2015; Doak *et al.* 2016).The advantage of peptides therapeutics compared to antibodies is that they have a lower manufacturing cost because they can be manufactured synthetically (compared to recombinant production of antibodies), show high biological activity associated with low toxicity (reviewed in (Ladner *et al.* 2004), (Pichereau 2005)). In addition, peptides have a potential to penetrate further into tissues compared to antibodies due to their smaller size (McGregor 2008).

Despite this great potential of biologics such as therapeutic peptides, antibodies and nucleic acid derivatives to cure disease, their poor absorption and permeability across biological barriers and delivery to their intracellular targets largely limits their therapeutic use.

1.2   Requirements for intracellular delivery

Absorption, distribution, metabolism and excretion (ADME) processes in the body are critical when developing drugs. Especially cell permeability of a drug in order to reach its intracellular target is critical to the successful development of drugs. Factors that play a key role in the absorption of drugs are solubility and permeability.

For small molecule drugs the chemical properties to achieve optimal solubility and permeability are well defined. Christopher Lipinski and his colleagues proposed the key chemical criteria to achieve optimal solubility and permeability of a drug in

1997 (Lipinski *et al.* 1997). Lipinski's Rule of Five implies that poor absorption and permeation of a drug is more likely if it meets the following criteria: the number of groups that donate hydrogen to form a hydrogen bond is more than five (sum of hydroxyl and amine groups); the number of groups that accept hydrogen to form a hydrogen bond is more than 10 (sum of oxygen and nitrogen atoms); the molecular weight is greater than 500 Daltons and the calculated Log P (logarithm of the partition coefficient between water and 1-octanol) is greater than 5 (Lipinski *et al.* 1997). These rules apply to the absorption by passive diffusion of drugs and are used as criteria to determine the overall 'drug-likeliness' of small molecule drugs rule and has led to the decrease in attrition rates of drugs (Leeson 2012). Lipinski's observations show that oral bioavailability and cell permeability is mainly dependent on molecular weight and polarity and is increased for small lipophilic molecules.

1.2.1   Inability of biologics to pass the plasma membrane

Lipinski's Rule of Five defines the optimal characteristic of a drug in order to permeate the plasma membrane. Key characteristics are molecular weight and polarity. Investigating the characteristics regarding molecular weight and polarity of the small molecule drug aspirin compared to biologics sheds light on as to why biologics do not comply with the rule of five and have a poor permeability across biological membranes. Figure 1-2 shows the structure and molecular weight of the small molecule drug Aspirin as well as three examples of biologics, Glucagon-like peptide 1, Insulin and a monoclonal antibody. Aspirin consists of 21 atoms with a molecular mass of 0.18 kDa. In contrast, biologics are complex macromolecules with increased molecular weight; Glucagon-like peptide 1 with 3.27 kDa; Insulin with 5.8 kDa or a monoclonal antibody with 26 kDa. The molecular weight of biologics compared to aspirin is increased by 18.1 times for Glucagon-like peptide 1, 32.2 times for Insulin and 144.4 times for a monoclonal antibody. This increased molecular weight limits their ability to passively diffuse across the plasma membrane.

Furthermore, aspirin is lipophilic in the acidic environment of the stomach which allows absorption of the drug by diffusion across the plasma membrane (Gutknecht and Tosteson 1973). Therapeutic proteins and peptides are of hydrophilic nature which makes them impermeable to the lipidic plasma membrane.

The rule of five not only defines the 'drug-likeliness' of small molecule drugs but also allows to predict small molecule 'druggable' protein targets. These are limited to proteins where ligand and substrate binding pockets are solvent-accessible and susceptible to small molecule interaction (e.g. inhibition) (Naylor *et al.* 2017). Due to the small size of a small molecule drug (<0.5 kDa) it has a limited surface area and the interaction site with its target protein represents no more that 2-5% of the surface area of the protein (Lazo and Sharlow 2016). The classes of proteins that were defined as 'druggable' targets of small molecules are mainly enzymes and G protein coupled receptors (Hopkins and Groom 2002). However, these targets only reflect a small portion of the interactions mapped in the human genome (Venkatesan *et al.* 2009). Especially targets like protein-protein interactions are important novel targets in drug discovery (McFedries *et al.* 2013). With their large interaction surface that contain few opportunities for molecular interaction, these targets do not comply with Lipinski's Rule of Five and were therefore believed to be 'undruggable'. (Doak *et al.* 2016). In contrast, biologics are macromolecules (>0.5 kDa) that do not comply with Lipinski's Rule of Five which limits their permeability across the plasma membrane. However, their large surface area and biological activity offers novel possibilities of molecular interaction with their targets beyond 'Rule of five drugs' (Doak *et al.* 2016; Lazo and Sharlow 2016).

Hence, in order to make use of the full potential of biologics to cure disease, drug delivery systems are needed that facilitate the delivery of biological macromolecules across that plasma membrane to their intracellular targets.
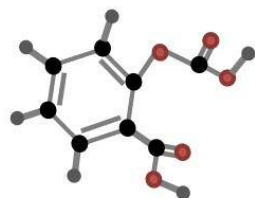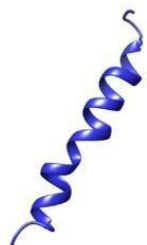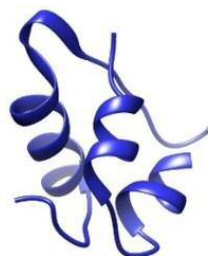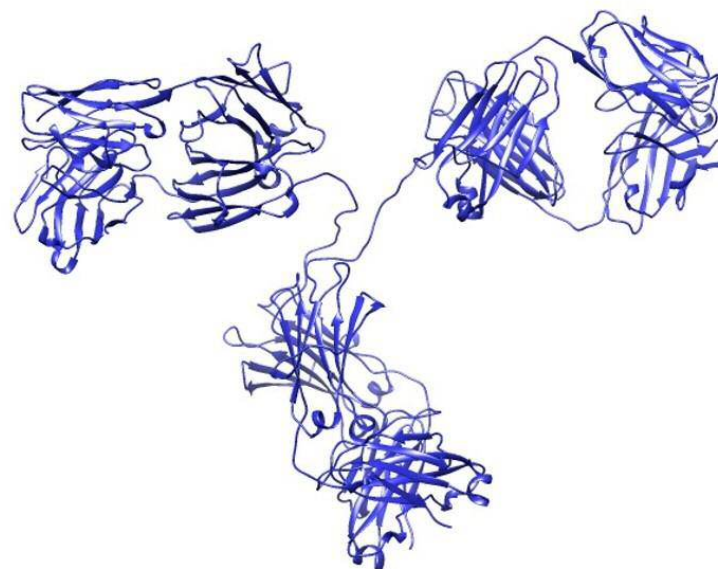
Figure 1-2 Comparison of the size of a small molecule drug and biologics.
Aspirin represents a small molecule drug. The structure was obtained from the PubChem website (CID 2244). Carbon molecules are shown in black, Hydrogen molecules are shown in dark grey and Oxygen molecules are shown in red. Glucagon like peptide 1 (GLP-1) receptor agonist is a popular choice for peptide therapeutics (Kaspar and Reichert 2013). Presented here is the structure of Glucagon-like peptide 1 (PDB ID: 1D0R) (Chang 2001) . Furthermore, structures of Insulin (PDB ID: 3I40) (Timofeev *et al.* 2010) and an IgG2a monoclonal antibody (PDB ID 1igt) (Harris *et al.* 1997) are shown as an example for biologics. All structures were modelled using Chimera.

1.3 Cell penetrating peptides for delivery of biologics

1.3.1 Natural peptides

Cell penetrating peptides (CPPs) are currently attracting a lot of interest in the drug delivery field, as it is hoped they can be exploited as a novel drug delivery system for macromolecular delivery (Foged and Nielsen 2008; Munyendo *et al.* 2012).

As their name suggests, CPPs have the ability to penetrate the cell membrane and gain access into the cell. CPPs are short peptide sequences, usually consisting of no more than 30 residues and were first found in organisms that are known to be able to penetrate membranes (e.g. viruses). These sequences are also called protein transduction domains (PTD). The best characterised examples are the human immunodeficiency virus (HIV) derived CPP Tat which plays a major role in the virus transduction into cells (Fawell *et al.* 1994; Vives *et al.* 1997), or the amphipathic Antennapedia homeobox protein, penetratin which was discovered in *Drosophila* where it acts as a transcription factor that can translocate between cells (Derossi *et al.* 1994). The amphipathic character of penetratin is revealed upon interaction with the plasma membrane when there is a structural change in the peptide conformation (helix formation) and insertion into the membrane (Dom *et al.* 2003; Ziegler 2008) .

In contrast, the Tat peptide is classed a non-amphipathic peptide and binds to plasma membranes with a high local concentration of anionic lipids (Madani *et al.* 2011). The cell penetrating character of Tat is attributed to its charge as the peptide consists of mainly basic amino acids; predominantly Arginine and Lysine residues, giving the peptide a cationic character that allows the peptide to bind and translocate through the membrane (Vives *et al.* 1997).

1.3.2 Synthetic peptides

Based on these natural examples highly positively charged synthetic peptides were generated to test their cell penetrating ability. Potential peptides for this were polymers consisting of the basic amino acids Histidine, Lysine and Arginine. It was found that peptides with a length of less than 6 amino acids are ineffective to enter the cell. Furthermore, a comparison of polypeptide sequences consisting of Arginine, Lysine or Histidine residues revealed that (L-or D-) Arginine is the most efficient to enter cells (Mitchell *et al.* 2000).

In a study by Gisela Tuennemann the penetration ability of polyarginines was further investigated. It was shown that the cell penetrating character is dependent on the length of the polyarginine chain and successful cell penetration requires a minimum of 7 Arginine residues. The transduction efficiency of polyarginines increases with increasing number of arginine residues and concentration. This effect however is accompanied with increased toxicity (Tunnemann *et al.* 2008). Peptides between 8 and 10 arginine residues are commonly used to study uptake of polyarginines into cells (Futaki *et al.* 2003; Tunnemann *et al.* 2008).

The chemically synthesised peptide Octaarginine, R8, is of special interest for this study. For this reason uptake mechanisms and cargo delivery are discussed focused on R8 or arginine rich peptides.

1.3.3 The uptake of CPPs

1.3.3.1 Methods to study the uptake of CPPs

A popular strategy in order to investigate the uptake of CPPs like R8 into cells is the attachment of a fluorophore to the CPP and quantification using fluorescent microscopy or flow cytometry. Commonly used methods included methanol or paraformaldehyde fixation of cells after incubation with the fluorophore tagged CPP and microscopic analysis of the localisation of the fluorophore. However microscopic

analysis showed that fixation introduced an artificial redistribution of arginine rich CPPs to the nucleus compared to live cells where the fluorescence was located in vesicular structures throughout the cytosol (Lundberg and Johansson 2002; Richard *et al.* 2003). Due to these experimental artefacts, it is critical to perform uptake studies of cell penetrating peptides and quantify cellular fluorescence using live cells.

Furthermore it is important to be able discriminate between fluorescently tagged CPP that is bound to the cell surface and CPP that has internalised into the cell. Richard and colleagues have demonstrated in their studies that fluorescently tagged CPPs are associated to the plasma membrane and quantification using flow cytometry measurement not only measures the fluorescence of internalised CPPs but also extracellular CPP bound to the plasma membrane (Richard *et al.* 2003). For this reason it is important to remove extracellular membrane bound CPP. Methods to achieve this are treatment of cells with trypsin in order to digest the membrane bound CPP without damaging the plasma membrane (Richard *et al.* 2003) or heparin washing of the cells which competitively removes CPPs bound to heparan sulfates on the plasma membrane (Lundberg *et al.* 2003). Utilising these improved methods it is possible to quantify the uptake of fluorescently tagged CPPs using microscopy or flow cytometry measurement (Fretz *et al.* 2007; Tunnemann *et al.* 2008; Sayers *et al.* 2014). Attachment of fluorescent probes to the CPP, however have been shown to influence the uptake of CPPs into cells. Depending on the charge of the fluorescent probe itself it can increase the uptake of CPPs into cells (Jones and Sayers 2012; Hyrup Moller *et al.* 2015). An alternative to the attachment of fluorescent probes to CPPs in order to monitor their uptake into cells is quantification using mass spectrometry where molecules can be analysed according to their mass. This technique however requires the lysis of cells and does not allow to monitor the subcellular distribution of CPPs in live cells (Burlina *et al.* 2005).

1.3.3.2 L and D amino acid enantiomers

When CPPs are synthesised, they can be chemically synthesised using L or D amino acids, however, the choice of the L or D isoform has an effect on uptake dynamics into cells. The human body only produces and recognises L-amino acid isoforms. Thus, CPPs that are produced as an L-amino acids isoforms can be recognised by cellular proteases and are at risk of degradation. In contrast, it has been shown that CPPs composed of the D-isoform were more stable in HeLa cells than CPPs composed of L-amino acids because they are not recognised by cellular proteases (Derek S. Youngblood *et al.* 2006). This could lead to the assumption that CPPs composed of the D-isoform should be utilised over the L-isoform. However, due to the fact that the D-isoform is foreign to the body, it was also demonstrated that the uptake of D-CPPs was decreased compared to L-CPPs (Verdurmen *et al.* 2011). For this reason it is preferred use L-CPPs compared to D-CPPs even though this is associated with an increased susceptibility to protease degradation once internalised.

How CPPs enter the cell is widely discussed and an ongoing field of CPP research. Thus far, two modes of cell entry are considered for cationic CPPs, direct translocation of the plasma membrane and uptake via endocytosis (reviewed in (Koren and Torchilin 2012; Layek *et al.* 2015)) (Figure 1-3).

1.3.3.3 Direct translocation

One mechanism for arginine rich peptides to gain entry to the cytosol is direct penetration of the plasma membrane (Figure 1-3 A) and this process has been found to be concentration dependent (Tunnemann *et al.* 2008). Once the peptides reach a threshold concentration, direct translocation across the plasma membrane can occur (Fretz *et al.* 2007; Jones 2007). When the direct translocation efficiency of polyarginines into cells was assessed it was found that the threshold started at concentrations as low as 5 µM. However, only a low proportion of cells was seen to

be positive for translocation (<5%). Direct translocation for this study was considered to occur when the fluorescent signal of the fluorophore tagged CPP is distributed within the whole cytosol and not seen as punctate structures enclosed in vesicles, where the uptake would be classed as occurring via endocytosis (Tunnemann *et al.* 2008).

Direct penetration of the cell by positively charged CPPs involves interaction with the negatively charged components of the plasma membrane like proteoglycans and phospholipids that leads to destabilisation of the membrane (reviewed in (Layek *et al.* 2015)). The mode by which penetration of lipid membranes by Arginine residues occurs was shown to be due to the formation of stable arginine-phosphate clusters that were formed in the membrane. This leads to binding, membrane perturbations and can result in pore formation in the membrane (Li *et al.* 2013). However, even though direct penetration of the plasma membrane is seen from a concentration of 5 μM (<5% transduced cells), it was shown that this was not associated with toxicity up to a concentration of 50 μM (35% of transduced cells) when polyarginines (R7-R9) were incubated with HeLa cells (Tunnemann *et al.* 2008).

There is evidence that damage to the membrane caused by the entry of CPPs trigger cellular repair mechanisms that involve internal vesicles being mobilized to the site of the disrupted plasma membrane resealing it to prevent leakage of intracellular molecules (Palm-Apergi *et al.* 2009).
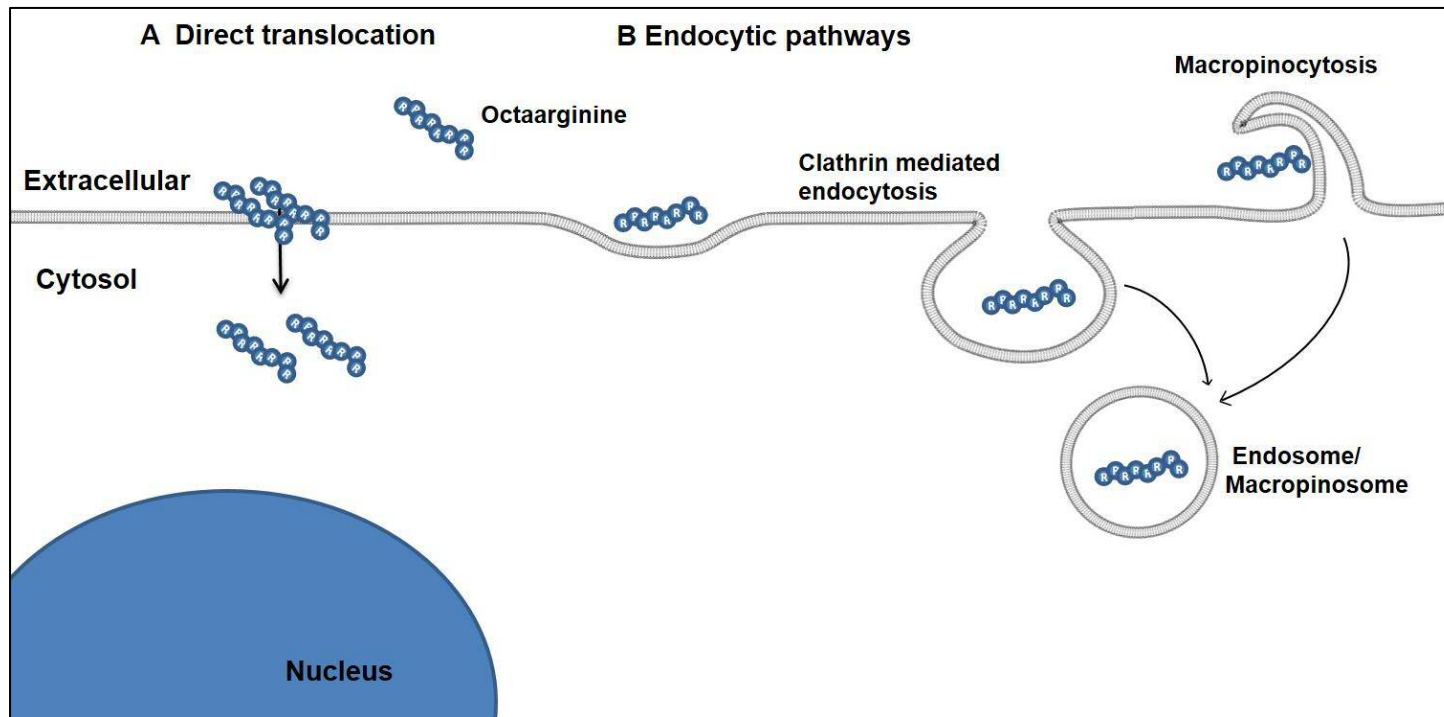
Figure 1-3 Mode of uptake of Cell penetrating peptides.
(A) Cell penetrating peptides can enter the cell through direct penetration of the plasma membrane (direct translocation).
(B) A second way of uptake is via endocytic pathways like macropinocytosis or clathrin dependent endocytosis. Once CPPs are internalised they are enclosed in an endosome/macropinosome.
R8 is shown as an example for CPP uptake.

1.3.3.4 Endocytic uptake

A second mechanism by which Arginine rich CPPs can enter the cells is through endocytosis (Figure 1-3 B). Endocytosis is a process where membrane impermeable molecules are internalized into the cell by engulfing them with plasma membrane in order to form vesicles. Through this process, the molecule is enclosed in a membrane vesicle that buds inside the cell to form an endosome. Hence, the endocytic process leads to internalisation of membranes originating from the plasma membrane bilayer. It can be dependent on different co-factors defining several endocytic pathways (reviewed in (Doherty and McMahon 2009)). Endocytic uptake of CPPs is usually studied in low concentrations ranging from 1 µM to 10 µM (Ikuhiko Nakase *et al.* 2006; Sayers *et al.* 2014; Kawaguchi *et al.* 2016).

CPPs like Tat and R8 were shown to be taken up by an endocytic process called macropinocytosis (Kaplan *et al.* 2005; Ikuhiko Nakase *et al.* 2006). Macropinocytosis is a process of ruffling of the plasma membrane to engulf fluid and cargo into macropinosomes (Figure 1-3 B). This fluid phase uptake process was first described in 1931 by Warren Lewis in rat macrophages (Lewis 1931). Macropinocytosis can be initiated by signalling molecules like epidermal growth factor (EGF). Stimulation with EGF leads to reorganisation of the actin skeleton and ruffling of the plasma membrane which leads to internalisation of EGF receptor (Orth *et al.* 2006).

Uptake of R8 through macropinocytosis was shown to be dependent on interaction with heparan sulfate proteoglycans, negatively charged components of the plasma membrane, and it was suggested that interaction with these components activates signals that lead to actin organisation and macropinocytosis (Ikuhiko Nakase *et al.* 2006). Knockdown of macropinocytosis by an actin cytoskeleton inhibitor was also shown to significantly suppress uptake of R8 into HeLa cells. (Nakase *et al.* 2004).

A second endocytic mechanism for the CPP Tat was shown to be clathrin mediated endocytosis (CME) (Richard *et al.* 2005) ((Figure 1-3 B). CME is a process

of the cell used in order to internalise receptors from the cell surface. One example is the internalisation of transferrin receptor (TR) which leads to uptake of iron into the cell through the TR bound ligand transferrin (Dautry-Varsat *et al.* 1983). Clathrin mediated endocytosis characteristically involves the formation of a clathrin coated pit. This coat forms at the cytoplasmic face of the plasma membrane and consists of the scaffold protein clathrin and adaptor protein complexes such as the adaptor protein AP-2 (Pearse 1976). Inhibition of this pathway can be achieved by utilising siRNA knockdown of the AP-2 subunit involved in the clathrin coat formation (Motley *et al.* 2003). In a study by Shiru Futaki's lab, syndecan-4, a heparin sulfate proteoglycan, was most recently identified to act as an receptor for R8 and that mediates uptake via clathrin mediated endocytosis (Kawaguchi *et al.* 2016).

Independent of which endosomal mechanism uptake occurs, it is important to consider that once a CPP has been taken up it is enclosed in a vesicle (endosome/macropinosome) and has not yet entered the cytosol (Figure 1-3 B). In order to understand the fate of a CPP enclosed in an endocytic vesicle it is important to outline the pathways and function of the endolysosomal system (Figure 1-4). The endolysosomal system carries out important functions such as recycling plasma membrane and their back to the cell surface (Steinman *et al.* 1983) as well as internalisation of receptors and targeting of specific cargo to the lysosome in order degrade it.

Once a cargo has entered the cell via an endocytic pathway it is enclosed in an endosome. Endosomes will fuse to form the first compartment of the endocytic pathway, the early endosome (Gruenberg *et al.* 1989). From this compartment cargo can be recycled back to the cell surface via recycling endosomes (van IJzendoorn and Hoekstra 1999). One example of a cargo that utilises this pathway is the transferrin receptor that is internalised via CME. This receptor is constitutivly internalised (Hopkins *et al.* 1985) and when bound to its ligand transferrin it transports

iron into the cell. Endocytic recycling can be as fast as 8-15 min (Huotari and Helenius 2011) and is not only important in order to maintain the presence of this receptor at the cell surface but also to recycle plasma membrane material back to the cell surface. Another example is the EGFR that is internalised via CME when bound to its EGF ligand and recycled back to the cell surface in order to achieve prolonged signalling (Sigismund *et al.* 2008).

However, this receptor can also be internalised via other endocytic routes which will lead degradation of the receptor (Figure 1-4). This is an important pathway in order to downregulate the presence of receptors on the cell surface. When cargo is targeted for degradation in the lysosome (ubiquitination of the cytosolic domain of EGFR) the cargo resides in the early endosome which matures into a late endosome. Characteristic of this maturation is a drop in pH in the late endosomal compartment (Maxfield and Yamashiro 1987). These late endosomal compartments then fuse with lysosomes in order to degrade the cargo material. Lysosomes are cellular organelles that contain enzymes that can break down proteins and other organic materials. These enzymes only function at acidic pH for which reason it is important to maintain the acidic pH (pH 5) in the lysosome.

Thus, CPPs that enter the cell through endocytic pathways largely remain trapped in the endolysosomal system where they recycle back to the cell surface or reside in the endosome to undergo degradation in the lysosome. However, in order to function as novel DDSs to facilitate uptake and delivery of target molecules to their intracellular targets it is critical that the CPP and its cargo escape the endosome. Endosomal escape of CPPs will further be discussed with their function as macromolecular drug delivery systems.
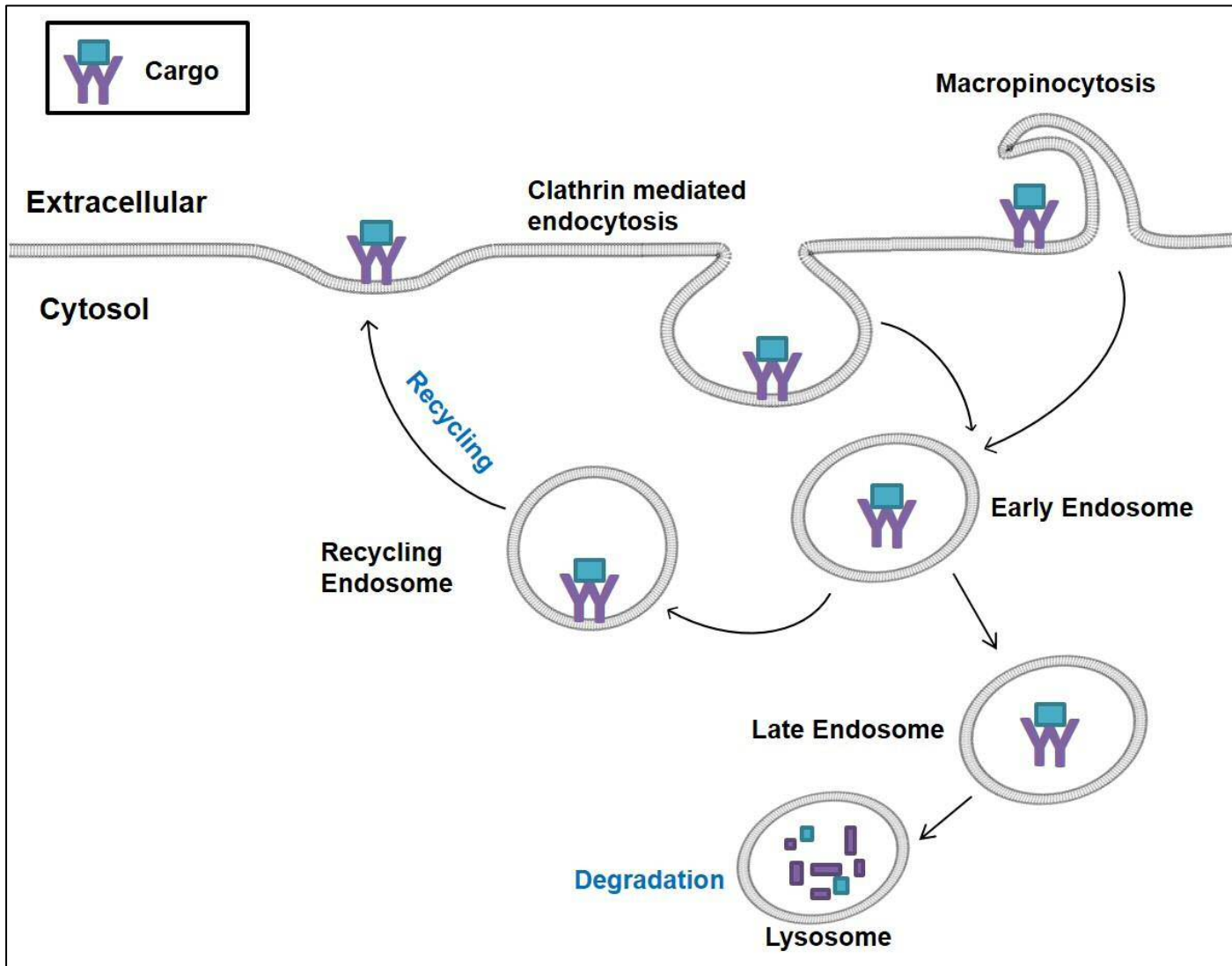
Figure 1-4 The endolysosomal system
Cargo can enter the endolysosomal system through various endocytic pathwyas like clathrin mediated endocytosis or macropinocytosis.
Endosomes fuse together to an organelle called the early endosome. From this location the receptor can undergo different fates; it can recycle back to the cell surface through a recycling endosome or remain in the early endosome, which matures into a late endosome and will be degraded in the lysosome.

1.3.3.5 Macromolecular cargo delivery and endosomal escape

Due to their cell penetrating ability, CPPs are a popular choice for the delivery of biological macromolecules such as peptides that cannot pass the plasma membrane by themselves (Foged and Nielsen 2008; Munyendo *et al.* 2012). CPPs are also termed 'Trojan horses' because they have the ability to facilitate the uptake of macromolecules into the cell that would not gain access to the cell by itself. They have been shown to be able to facilitate the uptake of macromolecular cargo such as peptide, proteins, nucleic acids and nanoparticles by covalent conjugation of the cargo to the peptide or by complexation with the peptide. Uptake of cargo molecules by CPPs can be shown by conjugation of a fluorescent label to the cargo and measurement of fluorescent intensity of the cell. Using this method the uptake of siRNA can be shown by Tat when the nucleic acid is labelled with the fluorescent probe Cy5 (Arthanari *et al.* 2010). Penetratin has been shown to facilitate the uptake of BSA into cells when complexed with the protein; in the same study it has been demonstrated that R8 can facilitate the uptake of quantum dots into cells. Interestingly, the uptake of quantum dots dots as well as BSA was enhanced when a Phenylalanine residue was substituted for the Glycine residue in the N-terminal GSGSGSGSG linker sequence attached to the CPP (Sayers *et al*. 2014). The uptake was validated through attachment of the fluorophore Alexa647 to BSA or by utilising the optical properties of quantum dots. Investigating the uptake of these fluorescently tagged cargos through CPPs by microscopy, it can be seen that the fluorescence is mainly localised in endosomes and the concentration of CPP used in this study (2 µM) suggest endosomal uptake of the CPP and its cargo (Sayers *et al*. 2014).

It has been shown that a macromolecular cargo influences uptake of the CPP-cargo complex and can be different as seen with the CPP alone. Uptake is dependent on the size and the charge of the cargo if uptake is facilitated through direct translocation or via an endocytic mechanism (Maiolo *et al.* 2005; Tunnemann *et al.*

2006). Large cargos like globular proteins remain trapped in endocytic vesicles and smaller cargos like non globular peptides are to some extent internalised by endocytosis but can also enter the cell through direct penetration (Tunnemann *et al.* 2006). Thus, macromolecular cargo is likely to be internalised through endocytic mechanisms.

When investigating intracellular cargo delivery by CPPs it is critical to differentiate between <u>uptake</u> and <u>functional delivery</u> of the cargo to its intracellular target. A cell penetrating peptide can facilitate uptake of cargo via direct translocation or endocytosis (Figure 1-5). When the CPP-cargo complex enters the cell via direct translocation, it has direct access to its intracellular target (Figure 1-5 A). However, if it utilises the endocytic route it is at risk to recycling back to the cell surface or degradation in the lysosome (Figure 1-5 B). In order to function at its intracellular target, the cargo has to reach the cytosol through endosomal escape.

Hence, endosomal escape is critical for the cargo in order to reach its intracellular target (Figure 1-5 B). Endosomal escape of CPPs and other novel drug delivery vectors and their cargos is highly inefficient and is believed to be the limiting factor for cargo delivery to their intracellular targets (El-Sayed *et al.* 2009; Erazo-Oliveras *et al.* 2012). Hence, the cargos remain trapped in the endosome are recycled back to the cell surface or undergo degradation in the lysosome and will therefore not be able to function at their intracellular targets (Sahay *et al.* 2013).

For this reason novel DDSs are needed that not only facilitate uptake of their cargo, but also deliver it to its intracellular target.

A Direct translocation

B Endocytic pathways

Extracellular

Cytosol

Macromolecular cargo conjugated to R8

Macropinocytosis

Clathrin mediated endocytosis

Recycling

Endosomal escape

Endosome/ Macropinosome

Lysosome

Degradation

Nucleus
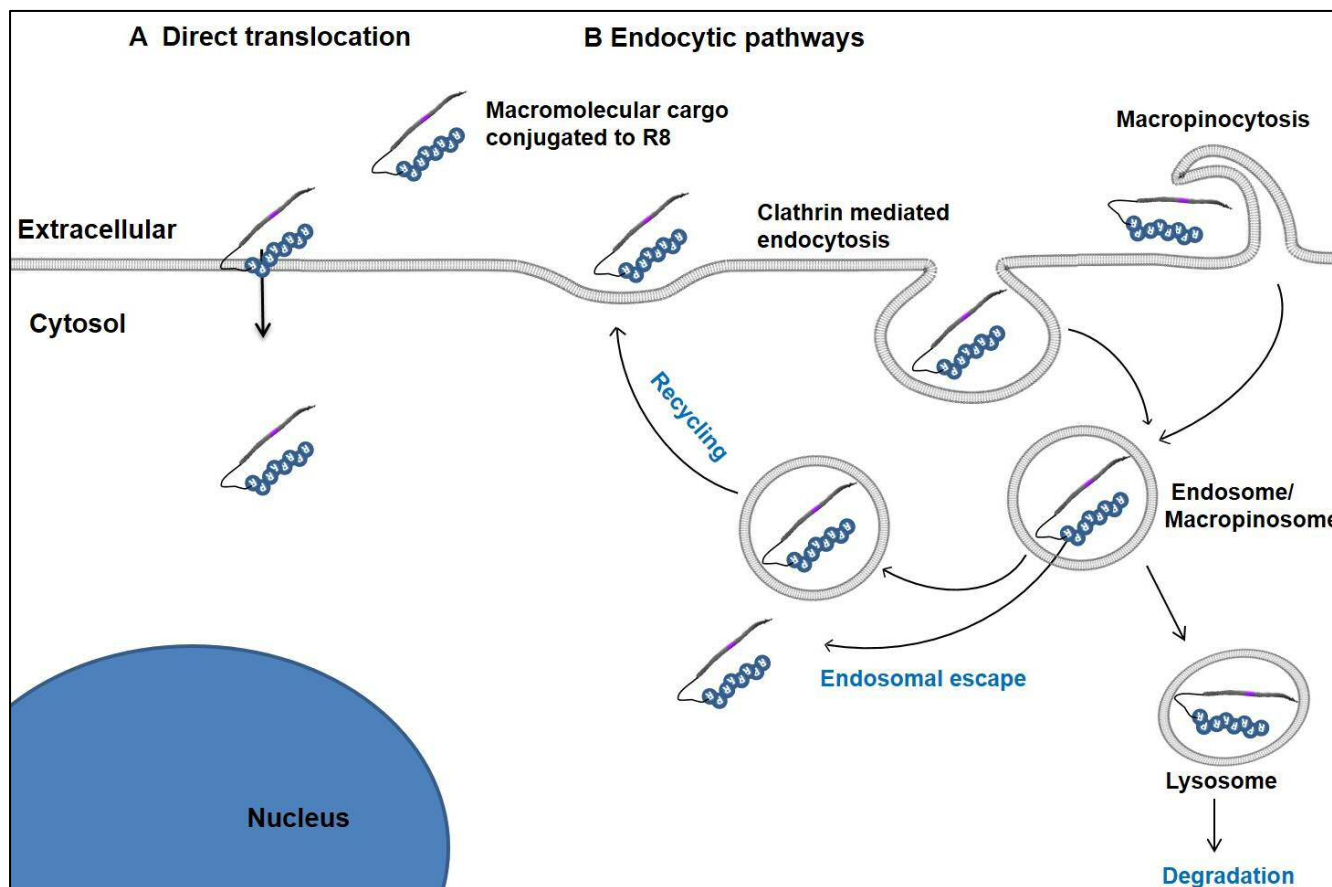
Figure 1-5 Delivery of macromolecular cargo by R8. Macromolecular therapeutics are too large to cross the plasma membrane by themselves.
Their delivery across the plasma membrane can be facilitated by drug delivery systems such as the cell penetrating peptide R8. Delivery to intracellular targets can be achieved through direct translocation (A) or endocytosis followed by endosomal escape (B) to avoid recycling to the cell surface or degradation in the lysosome.

In order to pursue this strategy CPPs are being modified to enhance endosomal escape mechanisms by endosomal leakage. For Tat it has been shown that dimerization of the peptide increases endsosomal escape which was shown by attatchment of the fluorescent probe rhodamine to the CPP. Tat monomer was mainly localised in endosomes when incubated at 20 µM whereas the fluorescently labelled dimer was distributed across the cytosol of the whole cell. Other endosomal escape mechanisms include fusion of the CPP to membrane lytic peptides (Arthanari *et al.* 2010). These lytic peptides can make use of the acidification of the endosome during its maturation process. Recently it has been shown that even macromolecules like an Alexa 488 labelled IgG antibody can be delivered with the help of lytic peptides. Critical residues of this peptide consisted of glutamic acid which is negatively charged in the extracellular region and does not penetrate membranes. When it is entrapped in the endosome with the antibody cargo, acidification of the maturing endosome causes protonation of glutamic acid which allows the less charged peptide to form a helical structure that pertubs the endosomal membrane (Akishiba *et al.* 2017).

Attachment of a fluorescent probes in order to investigate the location of a cargo inside the cell is an effective technique in order to differentiate between cargos trapped in endosomes and cytosolic distribution of the cargos (Fretz *et al.* 2007; Tunnemann *et al.* 2008; Sayers *et al.* 2014). However, fluorophores where shown to influence uptake dynamics of CPPs (Jones and Sayers 2012) and utlising this method does not answer an important question when delivering biological macromolecules:

Is the cargo still functional once it reaches the cytosol?

When fluorescently tagged splice correcting oligonucleotides were delivery by CPPs it was shown that intracellular fluorescence did not correlate with splice correcting activity of the oligonucleotides (Hassane *et al.* 2011). This study shows that simple attachment of a fluorophore to a CPP-cargo complex does not sufficiently represent its delivery or biological activity and this method is not suitable to investigate cargo delivery into the cell. For this reason, techniques are needed that not only prove cytosolic delivery of biologics but also assess their <u>functionality</u>.

It is also important to consider that covalent attachment of a cargo to CPPs can change the intracellular localization of the cargo. It has been demonstrated that CPPs with positively charged amino acids like TAT or R8 accumulate at the nucleolus of cells (Tunnemann *et al.* 2006; Martin *et al.* 2007). Covalent attachment of a cargo to these CPPs can result in the localisation of cargo in the nucleolus and is therefore not able to carry out its function at a target located in the cytosol of the cell.

For this reason it is not only important to develop techniques that assess the functionality of the cargo but more importantly techniques that assess the biological function of the cargo at its intracellular target.

1.3.4 Strategies to investigate the delivery of biologics

Promising biologics that carry out their function at intracellular targets are therapeutic peptides or proteins, antibodies and nucleic based therapeutics. In order to characterise novel DDSs that facilitate the functional delivery of these biologics to their intracellular targets, robust methods have to be in place to assess the biological activity of the delivered cargo.

The biological activity of delivered nucleic acids such as ASO or siRNA can easily be determined using splice correction assays or by testing gene silencing (Hassane *et al.* 2011). Popular gene silencing targets for colorimetric assays are proteins that

are introduced to the cell to be stably expressed such as green fluorescent protein (GFP) or luciferase. Gene silencing of GFP can be determined in live cells by monitoring the decrease of the fluorescence of the expressed protein (Kim *et al.* 2006).

In order to investigate the delivery of therapeutic proteins such as enzymes, several methods are available. These include the delivery of enzymes such as RNAse A, Luciferase or beta lactamase and measuring their enzymatic activity as an indication for delivery (D'Astolfo *et al.* 2015; Niikura *et al.* 2015). However, these methods cannot be assessed in live cells. Delivery of molecules such as RNAse requires further RNA purification steps to obtain a quantitative readout of delivery. The delivery of luciferase involves lysis of cells and preparation for luciferase measurement. When beta lactamase is delivered into cells its activity is measured by a shift of a fluorescent signal of a compound that requires cellular treatment with that compound (D'Astolfo *et al.* 2015; Niikura *et al.* 2015). Protein delivery into live cells can be investigated by the delivery of the protein GFP into cells, however this does not include assessment of therapeutic activity of the protein cargo (Erazo-Oliveras *et al.* 2014). The functional delivery of small cell penetrating antibodies (nanobodies) into cells has recently been shown by targeted relocation of their specific antigen from the cytosol to the nucleolus (Herce *et al.* 2017). This was shown by the change of the location of GFP fom the cytosol to the nucleolus. Binding of GFP was facilitated by the anti GFP binding nanobody, penetration into the cell as well as relocation of the GFP cargo-nanobody complex was facilitated by cyclic decarginine attachted to the nanobopdy.

Another class of therapeutics that have potential to act at intracellular targets are therapeutic peptides. Therapeutic peptides have a lower manufacturing cost compared to antibodies and show high biological activity associated with low toxicity. However, it is more challenging to determine the functional delivery of a peptide in

order to assess the DDS delivering the peptide. Hence, we require a method in order to assess functional delivery of a peptide to its intracellular target.

1.3.5   Requirements for a method to determine functional peptide delivery

A method to determine functional delivery of a peptide in order to evaluate their DDSs should be a robust and reproducible method. The method has to give information about the delivery of a peptide to its intracellular target as well as its biological activity at its target. The delivery of enzymes are great methods to determine functional delivery of macromolecules, however, these methods do not give a direct readout of engagement with their target or their functionality because of further purification and cell preparation steps.

Hence, when developing a method to investigate functional delivery of a peptide, a direct correlation of targeted engagement and biological activity would be desirable. Especially obtaining a readout of delivery in a live cell would be advantageous.

1.4 Green fluorescent protein (GFP)

As previously mentioned, GFP is a popular tool to be utilised to prove the delivery of various biologics into live cells. These include siRNA delivery resulting in gene silencing of GFP expression; GFP delivery representing a 27 kDa protein cargo; and anti GFP nanobody delivery which leads to GFP antigen binding which allows us to investigate the subcellular localisation of the antibody-antigen complex (Kim *et al.* 2006; Erazo-Oliveras *et al.* 2014; Herce *et al.* 2017). Furthermore, GFP has found a wide range of applications in cells such as protein labelling, defining subcellular localisations of proteins within cells, acting as biosensors, cell and tissue labelling, DNA and RNA labelling or studying protein-protein interactions (reviewed in (Chudakov *et al.* 2010)). It is a powerful tool because of its ability to give a readout without the need of additional cofactors or substrates and allows us to visualise the spatial and temporal patterns of GFP tagged targets in live cells.

1.4.1 History of GFP

The discovery of GFP was a Nobel Prize winning finding and a major discovery in the last century. Osam Shimura, Martin Schalfie and Roger Y. Tsien contributed to the discovery and characterisation of GFP and were awarded the Nobel Prize in chemistry in 2008 (*Nobelprize.org* Last accessed 07/2017).

GFP was first described in 1955 as yellow-green fluorescent masses appearing in the marginal canal of the jellyfish *Aequorea Victoria* upon mechanical stimulation (Davenport and Nicol 1955). In 1962 Osamu Shimomura discovered GFP while he was studying and isolating the photoprotein aequorin from *Aequorea Victoria* that emits light in the presence of calcium ions. During the purification process of aequorin a second protein was identified that is known as GFP today (Shimomura *et al.* 1962; Shimomura 2009). Over 30 years later the DNA of the 238 amino acid protein was first cloned (Prasher *et al.* 1992) and then introduced as a tool in molecular biology to

monitor gene expression and protein localisation in living cells by Martin Chalfie. Using GFP, gene expression could be detected in the prokaryotic organism *E.coli* and the sensory neurons of the eukaryotic organism *C.elegans* (Chalfie *et al.* 1994). GFP was then further characterised with respect to the process of chromophore formation, fluorescent properties and its structure.

1.4.2 Structure of GFP

The crystal structure of the protein was obtained by Ormo and colleagues 1996 (Ormo *et al.* 1996) (Figure 1-6). It revealed that the protein consists of 11 beta sheets with a central coaxial alpha-helix inserted between the 3rd and the 4th beta strand which contains the chromophore (star in Figure 1-6 A). In the 3 dimensional structure of GFP, the beta sheets build a barrel surrounding the central alpha helix (Figure 1-6 B).
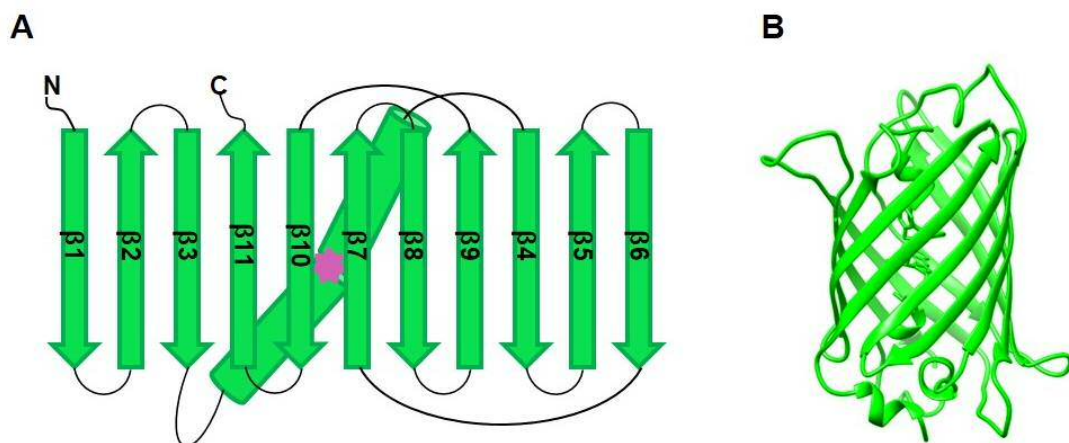
Figure 1-6 Structure of GFP
(A) Two dimensional structure of GFP showing 11 beta sheets (β1 – β11) and the central alpha helix containing the chromophore (pink star). (B) Three dimensional structure of GFP. The structure was modelled using Chimera (PDB ID: 1EMA) (Ormo *et al.* 1996).

It was found that the chromophore of wild type GFP is formed by an autocatalytic cyclisation of the three amino acids Ser65-Tyr66-Gly67 (Cody *et al.* 1993). It was identified that this reaction consists of three steps: cyclisation, oxidation and dehydration (Heim *et al.* 1994; Rosenow *et al.* 2004). For these steps, not only the three amino acids that form the chromophore, but also surrounding amino acids within the GFP structure play a key role in the maturation of the chromophore. Highly conserved residues are Arg96 and Glu222 which act as catalysts for the chromophore formation and are therefore in close proximity of the central helix (Sniegowski *et al.* 2005). Roger Y. Tsien not only contributed to the understanding how GFP fluoresces but also identified key residues that could be mutated in order to improve the properties of GFP for scientific applications.

1.4.3   Mutations of GFP

Wildtype GFP is a protein consisting of 238 residues, 27 kDa in size, with two excitation peaks at 395 and 475 nm and a single emission peak at 509 nm wavelength. The two excitation peaks represent two different states of the chromophore. The larger excitation peak at 395 nm wavelength light is found in a neutral chromophore (protonated) and the minor excitation peak at 475 nm wavelength light is caused by an anionic chromophore (deprotonated) (Heim *et al.* 1994; Brejc *et al.* 1997).

Major drawbacks of GFP for scientific use were the low maturation at 37 °C and its low fluorescent intensity when excited with blue light due to the low excitation peak at 475 nm wavelength light. Substitution of Phenylalanine to Leucine at position 64 (F64L) resulted in a protein with greater stability and therefore rate of fluorophore generation at 37°C (Cormack *et al.* 1996). Mutation of Ser65 to Thr65 (S65T), contained in the chromophore, suppresses the 395nm excitation peaks and leads to increased brightness and with a single excitation peak at 488 nm wavelength (emission 512nm) (Heim *et al.* 1995). The protein with improved folding and

brightness was named enhanced GFP (EGFP) (Heim *et al*. 1995; Cormack *et al*. 1996). Further mutations lead to the generation of colour variants of GFP such as yellow (T203Y) or cyan (Y66W) fluorescent proteins (Heim *et al*. 1994; Heim and Tsien 1996; Ormo *et al*. 1996).

An improvement to live cell imaging to track dynamics of proteins in cells was made by introducing photoactivatable GFP (PA-GFP). PA-GFP was developed based on GFP carrying two excitation peaks. Introduction of a Thr203His mutation, produces mostly neutral chromophore form of GFP with its main excitation peak at 400 nm wavelength light (Patterson and Lippincott-Schwartz 2002). This is termed the low fluorescent state of the fluorophore when excited with 488 nm wavelength light. Photoactivatable GFP relies on a conversion from the fluorescent protein from a low fluorescent state to a higher fluorescent state. This is achieved by irradiation of the fluorophore in the low fluorescent state with 413 nm wavelength light which shifts the excitation wavelength from 400 nm of the neutral form to the anionic form of the fluorophore which absorbs at 507 nm. This leads to an irreversible photoactivation of the fluorophore with a 100 times increase in fluorescence of the higher fluorescent state to the lower fluorescent state when excited with 488 nm wavelength light. This conversion can be achieved selectively for the protein of interest which can be tracked and imaged over the low GFP fluorescent background. Further improvement was the photoconversion from cyan fluorescent protein to green fluorescent protein in response to 405 nm wavelength light irradiation termed photoswitching (PS) (Chudakov *et al*. 2004).

Improvements to expression of GFP in *E.Coli* were made with the generation of folding reporter GFP. Wild type GFP missfolds when expressed in *E.Coli* and is expressed in inclusion bodies. Folding reporter GFP includes the improvements that were previously made for EGFP, the S65T and F64L mutation in order to ensure the maturation at 37 °C and the brightness of the protein as well as three additional

mutations (F99S, M153T, V163A). This folding reporter had improved brightness as well as improved solubility when expressed in *E.Coli* (Crameri *et al.* 1996).

GFP and its variants have found useful applications as fusion proteins, however, the fluorescence and folding of the protein is susceptible to the ability of their fusion partners to fold correctly. Their folding can decrease the folding yields of GFP and its brightness. Bright fluorescence is only seen when GFP is expressed as a fusion protein to well folded proteins (Waldo *et al.* 1999). For this reason, Waldo and colleagues generated a new GFP mutant, superfolder GFP (sfGFP), with improved folding characteristics that even folds well when fused to poorly folding polypeptides. This mutant was based on a previously generated well-folding variant of GFP, folding reporter GFP (Crameri *et al*. 1996). In addition to the mutations present in folding reporter GFP sfGFP contained six new mutations (S30R, Y39N, N105T, Y145F, I171V and A206V). sfGFP folds well and is bright fluorescent even when expressed as a fusion to poorly folded polypeptides (Pedelacq *et al*. 2006).

1.4.4   Disadvantages of GFP

It is also important to mention that using GFP can have disadvantages. GFP as a protein label is expressed as a C- or N-terminal fusion protein to its protein target. However, the addition of a 27kDa fluorescent protein to a protein can impair its biological function. It is therefore critical to not only study the fusion protein but also to obtain data from the endogenous protein without a fluorescent protein tag (Michaelson and Philips 2006). In addition to that, GFP tagging as well as the choice of C- or N-terminal fusion to the target protein can have an influence of its subcellular localisation (Palmer and Freeman 2004). However, an analysis of the localisation of >500 human proteins showed that 80% of proteins had the same localisation when expressed as fluorescent protein fusions compared to the localisation of an endogenous protein that was shown using immunofluorescence (Stadler *et al.* 2013).

Another factor to be considered when performing expreiments where endogenous DNA is expressed is the change of localisation of the protein by its overexpression. GFP fusion proteins are generally expressed by introduction of an expression plasmid encoding for the exogenous fusion protein. Protein expression from an expression plasmid can lead to overexpression of the protein introducing overexpression artifacts compared to the endogenous protein.

Another disadvantage is that the emission spectrum of GFP lies within the 500 – 600 nm spectral region where autofluorescence is detected in cultured mammalian cells. The source of this autofluorescence are endogenous fluorophores like nicotinamide adenine dinucleotide (NADH) or flavins like flavin adenine dinuclotide (FAD) which were shown to be localised in the perinuclear region (Aubin 1979; Benson *et al*. 1979). Their fluorescent excitation/emission spectra are 350/460 nm for NADH and 450/535 nm for FAD (Ramanujam *et al*. 1994). Because NADH and FAD are important cofactors in the mitochondrial electron transport chain where they function as coenzymes for cell metabolism and energy production, it was shown that their fluorescent properties can be utilised to develop an imaging technique investigating cellular metabolic activity or using it to determine mitochondrial cytotoxicity of chemical compounds (Skala and Ramanujam 2010; Bednarkiewicz *et al*. 2011; Rodrigues *et al*. 2011). FAD with its emission spectrum of 535 nm lies within the spectral range that is collected when GFP emission is measured. Thus, the autofluorescence of cells can create a fluorescent background signal when choosing GFP as a fluorescent protein for imaging.

Nevertheless, GFP and its derivatives have turned out to be a very powerful tool for live cell imaging to determine protein localization or to study dynamic events inside cells using a fluorescent microscope.

1.4.5   Split GFP to show protein-protein interaction

To test the delivery of biologics by DDSs, GFP can serve as a 27 kDa model protein cargo. Its fluorescence will give information about its subcellular localisation as well as if the protein is intact at this localisation. However, this does not give information about the engagement of the cargo with an intracellular target. When developing a new method to investigate functional delivery of a therapeutic peptide by DDSs, not only the success of delivery is important but it would also be a major improvement to be able to show its biological activity at its intracellular target.

One technology where GFP fluorescence is utilised as a biosensor for the readout of the biological engagement of two proteins is split GFP (Hu and Kerppola 2003; Cabantous and Waldo 2006).

The idea of split GFP was first mentioned in 2000. GFP was divided into two large parts between residues 157 and 158 to create two non fluorescent fragments, CGFP and NGFP containing 157 and 81 residues, respectively. The chromophore was contained on NGFP. Both fragments were connected to antiparallel leucine zippers via a flexible linker. The fragments connected to the designed leucine zippers were termed NZGFP and CZGFP respectively. Reassembly of NZGFP and CZGFP to from full length fluorescent GFP was achieved by the non-covalent association of the two leucine zippers and reassembly was shown to be dependent on the leucine zippers *in vitro* and *in vivo* (Ghosh *et al.* 2000).

Based on this leucine zipper mediated reassembly split fluorescent proteins were used to study protein-protein interactions inside cells (bimolecular fluorescence complementation (BiFC) (Hu *et al.* 2002). The broad range of GFP variants that were split using leucine zipper mediated re-association allowed the visualisation of multiple interaction events in the same cell (Hu and Kerppola 2003). For this application it was important that the re-association of the two fragments found not to be spontaneously initiated by the split fragments but dependent on the protein-protein interaction (e.g. leucine zipper association) of the fusion proteins (Chudakov *et al.* 2010).

Waldo and colleagues wanted to utilise this split GFP system as a folding reporter for proteins and detect soluble or insoluble proteins in living cells and cell lysates. However existing split GFP could not be utilised because of insufficient folding when expressed as fusion proteins as well as the dependence of fusion protein interaction in order to achieve GFP complementation. Thus, they improved this system and designed split GFP fragments that were able to self-assemble independent of a fusion proteins and fragments with improved folding (Cabantous *et al.* 2005). In order to improve the folding of split GFP fragments, experiments were based on the two well-folding GFP variants, folding reporter GFP (Crameri *et al*. 1996) and superfolder GFP (Pedelacq *et al*. 2006). They split both GFP variants assymatrically into two non fluorescent split GFP fragments, a large fragment consisting of amino acids 1-214 termed GFP1-10 and the small fragment, GFP11, comprising amino acids 215-230. When they coexpressed both fragments in *E.Coli* only coexpression of the superfolder fragments led to complementation of the fragments and rescued GFP fluorescence. However superfolder GFP1-10 was insoluble. In a stepwise improvement through introduction of mutations they designed two fragments with maximal solubility and brightest *in vitro* complementation. They named these split GFP variants GFP1-10 OPT and GFP11 M3 (containing 16 amino acids). GFP1-10OPT contains all amino acid substitutions found in superfolder GFP and seven additional mutations (N39I, T105K, E111V, I128T, K166T, I167V and S205T).

In vitro complementation of both fragments to form full length GFP was shown to occur shortly after incubation of the fragments and saturation of GFP complementation of 50 pmol GFP11 M3 with 800 pmol GFP 1–10 OPT was reached after ~400 min (Cabantous *et al.* 2005).

A Key components of GFP

I

II

Chromophore
(THR65-TYR66-GLY67)

Proton acceptor
(GLU222)
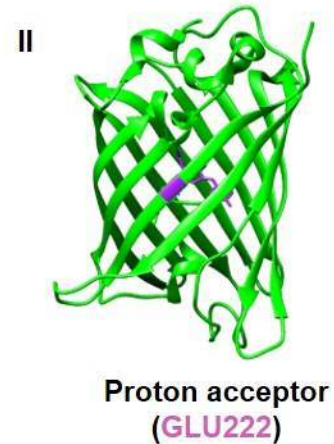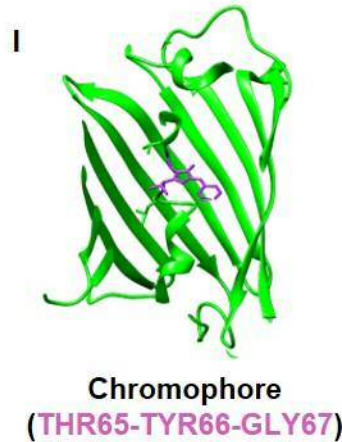
B Split GFP

GFP1-10 OPT

+

GLU 222
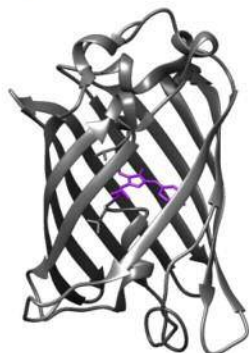
GFP11 M3
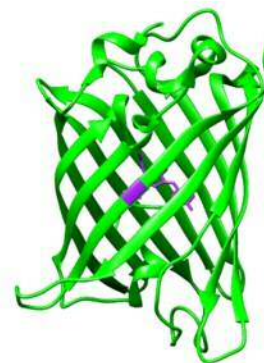
Complemented GFP

Figure 1-7 Split GFP
(A) Key components of GFP (pink) are the chromophore located on the central alpha helix consisting of the amino acids Thr65-Tyr66-Gly67 as well as the highly conserved residue glutamic acid (GLU222) which is located on the 11th beta sheet of the beta barrel. (B) GFP can be split into two non- fluorescent fragments, GFP1-10 OPT containing the chromophore and GFP11 M3 containing GLU222. These fragments can complement to form full length GFP and the green fluorescence of the protein is rescued (Kent *et al.* 2008).
The structures are based on the crystal structure of superfolder GFP (PDB ID: 2B3P) (Pedelacq *et al.* 2006). All structures were modelled using Chimera.

The underlying mechanism of split GFP generated by Waldo and colleagues is shown in Figure 1-7. Key components of GFP that are important to the fluorescence of the protein are the chromophore located on the central alpha helix consisting of the amino acids Thr65-Tyr66-Gly67 as well as the highly conserved glutamic acid residue (GLU222) which is located on the 11th beta sheet of the beta barrel (Figure 1-7 A). These can be separated to obtain two non- fluorescent fragments, GFP1-10 OPT containing the chromophore and GFP11 M3 containing GLU222. These fragments can complement to form full length GFP and the green fluorescence of the protein is rescued (Figure 1-7 B) (Kent *et al.* 2008).

Furthermore it was shown that *in vitro* complementation was linear to the concentration of the fragments when 0.1 to 200 pmol of GFP11 M3 was mixed with 800 pmol GFP1-10 OPT. Moreover the complementation of the split GFP fragments was analysed regarding pH dependency. It was found that complementation below a pH of 6.5 was inefficient (Cabantous *et al.* 2005).

Investigation of absorption and excited-state proton transfer dynamics revealed that complemented GFP (not containing the S65T mutation) had identical characteristics to the full length protein. It was also noted that complemented GFP can be separated by denaturation and the GFP1-10 fragment containing the matured chromophore emits weak fluorescence (Kent *et al.* 2008).

With the development of spontaneously assembling split GFP fragment a new powerful tool has been created to investigate intracellular processes.

Importantly, split GFP allows us to investigate functional complementation of a large protein fragment, GFP1-10OPT and a small peptide fragment, GFP11 M3 which has a great potential to investigate a functional biological interaction of a cargo (GFP11 M3) at its intracellular target (GFP1-10OPT).

One key publication that has led to the development of the split GFP based method presented in this study utilised split GFP for the selective detection of single biomolecules using complementation-activated light microscopy (CALM). It was shown that split GFP complementation can be directly imaged when the M3 peptide conjugated to biotin was fixed to an avidin-functionalized coverslip and subsequently incubated with GFP1-10. GFP complementation occurred within 10 minutes and lasted for 2 hours until it reached saturation. Importantly, they also showed that extracellular membrane proteins on live cells fused with GFP1-10, complemented to full length GFP upon incubation with the M3 peptide. Complementation was achieved by incubation of M3 peptide (50 µM) with live cells within 45-60 min. Furthermore, intracellular GFP complementation was investigated by microinjection of M3 to an intracellular expressed GFP1-10 target. Importantly, it was briefly described that short amphipathic peptide carrier, Pep-1 was used to deliver M3 across the membrane by co-incubation to complement with its intracellular target as an alternative to microinjection (Pinaud and Dahan 2011).

1.5   Hypothesis and aims

1.5.1   Utilising split GFP to show functional peptide delivery by DDSs

Because of insufficient delivery of macromolecular therapeutics such as peptides across the plasma membrane, there is a need for novel DDSs that facilitate uptake of these macromolecules. Hence, novel DDSs have to be assessed regarding their delivery efficiency of peptides. For this reason methods need to be developed to evaluate and quantify the functional delivery of their functional peptide cargo across biological barriers.

The split GFP system by Waldo and colleagues holds great potential in order to achieve this. The idea for the development of a method to investigate functional peptide delivery utilising the Split GFP is shown in Figure 1-8. Non-fluorescent GFP1-10OPT (named GFP1-10 in this thesis) (Cabantous *et al.* 2005), is expressed in the cytosol of HeLa cells and mimics an intracellular target protein. The M3 peptide consisting of 16 amino acids as described (GFP11 M3) (Cabantous *et al.* 2005) acts as a peptide cargo that cannot pass the plasma membrane. Attatchment of a drug delivery system (DDS) (e.g. octaarginine) to M3 can facilitate its uptake through direct translocation across the plasma membrane or via endocytic pathways. The M3 peptide only reaches the cytosol by direct entry or endosomal escape, avoiding recycling back to the cell surface or degradation in the lysosome. If the M3 peptide enters the cytosol, GFP1-10 and M3 are localised in the same cellular compartment and can undergo spontanous complementation to form full length GFP. This implies that the M3 peptide is fully functional and has not been degraded before reaching its intracellular GFP1-10 target. Hence, intracellular GFP fluorescence is a proof of the delivery of functional M3 peptide cargo by the DDS. [1]

---

[1] This idea was first described within my Master's project that preceded this project (Riester P., Characterising the cellular uptake and targeting of novel drug delivery systems, 2014, Department of Biology, Universitaet Konstanz.).
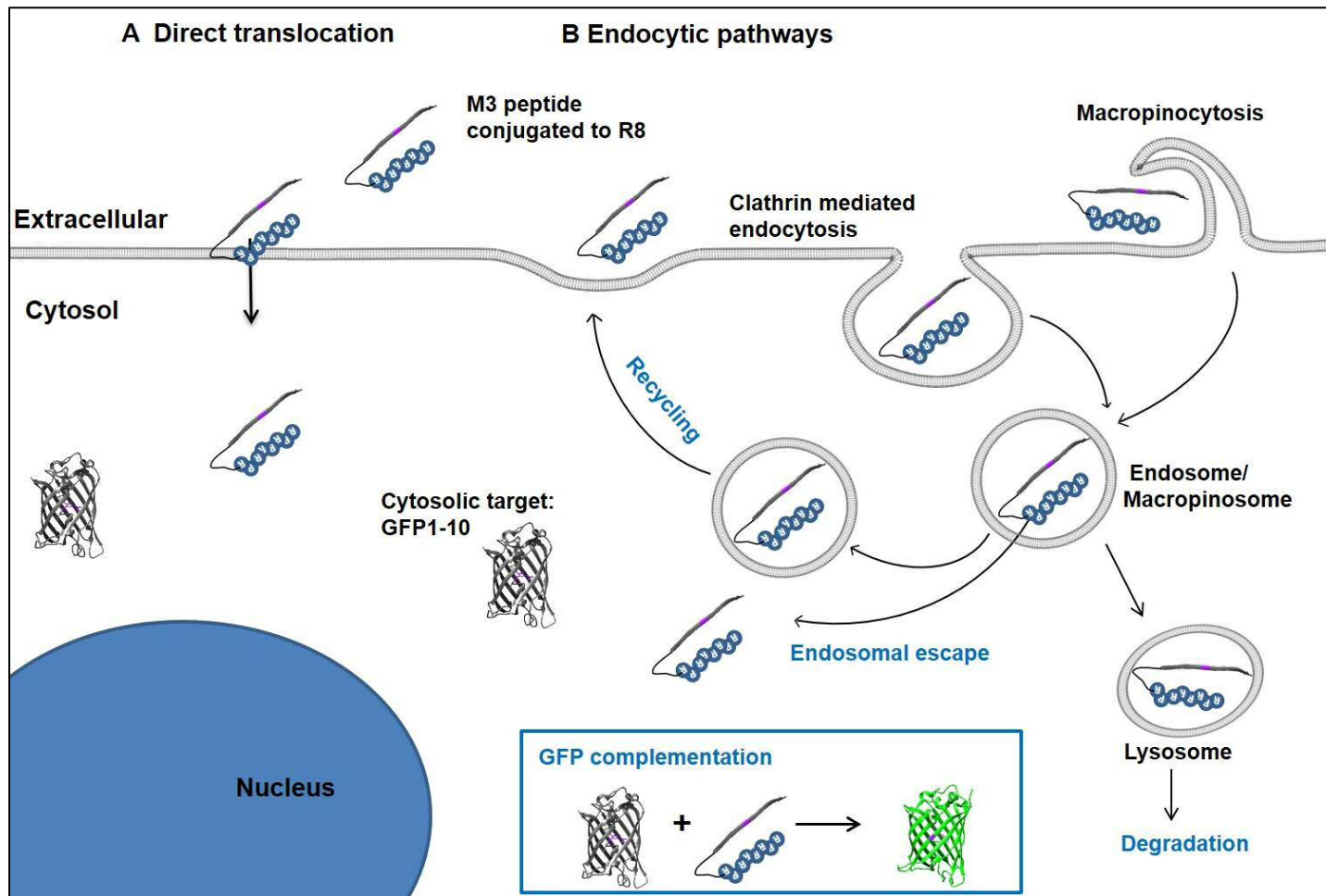
Figure 1-8 Split GFP complementation assay to determine functional delivery of a peptide by DDSs

GFP1-10 is expressed in the cytosol of HeLa cells and mimics an intracellular target protein. The M3 peptide consisting of 16 amino acids acts as a model peptide cargo that cannot pass the plasma membrane. Attachment of the drug delivery vector R8 to M3 can facilitate its uptake through direct translocation across the plasma membrane or via endocytic pathways. The M3 peptide only reaches the cytosol by direct entry or endosomal escape, avoiding recycling back to the cell surface or degradation in the lysosome. If the M3 peptide enters the cytosol, GFP1-10 and M3 undergo spontaneous complementation to form full length GFP. Functional peptide delivery can be measured by GFP fluorescence upon illumination with 490 nm wavelength light,

R8 has been extensively investigated by our research group and will act as a model DDS for the development of this assay (Fretz *et al.* 2007; Sayers *et al.* 2014). However, this method has the potential to can act as a platform to evaluate <u>any</u> peptide delivery vector regarding its efficiency to funtionally deliver peptide cargo.

The advantage of this technique over commonly used techniques (e.g. measurement of enzymatic activity of delivered enzyme) is that functional delivery to an intracellular target can be visualized in live cells in real time upon illumination of the cells with 490 nm wavelength light.

1.5.2 Existing Split GFP complementation assays to prove functional peptide delivery

Split GFP complementation assays utilising the method described above to determine the functional delivery of the M3 peptide by CPPs were published by other research groups after 1.5 years into the development of the assay presented in this work (Milech *et al.* 2015; Schmidt *et al.* 2015b).

Schmidt *et al.* first published the split GFP complementation assay using the CPP nonarginine (R9) to deliver the small fragment of split GFP (called GFP11 in that study) to its cytosolic GFP1-10 target. In this publication it was shown that the CPP conjugated GFP11 peptide as well as the pure GFP11 peptide can be introduced to the cytosol of the cell by electroporation to complement with GFP1-10 resulting in green fluorescence. Furthermore, Schmidt *et al.* demonstrated that R9 functionally delivers GFP11 to cells transiently expressing GFP1-10 along with the co-expression marker mCherry in a concentration dependent manner (Schmidt *et al.* 2015b). The majority of this work, however, is presented from two independent experiments only.

Shortly after the first publication, Milech *et al.* published the same split GFP complementation approach to prove the functional delivery of the short fragment of GFP (called S11 in that study) to its intracellular GFP1-10 target. In this study the delivery efficiency of a large range of different CPPs to facilitate functional S11

delivery is compared. Concentration dependent delivery of S11 is shown for the CPPs Tat, R9 and penetratin (Milech *et al.* 2015). In both papers analysis of functional peptide delivery resulting in GFP complementation was detected by flow cytometry and it was not utilised as a microscopy based technique. Microscopy images were shown in the paper by Schmidt et al. but solely to identify if the peptide fragment of GFP was delivered to the cytosol. Using microscopy has the huge potential to gain additional information from the assay such as time dependent delivery of the M3 peptide as well as assessment of the subcellular localisation of delivered peptide.

1.5.3   Aims of this work.

The aim of this project is to develop and characterise a method to investigate functional peptide delivery by DDSs based on split GFP technology. This method will enable us to determine the functional cytosolic delivery of a peptide thereby evaluating different drug delivery systems regarding their efficiency to functionally deliver peptide cargo. The assay will be developed in the well characterised model cell line HeLa due to its ease of manipulation and well characterised cell biology. Once the system is verified in this cell model it can further be applied to detect delivery of peptides into pharmaceutically relevant endothelial barriers (e.g. intestine, lung, skin, and blood-brain-barrier) or utilized *in vivo* to investigate functional delivery into target tissues. Furthermore, it is important to be able to assess M3 peptide delivery by a DDS in a concentration dependent manner in order to determine effective concentrations for peptide delivery. Analysis of concentration dependent delivery of the M3 peptide by different DDSs by flow cytometry will be comparable to split GFP complementation assays shown by Milech *et al* and Schmidt *et al.*.

In this work, however, the focus is to develop the split GFP complementation assay to be utilised as a microscopy based technique and detailed characterisation of the split GFP system on a fluorescent widefield microscope will be performed. Detection of split GFP complementation upon M3 delivery to the cytosol using a

microscope allows us to visualize real time delivery of a functional peptide cargo to its intracellular target. Fluorescent microscopy on a widefield microscope will ensure the visualisation of live cell processes with sufficient speed.

In addition to this, microscopic analysis of M3 delivery will also elucidate the subcellular localisation of the complemented target-cargo complex once delivered into the cell. This will emphasize the influence of the DDS on intracellular localisation of the cargo.

The additional information gained in this work by analysing when a peptide is delivered to its intracellular target as well as where it is located inside the cell will go above and beyond what has been published previously and add valuable information to the characterisation of drug delivery systems.

2   Materials and Methods

2.1   Consumables

Tissue culture plastic-ware and laboratory disposables were obtained from Fisher Scientific. General usage chemicals and reagents were supplied by Sigma-Aldrich.

2.2   Peptides

All peptides were obtained from EZBiolabs. Peptides were synthesised of L-amino acids and were obtained at >95% purity and aliquoted to 1 mg as lyophilized powder. When necessary, peptides were modified with an acetylation (Ac-) at the N-terminus or an amidation (-NH2) at the C-terminus. Peptides were resuspended in DMSO to a final concentration of 10 mM. Lyophilized powder was stored at -20˚C, once resuspended in DMSO, peptides were stored in 5 µl aliquots at -80˚C. Table 2-1 shows an overview of peptides used in this study and the volume of DMSO that was used to dilute peptides to obtain a final concentration on 10 mM.

Table 2-1 List of peptides used in this study.

Peptide Name	Sequence	Molecular weight	Amount	Volume DMSO	Final concentration
M3	Ac-RDHMVLHEYVNAAGIT	1869.12 g/mol	1.1 mg	58.85 µl	10 mM
L-M3	Ac-GSGGGSTSRDHMVLHEYVNAAGIT	2458.67 g/mol	1.0 mg	40.67 µl	10 mM
R8	RRRRRRRR-NH$_2$	1266.54 g/mol	3.0 mg	236.9 µl	10 mM
R8-M3	RRRRRRRRGSGGGSTSRDHMVLHEYVNAAGIT	3666.06 g/mol	1.0 mg	27.27 µl	10 mM
FR8-M3	FRRRRRRRRGSGGGSTSRDHMVLHEYVNAAGIT	3813.32 g/mol	1.0 mg	26.22 µl	10 mM
FFR8-M3	FFRRRRRRRRGSGGGSTSRDHMVLHEYVNAAGIT	3960.50 g/mol	1.0 mg	25.24 µl	10 mM
GR8-M3	GRRRRRRRRGSGGGSTSRDHMVLHEYVNAAGIT	3723.19 g/mol	1.0 mg	26.85 µl	10 mM
GGR8-M3	GRRRRRRRRGSGGGSTSRDHMVLHEYVNAAGIT	3780.25 g/mol	1.0 mg	26.45 µl	10 mM
Rhodamine-R8-M3	Rh-RRRRRRRRGSGGGSTSRDHMVLHEYVNAAGIT	4136.64 g/mol	1.1 mg	26.59 µl	10 mM

2.3   Tissue culture methods and cell preparation for microscopy

2.3.1   Cell culture

The human cervical cell line HeLa was obtained from the American Type Culture Collection (ATCC) and had been Mycoplasma tested. Cells were cultured at 5% CO_2 and 37°C in a humidified incubator. Their growth was monitored every day using brightfield microscopy. Cells were grown in a cell culture petri dish with 55 cm^2 growth area.

2.3.1.1 Media

Cells were maintained in Minimal Essential Medium (MEM) containing GlutaMAX(TM) (Thermofisher) which was additionally supplemented with 10% Foetal Bovine Serum (FBS) (Thermofisher), 1X Non Essential Amino Acids (NEAA) and 1 mM Sodium Pyruvate to be used as complete medium. Cells were grown in absence of antibiotics. When serum free conditions were required for experiments MEM containing GlutaMAX(TM) was supplemented with 1X Non Essential Amino Acids (NEAA) and 1 mM Sodium Pyruvate only. For generation of stable cell lines, selection media containing 400 mg/ml G418 (Geneticin®) was used. Table 2-2 displays an overview of the types of media used in this study.

Table 2-2: Media composition.

Name of Medium	Medium	Supplements
Complete Medium	Mem, GlutaMAX (TM)	10% FBS 1X NEAA 1 mM Sodium Pyruvate
Serum free Medium	Mem, GlutaMAX (TM)	1X NEAA 1 mM Sodium Pyruvate
Selection Medium	Mem, GlutaMAX (TM)	10% FBS 1X NEAA 1 mM Sodium Pyruvate 400 mg/mL G418

2.3.1.2 Routine Cell culture

Cells were passaged every 3-4 days when cells had reached 75% confluency. All solutions were pre-warmed to 37°C in a water bath and passaging was performed in a sterile cell culture hood which was disinfected with 70% Industrial Methylated Spirit (IMS) prior to and following use. For passaging, cells were washed once with Phosphate Buffered Saline (PBS) (Thermofisher) and incubated with 1 mL 0.25% Trypsin/EDTA (Thermofisher) for 5 min at 37°C. Detachment of cells was confirmed using a brightfield microscope. The detached cells were resuspended using 9 mL of culture Media and transferred into a 15 mL falcon tube. Cell suspension was centrifuged at 250x g for 4 min and supernatant discarded. The remaining pellet was resuspended in 10 mL of fresh cell culture media. Cell number per mL was determined using a Hemacytometer and 0.37 x 104 cells per cm^2 were plated into a new cell culture dish. Cells were passaged to a maximum passage number of 30.

Number of Cells per ml was determined using the following equation:

* Vol. of square = W x H x D = 1 mm x 1mm x 0.1 mm = 0.1 mm^3 = 0.0001 mL

The volume of cell suspension required for seeding cells was determined using the following equation:

2.3.2 DNA transfection of cells

DNA transfection was performed using Fugene6 (Promega). This method describes volumes and quantities for transfections per well of a 6-well plate (Corning) or a single MatTek dish with 35 mm^2 growth area (Mattek Corporation). For the transfection mix 3 µl of Fugene6 was added to of 100 µl Optimem (Thermofisher), mixed and incubated for 5 min at room temperature. Then 1000 ng of DNA was added, mixed and incubated for 25 min. After incubation, 94 µl of transfection mix was pipetted into the cell culture media of the cells. When co-expression experiments were performed in which multiple DNA types were co-transfected, a total amount of 1000 ng DNA consisting of equal amounts of the different types of DNA was added. For Mock transfections, no DNA was added to the transfection mix. The transfection mix was incubated with the cells in 2 mL complete media overnight (~16 h) at 37˚C.

2.3.2.1 DNA constructs for DNA transfection

Plasmids used in DNA transfections are listed in Table 2-3.

2.3.3 Paraformaldehyde (PFA) fixation and triton-X100 permeabilisation of cells

Prior to fixation of cells, 4%PFA/PBS (Affymetrix) was warmed to 37˚C. For fixation, cell culture media of cells was removed and replaced with 4% PFA/PBS for 20 min. Fixed wells were incubated with 30mM Glycine/PBS for 5 min to quench the active groups of PFA and washed once in PBS. If permeabilisation was required, PBS was removed and the plasma membrane was pemeabilised with 0.1% Triton-X-100/PBS for 4 min and washed once with PBS.

Table 2-3 Plasmids for DNA transfection.

Name	Background Vector	Expression of	Source
pEGFP-C1	pEGFP-C1	EGFP	Watson lab
pGRASP65-GFP1-10-N2	pEGFP-N2	GRASP65-GFP1-10	Generated (see 2.11.1)
pGFP1-10-N1	pEGFP-N1	GFP1-10	Generated (see 2.11.2)
pET3A-H6-Xa-R8-M3	pET3a	H6-Xa-R8-M3	Generated (see 2.11.3)
pH6-Xa-R8-M3-N2	pEGFP-N2	H6-Xa-R8-M3	Generated (see 2.11.4)
pcDNA3.1-mCherry-H6-Xa-R8-M3	pcDNA3.1	mCherry-H6-Xa-R8-M3	Generated (see 2.11.5)
pcDNA3.1-mCherry-GFP1-10	pcDNA3.1	mCherry-GFP1-10	Generated (see 2.11.6)
pcDNA3.1-mCherry-GFP	pcDNA3.1	mCherry-GFP	Generated (see 2.11.7)
pGRASP65-GFP-N2	pEGFP-N2	GRASP65-GFP	Kind gift from Lane J.D. et al., 2002
pCav1-GFP1-10(h)-N1	pEGFP-N1	Caveolin1-GFP1-10	Kind gift from Pinaud F. et al., 2011
pcDNA3.1-mCherry	pcDNA3.1	mCherry	Kind gift from Reddington S.C. et al., 2015

2.3.4 Widefield fluorescence Microscopy

Fluorescence microscopy was carried out using an inverted Olympus IX73 widefield fluorescent microscope. Images were collected with an Orca flash 4.0 camera (Hamamatsu) using HCImaging software and a Prior Lumen200Pro light source. Fluorescence emission was separated by a multiband dichroic emission filter set #69002 (Chroma). For live cell imaging, cells were kept at 37˚C and 5% CO_2 throughout the imaging process. Microscopy and settings were kept consistent within each experiment. Excitation and emission filter settings as well as type of objectives are listed in Table 2-4 and Table 2-5 below.

Table 2-4 Excitation and emission filter settings.

Filter	λ Excitation [nm]	λ Emission[nm]
DAPI	350/50	455/50
GFP	490/20	525/36
Alexa568/mCherry	555/25	605/52
Alexa647	645/30	705/72

Table 2-5 Objectives used in this study.

Objective	Magnification	Air/Oil	Numerical aperture
UPlanSApo	100x	Oil	1.4
UPlanSApo	40x	Air	0.95
UPlanSApo	20x	Air	0.75
UPlanFL N	10x	Air	0.3

2.3.4.1 Image processing

Images were processed using ImageJ adjusting the brightness and contrast settings and applying a scale bar on images. Merged images were separated to obtain single images representing the green, red and blue channel. Brightness and contrast settings were kept consistent between images derived from the same experiment.

2.4 Investigation of GFP1-10 expression and testing of the complementation of GFP1-10 with M3

2.4.1 Immunofluorescent staining to detect GFP1-10 expression

For immunofluorescent staining, 1.0×10^5 cells were seeded in 6 well plates (Corning) and grown on No. 1.5 coverslips, 25 mm in diameter (VWR) in complete medium (Table 2-2). When DNA transfection was needed cells were transfected with a DNA construct coding for GFP1-10/mCherry-GFP1-10/GRASP65-GFP1-10 (Table 2-3) one day after seeding as described previously (2.3.2). Cell lines stably expressing GFP1-10 or mCherry-GFP1-10 were left untreated. The next day cell were PFA fixed and Triton-X-100 permeabilised (2.3.3). For immunofluorescent staining, cells were blocked for non-specific anti body binding in 3% BSA/PBS (Sigma) for 30 min. Then cells were incubated with an anti-GFP antibody (Vector Laboratories) in 3% BSA/PBS (1:500) for 1h, followed by three washes in PBS for 5 min each. Next, cells were stained with secondary anti-goat-647 antibody (Invitrogen) in 3% BSA/PBS (1:300) for 1h and washed twice with PBS for 5 min each. For secondary antibody controls, cells were only stained with the secondary anti-goat-647 antibody in 3% BSA/PBS (1:300) for 1h after cells were blocked in 3% BSA/PBS for 30 min. Finally the nucleus was stained with DAPI/PBS (1:10,000) for 5 min, washed in PBS and mounted on glass slides using 15 ul Mowiol (Appendix 9.1). Antibodies are listed in Table 2-6. All steps were carried out at room temperature. Antibody staining was investigated using microscopy (2.3.4).

Table 2-6 Antibodies used for Immunofluorescence

Antibody	Target	Supplier	Derived from	Concentration	Dilution
Primary	Anti-GFP/GFP1-10	Vectorlabs (SP0702)	Goat	1 mg/mL	1:500
	Anti-GFP	Roche (11814460001)	Mouse	0.4 mg/ml	1:500
Secondary	Anti-Goat-Alexa 647	Life Technoligies (#A-21447)	Donkey	0.66 mg/mL	1:300
	Anti-mouse-Alexa488	Invitrogen (#A-11001)	Donkey	1 mg/mL	1:500

Quantification of Antibody stain

Microscopy images of antibody staining were analysed with ImageJ. Single cells were encircled at their cell membrane using the brightfield image. The integrated density (Area of the cell * mean fluorescence within that area) of red fluorescence representing total protein levels of the antibody stain was measured within this area using the image obtained in the Alexa647 channel. On the same image, two measurements were taken of the background without cells. The mean fluorescence was measured and the average of two mean fluorescence measurements represented the red fluorescence of the average background. The corrected total cell fluorescence (CTCF) was calculated with the following formula:

CTCF= Integrated density - (Area of the cell * Average background)

2.4.2   Western Blot analysis of GFP and GFP1-10 expression

For Western Blot analysis 1x105 cells were seeded two days before the experiment. The next day cells were transiently transfected with plasmids coding for EGFP or GFP1-10 expression (2.3.2). On the day of the experiment cells were washed with ice cold PBS once, then cells were lysed using ice cold non-denaturing lysis buffer (Appenidx, 9.1). Cells were scraped off the dish and the suspension was transferred into an Eppendorf tube and kept at 4˚C for 30 min. Cell suspension was

pelleted using a microcentrifuge and the supernatant was placed into a new tube and placed on ice for further analysis. For western blot analysis of cell lysates, a 4-12% Bis-Tris Gel (Invitrogen) with 1x MOPS running Buffer (Invitrogen) was used. Samples were prepared following the Bis-Tris Mini Gels Electrophoreses Protocol for reduced samples. Gel was run at 200V for 70 minutes. Proteins were transferred on a membrane using 1x NuPage Transfer Buffer (Invitrogen) supplemented with 20% Methanol at 30V for 1h. For antibody detection, membrane was blocked in 5% Marvel in PBS/0.05% Tween20 for 1 hour. Membrane was incubated with 1ug/mL anti-GFP (Vectorlabs) in 5% Marvel in PBS/0.05% Tween20 at room temperature overnight. The next day membrane was washed with PBS/0.05% Tween20 for 3 times for 5 minutes before the secondary (anti goat-HRP) was incubated in 5% milk in PBS/0.05% Tween20 for 1 hour at room temperature and washed with PBS/0.05% Tween20 for 3 times for 5 minutes. Antibodies are listed in Table 2-7. Membrane was incubated with Enhanced Chemiluminescent Substrate (Invitrogen) for 5 minutes. Luminescence was detected using the ChemiDoc (BioRad) detection system.

Table 2-7 Antibodies used for Western Blotting

Antibody	Target	Supplier	Derived from	Concentration	Dilution
Primary	Anti-GFP/GFP1-10	Vectorlabs (SP0702)	Goat	1 mg/mL	1:1000
Secondary	Anti-Goat-HRP	Invitrogen (A10547)	Rabbit	1 mg/mL	1:2000

2.4.3   GFP complementation using co-transfection

2.4.3.1 Investigation of GFP complementation using microscopy

To investigate GFP complementation using co-transfection 1×10^5 cells were seeded in 6 well plates on 25 mm coverslips in complete medium and left to adhere overnight. The next day cells were transfected with indicated DNA constructs using Fugene6 (2.3.2) and incubated overnight. The next day cells were fixed using PFA (2.3.3). Nuclei were stained with DAPI/PBS (1:10,000) for 5 min and washed in PBS once. Coverslips were mounted on glass slides using Mowiol and analysed by microscopy (2.3.4).

2.4.3.2 Investigation of GFP complementation using a microplate reader

To investigate GFP complementation using a microplate reader, 1×10^5 cells were seeded in 6 well plates in complete medium and left to adhere overnight. The next day cells were transfected with indicated DNA constructs using Fugene6 (2.3.2). On the day of the experiment, transfected cells were detached using 250 µl 0.25% Trypsin/EDTA per well of a 6 well plate. Cells were left to detach for 4min at 37˚C. Detached cells were resuspended in 750 µl PBS and transferred into eppendorf tubes. Cells were pelleted at 250xg for 4 min. The supernatant was discarded and the cell pellet was washed in PBS and pelleted at 250x g for 4 min. The washing step was performed twice and the pellet containing transfected cells was resuspended in a final volume of 350 µl PBS. The cells in suspension were plated in triplicates (100 µl each, containing ~ 100,000 cells) into a clear bottom, black walled 96 well plate (Greiner) and immediately analysed on a microplate reader.

Settings and analysis on the microplate reader

Green fluorescence was detected using the microplate reader FLUOstar OPTIMA (BMG Labtech). The reader was set to measure fluorescent intensity. The

dimensions of the plate to be measured were set to Greiner 655096 Uclear96. The lid of the 96 well plate was removed before measurements and the sample was excited from the top and emitted fluorescence was detected from the top. Excitation and emission filters for GFP detection were set as 485 nm and 520 nm, respectively. The gain was adjusted to reach 88% for the co-transfection positive control and kept constant between experiments. The well scanning mode was set as orbital measurements.

Data processing

In order to display green fluorescence in a graph, all fluorescent values obtained from the plate reader were background subtracted. Values obtained from mock transfected cells, served as background readings. Readings are displayed in relative fluorescent units (RFU).

2.4.4 GFP complementation with a synthetic peptide

2.4.4.1 Microscopy approach: 'Fix and stain'

To test complementation of expressed GFP1-10 with the M3 peptides (Table 2-1), 1×10^5 cells were seeded on 25 mm coverslips two days prior the experiment and left to adhere overnight in complete media. Cells were transfected with DNA constructs coding for GFP1-10 or GRASP65-GFP1-10 one day after seeding as described previously (2.3.2). On the day of the experiment cells were PFA fixed and permeabilised (2.3.3). Cells with permeabilised plasma membrane were then incubated with 20 µm of M3 containing peptide in PBS for 1h at room temperature. Cells were washed once in PBS. Finally the nucleus was stained with DAPI/PBS (1:10,000) for 5 min, washed in PBS and mounted on glass slides using 15 µL Mowiol. GFP complementation was analysed by microscopy (2.3.4).

2.4.4.2 Improved *in vitro* GFP complementation using cell lysate and detection with a microplate reader

To investigate reassembly of GFP1-10 and M3 peptides *in vitro*, M3 containing peptides were diluted in 30 µl PBS to a concentration of 80 µM or 20 µM. Stable cells or transiently transfected cells expressing GFP1-10 or mCherry-GFP1-10 were grown in 10 cm dishes until they had reached 80% confluency. For the experiment cells of two 10 cm dishes were detached using 0.25% Trypsin/EDTA and incubated for 4 min at 37˚C. Cells were resuspended in PBS and pooled in a 15 mL falcon tube. The cell suspension was centrifuged at 250x g for 4 min and supernatant discarded. The remaining pellet was resuspended in 10 mL of fresh PBS. Cell number per mL was determined using a Haemocytometer (2.3.1.2). Then the volume was calculated that was needed to obtain a cell suspension of 26.6×10^5 cells per mL. The cells in solution were pelleted at 250x g for 4 min and the cell pellet was resuspended in the calculated volume of 0.1% Triton-X-100/PBS. Cells were left to lyse for 4 min at RT.

To test GFP complementation *in vitro*, 30 µl of 80 µM /20 µM M3 containing peptides were mixed with 30 µl of cell lysate containing ~ 0.8×10^5 cells to obtain a final concentration of 40 µM /10 µM M3 containing peptides respectively. The mixture was transferred into a clear bottom, black walled 96 well plate (Greiner) and GFP fluorescence was monitored using a microplate reader. GFP fluorescence was detected after 5 min and then every hour. The plate was kept under constant agitation at the indicated temperature (4˚C or room temperature). The gain was set to 2750 unless indicated otherwise. All other settings of the microplate reader were kept as previously described (2.4.3.2).

Data processing

In order to display green fluorescence in a graph, all fluorescent values obtained from the plate reader were background subtracted. Values obtained from DMSO treated cells served as background readings. Readings are displayed in relative fluorescent units (RFU).

2.5 Live uptake assay for GFP complementation by M3 delivery

2.5.1 Microscopic analysis of M3 delivery into cells

For the live GFP complementation assay using transient transfected cells, $1x\ 10^5$ cells were seeded on 35 mm MatTek dishes (Mattek Corporation) with a 10 mm glass bottom two days prior to the experiment and left to adhere overnight. Cells were transfected to express GFP1-10 or mCherry-GFP1-10 on the next day using Fugene6 (2.3.2). For the live GFP complementation assay using stable cell lines, $1.8x\ 10^5$ cells were seeded on 35 mm MatTek dishes (MatTek Corporation) with a 10 mm glass bottom one day prior the experiment and left to adhere overnight. On the day of the experiment M3 containing peptides were diluted in serum free media (see Table 2-2) to the indicated concentration (10-40 µM). Cells were washed with prewarmed serum free media once. Serum free media was aspirated off and central glass bottom ring of cells was incubated with 100 µl of peptides in serum free media for 2 hours at 5% $CO2$ and 37˚C in a humidified incubator. Cells were washed with phenol red free RPMI once and incubated with Hoechst (1:2000) in RPMI for 5 minutes at 37°C, washed twice in RPMI and left in RPMI for imaging.

Imaging was performed on a widefield fluorescent microscope. GFP complementation was imaged using the following settings: 100x Oil objective, 2x binning, 500ms exposure time on GFP excitation and emission filter settings (see 2.3.4).

Quantification

When microscopy images were quantified, imaged were acquired randomly. Images were analysed using ImageJ. Single cells were encircled at their cell membrane using the brightfield image. The integrated density of green fluorescence representing total protein levels of complemented GFP was measured within this area using the image from the GFP channel. Then the mean fluorescence of two background measurements were taken on the same image where no cells were present. The average of those two measurements represented the average background fluorescence. The corrected total cell fluorescence (CTCF) was calculated with the following formula:

CTCF= Integrated density - (Area of the cell * Average background)

When uptake of Rhodamine labelled R8-M3 peptide was measured, the CTCF of the red channel was calculated from the same images where GFP complementation was assessed.

2.5.2 Flow cytometry analysis

2.5.2.1 Detection of morphologically intact cells and cell characterisation

In order to define FSC and SSC gating for morphologically intact cells, Hela cells, SCL1 cells and mCherry-SCL1 cells were grown in 10 cm dishes to 75% confluency and detached from the dish using 1 mL prewarmed 0.25% Trypsin/EDTA for 4 min at 5% CO_2 and 37˚C in a humidified incubator. To prepare cells for flow cytometry measurement, cells were resuspended in 9 mL ice cold PBS and transferred into an Eppendorf tube. Cells were pelleted at 300x g for 4 min, washed once in 5 mL PBS and pelleted again at 300x g for 4 min. To investigate the viability of these cells, cells were mixed with LIVE/DEAD™ Violet Stain (Invitrogen L34963) according to the manufacturer's protocol and incubated on ice for 30min. Cells were washed once in PBS and final cell pellet was resuspended in 500 µl PBS. Flow cytometry

measurement of FSC, SSC and cell viability was performed using FACSCanto II (BD Biosciences). Cells were mixed by flicking the tube before the measurement. To detect viable cells, samples were excited with 405 nm wavelength and emitted fluorescence was collected using the Pacific Blue filter (425 - 475 nm). Green and red fluorescence of untreated cells were measured using the 488nm excitation laser and FITC (515-545 nm wavelength) and PerCP-Cy5-5 (670 – 753 nm) emission filters, respectively. Fluorescence of a total of 50,000 per sample. Samples were measured in duplicates. Voltage settings were the following: FSC-A: 100 V; SSC-A 320 V; pacific blue 200 V; FITC: 400 V

Data processing

Data was analysed using the FlowJo software (V10) gating of cells was performed using FSC-A and SSC-A measurements. Single cells were gated using according to FSC-A and FSC-H measurements. Within the single cell population, fluorescence of GFP, mCherry and LIVE/DEAD™ Violet Stain was determined and shown as a histogram. FSC and SSC gating for morphologically intact cells was set where cells were negative for LIVE/DEAD™ Violet Stain fluorescence.

2.5.2.2 Flow cytometry analysis of M3 delivery into cells

For Flow cytometry analysis of M3 delivery into cells, 0.7x 10^5 SCL1 or mCherry-SCL51 cells were seeded into each well of a 12 well plate (Corning) and left to adhere for 48 hours. On the day of the experiment M3 containing peptides were diluted in serum free media (see Table 2-2) to the indicated concentration (10-40 µM). Cells were washed with prewarmed serum free media once and incubated in 300 µl prewarmed peptide solution in serum free media for 2 hours at 5% CO2 and 37˚C in a humidified incubator. After the incubation time the peptide solution was aspirated off and cells were washed twice with ice cold 0.5 mg/mL Heparin/PBS to remove

bound R8 containing peptides from the plasma membrane. Cells were washed once with PBS at room temperature and detached from the dish using 250 µl prewarmed 0.25% Trypsin/EDTA that was incubated with the cells for 4 min at 5% CO2 and 37˚C in a humidified incubator. The cell suspension was resuspended in 750 µl ice cold PBS and transferred into an Eppendorf tube. Cells were pelleted at 300x g for 4 min, washed once in 1000 µl PBS and pelleted again at 300x g for 4 min. Cells were resuspended in 500 µl PBS and transferred into round-bottom polystyrene tubes (Corning) for flow cytometry analysis and kept on ice.

Flow cytometry measurement of GFP complementation was performed using a BD FACSCanto II. Cells were mixed by flicking the tube before the measurement. Samples were excited with 488 nm wavelength and emitted fluorescence was collected using the FITC filter (515-545 nm wavelength). When mCherry-SCL51 was measured on the flow cytometer, red fluorescence was collected in addition to the FITC signal using the PerCP-Cy5-5 emission filter (670 – 753 nm). Green fluorescence of a total of 20,000 cells (SCL1) or 10,000 cells (mCherry-SCL51) was measured. Voltage settings were the following: FSC: 100 V; SSC 320 V; FITC 400 V; PerCP-Cy5-5 500 V.

Data processing

Data was analysed using the FlowJo software (V10) gating of morphologically intact cells was performed using FSC-A and SSC-A measurements. Single cells were gated using FSC-A and FSC-H measurements. The geometric mean of GFP fluorescence was determined within the single cell population. When fold change of GFP fluorescence is shown, geometric mean of the DMSO control was set to a value of 1 and all samples were normalised to the DMSO control. Percentage of GFP positive cells was determined using the population comparison tool in the FlowJo software using the Overton % Positive algorithm.

2.6 Spectral detection of green fluorescence of GFP1-10

Spectral detection of green fluorescence was performed using a Zeiss LSM 880 confocal microscope. $1.0x10^5$ HeLa cells and SCL1 cells were grown on No. 1.5 coverslips, 25 mm in diameter (VWR) in complete medium (Table 2-2) two days before the experiment. HeLa cells were transfected with DNA coding for EGFP, GFP1-10 expression or Mock transfected (2.3.2). SCL1 cells were left untreated. On the day of the experiment, coverslips were transferred into an imaging chamber and the fluorescent signal of HeLa cells transfected with EGFP, GFP1-10 or mock transfected cells as well as green fluorescence of untreated SCL1 cells was analysed. The green fluorescent signal of a chosen region of interest was analysed regarding its emission spectrum. The emitted fluorescent signal was collected on 22 detectors dividing the fluorescent signal between 495 nm 682 nm wavelength light with a collection range of 8-9 nm wavelength light for a single detector. Values were then plotted in Excel to obtain the full emission spectrum of each sample.

2.7 Confocal analysis of localisation of complemented GFP

For the analysis of the localisation of complemented GFP, $1.0X 10^5$ HeLa cells were seeded on 35 mm MatTek dishes (MatTek Corporation) with a 10 mm glass bottom two days prior to the experiment and left to adhere overnight. HeLa cells were transfected the next day with with DNA coding for GFP1-10 expression (2.3.2). On the day of the experiment M3 containing peptides were diluted in serum free media (see Table 2-2) to 40 µM. Cells were washed with prewarmed serum free media once. Serum free media was aspirated off and the central glass bottom ring of cells was incubated with 100 µl of peptides in serum free media for 2 hours at 5% CO_2 and 37˚C in a humidified incubator. Cells were washed with phenol red free RPMI once and incubated with Hoechst (1:2000) in RPMI for 5 minutes at 37°C, washed twice in RPMI and left in RPMI for imaging. Confocal analysis of complemented GFP was

performed using the Leica TCS SP2 AOBS confocal system using the inverted (Leica DMIRE2) microscope and the HCX PL APO 63x oil objective.

2.8 Generation of stable cell lines

2.8.1 Determination of the concentration of selection antibiotics

Before generating the stable cell line, the concentration for Geneticin (G418) (Invitrogen) selection was detected on untransfected HeLa cells. The optimal dose for antibiotic selection was defined when 90% cell death occurred after 7 days and corresponded to 400 µg/mL G418.

2.8.2 Generation of stable cell lines

To generate the stable cell lines SCL1 and mCherry-SCL51, HeLa cells were transfected with the DNA coding for GFP1-10 or mCherry-GFP1-10 and the Neomycine gene using Fugene6. Transfection was carried out when cells were ~60% confluent in a 10 cm cell culture dish (55 cm^2 growth area). The transfection mix consisted of 700 µl Optimem, 21 µl Fugene6 and 7000 ng DNA. Cells were maintained in complete media for 48 h to allow expression of the Neomycine gene for G418 resistance. Cell were then passaged (see 2.3.1.2) and divided into new dishes in the different dilutions 1:2, 1:5, 1:10, 1:20 and 1:40 containing selection media supplemented with 400 mg/ml G418. The media was changed regularly for 14 days. After 14 days the dish containing the highest number of clearly separated cell colonies was chosen for limiting dilution. To perform limiting dilution, cells were seeded into 96 well plates at a concentration of 0.5 cells/well or 2 cells/well to increase the chances of the cell colonies growing up from a single cell clone to obtain a monoclonal cell line. Selection media was regularly changed until cells had grown to confluence.

2.8.2.1 Selection of a colony expressing GFP1-10: SCL1

When cells had grown to confluency in a 96 well plate, cells were replica plated to maintain growth of the colonies and cells were additionally plated into a screening plate. This plate was used to screen colonies for expression levels of GFP1-10 by immunohistochemistry (2.4.1). Selection criteria to reduce number of colonies to the most promising clones were even antibody staining across the cell population. Most promising colonies were then tested for GFP complementation using co-transfection of DNA coding for M3 (0) and reassembly with M3 peptides (2.4.4.1). The colony expressing highest and even levels of GFP1-10 that was able to complement using co-transfection and reassembled with M3 peptides was chosen as the most promising colony and was named Split Cell Line 1 (SCL1). After selection of SCL1, cells were cultured in selection media for another 4 weeks until cultured in non-selective media. Expression of GFP1-10 was confirmed again when cells were cultured in complete media using immunohistochemistry (2.4.1).

2.8.2.2 Generation of stable cell line expressing mCherry-GFP1-10: mCherry-SCL51

When cells had grown to confluency in a 96 well plate, cells were replica plated to maintain growth of the colonies and cells were additionally plated into a screening plate. The screening plate was then imaged on a widefield fluorescent microscope (2.3.4) to investigate mCherry fluorescence in live cells. Selection criteria to reduce number of colonies to the most promising clones were even expression of mCherry across the cell population. Most promising colonies were then tested for GFP1-10 expression using immunofluorescence (2.4.1). When GFP1-10 expression was confirmed in these colonies, GFP complementation using co-transfection of DNA coding for M3 (0) and reassembly with M3 peptides (2.4.4.1). In the first round of limiting dilution it was not possible to obtain a monoclonal stable cell line. Hence another round of limiting dilution and screening as described above was performed.

The cell line that was obtained was named mCherry-SCL51 and was the cell line with the highest amount of mCherry-GFP1-10 expression cells. However, it is also a polyclonal cell line.

2.8.3 Freezing stable cell lines

For long-term storage, 75% confluent stable cells lines were detached from the cell culture dish and pelleted following the protocol for routine cell culture (2.3.1.2). Pellet containing ~1 x 10^6 cells was resuspended in 1mL freezing mix containing 50% complete media, 40% FBS and 10% DMSO and transferred into a cryovial. Cells were frozen in a temperature controlled freezing container to -80˚C and transferred to liquid nitrogen for long-term storage.

2.9 Statistical analysis

Statistical analysis was performed using R Statistical Software. Statistical examination of two populations was first performed by testing for normality of the data. This was performed by investigating the distribution of the data in a histogram as well as performing a Shaipiro-Wilk-Test. If $p < 0.05$, the data was not normally distributed and data was further tested for significant difference using a Mann–Whitney-U-Test for nonparametric data.

When multiple conditions were compared, data was tested using a One-Way-Annova. If residuals were normally distributed multiple condition were compared using a Turkey honest significant difference (HSD) test. If residuals were not normally distributed, data was tested using a Kruskal-Wallis test for nonparametric data and a Benjamini Hochberg test for multiple comparison. Significance levels are indicated the following *: $p < 0.05$, **: $p < 0.01$, ***: $p < 0.001$, n.s.: not significant.

2.10 Molecular biological techniques

2.10.1 Restriction digest

For DNA restriction digests the appropriate restriction enzymes were used and their according buffers to ensure optimal performance. Components were defrosted on ice. The volumes for the restriction digest were the following:

Component	Volume
DNA	1-5 µg
10X NEBuffer	5µl
Restriction Enzyme	10 Units per µg of DNA
Nuclease free water	to 50 µl
	50 µl

The restriction digest was mixed by pipetting up and down incubated at 37˚C for 1 h. The restriction digest was analysed using agarose gel electrophoresis (2.10.6) or cleared from restriction enzymes using QiaexII Gel extraction kit (2.10.7). When a test digest was performed, a total volume of 20 µl was used and volumes of reagents were adjusted accordingly.

2.10.2 Ligation using T4 DNA Ligase

When a traditional cloning technique was used, DNA fragments were ligated following the T4 DNA ligase protocol. Components were defrosted at room temperature. The volumes for the ligation were the following:

Component	Volume
10X T4 Ligase Buffer	2 µl
Vector DNA	x µl (50 ng)
Insert DNA*	x µ (x ng)
Nuclease free water	to 20 µl
T4 ligase	1 µl
	20 µl

* The amount of insert that was added to the ligation mix was in a molar ratio of 1:3 (Vector:Insert) and calculated using the following formula:

The ligation mix was mixed by pipetting up and down incubated at room temperature for 1 h. 1-5 µl were added to the transformation mix of Top10 chemically competent cells.

2.10.3 Ligation using Seamless cloning technique

New constructs were obtained following the GeneArt® Seamless Cloning and Assembly protocol. This technique relies on homologues recombination of DNA. In order to utilize this technique, Genestrings were designed, containing the genes of interest. These genestrings contained homologue regions to their linearised receiving vector at their N- and C-terminus (15 bp each). All genestrings that were utilised within this work were generated within the Master's Thesis: Riester P., Characterising the cellular uptake and targeting of novel drug delivery systems, 2014, Department of Biology, Universitaet Konstanz. Cloning of constructs was performed within this PhD thesis.

2.10.4 Transformation of bacteria

E.Coli were transformed using the heat shock method. The *E.Coli* strands that were used are listed below.

Table 2-8 *E.Coli* strands

Type of *E.Coli*	Used for
Top10 chemically competent cells	Cloning experiments
XL1-Blue	DNA expansion
DAM-	DNA expansion with non methylated XBAI and XMAI sites

For transformations, bacteria were defrosted on ice for 30 min and 50-400 ng of DNA was added to the tube and mixed. DNA was incubated with the bacteria on ice for 30 min. Then bacteria were heat-shocked for 45 seconds at 42°C followed by an incubation on ice for 2 minutes. 250 μl of SOC media (Invitrogen) was added and bacteria were incubated shaking at for one hour at 37°C to allow expression of the antibiotic resistance. Then 80 μl were plated out on LB-Agar plates containing the appropriate antibiotics and incubated at 37°C overnight.

2.10.5 Polymerase Chain reaction (PCR)

PCR was used to screen bacterial colonies or to amplify DNA sequences for cloning. PCR primers used in this study can be found in Table 2-9. Primers were obtained from eurofins genomics and diluted in nuclease free water to a final concentration of 100 pmol/ μl.

Table 2-9 List of primers

Primer Name	Sequence 5' -> 3'	Tmelt [°C]
CMV forward	CGCAAATGGGCGGTAGGCGTG	65.7
EGFPC1 reverse	CATTTTATGTTTCAGGTTCAGGG	57.1
T7 forward	TAATACGACTCACTATAGGG	53.2
T7 reverse	CTAGTTATTGCTCAGCGGT	54.5
pcDNA3.1 forward	GGCTAACTAGAGAACCCACTG	59.8
pcDNA3.1 reverse	GGCAACTAGAAGGCACAGTC	59.4
GFP1-10 forward	CAGTGGCGGCCGCTCGAGGTCAGATCCGCTAGCGC	>75
GFP1-10 reverse	AACCGCGGGCCCTCTAGATTATGTTCCTTTTTCAT	69.5
GFP forward	CAGTGGCGGCCGCTCGAGCAGTCGACGGTACCGCG	>75
GFP reverse	AACCGCGGGCCCTCTAGAGTCGCGGCCGCTTTACT	>75

2.10.5.1   PCR for screening bacterial colonies

In order to investigate if bacterial colonies had amplified DNA containing the correct insert resulting from molecular cloning, PCR was used to screen for positive colonies. Single colonies were picked from the LB agar plate and diluted in 100 μl nuclease free water and mixed well. To screen bacterial colonies, *Taq* Polymerase was used. Per PCR a PCR mix of a total volume of 10 μl was prepared. An example is shown below when PCR mix was prepared to screen 10 colonies. The template

DNA was added individually for every PCR by adding 1 µl of the bacterial colony mix in nuclease free water to 9 µl of PCR mix.

Component	100 µl	Final concentration
10X Standard Taq Reaction Buffer	10 µl	1x
10 mM dNTPs	2 µl	200 µM
10 µM Forward Primer	2 µl	0.2 µM
10 µM Reverse Primer	2 µl	0.2 µM
Taq DNA Polymerase	0.25 µl	1.25 U/50 µl PCR
Template DNA	1 µl	-
Nuclease-free Water	to 100 µl	
	100 µl	

The thermocycling conditions were the following:

Step	Temperature	Time	
Initial denaturation	95 °C	4 min	
Denaturation	95 °C	40 sec	
Annealing	45 -68 °C	40 sec	30 cycles
Elongation	68 °C	1 min per kb	
Final extension	68 °C	5 min	
Hold	4°C	∞	

The Annealing temperature was adjusted depending on the melting temperature (Tm) of the used primers. A list of primers used in this study can be found in Table 2-9. PCR products were visualised using Gel electrophoresis (2.10.6).

2.10.5.2   PCR to generate gene constructs for cloning

In order to amplify DNA sequences used for cloning, Phusion DNA polymerase was chosen exhibiting a proof reading function. Per sample a 50 µl reaction volume was used. An example for a 50 µl PCR mix is shown below.

Component	50 µl	Final concentration
5X Phusion HF buffer	10 µl	1x
10 mM dNTPs	1 µl	200 µM
10 µM Forward Primer	2.5 µl	0.5 µM
10 µM Reverse Primer	2.5 µl	0.5 µM
Phusion DNA Polymerase	0.5 µl	1.0 U/50 µl PCR
Template DNA	variable	~ 20ng
Nuclease-free Water	to 50 µl	
	50 µl	

The thermocycling conditions were the following:

Step	Temperature	Time	
Initial denaturation	98 °C	30 sec	
Denaturation	98 °C	10 sec	
Annealing	45 - 72 °C	30 sec	30 cycles
Elongation	72 °C	30 sec per kb	
Final extension	72 °C	5 min	
Hold	4°C	∞	

The Annealing temperature was adjusted depending on the melting temperature (Tm) of the used primers. PCR products were visualised using Gel electrophoresis (2.10.6) and DNA was purified using Gel extraction (2.10.7).

2.10.6 Agarose gel electrophoreses

DNA fragments from restriction digests and PCR products were separated and analysed by Gel electrophoresis. Therefore a 1.5 % Agarose gel was prepared by boiling Agarose in Tris-acetate- EDTA buffer (TAE-buffer). After cooling down, ethidiumbromide to a final concentration of 0.5 µg/mL was added. The gel was left to polymerise. Once gel was set it was placed in an electrophoresis tank and filled with TAE buffer. DNA samples were loaded using 10x loading buffer (Appendix 9.1). Gel

ran for at 90 V until bands were sufficiently separated and visualized under UV light using a GelDoc UV transilluminator (Bio-Rad).

2.10.7 Gel extraction

Gel extraction of DNA was carried out using a Qiaquick Gel extraction kit (Qiagen). If high yields of extracted DNA were required or restriction digests were purified from restriction enzymes, QiaexII Gel extraction kit (Qiagen) was used. Both gel extractions were performed following the manufacturer's protocol.

2.10.8 Plasmid preparation

A single colony of bacteria was picked and cultured in LB-media containing the appropriate antibiotics overnight shaking at 37°C. For minipreps a 5 mL overnight culture was grown; for a plasmid midiprep a 5 mL day culture was grown and 1 mL was transferred into 50 mL of fresh LB media containing the appropriate antibiotics for an overnight culture. Plasmid DNA was isolated following the manual of PureLink™ Quick Plasmid Miniprep or Midiprep Kit (Invitrogen).

2.10.9 Quantification of DNA

The concentration and purity of DNA obtained from plasmid preparations was determined using a NanoDrop2000 (Thermo Scientific).

2.10.10   Sequencing of DNA constructs

Purified plasmid DNA was submitted for sequencing with appropriate sequencing primers. Sequencing was carried out by Eurofins Genomics.

2.11 Generation of expression plasmids

2.11.1 Generation of pGRASP65-GFP1-10-N2

pGRASP65-GFP1-10-N2 was generated by using the seamless cloning technique (2.10.3) using a genestring carrying the DNA for GFP1-10 expression. This genestring was designed for mammalian expression of GFP1-10. The GFP1-10 sequence used was based on the GFP1-10$_{(h)}$ sequence, optimized for human codon usage (Pinaud and Dahan 2011) but still encoding the 16 mutations that are necessary for split GFP1-10 OPT (Cabantous *et al.* 2005). The genestring (Figure 2-1) was designed to be cloned into the multiple cloning site of pEGFP-N2 (Appendix9.2 Figure 9-1) when this vector was linearised by digest with the restriction enzymes XmaI and XbaI. Therefore, the genestring contained N- and C-terminal homologous regions to linearised pEGFP-N2, XmaI and XbaI restriction sites to restore restriction sites in the resulting plasmid and GFP1-10. This genestring was designed within a previous Master's project (Riester P., Characterising the cellular uptake and targeting of novel drug delivery systems, 2014, Department of Biology, Universitaet Konstanz.)

```
GTGAAGGCCCCTGGCCCGGGATCCACCGGCCGGTCGCCACCATGTCCAAAGGAGAAGAACTGTTTA
CCGGCGTGGTGCCCAATTCTCGTGGAACTGGATGGCGATGTGAATGGCCACAAATTTTCTGTCAGAG
GAGAGGGTGAAGGTGATGCCACAATCGGAAAGCTCACCCTGAAATTCATCTGCACCACTGGAAAGC
TCCCTGTGCCATGGCCAACACTGGTCACTACCCTGACCTACGGCGTGCAGTGCTTTTCCAGATACC
CAGACCATATGAAGAGGCATGACTTTTTCAAGAGCGCCATGCCCGAGGGCTATGTGCAGGAGAGAA
CCATCTCTTTCAAAGATGACGGGAAATACAAGACCCGCGCTGTGGTCAAGTTCGAAGGAGACACAC
TGGTGAATAGAATCGAGTTGAAGGGCACAGACTTTAAGGAAGATGGAAACATTCTCGGCCACAAGC
TGGAATACAACTTTAACTCCCACAATGTGTACATCACAGCCGACAAGCAAAAGAATGGCATCAAGG
CTAACTTCACAGTCAGACACAACGTCGAGGATGGAAGCGTGCAGCTGGCCGACCATTATCAACAGA
ACACTCCAATCGGCGACGGCCCTGTGCTCCTCCCAGACAACCATTACCTGTCCACCCAGACAGTCC
TGAGCAAAGATCCAAATGAAAAAGGAACATAAAGCGGCCGCGACTCTAGATCATAATCAGCCAT
```

Figure 2-1 Genestring for GFP1-10 expression
DNA sequence of genestring coding for GFP1-10 expression is shown. Homologous base pairs to linearised pEGFP-N2 when digested with XmaI and XbaI are underlined. XmaI restriction site (red), XbaI restriction site (blue), GFP1-10 coding region (green) and the start of transcription is marked with an arrow.

To perform cloning, a plasmid encoding GRASP65 in the background vector pEGFP-N2 was received as a kind gift from Dr. John D. Lane (pGRASP65-EGFP-N2) (Lane *et al.* 2002). The plasmid was amplified in a DAM⁻ bacterial strain to prevent methylation of the XbaI site. Full length EGFP was removed by restriction digest of XmaI and XbaI sites. The linearised vector was purified by agarose gel electrophoresis (2.10.6.) followed by gel extraction (2.10.7). In order to insert the DNA encoding for GFP1-10 following the GeneArt® Seamless Cloning and Assembly protocol, a genestring was synthesised with a 15 bp overhang at the N- and C-terminus homologous to the linearized vector (2.11.1). Using the seamless cloning technology the genestring was ligated with the linearised vector via homologous recombination to obtain pGRASP65-GFP1-10-N2 (Figure 2-2). This was achieved following GeneArt® Seamless Cloning and Assembly ligation protocol. The ligation mix was transformed into Top10 chemically competent bacteria (2.10.4) and plated onto LB-Agar plates containing kanamycin. The next day four colonies were grown on the LB-Agar plates. Clones1-4 were picked and DNA was obtained using a PureLink™ Midiprep Kit (see 2.10.8). All clones were test digested with XmaI and BsrGI. The digest products were analysed using gel electrophoresis and visualised using a GelDoc UV transilluminator (Figure 2-3). The expected size for a GFP1-10 insert was 475 bp and 736 bp if the DNA was derived from the original plasmid pGRASP65-EGFP-N2. All clones (1-4) showed a correct sized insert and sent off for sequencing. Sequencing results were correct and clone 1 was selected to be used for GRASP65-GFP1-10 expression.
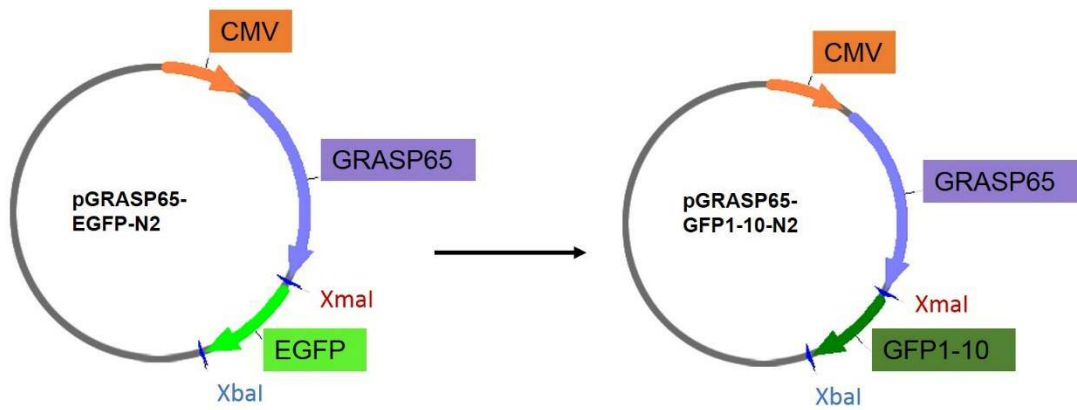
Figure 2-2 Cloning strategy to obtain pGRASP65-GFP1-10-N2
pGRASP65-EGFP-N2 was amplified in a DAM- bacterial strain to prevent methylation of the XbaI site. Full length EGFP was removed by restriction digest of XmaI and XbaI sites. Using the seamless cloning technology a genestring coding for GFP1-10 with homologous sequences to the linearised vector was ligated with the vector to obtain pGRASP65-GFP1-10-N2.
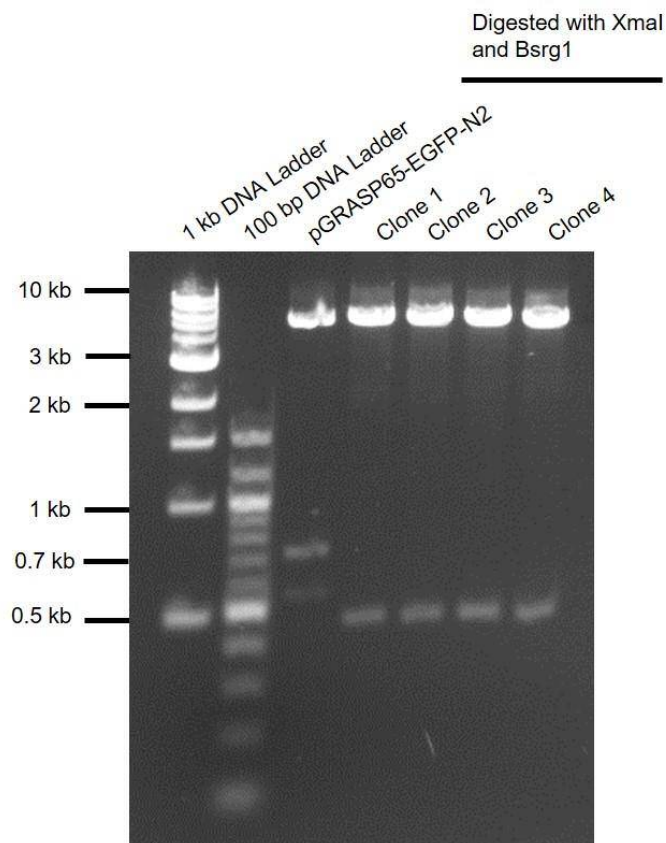
Figure 2-3 Test digest to identify pGRASP65-GFP1-10-N2
All clones as well as the original plasmid pGRASP65-EGFP-N2 were test digested with XmaI and BsrGI. Samples were run on a 1.5% agarose gel in TAE buffer. In addition to the samples, 1kb DNA ladder and 100 bp DNA (NEB) were run on the gel. Expected sizes were 475 bp when GFP1-10 has inserted correctly and 736 bp when EGFP was inserted back into the vector.

2.11.2 Generation of pGFP1-10-N1

The plasmid pCav1-GFP1-10$_{(h)}$-N1 coding for caveolin-GFP1-10 expression was received as a kind gift from F. Pinaud/ M. Dahan (Pinaud and Dahan 2011). Caveolin-1 was removed by double digest with BglII and BamHI. The digest was purified from restriction digest enzymes using QiaexII Gel extraction Kit (see 2.10.2). The digest with BglII and BamHI resulted in compatible cohesive ends that were religated following the T4 DNA ligase protocol (see 2.10.2) in frame to obtain pGFP1-10-N1 (Figure 2-4). The ligation mix was transformed into Top10 chemically competent bacteria (2.10.4) and plated onto LB-Agar plates containing kanamycin. The next day clones were screened using PCR (2.10.5.1) to identify clones where the DNA had religated to pCav1-GFP1-10-N1 and clones that contained the DNA for pGFP1-10-N1. PCR primers that were used were CMV forward and EGFPC1 reverse primer. Annealing temperature was 55°C annealing and elongation time 1min. The PCR products were analysed using gel electrophoresis and visualised using a GelDoc UV transilluminator (Figure 2-5). The expected size for a religated vector with GFP1-10 insert only was ~700 bp. When the vector had religated with the original Caveolin-GFP1-10 DNA, PCR product was expected to be a size of ~1300 bp. Clones 118, 121 and 122 showed the correct size of PCR product on the gel. Clone 118, 121 were mini prepped and sent off for sequencing. Sequencing results were correct and clone 121 was selected to be used for GFP1-10 expression.
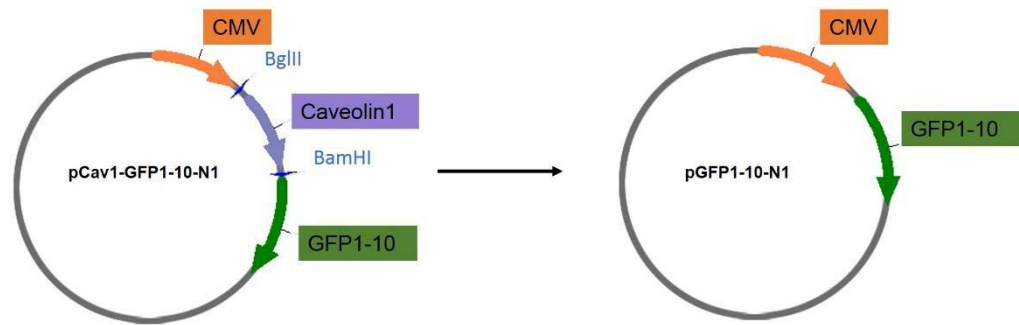
Figure 2-4 Cloning strategy to obtain pGFP1-10-N1

pCav1-GFP1-10(h)-N1 was digested with BglII and BamHI to remove Caveolin-1. Digest with BglII and BamHI resulted in compatible cohesive ends that were religated using T4 DNA ligase.
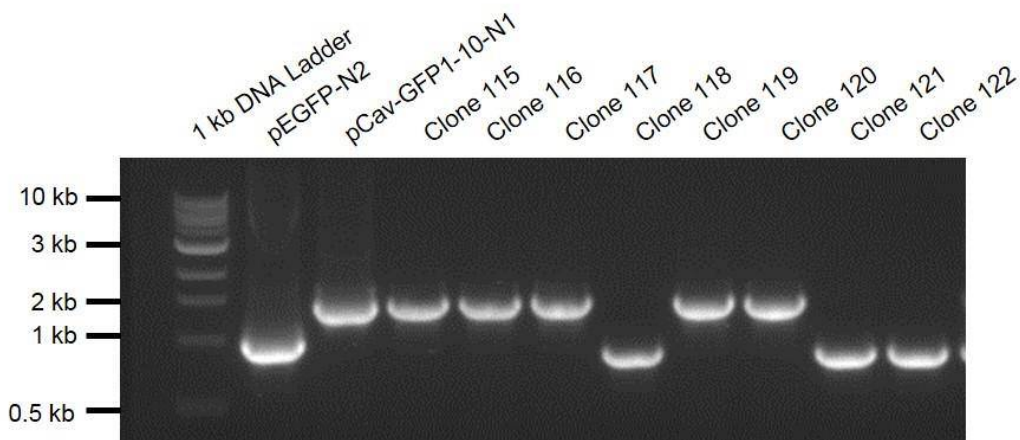
Figure 2-5 Screening of PCR products to identify pGFP1-10-N1.

Clones from bacterial colonies were screened using PCR to identify pCav1-GFP1-10-N1. PCR primers used were CMV forward and EGFPC1 reverse primer. Annealing temperature was 55°C annealing and elongation time 1min. Samples were run on a 1.5% agarose gel in TAE buffer. In addition to the samples, 1kb DNA ladder (NEB) were run on the gel. Expected sizes were ~700 bp when GFP1-10 has inserted correctly and ~1300 bp when Caveolin-GFP1-10 was inserted back into the vector.

2.11.3 Generation of pET3A-H6-Xa-R8-M3

pET3A-H6-Xa-R8-M3 was generated by using the seamless cloning technique (2.10.3) using a genestring carrying the DNA for H6-Xa-R8-M3 expression. The genestring was designed with the Master's thesis: Riester P., Characterising the cellular uptake and targeting of novel drug delivery systems, 2014, Department of Biology, Universitaet Konstanz. This DNA construct was generated and served as a precursor for a mammalian DNA construct coding for H6-Xa-R8-M3. The genestring was designed to be cloned into the multiple cloning site of pET3A when this vector is

by digest with the restriction enzymes NdeI and BamHI. To perform seamless cloning, the genestring contained N- and C-terminal homologous regions to linearised pET3A and a coding region carrying the DNA for H6-Xa-R8-M3 expression. Furthermore, the genestring was designed to restore NdeI and BamHI restriction sites (Figure 2-6). The full sequence of the genestring is shown in Figure 2-7. The sequence of M3 was based on the published GFP11 M3 sequence (Cabantous *et al.* 2005) and the flexible linker between octaarginine (R8) and M3 was used as described by (Pinaud and Dahan 2011).
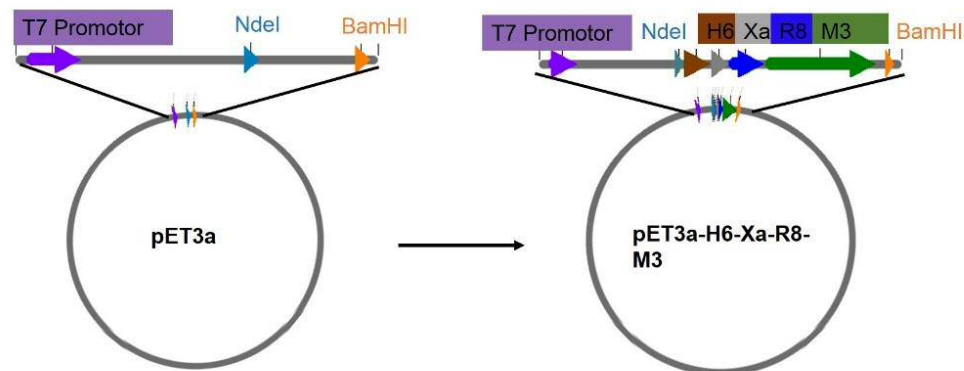
Figure 2-6 Cloning strategy to obtain pET3A-H6-Xa-R8-M3

Digest of pET3a with the restriction enzymes NdeI and BamHI leads to linearization of the vector. A genestring containing N- and C-terminal homologue regions to linearised pET3A and a coding region carrying the DNA for H6-Xa-R8-M3 expression can then be ligated into the vector using the seamless cloning technique.

Figure 2-7 Genestring for H6-Xa-R8-M3 cloning into pET3a.
DNA sequence of genestring coding for H6-Xa-R8-M3 expression expression is shown. Homologue base pairs to linearised pET3a when digested with NdeI and BamHI are underlined. NdeI restriction site (blue), BamHI restriction site (orange), coding region for H6 in brown, Xa cleavage site in grey, R8 in blue, M3 in green and the start of transcription is marked with an arrow.

To perform the cloning, the bacterial expression plasmid pET3a was linearized using the restriction sites NdeI and BamHI. The digest was purified from restriction

digest enzymes using QiaexII Gel extraction Kit (see 2.10.2). Making use of the seamless cloning technology the linearized vector and the homologous sequences of the genestring were recombined. The ligation mix was transformed into Top10 chemically competent bacteria (2.10.4) and plated onto LB-Agar plates containing Ampicillin. The next day clones on LB plates were screened using PCR (2.10.5.1) to identify clones where the DNA coding for H6-Xa-R8-M3 had inserted into pET3A. PCR primers that were used were T7 forward and T7 reverse. The PCR products were analysed using gel electrophoresis and visualised using a GelDoc UV transilluminator (Figure 2-5). The expected size for a vector with correct H6-Xa-R8-M3 insert only was ~300 bp. When the vector had religated to the original pET3a vector, PCR product was expected to be a size of ~100 bp. Figure 2-8 shows that clone 84, 85 and 86 had the correct size insert. All clones were sent off for sequencing. Sequencing results were correct and clone 86 was selected to be used for bacterial H6-Xa-R8-M3 expression.
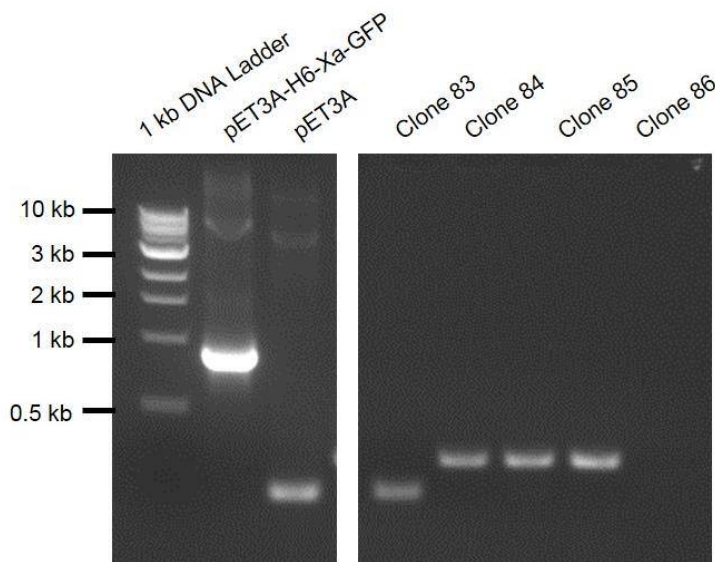
Figure 2-8 Screening of PCR products to identify pET3a-H6-Xa-R8-M3.
Clones from bacterial colonies were screened using PCR to identify pET3a-H6-Xa-R8-M3. PCR primers used were T7 forward and T7 reverse primer. Samples were run on a 1.5% agarose gel in TAE buffer. In addition to the samples, 1kb DNA ladder (NEB) were run on the gel. Expected sizes were ~300 bp when H6-Xa-R8-M3 has inserted correctly and ~100 bp when pET3a had not inserted DNA.

2.11.4 Generation of pH6-Xa-R8-M3-N2

For further subcloning of H6-Xa-R8-linker-M3 into the mammalian expression plasmid pEGFP-N2, H6-Xa-R8-linker-M3 was PCR amplified and inserted into the vector EGFP-N2 through restriction digest of both, vector an insert at the XmaI and XbaI restriction sites followed by ligation (Figure 2-9).

To perform the subcloning, the XmaI-H6-Xa-R8-linker-M3-XbaI insert was PCR amplified from pET3a-H6-Xa-R8-M3 using Phusion polymerase (2.10.5.2). Forward primer and reverse primer used were T7 forward and T7 reverse, respectively. The PCR product was purified and digested with XmaI and XbaI restriction enzymes. The insert was purified from restriction enzymes using the QiaexII Gel extraction Kit (2.10.7). The plasmid pEGFP-N2 was amplified in a DAM- bacterial strain to avoid methylation of restriction sites. The plasmid was linearised by restriction digest with XmaI and XbaI and EGFP was removed. The vector was purified using gel electrophoresis (2.10.6) followed by gel extraction (2.10.7). Then H6-Xa-R8-M3 and pEGFP-N2 were ligated using T4 ligase (2.10.2) to obtain mammalian expression construct pH6-Xa-R8-M3-N2. The ligation mix was transformed into Top10 chemically competent bacteria (2.10.4) and plated onto LB-Agar plates containing Kanamycin. The next day clones on LB plates were screened using PCR (2.10.5.1) to identify colonies where the DNA coding for H6-Xa-R8-M3 had inserted into pEGFP-N2. Colonies were screened using CMV forward and EGFPC1 reverse primers and an annealing temperature of 55°C. The PCR products were analysed using gel electrophoresis and visualised using a GelDoc UV transilluminator (Figure 2-10). The expected size for a vector with correct H6-Xa-R8-M3 insert only was ~300 bp. Figure 2-10 shows that all clones (1-5) show different sized inserts below 500 bp. All clones were sent off for sequencing. Sequencing results were correct for clone 1 which was selected to be used for mammalian H6-Xa-R8-M3 expression.
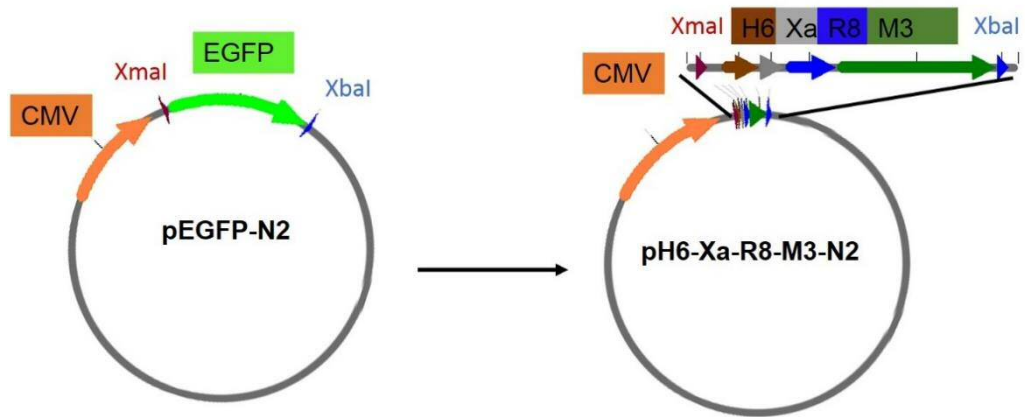
Figure 2-9 Cloning strategy to obtain pH6-Xa-R8-M3-N2.
The XmaI-H6-Xa-R8-linker-M3-XbaI insert is amplified using PCR from the vector pET3a-H6-Xa-R8-M3 and T7 forward and reverse primers. The mammalian expression pEGFP-N2 and the XmaI-H6-Xa-R8-linker-M3-XbaI insert are digested using restriction enzymes XmaI and XbaI and vector and insert a ligated to obtain p-H6-Xa-R8-M3.
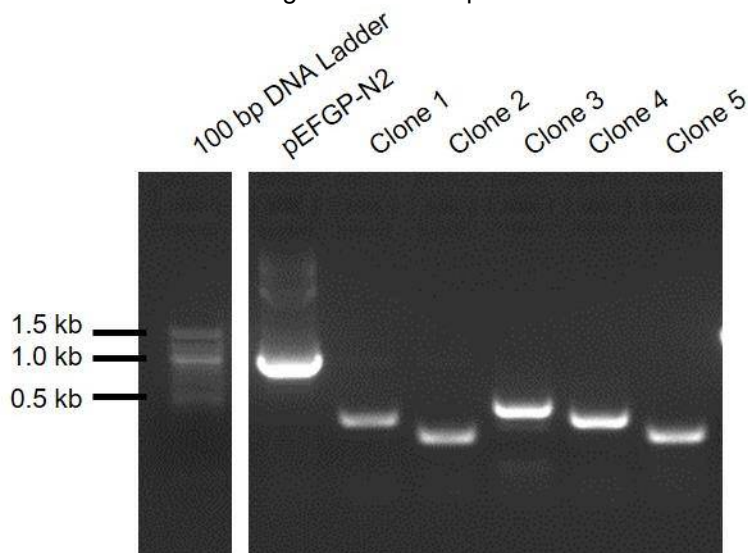
Figure 2-10 Screening of PCR products to identify pH6-Xa-R8-M3-N2.
Clones from bacterial colonies were screened using PCR to identify pH6-Xa-R8-M3-N2. PCR primers that were used were CMV forward and EGFPC1 reverse primer. Samples were run on a 1.5% agarose gel in TAE buffer. In addition to the samples, 100 bp DNA ladder (NEB) was run on the gel. Expected sizes were ~300 bp when H6-Xa-R8-M3 has inserted correctly. Samples were run on the same gel as the 100 bp DNA ladder but samples that were not relevant to this experiment were removed from the gel.

2.11.5 Generation of pcDNA3.1-mCherry-H6-Xa-R8-M3

To have a fluorescent readout of H6-Xa-R8-M3-N2 expression, another mammalian expression construct was generated where H6-Xa-R8-M3-N2 was introduced as a C-terminal fusion to mCherry using XhoI and XbaI restriction sites available in vector and insert (Figure 2-11). The plasmid pcDNA3.1 encoding mCherry was given as a kind gift from D. Dafydd Jones laboratory (Nasu *et al.* 2015). Both plasmids, pcDNA3.1.-mCherry and pH6-Xa-R8-M3-N2 were amplified in a DAM-bacterial strain to obtain a non-methylated XbaI site and digested with XbaI and XhoI. Digested vector and insert were purified (2.10.7) and the insert H6-Xa-R8-M3 was ligated (2.10.2) into the linearised vector pcDNA3.1.-mCherry to obtain a new mammalian expression construct, pcDNA3.1.-mCherry-H6-Xa-R8-M3. The ligation mix was transformed into Top10 chemically competent bacteria (2.10.4) and plated onto LB-Agar plates containing Ampicillin. The next day clones on LB plates were screened using PCR (2.10.5.1) to identify colonies where the DNA coding for H6-Xa-R8-M3 had inserted into pCDNA3.1-mCherry. Colonies were screened using pcDNA3.1 forward and pcDNA3.1 reverse primers and an annealing temperature of 55°C. The PCR products were analysed using gel electrophoresis and visualised using a GelDoc UV transilluminator (Figure 2-10). The expected size for a vector with correct H6-Xa-R8-M3 insert only was ~1200 bp. Figure 2-12 shows that clone 217 shows a bigger size insert than all other clones screened. All other clones show the same size as original pcDNA3.1-mCherry construct. Clone 217 was sent off for sequencing. Sequencing results were correct and clone 217 was selected to be used for mCherry-H6-Xa-R8-M3 expression.
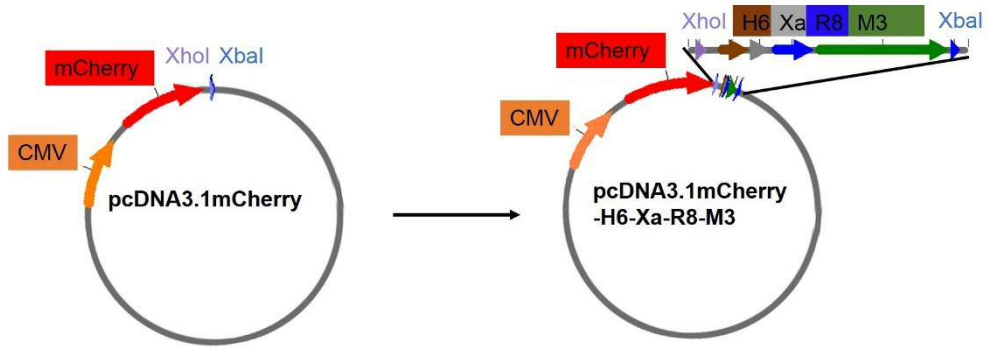
Figure 2-11 Cloning strategy to obtain pcDNA3.1-mCherry-H6-Xa-R8-M3.
To obtain pcDNA3.1-mCherry-H6-Xa-R8-M3, pcDNA3.1-mCherry and pH6-Xa-R8-M3-N2 were digested using XhoI and XbaI restriction sites. Vector and insert were then ligated using T4 ligase.
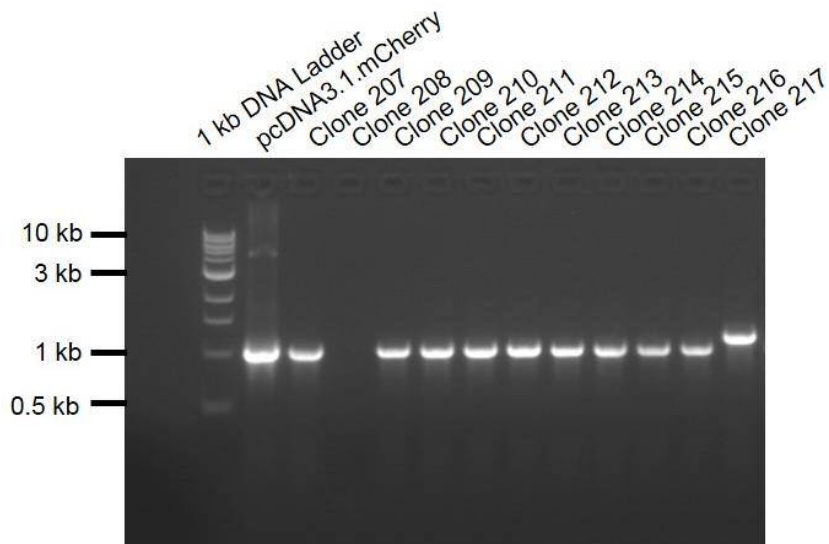
Figure 2-12 Screening of PCR products to identify pCDNA3.1-mCherry-H6-Xa-R8-M3.
Clones from bacterial colonies were screened using PCR to identify pCDNA3.1-mCherry-H6-Xa-R8-M3. PCR primers that were used were pcDNA3.1 forward and pcDNA3.1 reverse primer. Samples were run on a 1.5% agarose gel in TAE buffer. In addition to the samples a 1kb DNA ladder (NEB) was run on the gel. Expected sizes were ~1200 bp when H6-Xa-R8-M3 has inserted correctly.

2.11.6 Generation of pcDNA3.1-mCherry-GFP1-10

For the generation of a mammalian mCherry-GFP1-10 expression construct, a GFP1-10 insert was PCR amplified including restriction sites XhoI and XbaI and inserted into pcDNA3.1-mCherry (Figure 2-13).

To perform the cloning, GFP1-10 was PCR amplified from pGFP1-10-N1 using phusion polymerase (2.10.5.2). Primers used were GFP1-10 forward and GFP1-10 reverse primers. These primers ensured amplification of a XhoI and a XbaI site in addition to the GFP1-10 insert and an overhang sequence. PCR products were purified using the QiaexII purification kit (Qiagen). pcDNA3.1.-mCherry was amplified in a DAM- bacterial strain to obtain a non-methylated XbaI site. The purified GFP1-10 PCR product and the plasmid pcDNA3.1-mCherry encoding mCherry were cut with XhoI and XbaI, purified and the GFP1-10 insert was ligated C terminally to mCherry into pcDNA3.1 (2.10.2). The ligation mix was transformed into Top10 chemically competent bacteria (2.10.4) and plated onto LB-Agar plates containing Ampicillin. The next day clones on LB plates were screened using PCR (2.10.5.1) to identify colonies where the DNA coding for GFP1-10 had inserted into pcDNA3.1-mCherry. Colonies were screened using pcDNA3.1 forward and pcDNA3.1 reverse primers. The PCR products were analysed using gel electrophoresis and visualised using a GelDoc UV transilluminator (Figure 2-14). The expected size for a vector with correct GFP1-10 insert only was ~1700bp. Figure 2-14 shows that clone 322 was the correct size on the gel. Clone 322 was sent off for sequencing. Sequencing results were correct and clone 322 was selected to be used for mCherry-GFP1-10 expression.
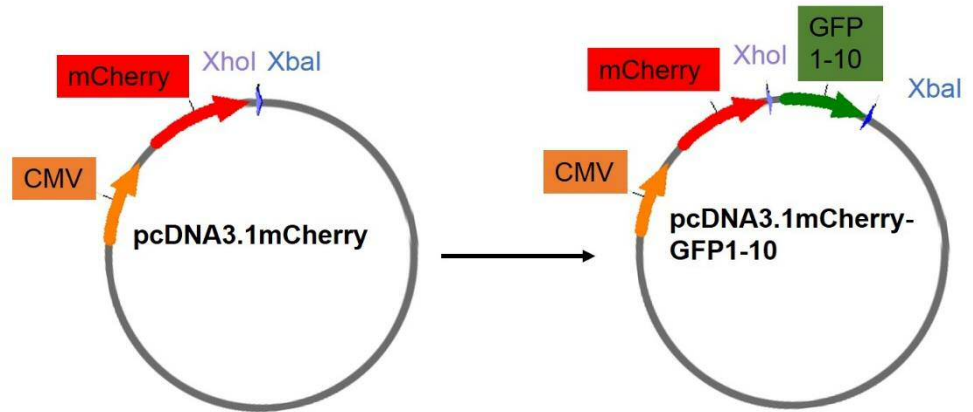
Figure 2-13 Cloning strategy to obtain pcDNA3.1-mCherry-GFP1-10.
To obtain pcDNA3.1-mCherryGFP1-10, pcDNA3.1-mCherry a PCR amplified insert XhoI-GFP1-10-XbaI were digested using XhoI and XbaI restriction sites. Vector and insert were then ligated using T4 ligase.
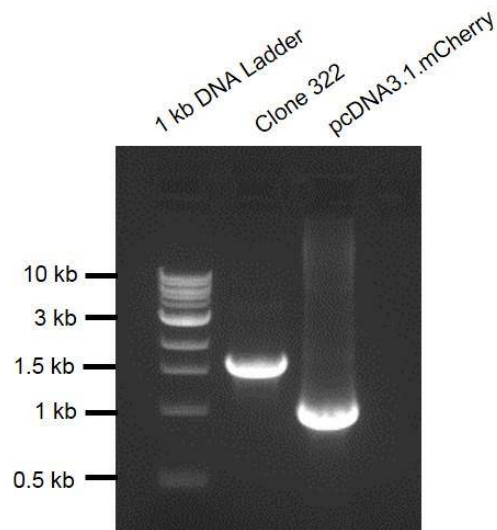
Figure 2-14 Screening of PCR products to identify pCDNA3.1-mCherry-GFP1-10.
Clones from bacterial colonies were screened using PCR to identify pCDNA3.1-mCherry-GFP1-10. PCR primers that were used were pcDNA3.1 forward and pcDNA3.1 reverse primer. Samples were run on a 1.5% agarose gel in TAE buffer. In addition to the samples a 1kb DNA ladder (NEB) was run on the gel. Expected sizes were ~1700 bp when H6-Xa-R8-M3 has inserted correctly.

2.11.7 Generation of pcDNA3.1-mCherry-GFP

For the generation of a mammalian mCherry-GFP expression construct, a GFP1-10 insert was PCR amplified including restriction sites XhoI and XbaI and inserted into pcDNA3.1-mCherry (Figure 2-15).

To perform the cloning, GFP was PCR amplified from pEGFP-C1 using Phusion polymerase (2.10.5.2). Primers used were GFP forward and GFP reverse primers. These primers ensured amplification of a XhoI and a XbaI site in addition to the GFP insert and an overhang sequence. PCR products were purified using the QiaexII prurification kit (Qiagen). pcDNA3.1.-mCherry was amplified in a DAM- bacterial strain to obtain a non-methylated XbaI site. The purified GFP1-10 PCR product and the plasmid pcDNA3.1-mCherry encoding mCherry were cut with XhoI and XbaI, purified and the GFP insert was ligated C terminally to mCherry into pcDNA3.1 (2.10.2). The ligation mix was transformed into Top10 chemically competent bacteria (2.10.4) and plated onto LB-Agar plates containing Ampicillin. The next day clones on LB plates were screened using PCR (2.10.5.1) to identify colonies where the DNA coding for GFP had inserted into pCDNA3.1-mCherry. Colonies were screened using pcDNA3.1 forward and pcDNA3.1 reverse primers. The PCR products were analysed using gel electrophoresis and visualised using a GelDoc UV transilluminator (Figure 2-14). The expected size for a vector with correct GFP insert only was ~1770 bp. Figure 2-16 shows that clone 327 and clone 331 were correctly sized. Clone 327 and clone 331 were sent off for sequencing. Sequencing results were correct and clone 327 was selected to be used for mCherry-GFP expression.
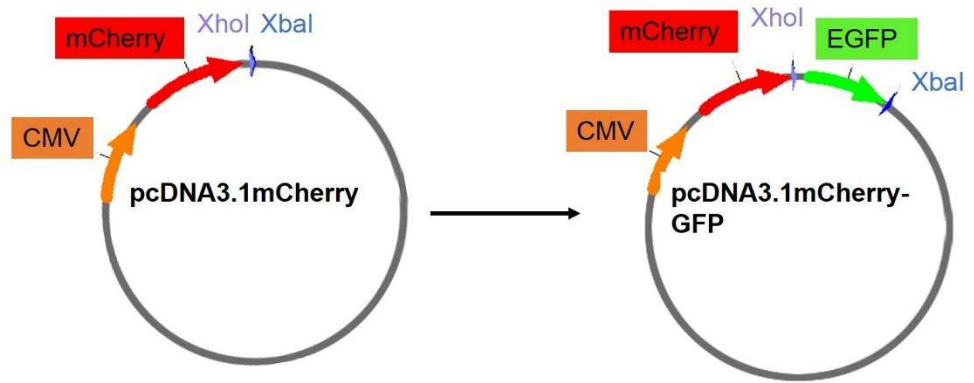
Figure 2-15 Cloning strategy to obtain pcDNA3.1-mCherry-GFP.
To obtain pcDNA3.1-mCherryGFP, pcDNA3.1-mCherry a PCR amplified insert XhoI-GFP1-XbaI were digested using XhoI and XbaI restriction sites. Vector and insert were then ligated using T4 ligase.
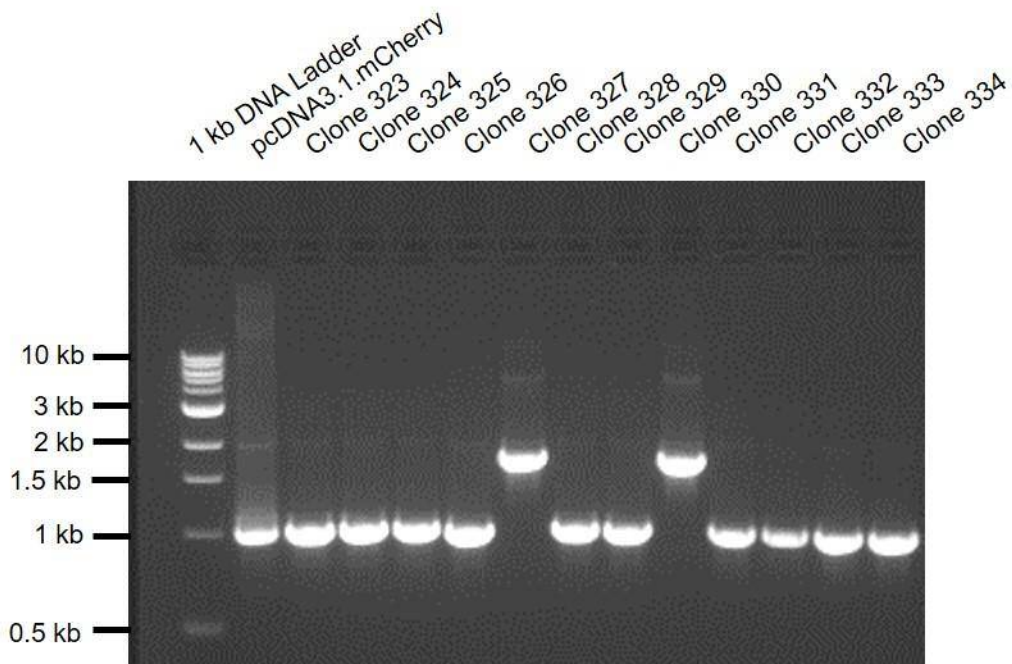
Figure 2-16 Screening of PCR products to identify pCDNA3.1-mCherry-GFP.
Clones from bacterial colonies were screened using PCR to identify pCDNA3.1-mCherry-GFP. PCR primers that were used were pcDNA1.3 forward and pcDNA3.1 reverse primer. Samples were run on a 1.5% agarose gel in TAE buffer. In addition to the samples a 1kb DNA ladder (NEB) was run on the gel. Expected size was ~1770 bp when GFP has inserted correctly.

3 Development of a spit GFP assay to detect functional cytosolic delivery of a peptide

3.1 Introduction

The success of the proposed method (1.5.1) to evaluate the efficiency of drug delivery systems to functionally deliver M3 peptide cargo to the cytosol of target cells that express GFP1-10 relies on three important factors. Firstly, that GFP1-10 can be expressed in the cytosol of HeLa cells and remain non-fluorescent. Secondly, GFP1-10 and M3 are able to complement to form full length GFP in the cytosolic environment of HeLa cells. Thirdly, the chemically synthesised DDS conjugated M3 peptide (R8-M3) as well as the M3 peptide alone can complement with GFP1-10 of cellular origin in an *in vitro* system where direct access of the two fragments is guaranteed, and complementation is not dependent on delivery of M3 across a biological membrane.

The primary focus of this chapter lies on the development of appropriate methods to prove that non-fluorescent GFP1-10 can be expressed in target cells and is able to complement with M3 in the cytosolic environment as well as *in vitro* with synthetic M3 peptide. Moreover, one of the main benefits of this assay will be to monitor peptide delivery in live cells in real time using fluorescent widefield microscopy. Hence, it is important to develop this assay and its methods to prove GFP complementation using a fluorescent widefield microscope to ensure that its sensitivity is adequate for it to be utilised as a detection platform to observe GFP complementation.

A second aim of this chapter is to demonstrate that the proposed split GFP assay can be utilised to show functional M3 peptide delivery by the drug delivery system R8 in live cells and that this delivery is indeed drug delivery system dependent.

3.2 Assay development

3.2.1 Cytosolic expression of the intracellular GFP1-10 target

The first aim in the development of an assay to determine the functional delivery of the M3 peptide to its cytosolic GFP1-10 target was to ensure that GFP1-10 can be expressed in the cytosol of HeLa cells (Henrietta Lacks). HeLa cells were chosen for the development of this assay because it is a well characterised cervical carcinoma cell line in which gene expression can be easily manipulated. To be able to transfect HeLa cells with the DNA coding for GFP1-10, the expression plasmid pGFP1-10-N1 was generated (2.11.2). To further prove that GFP1-10 can be expressed in the cytosol, HeLa cells were transiently transfected with pGFP1-10-N1. GFP1-10 expression cannot be detected using microscopy of live cells due to the lack of its green fluorescence, therefore, immunofluorescence was the proposed method to detect its expression. In order to perform immunofluorescent staining, HeLa cells were PFA fixed 16h after transfection and the plasma membrane was permeabilised. GFP-10 expression was detected using a primary anti-GFP antibody and stained with a fluorophore conjugated secondary antibody. Immunofluorescent staining against GFP was analysed using a widefield fluorescent microscope.

Antibodies are highly specific to detect epitopes of proteins. Due to the lack of the 11th beta sheet in GFP1-10, the epitope of GFP1-10 was changed compared to full length GFP. For this reason two different anti GFP antibodies were tested to detect GFP1-10 (Table 2-6). It was shown that both antibodies can detect full length GFP but only one antibody (Vector Laboratories) that was manufactured to detect GFP and GFP variants did detect GFP1-10 expression (Appendix 9.3, Figure 9-2). Hence, further experiments were performed using the anti-GFP antibody that was able to detect GFP1-10 expression.

When cytosolic GFP1-10 compared to EGFP expression was investigated using immunofluorescence it can be shown that control cells expressing full length GFP

showed green fluorescence in their cytosol (Figure 3-1 C). The fluorescent signal of the antibody co-localised with the GFP fluorescence indicating that the antibody specifically detects GFP (Figure 3-1 D). When the truncated version, GFP1-10, was expressed in HeLa cells, the green fluorescence of the protein was absent (Figure 3-1 G) but the anti GFP antibody still detected its expression in the cytosol (Figure 3-1 H). To exclude the possibility that the antibody detected non-specific cytosolic proteins, immunofluorescent staining was also performed on mock transfected cells. These cells were not green fluorescent (Figure 3-1 K) and the anti GFP antibody did not detect any proteins in the cytosol (Figure 3-1 L).
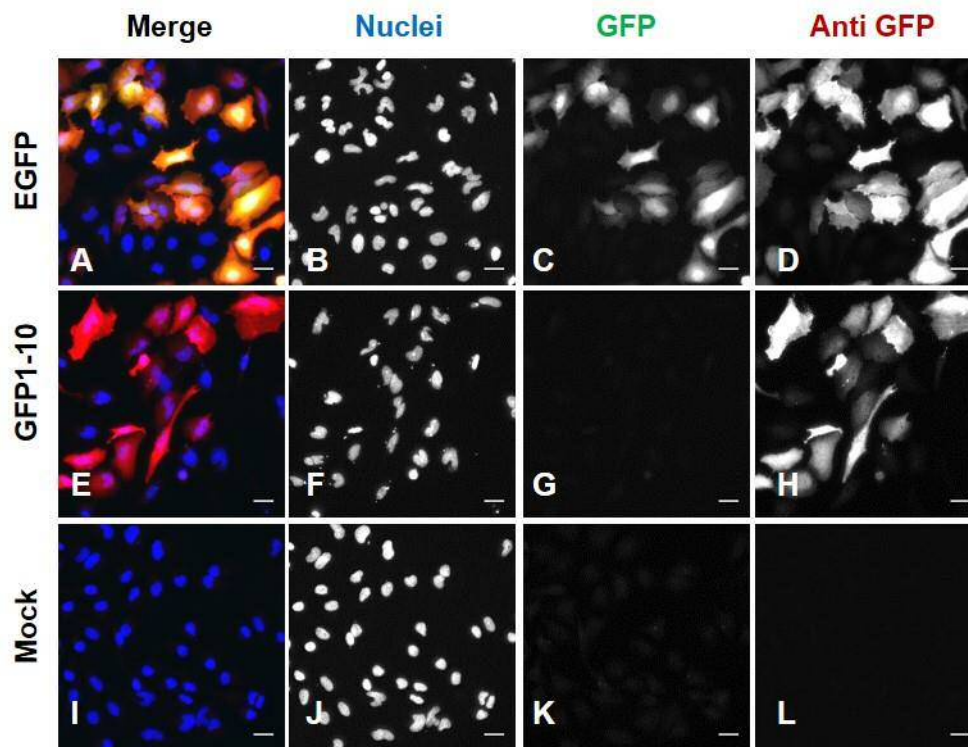
Figure 3-1 Detection of GFP1-10 expression in HeLa cells using immunofluorescence.
HeLa cells were transiently transfected with DNA constructs coding for GFP1-10 or full length EGFP. The transfection mix of mock transfected cells did not contain DNA. Cells were incubated in transfection mix overnight and PFA fixed the next day. The plasma membrane was permeabilised with 0.1 % Triton-X-100 and GFP or GFP1-10 expression was detected using a primary anti-GFP antibody raised in goat. A secondary anti-goat antibody conjugated to Alexa-647 was used to visualise GFP expression (Anti GFP). Nuclei were counterstained with DAPI. Representative images are shown for each condition. Scale bars: 30 µm. n=3.

To further ensure that the detected fluorescence of the antibody was specifically due to the primary anti GFP antibody and not an artefact of a cross reaction of the Alexa-647 labelled secondary antibody, a second experiment was conducted. As control cells, cells transiently expressing EGFP were treated with the primary anti-GFP antibody and the secondary Alexa-647 labelled antibody. As shown in the first experiment, cytosolic green fluorescence co-localised with the protein detected by the antibody (Figure 3-2 C, D). When the primary antibody was omitted and only the Alexa-647 conjugated secondary antibody was applied on cells expressing EGF, no antibody fluorescence could be detected (Figure 3-2 H). There was also no antibody fluorescence detected on cells expressing GFP1-10 or on Mock transfected cells (Figure 3-2 L, P). These findings demonstrate that the staining of the antibody was specific to GFP. Furthermore, this experiment proves that the chosen primary anti GFP antibody (vectorlaboratories) not only detects expression of full length EGFP but can also be utilised to detect superfolder GFP derived GFP1-10.

Taken together, these results show that HeLa cells can transiently express the GFP1-10 target protein and, importantly, GFP1-10 is non-fluorescent when excited with 488nm wavelength light (Figure 3-1 G). Moreover, its intracellular distribution was located in the cytosol (Figure 3-1 H).
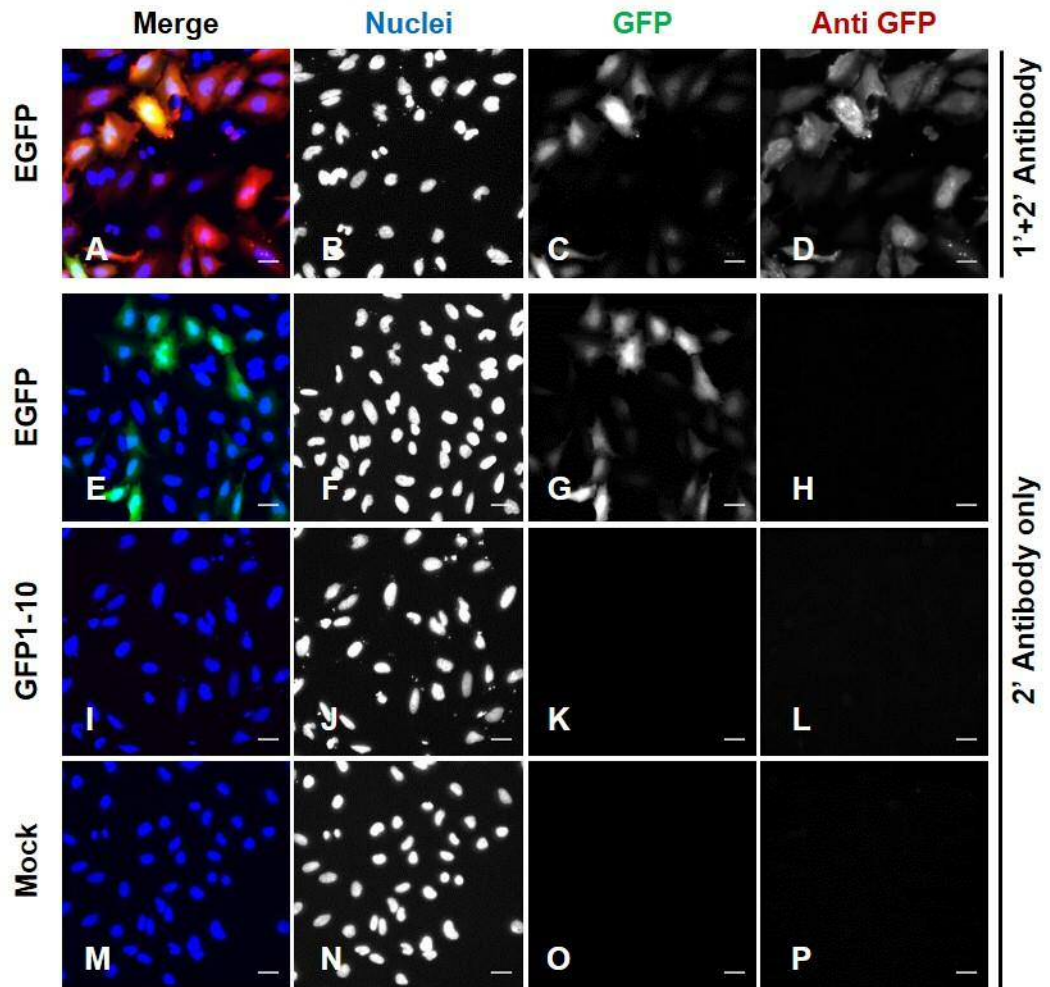
Figure 3-2 Secondary antibody control for anti GFP detection in HeLa cells.
HeLa cells were transiently transfected with DNA constructs coding for GFP1-10 or full length EGFP. The transfection mix of mock transfected cells did not contain DNA. Cells were incubated in transfection mix overnight. They were fixed the next day and the plasma membrane was permeabilised with 0.1 % Triton-X-100. Control cells expressing EGFP were incubated with the primary anti-GFP (goat) antibody followed by incubation with the secondary anti-goat-Alexa-647 antibody (1'+2' Antibody). Other samples were incubated with the secondary anti-goat-Alexa-647 antibody only (2' Antibody). Nuclei were counterstained with DAPI. Representative images shown for each condition. Scale bars 30 μm. n=3.

As a second method to confirm the expression of GFP1-10 in Hela cells, western blot analysis of cell lysates of cells transiently expressing EGFP and GFP1-10 was performed. To achieve this, cell lysates containing the cytosolic protein content of transfected cells were separated by their molecular weight using SDS gel electrophoresis and transferred onto a membrane. This membrane was probed with the same primary anti-GFP antibody that was previously used for immunofluorescence and detected with a secondary antibody conjugated to horseradish peroxidase.

Analysis of the blot showed that one clear band was detected in each of the cell lysates. The molecular weight of the protein detected in the lysate of cells expressing EGFP was ~30 kDa (Figure 3-3). The expected molecular weight of EGFP is 27 kDa which is in the region of the weight detected on the western blot. The protein detected in the cells expressing GFP1-10 had a molecular weight of ~25kDa (Figure 3-3). As expected, the truncated protein carried a lower molecular weight compared to full length GFP and these results were a second indication that GFP1-10 can be expressed by HeLa cells.
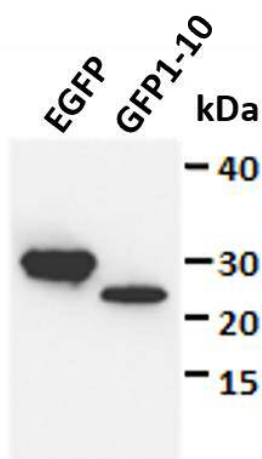
Figure 3-3 Western blot analysis of EGFP and GFP1-10 expression.
Cell lysates were obtained from cells transiently expressing EGFP (left) or GFP1-10 (right). Lysates were analysed using SDS gel electrophoresis and blotted onto a membrane. The membrane was probed against GFP using an anti-GFP (goat) antibody followed by a secondary anti-goat-HRP antibody. Sizes of proteins are shown in kDa. n=1.

3.2.2 Complementation of GFP1-10 with M3 in the cytosol – the 'co-transfection experiment'.

Once it was ensured that the intracellular GFP1-10 target protein can be expressed in the cytosol of HeLa cells it was important to test that GFP1-10 can complement with M3 to form full length GFP in the cytosolic environment. A possibility to investigate this, was to co-transfect HeLa cells with the DNA constructs encoding for the single split GFP fragments, GFP1-10 and M3, so that the cell expresses both fragments in its cytosol and GFP complementation can occur. GFP complementation can then be observed using a widefield fluorescent microscope. To perform this experiment, mammalian DNA expression constructs for GFP1-10 and M3 had to be in place. As previously confirmed using immunofluorescence, the generated DNA construct for GFP1-10 expression can be used to express GFP1-10 in the cytosol of HeLa (3.2.1).

To achieve the expression of the M3 fragment in Hela cells, a plasmid encoding for M3 needed to be generated. An existing plasmid for bacterial expression was utilised as a starting point for the generation of a mammalian expression plasmid and coded for the protein H6-Xa-R8-M3. This expression plasmid, pET3A-H6-Xa-R8-M3 was generated within this project (2.11.3) to obtain the peptide R8-M3 as a result of bacterial expression. Hence, additionally to R8-M3, it contained the N-terminal H6, a Histidine tag and a Factor Xa protease cleavage site for purification steps. Due to time constraints, the plasmid pET3A-H6-Xa-R8-M3 was never utilised for bacterial expression to obtain R8-M3 and this peptide was chemically synthesised (2.2). Another reason why the plasmid pET3A-H6-Xa-R8-M3 was never utilised for bacterial expression to obtain R8-M3 was that the presence of bacterial factors present in the protein even after purification could affect cells in a live cell assay.

Nevertheless, pET3A-H6-Xa-R8-M3 served as a precursor to sub-clone an expression construct for mammalian expression coding for M3.

Ideally, this expression construct would have coded for M3 expression only. But due to the absence of restriction digest sites, the entire DNA encoding H6-Xa-R8-M3 was sub-cloned from the bacterial expression vector pETA3a into the mammalian expression vector EGFP-N2 to obtain pH6-Xa-R8-M3-N2 (2.11.4). The successful generation of this expression construct was confirmed by sequencing but the cytosolic expression of H6-Xa-R8-M3 was not tested because of the lack of fluorescence of M3 and antibodies to detect the epitopes in the construct. Antibodies against a Histidine tag are available but results would have been difficult to interpret because no positive control was available (e.g. expression construct for mammalian protein expression fused to a Histidine tag). Hence, co-expression experiments were conducted with the confirmation of the sequencing results only, that a mammalian expression vector encoding for H6-Xa-R8-M3 had been generated.

When H6-Xa-R8-M3 was co-expressed with GFP1-10, no GFP fluorescence could be detected indicating that no complementation of GFP had occurred (Figure 3-4 C). Lack of GFP complementation could have been due to the failure of the GFP1-10 and M3 fragment to complement to full length GFP. Another reason could have been failure of expression of one of the fragments and the resulting absence of one of the complementation partners. It was shown that GFP1-10 can be expressed in the cytosol of Hela cells, so that was highly likely that H6-Xa-R8-M3 was faulty. Thus, H6-Xa-R8-M3 expression was further investigated.

An idea to be able to visualise H6-Xa-R8-M3 expression was to express it as a fusion protein to the fluorescent protein mCherry which can serve as a fluorescent expression partner. For this reason the plasmid pcDNA3.1.mCherry-H6-Xa-R8-M3 was generated coding for the protein mCherry-H6-Xa-R8-M3 (0).

When Hela cells were transfected with this construct, it enabled us to monitor if and where M3 is expressed inside the cell because it contained the fluorescent expression marker mCherry. The red fluorescence of mCherry-H6-Xa-R8-M3

fluorescence was accumulated in the nucleus, located at the nucleolus (Figure 3-5 C). An explanation for the nucleolar staining could be that the highly positively charged cell penetrating peptide R8 targeted the whole protein to this location. R8 is known to localise to the nucleolus and can be used as a nucleolar marker in live cells (Martin *et al.* 2007). Hence, the presence of red fluorescence at the nucleolus was an indication that not only mCherry was expressed in the cytosol of HeLa cells but also the mCherry fusion protein coding for H6-Xa-R8-M3.

It was further investigated if mCherry-H6-Xa-R8-M3 was exclusively located at the nucleolus. When the fluorescence of mCherry-H6-Xa-R8-M3 expression was oversaturated using ImageJ, it was visible that it was mainly located in the nucleus but was also located in the cytosol (Figure 3-5 F).
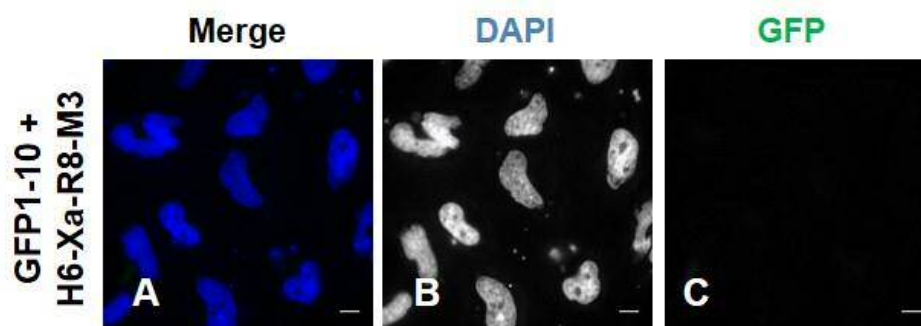
Figure 3-4 Co-expression of GFP1-10 and H6-Xa-R8-M3.
Cells were co-transfected with DNA encoding GFP1-10 and H6-Xa-R8-M3. Cells were left in transfection mix overnight and PFA fixed on the next day. Nuclei were counterstained with DAPI. Representative images show that no GFP fluorescence was detected (C). Scale bars: 10 μm. n=1.
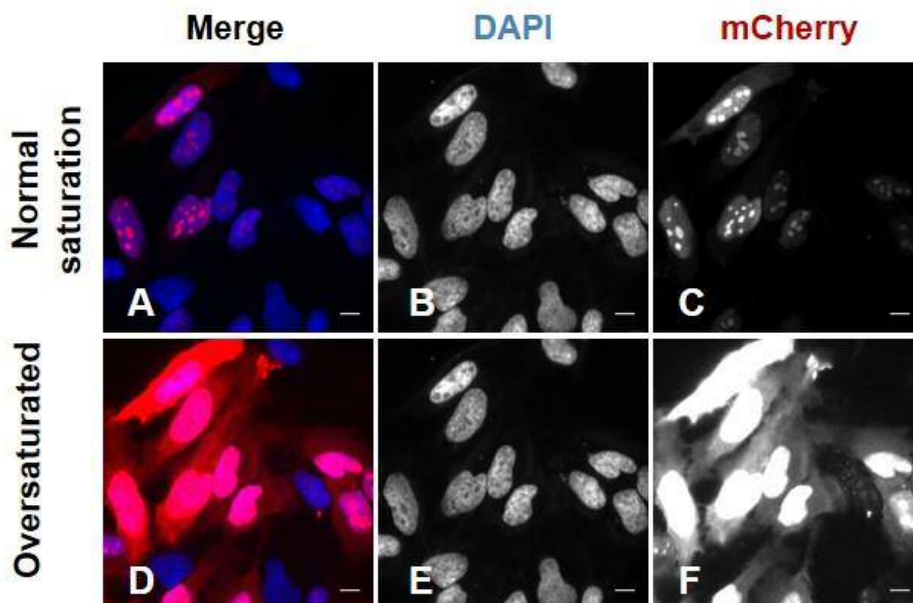
Figure 3-5 Expression pattern of mCherry-H6-Xa-R8-M3 in HeLa cells.
HeLa cells were transfected with DNA encoding for mCherry-H6-Xa-R8-M3. Cells were left in transfection mix overnight and PFA fixed the next day. Nuclei were counterstained with DAPI. Localisation of mCherry-H6-Xa-M3 is found at the nucleolus (normal saturation). Cytosolic localisation can be seen when the same image is shown oversaturated. Representative images are shown. Scale bars: 10 µm. n=3.

Having confirmed that GFP1-10 and mCherry-H6-Xa-R8-M3 can both be expressed in the cytosol, the co-expression experiment was repeated to investigate if GFP1-10 and mCherry-H6-Xa-R8-M3 can complement to form full length GFP. Cells were transfected with DNA constructs coding for GFP1-10 and mCherry-H6-Xa-R8-M3 and incubated for 16 h with the transfection mix. According with previous results, GFP1-10 and mCherry-H6-Xa-R8-M3 did not fluoresce in green when single proteins were expressed (Figure 3-6 C, G). When GFP1-10 and mCherry-H6-Xa-R8-M3 were co-expressed in HeLa cells, cells did fluoresce in green indicating that GFP complementation had occurred (Figure 3-6 K). The green fluorescence was observed as concentrated spots at the nucleolus as well as in the nucleus and low amounts in the cytosol. This distribution correlated with the location where mCherry-H6-Xa-R8-M3 was expressed (Figure 3-6 L) indicating that GFP complementation had only occurred where the M3 fragment was localised inside the cell.

The key role of M3 is to act as a proton acceptor in order for the GFP fluorophore to mature. To ensure that the GFP complementation with mCherry-H6-Xa-R8-M3 is specific to M3 and to rule out that the fluorophore mCherry is capable of acting as a proton acceptor and therefore replace the function of M3, cells were also co-transfected with GFP1-10 and mCherry. When mCherry was expressed alone, its fluorescence was distributed throughout the cells (Figure 3-6 P). Co-expression of GFP1-10 with mCherry did not result in GFP complementation because no green fluorescence was detected in those cells (Figure 3-6 S). This indicates that GFP complementation cannot occur through interaction of GFP1-10 with the fluorescent protein mCherry. Thus, GFP complementation is specific to the H6-Xa-R8-M3 fragment and therefore complementation of GFP1-10 with M3 can be assumed.

This experiment also indicated that detected GFP fluorescence is due to true GFP fluorescence and not an artefact of bleed through from the mCherry into the GFP channel on the microscope. When mCherry-H6-Xa-R8-M3 was expressed alone its red fluorescence was detected in the mCherry channel (Figure 3-6 H) but there was no bleed through into the GFP channel as there was no green fluorescence detected (Figure 3-6 G). When mCherry-H6-Xa-R8-M3 was co-expressed with GFP1-10, mCherry fluorescence, detected with the same microscope settings, was less than the fluorescence of mCherry-M3 alone (Figure 3-6 L, H) but green fluorescence was detected in the GFP channel (Figure 3-6 K). This confirmed that the green fluorescence was a true signal detected in the GFP channel and not an artefact of fluorescence that was collected from exciting mCherry.

GFP complementation using co-transfection was further verified using a microplate reader to obtain quantitative information of complemented GFP fluorescence. HeLa cells were left to transfect with transfection mix for 16 h and the next day cells were trypsinised and green fluorescence of 1×10^5 cells was measured with a microplate reader. Green fluorescence of mock transfected cells where the

transfection mix did not contain DNA were used for background subtraction. No green fluorescence was measured when cells were transfected with GFP1-10 or mCherry-H6-Xa-R8-M3 (Figure 3-7 A). Co-expression of GFP1-10 and mCherry-H6-Xa-R8-M3 resulted in GFP complementation which resulted in detection of significant GFP fluorescence compared to when single fragments were expressed. There was no fluorescence from GFP complementation observed when GFP1-10 was co-expressed with mCherry or when mCherry only was expressed. The fluorescence of complemented GFP1-10 and M3 was also compared to the green fluorescence when full length EGFP is expressed in HeLa cells. Interestingly, the brightness of complemented GFP was six fold lower than the green fluorescence that was measured when full length EGFP was expressed in HeLa cells (Figure 3-7 B).

In all, the results obtained with the microplate reader (Figure 3-7) correlate with the co-expression results obtained by microscopy (Figure 3-6). These experiments demonstrate that GFP1-10 and mCherry-H6-Xa-R8-M3 can complement in the cellular environment of HeLa cells to form full length GFP that fluoresces upon illumination with 490nm wavelength light and this complementation is specific to the two fragments GFP1-10 and H6-Xa-R8-M3 where a complementation of GFP1-10 and M3 can be assumed.
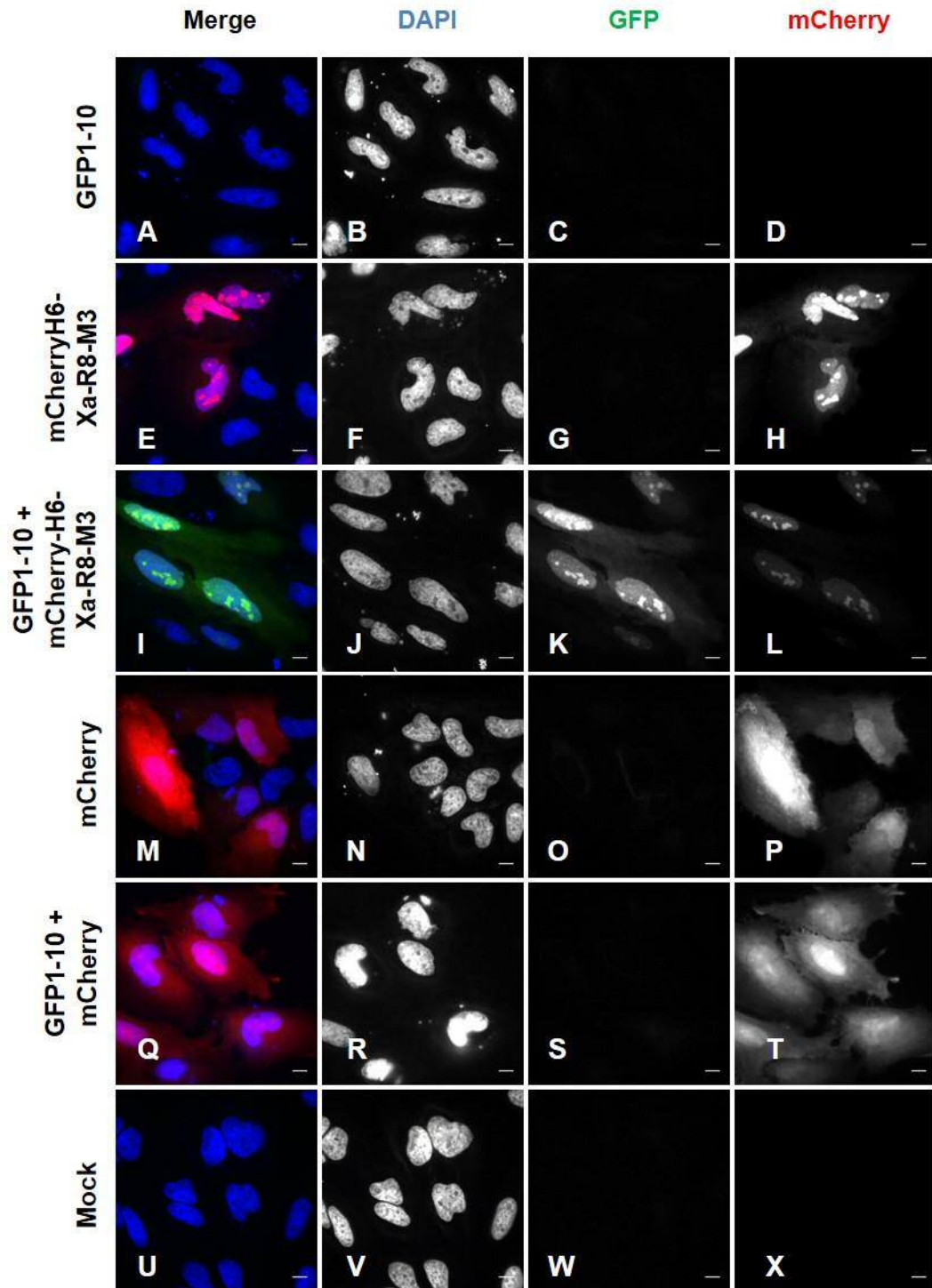
Figure 3-6 Co-transfection of GFP1-10 and mCherry-H6-Xa-R8-M3.
Transfections or co-transfections of HeLa cells were performed with DNA encoding for GFP1-10, mCherry-H6-Xa-R8-M3 and mCherry. The transfection mix of mock transfected cells did not contain DNA. Cells were left in transfection mix overnight and PFA fixed on the next day. Nuclei were counterstained with DAPI. Representative images are shown for each condition. Scale bars: 10 µm. n=3.
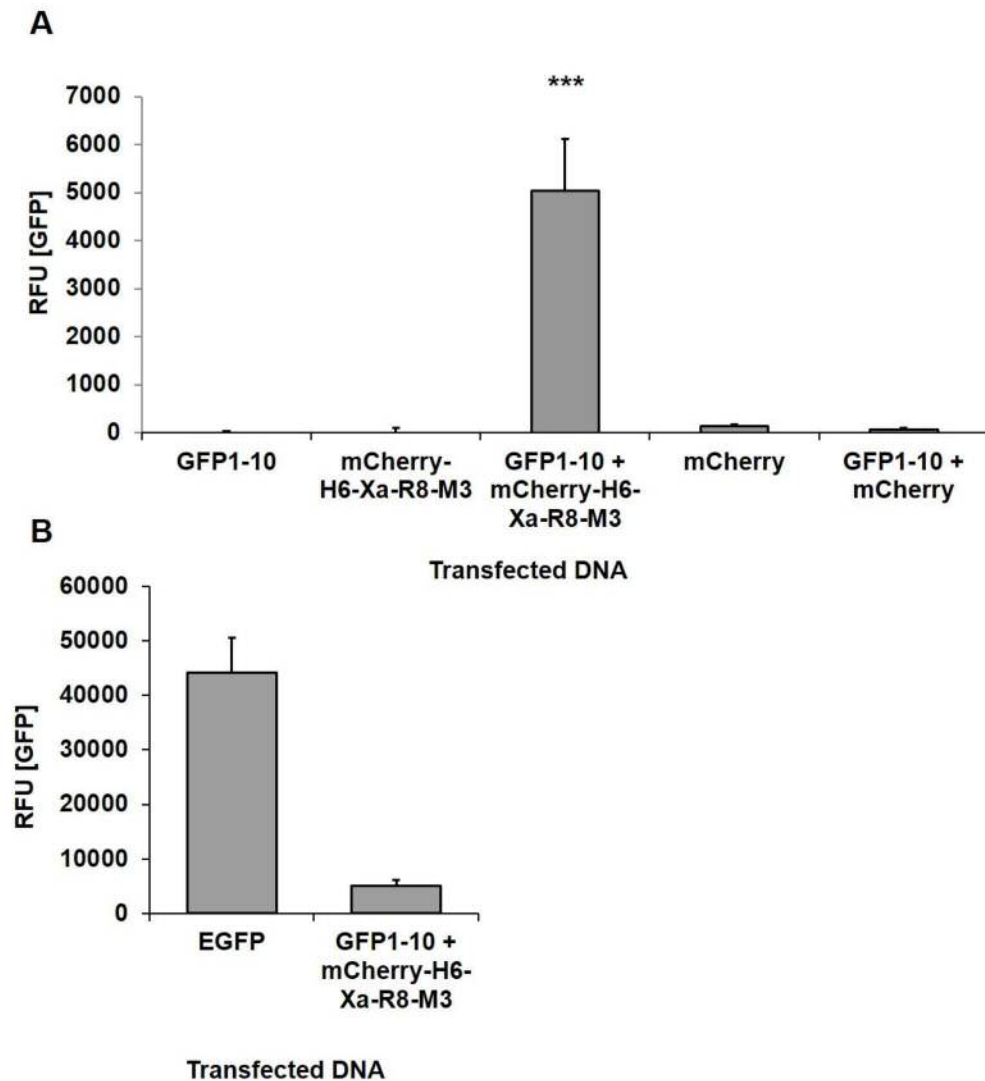
Figure 3-7 Detection of GFP complementation after co-tranfection using a microplate reader.
Single transfections or co-transfections of HeLa cells were performed with DNA encoding for GFP1-10, mCherry-H6-Xa-R8-M3 and mCherry. The transfection mix of mock transfected cells did not contain DNA. Cells were left in transfection mix overnight. The next day, cells were detached from their dish using trypsin, washed and transferred into a clear bottom, black walled microwell plate. Green fluorescence was monitored using a microplate reader (A) Comparison of green fluorescence of single DNA fragments and co-transfection of GFP1-10 and M3. For statistical analysis data was tested using a Kruskal-Wallis test. Significance of GFP1-10 + mCherry-H6-Xa-R8-M3 is shown compared to all other conditions. *: p<0.05, **: p<0.01, ***: p<0.001, n.s.: not significant. (B) Comparison of the green fluorescence of full length EGFP and complemented GFP. RFU=Relative Fluorescent Units. Error bars present Standard error of the mean. n=3.

3.2.3 The extracellular DDS-M3 peptide cargo

In the split GFP assay to determine functional delivery of a peptide, GFP1-10 is expressed in the cytosol of cells and mimics the intracellular target and the M3 peptide acts as an extracellular cargo that requires delivery across the plasma membrane to complement with cytosolic GFP1-10 to form full length GFP. In preliminary experiments, it was shown that GFP1-10 can be expressed in the cytosol of target cells (3.2.1) and the cytosolic environment allows GFP complementation of GFP1-10 and M3 (3.2.2).

The next important step for the assay development was to acquire M3 cargo peptide that was conjugated to a drug delivery system that can facilitate its delivery across the plasma membrane. The aim of the assay to determine functional delivery of the M3 peptide, is to be able to evaluate the ability of its drug delivery system to deliver the peptide across the plasma membrane and thereby characterise novel DDSs. For the development stage of this assay, a model DDS candidate was chosen that was already well characterised and had previously been used for multiple uptake experiments by our lab, the cell penetrating peptide Octaarginine (R8) (Jones and Sayers 2012; Sayers *et al.* 2014). This peptide was chemically synthesised by EZ Biolabs, USA.

When peptides are synthesised, an important key factor to consider is the chirality of the amino acids used for synthesis as mentioned before (1.3.3.2). Hence, to achieve best uptake characteristics, all peptides in this study were synthesised using all L-amino acids which are displayed in Table 3-1.

For the generation of a drug delivery system conjugated M3 peptide, R8 was conjugated to M3 using a flexible Serine-Glycine-linker (GSGGGSTS). This amino acid linker was used to provide a spacer between the high positive charge of R8 and M3. It was previously shown by Pineaud and his colleagues that GFP complementation can take place in presence of this N-terminal linker to M3 (Pinaud and Dahan 2011).

In addition to R8-M3, experimental control peptides were purchased. These included the DDS R8 alone without the M3 cargo peptide (R8) to serve as a control that GFP complementation is specific to the M3 peptide and R8 itself cannot complement GFP1-10; M3 alone without the cell penetrating peptide R8 (M3) to confirm that M3 itself cannot cross the plasma membrane; and a Linker-M3 peptide consisting of the flexible GSGGGSTS linker and the M3 peptide (L-M3) to exclude the possibility that the GSGGGSTS linker itself has a cell penetrating ability.

When peptides are chemically synthesised they carry charged amino and carboxy termini. Hence, this charge can be removed using an acetylation or amidation of the N- or C-terminus, respectively. These modifications were also added to the purchased peptides. The C-terminus of R8 was amidated to remove its C-terminal charge to act as an appropriate control peptide for R8-M3 where the C-terminus of R8 lies within an amino acid sequence and therefore does not carry a charge. The M3 peptide is a fragment of full length GFP and the N-terminus of the amino acid in full length GFP that corresponds to the first amino acid in the M3 peptide is not charged. Hence, the N-terminus of the M3 peptide was modified with an acetylation to remove its charge. For the L-M3 peptide an N-terminal acetylation was added to remove the charge of the linker that is not charged within the R8-M3 peptide.

Table 3-1 M3 Peptides and DDS-M3 peptides.

DDS	Cargo	Peptide name	Sequence DDS-linker-M3		Modifications		Number of amino acids	Molecular weight [kDa]
					N-terminal acetylation	C-terminal amidation		
R8	M3	R8-M3	RRRRRRRRGSGGGSTSRDHMVLHEYVNAAGIT		-	-	32	3.64
R8	-	R8	RRRRRRRR		-	Yes	8	1.25
-	M3	M3	RDHMVLHEYVNAAGIT		Yes	-	16	1.81
-	M3	L-M3	GSGGGSTSRDHMVLHEYVNAAGIT		Yes	-	25	2.40

Table displays sequences, modification and characteristics of M3 and CPP-M3 peptides and used in this study. All peptides use L-amino acids, blue letters denote the sequence of the cell penetrating peptide R8 (octaarginine) and M3 sequence is coloured in green. R8 is conjugated to M3 via a linker (grey).

3.2.4 *In vitro* testing of complementation of GFP1-10 with synthetic M3 peptides – the 'fix and stain experiment'.

Before a live cell assay could be performed using the synthetic M3 peptides to test a DDS dependent delivery of M3 to GFP1-10, it was important to determine if the chemically synthesised M3 peptides are able to complement with cytosolic GFP1-10 to form full length GFP *in vitro*. For this reason an '*in vitro*' system was created where the plasma membrane barrier of cells expressing GFP1-10 was removed to allow direct access of the synthesised peptides to reassemble to full length GFP. Using this '*in vitro*' system, GFP complementation was not dependent on the delivery of M3 by a drug delivery system.

In order to investigate GFP complementation of synthetic M3 peptides with cytosolic GFP1-10 an *in vitro* system was established where HeLa transiently expressing GFP1-10 were PFA fixed and the plasma membrane was permeabilised using 0.1% Triton-X-100. All M3 peptides shown in Table 3-1 were incubated at 20 µM in PBS with the permeabilised cells for 1 hour at room temperature to allow GFP complementation. As a negative control in this experiment DMSO was chosen because it served as the diluent for the synthetic peptides. Cells were washed once after incubation and analysed with a widefield fluorescent microscope.

Negative control cells incubated with DMSO did not show any green fluorescence in their cytosol (Figure 3-8 C). Cells incubated with R8 alone was also not able complement with GFP1-10 and rescue GFP fluorescence (Figure 3-8 F). Incubation with M3 or L-M3 did not result in GFP complementation showing no difference to the DMSO and R8 control sample (Figure 3-8 I, L). GFP complementation only occurred and was clearly detectable when cells were incubated with the R8-M3 peptide (Figure 3-8 O). These results indicated that complementation of synthetic R8-M3 peptide with cytosolic GFP1-10 results in functional GFP complementation. However, the complementation must have been specifically to the M3 peptide as incubation with R8 alone did not lead to GFP

complementation. For this reason, it was surprising the M3 and L-M3 did not complement with GFP1-10. One reason for this could have been that the plasma membrane was not sufficiently permeabilised and denied access to the non DDS conjugated M3 peptides. For this *in vitro* assay the same fixation and permeabilisation protocol as for the immunofluorescent staining was used where the plasma membrane had been permeabilised to allow access of the antibody to the cytosolic target. The molecular weight of an antibody is ~150 kDa which is considerably higher compared to M3 and L-M3 (1.8 kDa and 2.4 kDa respectively).

Hence, sufficient permeabilisation can be assumed and it was next investigated if M3 peptides would complement with GFP1-10 when the incubation time was increased. To explore this, cells transiently expressing GFP1-10 were PFA fixed, 0.1% Triton-X-100 permeabilised and peptides were incubated on cells for 36 hours at 20 µM M3 peptides in PBS. GFP complementation was observed with a microscope in the presence of peptides (Figure 3-9). After 36 hours of incubation there was clear GFP complementation observable for all the peptides containing M3. Cells incubated with M3 itself, L-M3 and R8-M3 did fluoresce in green (Figure 3-9 C, D, E) and there was no green fluorescence detectable in cells treated with DMSO or R8 (Figure 3-9 A, B). Due to the transient transfection of GFP1-10 not every cell expressed the GFP1-10 target protein; hence not every cell was positive for GFP complementation. This experiment indicated that all synthetic peptides containing M3 were able to complement with GFP1-10 in an *in vitro* situation where the plasma membrane barrier is removed and confirmed that R8 alone cannot complement with GFP.

The finding that M3 and L-M3 will complement with GFP1-10 but not as efficient as R8-M3 raised the question if this is an effect of the applied method rather than inability of the peptide to complement with GFP1-10. PFA fixation and Triton-X-100 permeabilisation can cause extraction of cytosolic proteins (Schnell *et al.* 2012). It was shown that the fluorescence of cytosolic EGFP is concentrated in the nucleus

after PFA fixation and Triton-X-100 permeabilisation which is an effect of the decrease of cytosolic EGFP fluorescence compared to the nucleus rather than relocation. When using this fixation and permeabilisation method to investigate complementation of GFP1-10 with a synthetic M3 peptide, the same effect was seen (Figure 3-9). The green fluorescence was mainly localised at the nucleus and less in the cytosol. Proteins can be better preserved during fixation and permeabilisation when they are located to organelles or associated with membranes (Stadler *et al.* 2010).

The assumption that GFP1-10 does not remain in the cytosol in high amounts in order to generate a sufficient GFP 1-10 with M3 and L-M3 leads to the question as to why R8-M3 did still complement with GFP1-10. R8 is highly positively charged and could interact with fixed and permeabilised cells through its charge. This interaction could favour a higher affinity for R8-M3 to the cells and gain access to the low levels of fixed GFP1-10.

Due to the fact that M3 and L-M3 are not charged and these pure peptides had to be tested in an *in vitro* assay without alteration, the idea was further investigated, to achieve higher internal GFP1-10 levels after fixation by fusing GFP1-10 to an intracellular organelle.
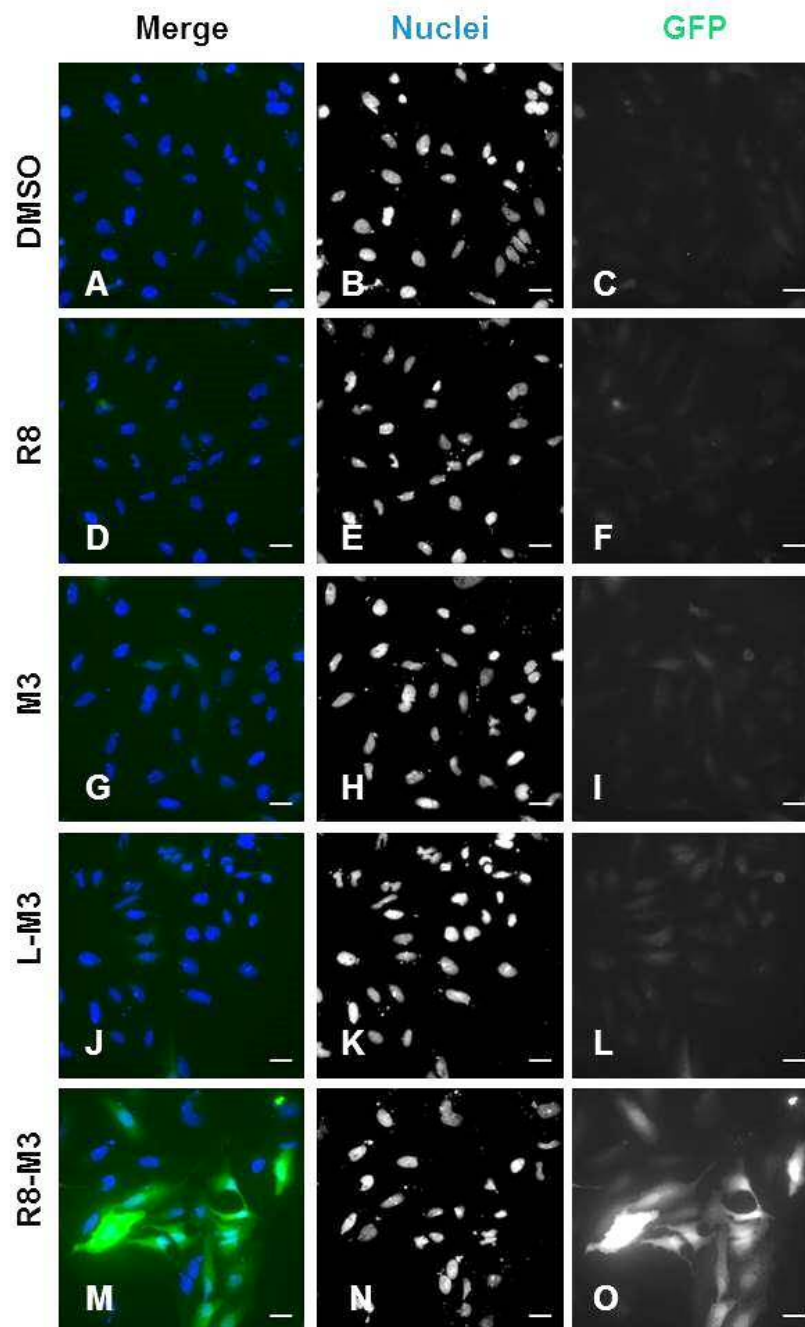
Figure 3-8 Complementation of GFP1-10 and M3 peptides '*in vitro*' after 1 hour.
Hela cells transiently expressing GFP1-10 were PFA fixed and the plasma membrane was permeabilised using 0.1% Triton-X-100. Peptides were incubated at 20 μM in PBS for 1 hour at room temperature to allow complementation of GFP1-10 with M3 to form full length GFP. Cells were washed once in PBS and nuclei were counterstained with DAPI. Representative images are shown for each condition. Scale bars: 30 μm. n=3.
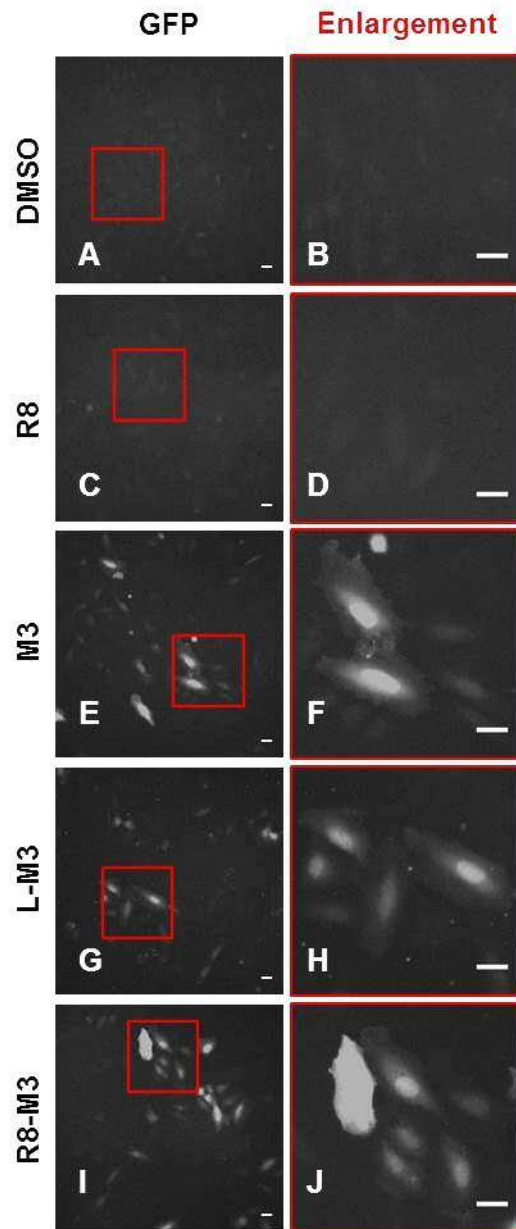
Figure 3-9 Complementation of GFP1-10 and M3 peptides 'in vitro' after 36 hours.
Hela cells transiently expressing GFP1-10 were PFA fixed and the plasma membrane was permeabilised using 0.1% Triton-X-100. Peptides were incubated at 20 µM in PBS for 36 hours at room temperature to allow complementation of GFP1-10 with M3 to form full length GFP. Peptides were left on the cells and GFP complementation was investigated using a widefield fluorescent microscope. Representative images are shown for each condition. Scale bars: 30 µm. n=2.

To test if the weak GFP complementation with M3 and L-M3 can be enhanced by using an organelle fused GFP1-10 that allows better preservation during the fixation and permeabilisation process, an expression construct was generated to express GFP1-10 as a C-terminal fusion of the Golgi stacking protein GRASP65 to obtain pGRASP65-EGFP-N2 (2.11.1). GRASP65 is a peripheral Golgi membrane protein on the cytoplasmic surface of the Golgi Apparatus which is retained at the plasma membrane through myristic acid at its N-terminus (Zhang and Wang 2015). The N-terminal domain is also the interaction surface to build a transoligomer with another GRASP65 molecule to form a Golgi stack (Wang *et al.* 2005). Hence, fusion of GFP1-10 to the C-terminus of GRASP65 ensured that GFP1-10 was localised to an organelle but was still accessible in the cytosol to complement with the M3 peptides.

To observe the expression pattern of GRASP65 it was first expressed as a fusion protein to EGFP. Cells were PFA fixed and triton-X100 permeabilised to investigate the remaining protein within the cell. In Figure 3-10 the phenotype of GRASP65-EGFP can be seen. It varies from being solely localised to the Golgi apparatus to being overexpressed in the cytosol, but more importantly, the protein did remain present in the cell after fixation and permeabilisation. It was further tested if GRASP65-GFP1-10 could be expressed, and detected in the cell using immunofluorescence. When GRASP65-GFP1-10 was expressed in HeLa cells, it did not fluoresce in green but the antibody labelling showed expression of the protein at the Golgi apparatus as well as overexpressed in the cytosol (Appendix Figure 9-3). Complementation of GRASP65-GFP1-10 with mCherry-H6-Xa-R8-M3 was tested when both proteins were co-expressed in HeLa cells. Single fragments did not show green fluorescence, co-expression resulted in GFP complementation and detection of green fluorescence on the plate reader (Appendix Figure 9-4).

Having confirmed that GRASP65-GFP1-10 can be expressed in HeLa cells, it is localised to the Golgi apparatus and it can complement mCherry-H6-Xa-R8-M3 to form full length GFP, GRASP65-GFP1-10 was tested for complementation with synthetic peptides. For the GFP complementation experiment with synthetic M3 peptides, cells transiently expressing GRASP65-GFP1-10 were PFA fixed and permeabilised using 0.1% Triton-X-100. Different peptides were incubated on cells at 20 µM in PBS for 1 hour at room temperature to allow GFP complementation. Cells were washed in PBS, nuclei were stained with DAPI and the coverslips were mounted onto a glass slide to be analysed with a widefield fluorescent microscope. When R8 itself was incubated with GRASP65-GFP1-10 expressing cells, no green fluorescence was observed (Figure 3-11 F) which correlated with cells incubated with DMSO (Figure 3-11 C). When L-M3 and M3 were incubated with the cells, weak GFP fluorescence was detected indicating that M3 had complemented with GRASP65-GFP1-10 (Figure 3-11 I, L). When R8-M3 was incubated with the cells, bright green fluorescence was observed (Figure 3-11 O). The fluorescence of cells incubated with R8-M3 was much brighter compared to cells incubated with M3 or L-M3 peptides. Nevertheless, M3 and L-M3 did complement with GRASP65-GFP1-10 within 1 hour which can clearly be observed when the brightness levels of these samples are adjusted independently from the R8-M3 control (Figure 3-11 R, U). When the localisation of GFP fluorescence is examined, it correlates with the localisation when GRASP65-EGFP is expressed in the cell. Fluorescence is predominantly detected in overexpressing cells where GFP fluorescence is distributed throughout the cytosol but with a concentration of fluorescent signal in the perinuclear region where the Golgi apparatus is localised.

Summing up the 'in vitro' complementation experiments of synthetic peptides with expressed GFP1-10 or GRASP65-GFP1-10, it was seen that R8-M3 can complement with cytosolic or Golgi localised GFP1-10 within one hour. M3 and L-M3

did complement with cytosolic GFP1-10 after a longer incubation time of 36 hours and as fast as 1 hour with GRASP65-GFP1-10. The GFP fluorescence detected in the experiments were generally weaker for M3 and L-M3 then when cells were incubated with R8-M3.

Taken together, the experiments clearly show that GFP complementation with GFP1-10 or GRASP65-GFP1-10 occurs when peptides carry the M3 fragment. The complementation is specific to the M3 fragment, as neither the DMSO diluent nor R8 by itself are able to replace the function of the proton acceptor which is located on the M3 peptide.

The efficiency of M3 and L-M3 to complement with GFP1-10 seems to be dependent on where the intracellular GFP1-10 target is localised during the fixation and permeabilisation process, low success of complementation could therefore be due to the experimental design. It also has to be considered that the *in vitro* system is an artificial system and GFP complementation dynamics could vary significantly in live cells from this '*in vitro*' system. Nonetheless, these experiments gave enough confidence that the synthetic M3 containing peptides will complement with expressed GFP1-10 which led to the next step to investigate M3 delivery in live cells.
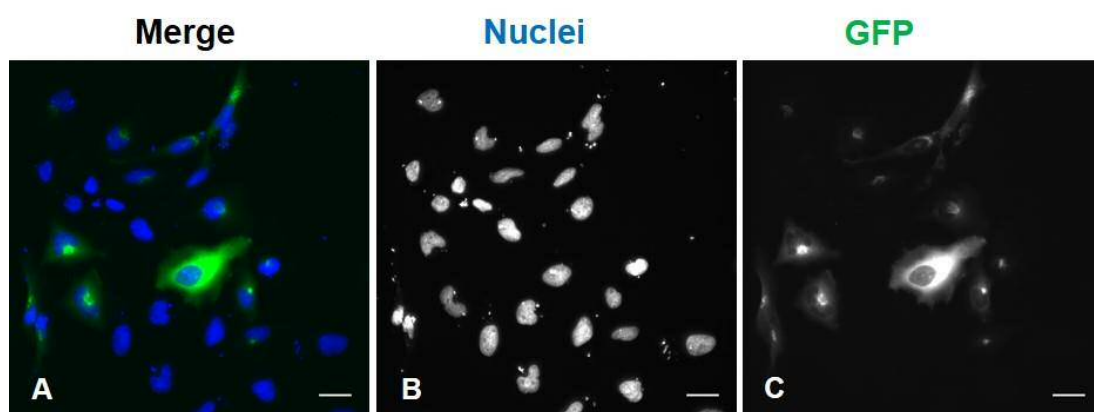
Figure 3-10 Phenotype of GRASP65-EGFP.
HeLa cells were transiently transfected with GRASP65-EGFP. The next day the cells were PFA fixed and 0.1% Triton-X100 permeabilised. Scale bar: 30 µm. n=1.
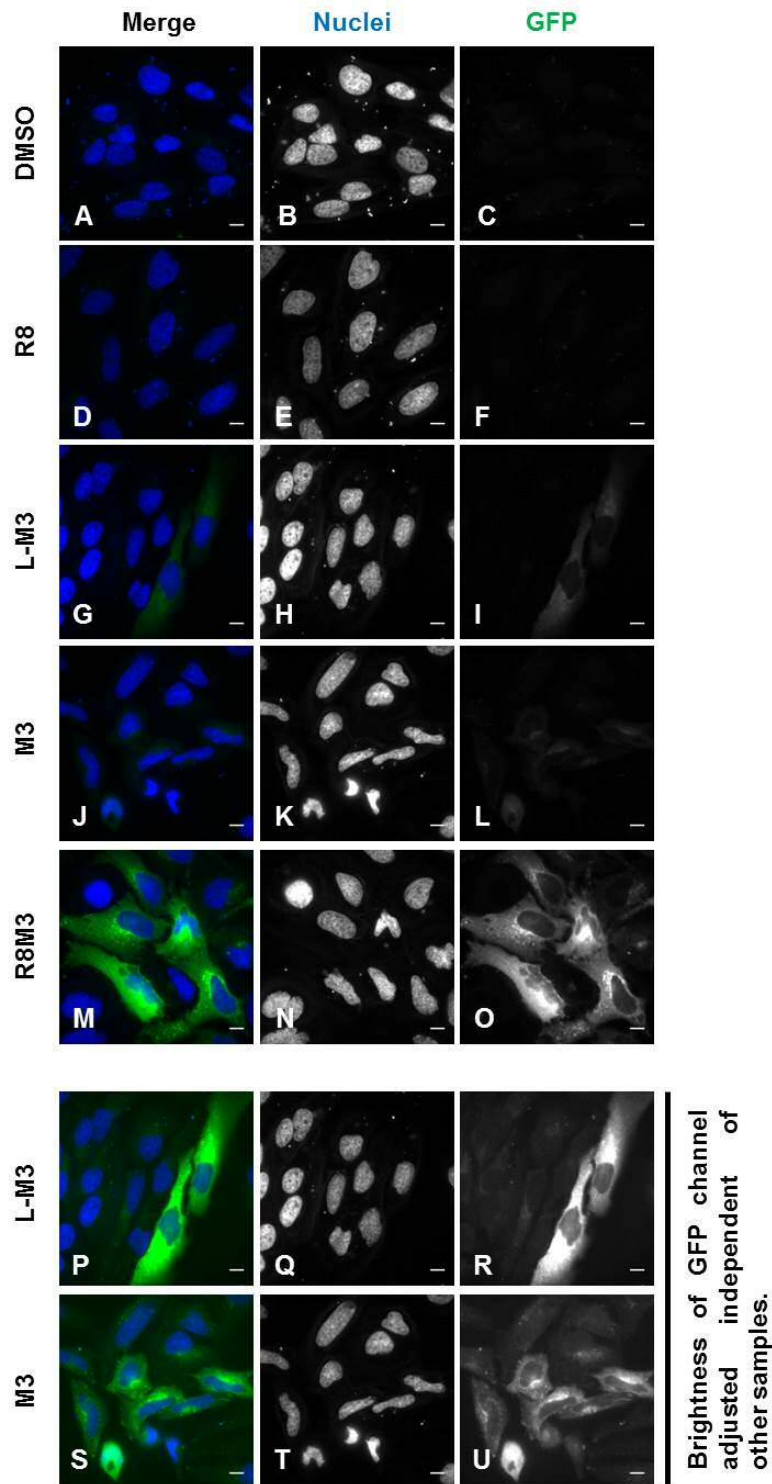
Figure 3-11 Complementation of GRASP-65-GFP1-10 and M3 peptides 'in vitro'.
Hela cells transiently expressing GRASP65-GFP1-10 were PFA fixed and the plasma membrane was permeabilised using 0.1% Triton-X-100. Peptides were incubated at 20 µM in PBS for 1 hour at room temperature to allow complementation of GRASP65-GFP1-10 with M3 peptides to form full length GFP. Cells were washed once in PBS and nuclei were counterstained with DAPI. Images A-O were processed using exactly the same GFP saturation. Images P-U display images shown in G-L but the brightness of the GFP channel is increased. Scale bars: 30 µm. n>3. The data displayed is taken from an experiment that was performed by Alexander Dudziak under my supervision.

3.3 Investigation of real time functional delivery of M3 by the DDS R8 using the split GFP system.

Previous experiments have ensured that the intracellular target GFP1-10 can be expressed in the cytosol of Hela cells (3.2.10) and that GFP1-10 complements with M3 when co-expressed in HeLa cells (3.2.2) as well as with synthetic M3 peptides in an *in vitro* assay (3.2.4). These are important results that lead up to the successful development of a live cell assay to investigate if M3 can be functionally delivered across the plasma membrane using the DDS R8.

3.3.1 Delivery of M3 by the DDS R8

To test if functional delivery of the M3 peptide by R8 can be detected using a widefield fluorescent microscope in live cells, HeLa cells were transiently transfected in MatTek glass bottom dishes with pGFP1-10-N1 to express cytosolic GFP1-10. On the day of the experiment the transfected cells were washed once in serum free medium and peptides were incubated with cells at 20 µM in serum free medium. Serum free medium was chosen as a diluent to avoid peptide degradation by proteases that are contained in FBS. In previous experiments within our lab, uptake of labelled R8 containing peptides was monitored after 1 hour and found in endocytic compartments when incubated at 2 µm or 5 µm (Sayers *et al.* 2014). For the live experiments an incubation time of 2 h was used to allow R8-M3 to be taken up by the cell, reach the cytosol and for GFP complementation to take place. After 2 hours cells were washed in phenol red free RPMI, nuclei were counterstained with Hoechst and cells were imaged in phenol red free RPMI on a widefield fluorescent microscope at 37°C and 5% CO_2.

Control cells that were incubated with DMSO in serum free media only showed background levels of green fluorescence in the GFP channel (Figure 3-12 C). When cells were incubated with the L-M3 peptide the same background levels as in the

DMSO control were detected indicating that GFP complementation had not occurred (Figure 3-12 F). Incubation with R8-M3 resulted in the occurrence of green fluorescent cells (Figure 3-12 I), indicating that M3 had been functionally delivered to its intracellular GFP1-10 to form full length GFP. Here, the L-M3 peptide was tested as due to the presence of the N-terminal linker it represents a better control to R8-M3, where R8 is connected to M3 via the same linker.

To further verify this outcome, green fluorescent intensities of the cytosol of single cells where quantified from microscopy images that were randomly taken during the experiment (Figure 3-13 A). The corrected total cell fluorescence (CTCF) of the green fluorescence was calculated for 25-30 cells per condition. DMSO control cells show a distribution of a cytosolic CTCF between 0-8 (Figure 3-13 A) with a mean value of 2.5 between experiments (Figure 3-13 B). When cells were incubated with L-M3, fluorescent CTCF of single cells ranged from 0-6 (Figure 3-13 A) with an overall average CTCF of 2.5 between experiments (Figure 3-13 B). This data correlates with the images displayed in Figure 3-12, that cells incubated with DMSO or L-M3 have the same level of green background fluorescence in their cytosol indicating that L-M3 did not functionally reach the cytosol to complement with GFP1-10. Analysis of green fluorescent intensity of cells that were incubated with 20 µM R8-M3 revealed that there was a large distribution of CTCF ranging from zero to the highest value of 17 (Figure 3-13 A). The average fluorescent intensity was 3.9 (Figure 3-13 B). This is a 1.5 increase in mean fluorescence compared to the DMSO negative control.

These important results prove the principle of this assay: L-M3 cannot pass the plasma membrane by itself and the flexible linker connecting it to its drug delivery system has no ability to facilitate delivery of the peptide. When the M3 peptide is attached to the DDS R8, the cell penetrating peptide facilitates delivery of M3 to the cytosol where it complements with GFP1-10 resulting in green fluorescence. Hence, functional M3 delivery to its intracellular target is dependent on R8 and this data set

supports the hypothesis that the split GFP assay can be utilized to investigate functional delivery of the M3 peptide by a drug delivery system such as R8.

When cells were incubated with 20 μM R8-M3 for 2h, the green fluorescence had not increased in every single cell indicating that GFP complementation had not occurred in every cell that was exposed to R8-M3. This could either be due to transient expression of GFP1-10 and that cells were not expressing the intracellular GFP1-10 target or lack of the delivery of M3 to a GFP1-10 expressing cell. Figure 3-13 C shows an example image that was obtained when cells were incubated with 20 μM R8-M3 and their corresponding green fluorescent values can be seen in Figure 3-13 D. Delivery of M3 and GFP complementation had clearly occurred in cell 1 and its fluorescence corresponds to 17 which is highly increased compared to the average fluorescent intensity obtained from DMSO control cells (2.5). The fluorescence seen in cell 2 and 3 corresponds to 6.4 and 4.5, respectively. This amount of fluorescence lies within the range of fluorescence that was detected for DMSO control samples and leads to the suggestion that those cells were negative for GFP complementation.

Because cells were transiently expressing GFP1-10, expression in single cells varies between high expression levels of GFP1-10 to not expressing the protein at all. Hence, only cells will complement with M3 that express GFP1-10 in their cytosol and the degree of complementation will be dependent on the amount of GFP1-10 that is expressed. It could be possible that cells 2 and 3 (Figure 3-13 C) do contain functionally delivered M3 but do not express GFP1-10 and therefore were not positive for GFP complementation.

Another possibility is that cells 2 and 3 are expressing GFP1-10 in their cytosol but R8-M3 has not been taken up by the cells or M3 was not functionally delivered and therefore GFP complementation had not occurred. R8-M3 is a non-fluorescent peptide, hence uptake of this peptide into cells cannot be monitored live. In order to investigate if the R8-M3 peptide is taken up evenly across the cell population and to

112

confirm that GFP1-10 expression is the limiting factor for lacking GFP complementation, a fluorescently labelled version of R8-M3 was synthesised: Rhodamine-R8-M3 (Rh-R8-M3).
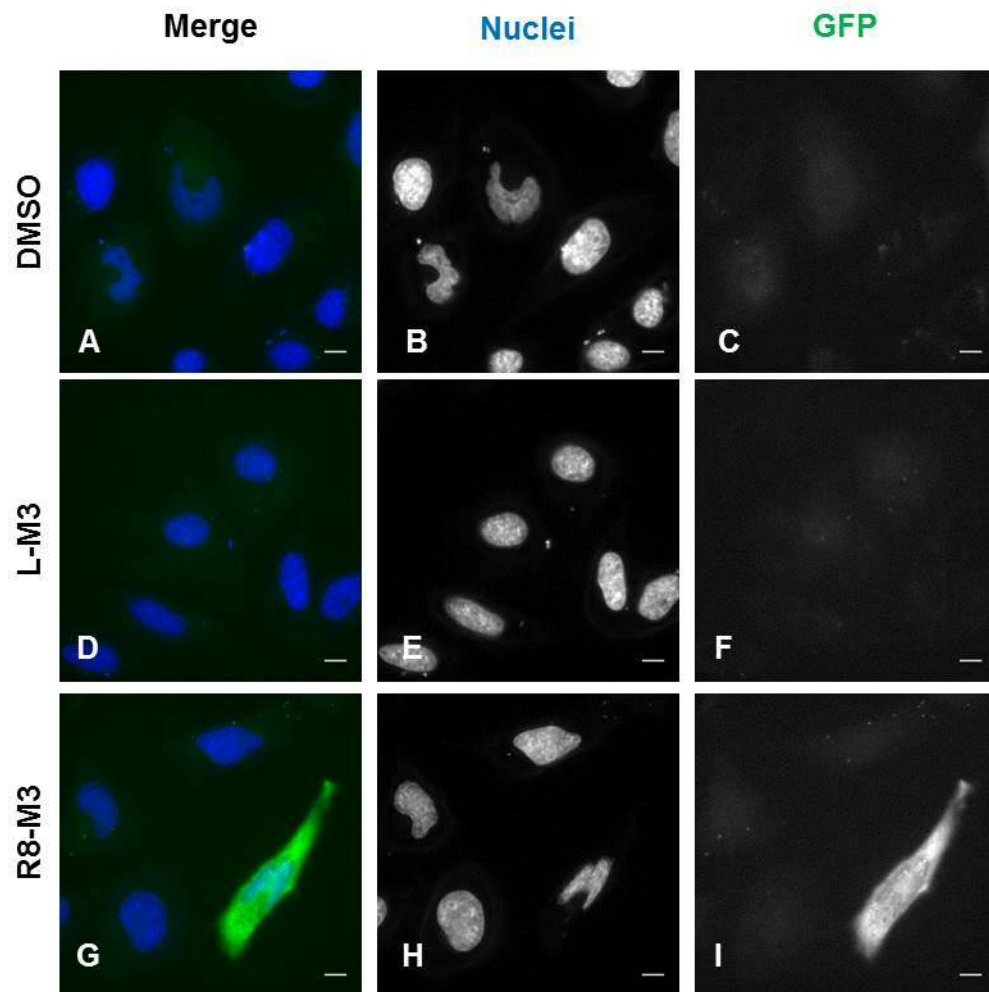
Figure 3-12 Delivery of M3 and GFP complementation in live cells.
Cells transiently expressing GFP1-10 were washed once in serum free media and incubated with DMSO, L-M3 or R8-M3 at 20µM in serum free media for 2 hours at 37°C. Cells were washed with phenol red free RPMI and counterstained with Hoechst nuclear dye. Live cells were images at 37°C and 5% CO_2 in phenol red free RPMI. Scale bar: 10µm.
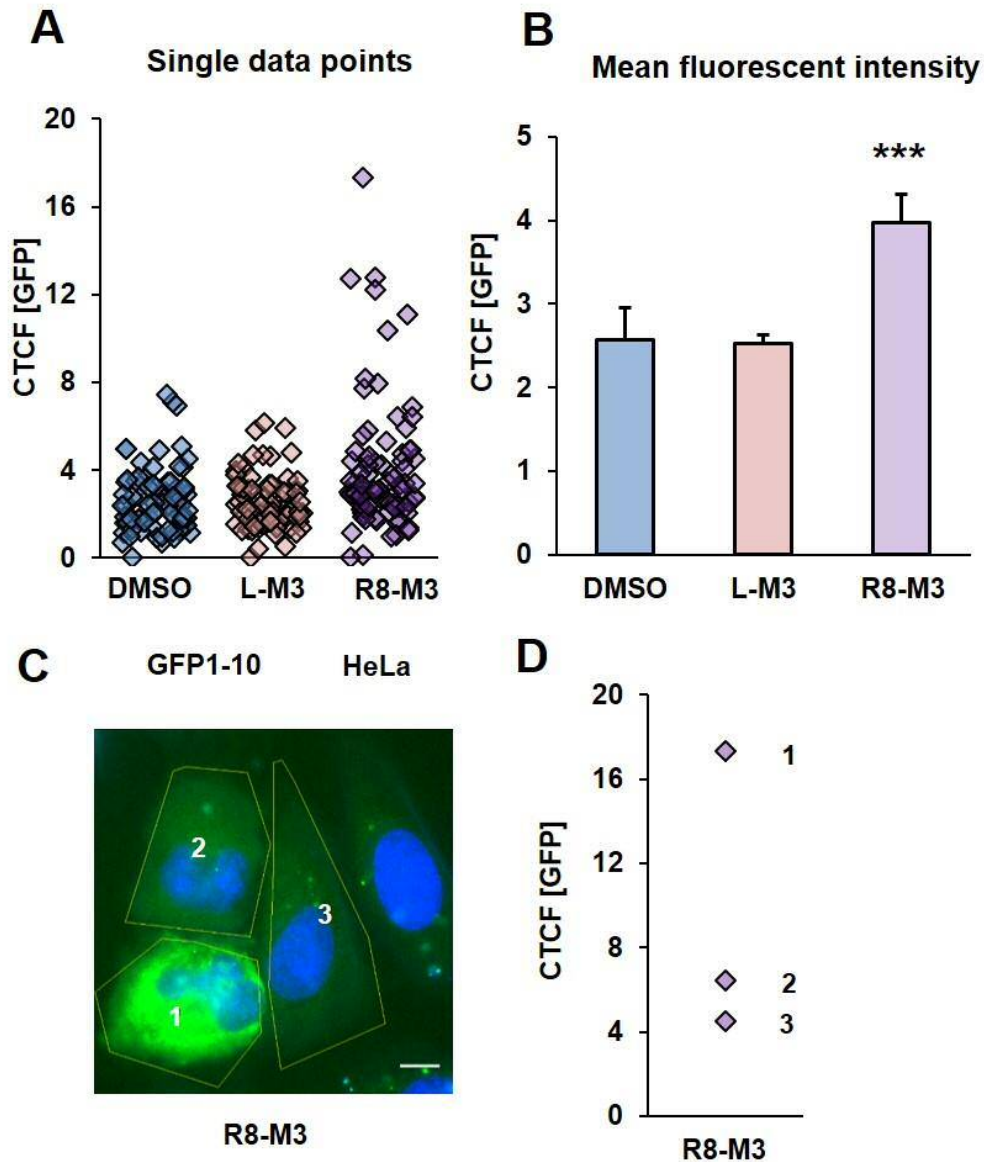
Figure 3-13 Quantification of R8 dependent delivery of M3 peptide into cells transiently expessing GFP1-10.
Quantification of random images taken on the microscope of cells transiently expressing GFP1-10 that were incubated with 20µM DMSO, L-M3 or R8-M3 in serum free media for 2 hours at 37˚C. CTCF=Corrected Total Cell Fluorescence. (A) Every data point represents a single cell treated with DMSO, L-M3 or R8-M3. (B) Mean fluorescence intensity represents the average CTCF from three individual experiments of cells treated with DMSO, L-M3 or R8M3. N=3, 25-30 cells were analysed per sample per experiment. Error bars display standard error of the mean between three experiments. For statistical analysis data was tested using a Kruskal-Wallis test. Significance is shown compared to M3 and DMSO. *: $p<0.05$, **: $p<0.01$, ***: $p<0.001$, n.s.: not significant. (C) Representative image of cells incubated with 20µM R8-M3. Scale bar represents 10µm. (D) Quantification of corrected total cell fluorescence (CTCF) of the cells three cells shown in image C.

3.3.2   Labelled peptide to monitor R8-M3 uptake: Rhodamine-R8-M3.

Rhodamine is a small fluorescent dye with an excitation and emission maximum of 555 nm and 580 nm, respectively. With these fluorescent properties, a minimal amount of bleed through into the green channel was expected which made it a suitable fluorophore to study the uptake of R8-M3 with little interference with the signal obtained from GFP complementation in the green channel (excitation and emission spectrum see Appendix Figure 9-5). To be able to conjugate Rhodamine to the N-terminus of R8-M3, an additional Glycine had to be added to the N-terminus of the amino acid sequence. Conjugation of Rhodamine to the R8-M3 peptide changed the molecular weight of the cargo complex from 3.64 kDa for R8-M3 (Table 3-1) to 4.14 KDa for Rh-R8-M3 (Table 3-2) which is a small change in the molecular weight of the peptide, which led to the expectation that uptake and delivery of M3 would not be altered significantly compared to unlabelled R8-M3.

Table 3-2 RhodamineR8-M3 peptide

| DDS | Cargo | Peptide name | Sequence

DDS-linker-M3 | Modifications | | Number of amino acids | Molecular weight [kDa] |
				N-terminal	C-terminal		
R8	M3	RhR8-M3	GRRRRRRRRGSG GGSTSRDHMVLH EYVNAAGIT	Carboxytetramethylrhodamine (TAMRA)	-	33	4.14

Table displays sequences, modification and characteristics of RhR8-M3. Blue letters denote the sequence of the cell penetrating peptide R8 (octaarginine) and M3 sequence is coloured in green. R8 is conjugated to M3 via a linker (grey) Rhodamine is conjugated to a Glycine (G) that was added N-terminally to the amino acid sequence (black).

In order to investigate the uptake of the Rhodamine labelled R8-M3 peptide (RhR8-M3), the live assay was performed with cells transiently expressing GFP1-10 that were incubated with 20 µM DMSO, L-M3, R8-M3 or RhR8-M3. After two hours cells were imaged using a widefield fluorescent microscope. No green fluorescence was detected in the cytosol of cells incubated with the DMSO and L-M3 control peptides, (Figure 3-14 C, H). For cells incubated with R8-M3, green fluorescence can be displayed in the GFP channel in this image (Figure 3-14 M). Cells incubated with RhR8-M3 showed that the peptide was taken up evenly across the cell population (Figure 3-14 S) and a high amount of GFP complementation could be detected in these cells, (Figure 3-14 R). Interestingly, the green fluorescence was mainly localised to the nucleolus.

When images were processed for Figure 3-14, all grey levels of the GFP channel were adjusted so that GFP fluorescence was clearly visible for cells incubated with RhR8-M3 and no sample was shown overexposed. Due to the large difference of green fluorescence that occurred in cells incubated with R8-M3 compared to RhR8-M3, only low green fluorescence could be shown for cells incubated with R8-M3 in Figure 3-14 M.

To emphasize low fluorescent GFP levels that were actually detected in cells over the black background of the image, all images of the GFP channel were converted to be displayed on a sepia lookup table (Figure 3-14 E, J, O, T). Images shown on a sepia scale reveal that no GFP complementation was detected on cells incubated with DMSO and L-M3 (Figure 3-14 E, J) whereas low levels of GFP fluorescence was detected in cells incubated with R8-M3 (Figure 3-14 O). This fluorescence was very low compared to GFP fluorescence detected in cells incubated with RhR8-M3 where the brightest GFP fluorescence was observed at the nucleolus (Figure 3-14 T). These results suggest that a DDS dependent functional delivery of the M3 peptide had occurred in cells incubated with R8-M3 and RhR8-M3.

As shown before, only one cell in the field of view was positive for GFP complementation when cells were incubated with R8-M3 (Figure 3-14 O). When the uptake of R8-M3 was monitored using the Rhodamine labelled peptide (RhR8-M3), it was clearly visible that the fluorescence of the peptide was associated with every cell. (Figure 3-14 S). GFP complementation was visible in most cells of the field of view confirming that the peptide had been taken up by the cell and the M3 peptide was delivered to cytosolic GFP1-10. Despite this even uptake of RhR8-M3 across the cell population, the degree of GFP complementation was decreased in one cell (Figure 3-14 R, marked with a star) compared to others. This could have been an effect of cells expressing a different amount of GFP1-10 in their cytosol and therefore GFP complementation was limited by intracellular GFP1-10 levels.

Surprisingly, the number of cells where GFP complementation had occurred was increased when cells were incubated with RhR8-M3 compared to R8-M3. A reason for this could be a different transfection efficiency between samples. However, cells that were incubated with R8-M3 and RhR8-M3 were transfected with the same DNA transfection mix to express GFP1-10 which means distribution of GFP1-10 expression levels should remain the same between these samples. Thus, it seems more likely that the observed effect is dependent on the incubation of the cells with Rh-R8-M3 and that this peptide delivers M3 more efficiently into the cells than R8-M3.

In summary, the above findings show that the number of cells where GFP complementation had occurred as well as the degree of GFP complementation is increased when cells are incubated with RhR8-M3 compared to R8-M3 meaning that the rhodamine label could have an increasing effect on functional delivery of the M3 peptide. However, red fluorescence of the rhodamine labelled R8-M3 peptide was extremely bright under the microscope, so that bleed through of rhodamine signal into the GFP channel is a concern. Originally the RhR8-M3 peptide was purchased

because it was thought that there was a low amount of bleed through signal between the red and the green channel. However the rhodamine labelled peptides showed extremely bright fluorescence. The capture settings on the microscope were set to 11% light power and 10 ms exposure time (Alexa 568 filter setting) compared to 100% light power and 500 ms exposure time to capture GFP fluorescence. This bright red fluorescence could be the source of more bleed through into the green channel than it was expected when this peptide was purchased.

Hence, to prove the that GFP complementation is increased with RhR8-M3 compared to R8-M3, it needs to be investigated if the GFP fluorescence seen in cells transiently expressing GFP1-10 is a true signal resulting from GFP complementation or an artefact of microscopy bleed through.
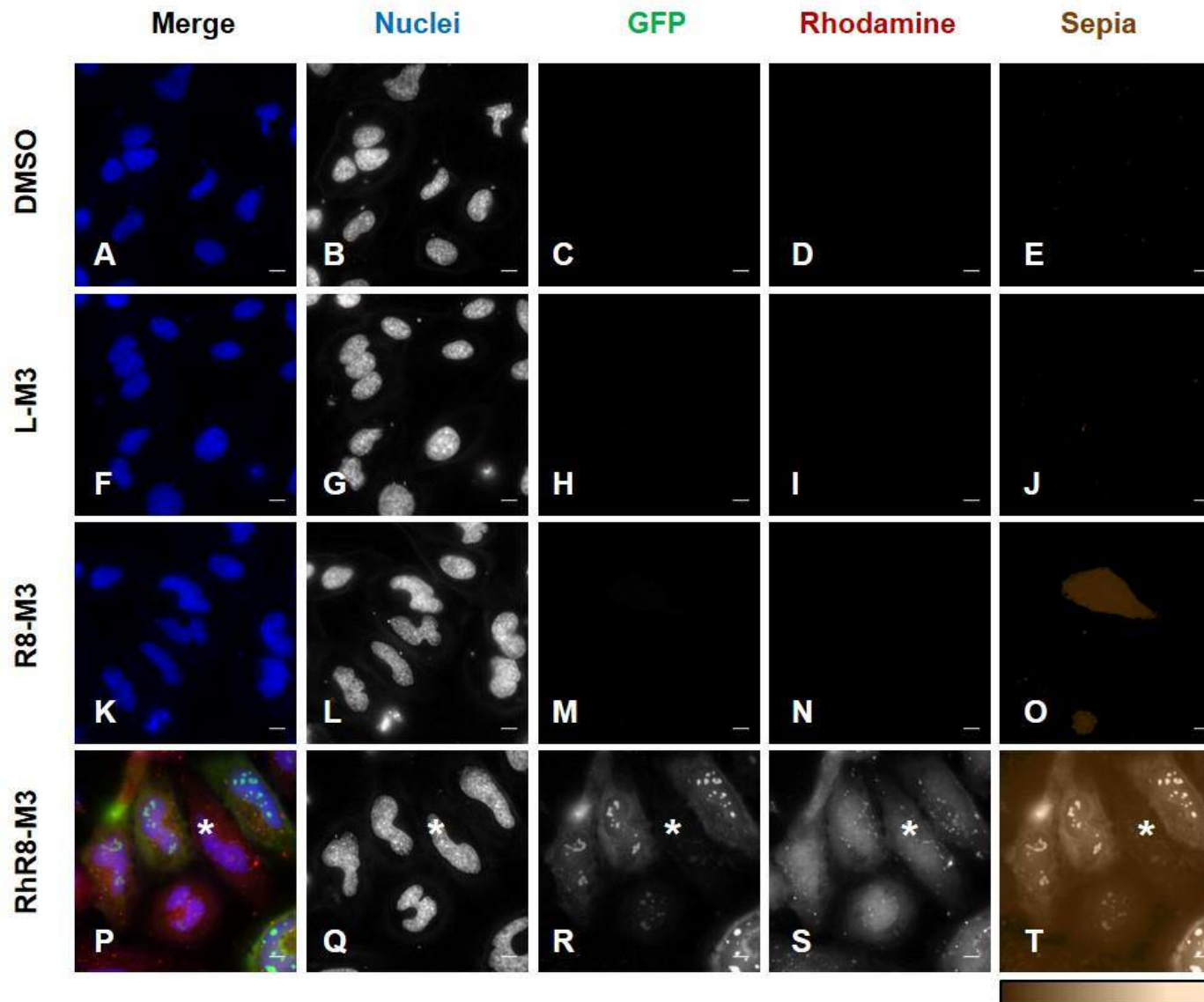
Figure 3-14 Monitoring peptide uptake using Rhodamine-R8-M3.
Cells transiently expressing GFP1-10 were washed once in serum free media and incubated with DMSO, L-M3, R8-M3 or Rhodamine labelled R8-M3 (RhR8-M3) at 20µM in serum free media for 2 hours at 37°C. Cells were washed with phenol red free RPMI and counterstained with Hoechst nuclear dye. Live cells were imaged at 37°C and 5% CO_2 in phenol red free RPMI. Images from the GFP channel are additionally shown with a sepia filter to enhance weak fluorescence of cells. Sepia lookup table calibration bar displays a range from 689 to 34627 grey levels. (P-T) Cell marked with a star shows a cell that has taken up the same amount of RhR8-M3 as other cells but shows lower levels of GFP. Scale bar: 10µm. n=3.

To investigate the amount of bleed through of the Rhodamine labelled peptide, cells incubated with RhR8-M3 on transiently expressing GFP1-10 were compared to untreated HeLa cells incubated with RhR8-M3 (Figure 3-15). Incubation of RhR8M3 on HeLa cells that are not expressing GFP1-10 cannot lead to GFP complementation because the cytosolic GFP1-10 target protein is not expressed in these cells. Thus, the fluorescence detected in the GFP channel will only be a result of "false" green fluorescence where Rhodamine was excited with 488 nm wavelength and the emission was collected as a bleed through signal that passed through the GFP emission filter.

Microscopy images suggest that there is little difference of RhR8-M3 uptake between cells transiently expressing GFP1-10 and untreated HeLa cells (Figure 3-15 A- IV, IX). Quantification of the corrected total cell fluorescence (CTCF) of single cells in three independent experiments confirms that the distribution of CTCF values of rhodamine fluorescence in single cells is similar between cells transiently expressing GFP1-10 and untreated HeLa cells (Figure 3-15 B). Surprisingly there is a high variation in the amount of rhodamine fluorescence in these cells, ranging from 0-2000. This high range of fluorescent intensities between cells suggests that cells do take up varying amounts of the peptide and uptake is not even across the cell population as expected. The mean fluorescent intensities of the CTCF of rhodamine between three experiments appeared to be slightly increased in HeLa cells compared to cells expressing GFP1-10 with values of 517 and a SEM of 77 compared to 448 and a SEM of 60, respectively (Figure 3-15 C). This difference is not significant, confirming that the overall uptake is not altered between GFP1-10 transfected cells and untransfected HeLa cells.

Investigation of the GFP fluorescence between GFP expressing cells and untreated HeLa cells that were incubated with RhR8-M3 using microscopy clearly shows that GFP fluorescence was only detected when cells were expressing GFP1-

10 (Figure 3-15 A- III, VIII). Moreover, this can be confirmed by quantification of the microscopy images. CTCF of GFP in single cells expressing GFP1-10 ranged from 8 to >1000 on a logarithmic scale compared to HeLa cells with values between 8 and 80 (Figure 3-15 D). Mean values of the CTCF of GFP between three experiments were 121 with and 16 for cells expressing GFP1-10 and untreated HeLa cells, respectively. This difference in green fluorescence is significant ($p<0.001$) confirming that green fluorescence detected in cells transiently expressing GFP1-10 is derived from GFP fluorescence that resulted from GFP complementation of GFP1-10 and M3.
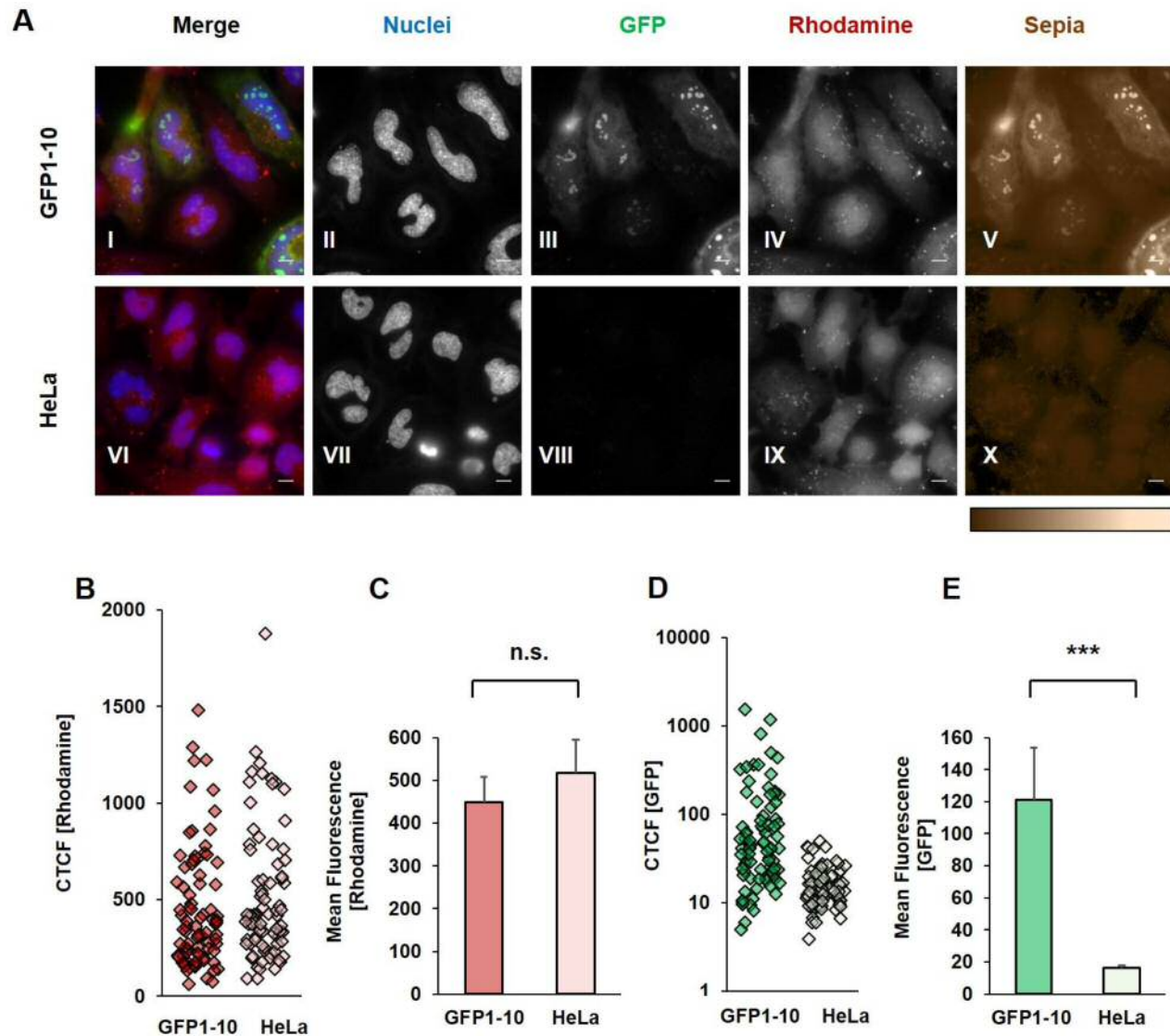
Figure 3-15 Comparison of RhR8-M3 uptake on GFP1-10 expressing cells and untransfectd HeLa cells.

Cells transiently expressing GFP1-10 (GFP1-10) or untransfected HeLa cells (HeLa) were washed once in serum free media and incubated with Rhodamine labelled R8-M3 (RhR8-M3) at 20μM in serum free media for 2 hours at 37°C. Cells were washed with phenol red free RPMI, counterstained with Hoechst nuclear dye and imaged live. (A) Representative images of cells shown. Images from the GFP channel is additionally shown with a sepia filter. Sepia calibration bar displays a range from 689 to 34627 grey levels. Scale bar: 10μm. (B-E) Quantification of fluorescence of microscopy images shown, 25-29 cells were analysed per sample per experiment. (B) CTCF of Rhodamine in the cytosol of single cells. Every data point represents CTCF of rhodamine of one cell. (C) Mean fluorescent intensity represents the average CTCF of Rhodamine fluorescence of cells. Error bars display SEM. (D) CTCF of GFP in the cytosol of single cells. Every data point represents CTCF of rhodamine of one cell. (E) Mean fluorescent intensity represents the average CTCF of Rhodamine fluorescence of cells. Error bars display SEM. For statistical analysis data was tested using a Shapiro-Wilk normality test followed by a Mann-Whitney Wilcoxon test. *: $p < 0.05$, **: $p < 0.01$, ***: $p < 0.001$, n.s.: not significant. n=3.

3.3.3 Comparison of delivery efficiency of R8-M3 and Rh-R8-M3

Finally, the ability to functionally deliver M3 into cells expressing GFP1-10 was compared between L-M3, R8-M3 and RhR8-M3 (Figure 3-16). As experimental controls were cells expressing GFP1-10 incubated with DMSO and untransfected HeLa cells incubated with RhR8-M3. Both of these samples cannot be positive for GFP complementation as Hela cells incubated with Rh-R8-M3 lack the intracellular GFP1-10 cargo and GFP1-10 expressing cells incubated with DMSO lack M3 cargo peptide. Nevertheless, it was visible that untransfected HeLa cells incubated with RhR8-M3 (RhR8-M3 HeLa) show a higher GFP fluorescence compared to GFP1-10 expressing cells incubated with DMSO (Figure 3-16 A). As untransfected HeLa cells will not be able to complement with M3 to form full length GFP, this increase in GFP fluorescence shows the amount of "false" GFP signal that is derived from the rhodamine fluorophore that is collected as GFP signal.

In order to be able to show the fold change of GFP fluorescence as a result of GFP complementation, this value was subtracted as the background from cells expressing GFP1-10 that were incubated with RhR8-M3 (green bar). For L-M3 (orange bar) and R8-M3 (purple bar), the value obtained from cells treated with DMSO was subtracted as the background.

The comparison of delivery of M3 between L-M3, R8-M3 and RhR8-M3 after background subtraction is shown in Figure 3-16 B. The fold change of GFP fluorescence as a result of GFP complementation is shown on a logarithmic scale. L-M3 shows very little change in GFP fluorescence indicating that this peptide was not able to cross the plasma membrane and M3 did not complement with cytosolic GFP1-10. Incubation of 20 µM R8-M3 led to GFP fluorescence suggesting that R8 facilitated the delivery of M3 to the cytosol of GFP 1-10 transfected cells. The Rhodamine labelled R8-M3 peptide that was originally purchased to enable to track the uptake of R8-M3 using a microscope, however when cells transiently expressing GFP1-10 were

incubated with this peptide, green fluorescence increased meaning that GFP complementation had occurred. Compared to R8-M3 the delivery efficiency of RhR8-M3 was increased. These results are based on the assumption that the transfection efficiency between the different samples were consistent because the same transfection mix was used between the samples.

In summary, these findings strongly suggest that Rhodamine can enhance the efficiency of R8 to deliver M3 across the plasma membrane to complement with cytosolic GFP1-10. The reason for enhancement of the delivery is further discussed at the end of this chapter.

A

Before background subtraction

B

After background subtraction
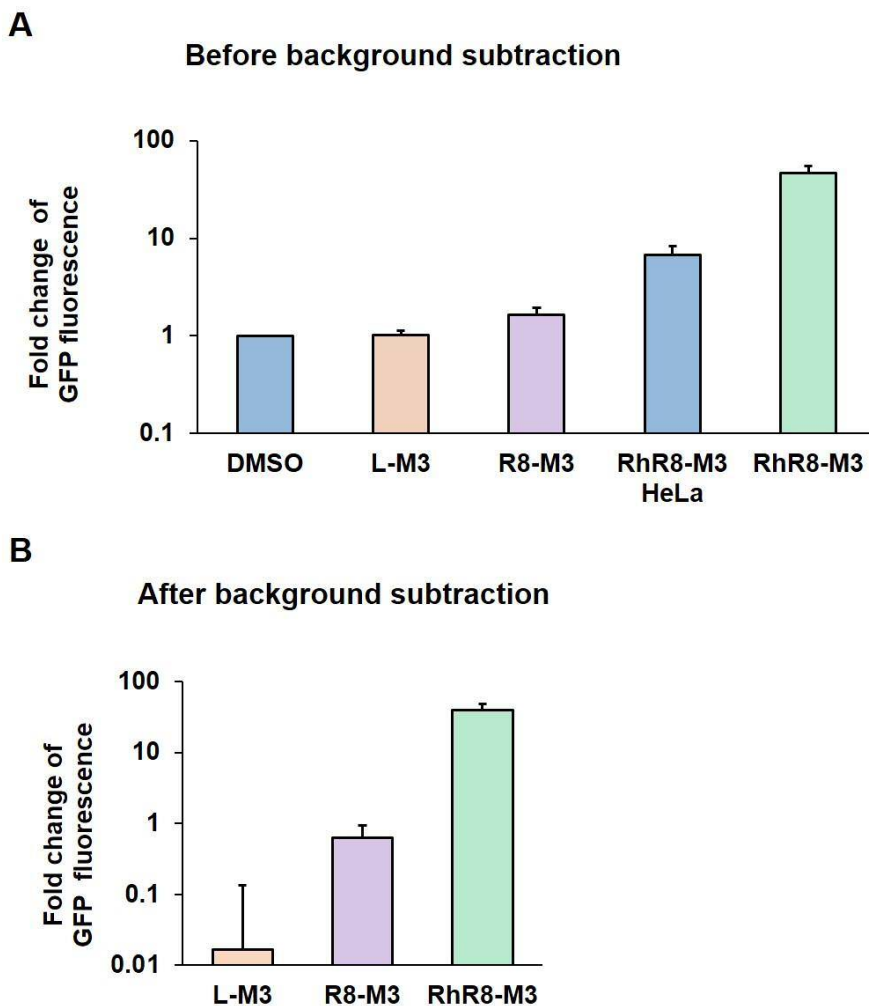
Figure 3-16 Comparison of M3 delivery into cells transiently expressing GFP1-10 using 20 μM L-M3, R8-M3 or RhR8-M3.
Cells transiently expressing GFP1-10 were washed once in serum free media and incubated with DMSO, L-M3, R8-M3 or Rhodamine labelled R8-M3 (RhR8-M3) at 20μM in serum free media for 2 hours at 37°C. Non transfected HeLa control cells were incubated with RhR8-M3 at 20 μM (RhR8-M3 HeLa). This figure combines data derived from three individual experiments shown in Figure 3-13 and Figure 3-15. (A) Fold change of GFP fluorescence of all samples shown. (B) DMSO background was then subtracted to obtain L-M3 and R8-M3 values. Background of RhR8-M3 HeLa was subtracted to obtain the fold change of GFP fluorescence of Rh-R8-M3 incubated with cells transiently expressing GFP1-10. n=3.

3.3.4 Localisation of complemented GFP at the nucleolus

When live uptake and delivery of the M3 peptide was investigated, it was striking that complemented GFP was strongly localised to the nucleolus when GFP1-10 expressing cells were incubated with 20 µM RhR8-M3 (Figure 3-14 K). This nucleolar localisation of complemented GFP was also investigated in previous experiments when mCherry-H6-Xa-R8-M3 was co-expressed with GFP1-10 (Figure 3-6). When R8-M3 was incubated with cell expressing GFP1-10, complemented GFP appeared to be mainly localised in the cytosol (Figure 3-12 I, Figure 3-13 C). Detailed analysis of HeLa cells expressing GFP1-10 incubated with 20 µM R8-M3, M3 or DMSO reveals that complemented GFP also localised to the nucleolar region when R8-M3 is used to deliver M3 into the cytosol of cells (Figure 3-17). After 2 hours of incubation with 20 µM R8-M3, the green fluorescence increases in the cytosol and concentration of green fluorescence can be detected in the nucleus, localised to the nucleolar region (Figure 3-17 L arrowheads). These structures cannot be seen in the nuclei of cells that were incubated with 20 µM DMSO or M3 (Figure 3-17 D, H). In DMSO and M3 control cells, green fluorescence is mainly localised around the nucleus or the whole nucleus appears to be fluorescent. This green fluorescence is weaker compared to cells were GFP complementation has occurred and it can be detected when cells were treated with M3 as well as with DMSO. As DMSO treated cells are not able to complement GFP1-10 with M3, this green fluorescence was assumed to be autofluorescence of the cell. When the concentration of R8-M3 is increased to 40 µM, the nucleolar structures can be seen more clearly (Figure 3-17 P arrowheads).

This data suggests that nucleolar localisation of complemented GFP can serve as an indication of functional delivery of M3 by R8 or Rh-R8. In addition to increasing levels of GFP fluorescence when M3 is delivered to GFP1-10, this fluorescence appearing at this defined localisation inside the cell can additionally be used to identify cells in which M3 has been delivered by R8 or RhR8-M3. This feature can be

especially advantageous when fluorescent levels of GFP complementation have little increase compared to DMSO control cells.

This data is a great example that a drug delivery system can have an influence on the intracellular localisation of its target and this will further be investigated in Chapter 6.
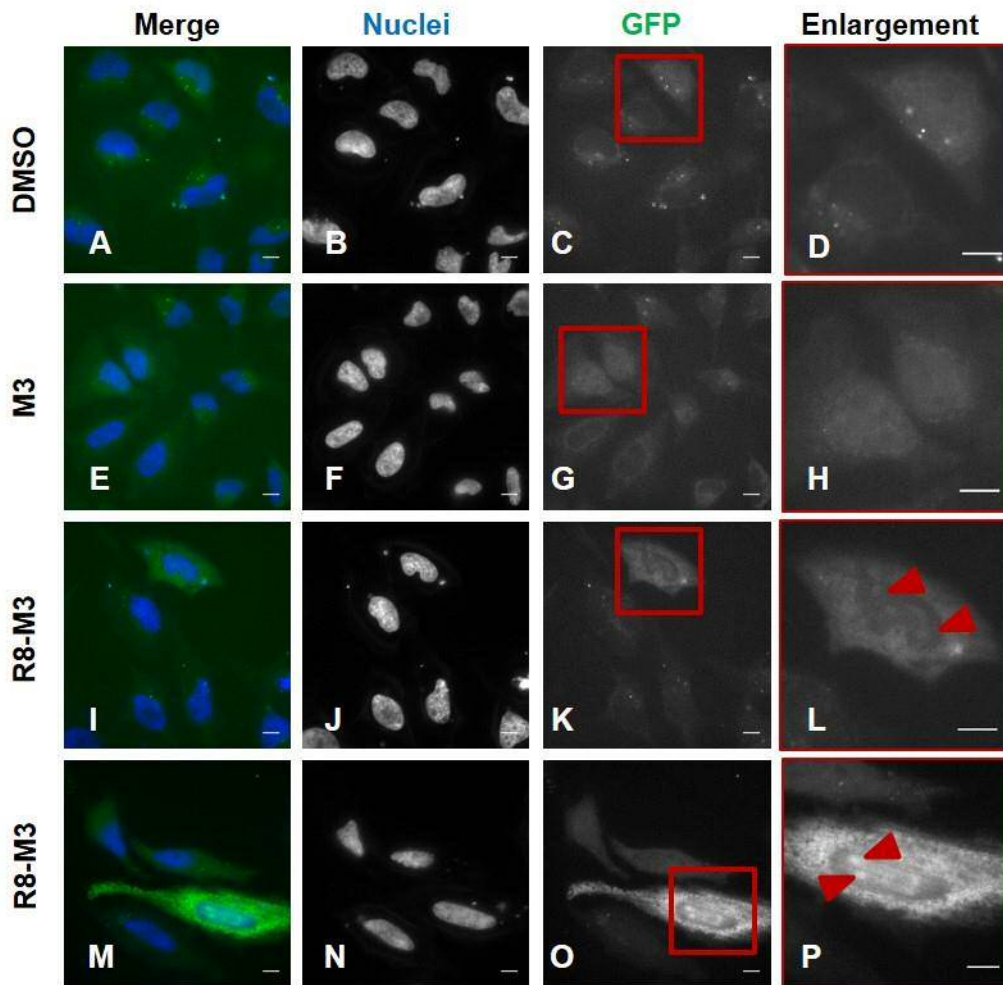
Figure 3-17 Localisation of complemented GFP in live cells.
Cells transiently expressing GFP1-10 were incubated with DMSO, L-M3 or R8-M3 at 20µM (A-K) or with 40µM R8-M3 (M-O) in serum free media for 2 hours at 37˚C. Cells were counterstained with Hoechst nuclear dye. Green fluorescence of cells in panel O was adjusted independently of other samples to show localisation of complemented GFP. Image would have been overexposed and nucleolar structures not visible if adjusted to the grey levels of other images. Red arrowheads point out nucleolar location of GFP. Scale bar: 10µm.

3.3.5 Visualisation of functional delivery of M3 in live cells.

One aim to utilise split GFP to show functional delivery of a peptide, is that it will enable us to detect GFP complementation in live cells as the peptide is delivered inside the cell with a microscope. Previous results demonstrated that M3 delivery and GFP complementation can be detected 2 hours after R8-M3 has been incubated on cells expressing GFP1-10.

It was next examined if functional delivery of the M3 peptide cargo to its intracellular GFP1-10 target, resulting in GFP complementation and an increase of GFP fluorescence can be shown in real time in live cells using a widefield fluorescent microscope. To investigate this, media of HeLa cells transiently expressing GFP1-10 was removed and replaced with serum free media containing 20 µM R8-M3. GFP complementation was then monitored every minute for 67 min (Movie Figure 3-18, Figure 3-19A). The movie shows increasing GFP fluorescence over time suggesting delivery of M3 and GFP complementation. Detailed examination of the single time points reveals that when the cell was first imaged on the microscope, green fluorescence was detected in the cytosol with increased green fluorescence located in the nucleus (Figure 3-19, 0 min). This green fluorescence decreased in the first 10 minutes of the experiment (Figure 3-19, 10 min). The nuclear green fluorescence was similar to the fluorescence detected in earlier experiments in DMSO control cells (Figure 3-17) which could mean that this is green auto fluorescence of the cell that photobleaches within the first 10 frames of the movie.

It was hypothesised earlier that complemented GFP mainly localises in the cytosol where GFP1-10 is expressed or to the nucleolus where R8 could target it to, thus, it was of interest to analyse how the GFP fluorescence in different compartments of the cell changes over time. Detailed analysis was performed to monitor the change in green fluorescence in the cytosol, nucleolus and the nucleus (Figure 3-19 B). To do so, a region of interest (ROI) was drawn in those localisations as well as the background. Measurements of the mean green fluorescence in the ROI were taken

between 0 and 66 minutes. The mean fluorescence displayed in Figure 3-19 B equals the mean fluorescence in that ROI after background subtraction. The mean fluorescent intensity measured in each ROI decreased slightly in the first 10 minutes, which is in alignment with what was seen on the microscopy images. In the cytosol GFP fluorescence changed linear with time and increased by 8 fold over 66 minutes (from 225 to 1873) indicating that GFP complementation had taken place in the cytosol. The fluorescence in the nucleus and the nucleolus increased by 2.8 fold and 4.7 fold, respectively in 66 minutes.

This data shows that complemented GFP is present at all three localizations of the cell, with the highest amount being localised in the cytosol where GFP1-10 is expressed and which is the first location where M3 is present after it has overcome the plasma membrane barrier. The change in green fluorescence at the nucleolus was higher than in the nucleus suggesting that this complemented GFP could be targeted to this position rather than being a result of passive diffusion into the nucleus.

Importantly, this movie proves that the developed split GFP assay can be utilised to investigate M3 peptide delivery by the drug delivery system R8 in real time using a microscope.
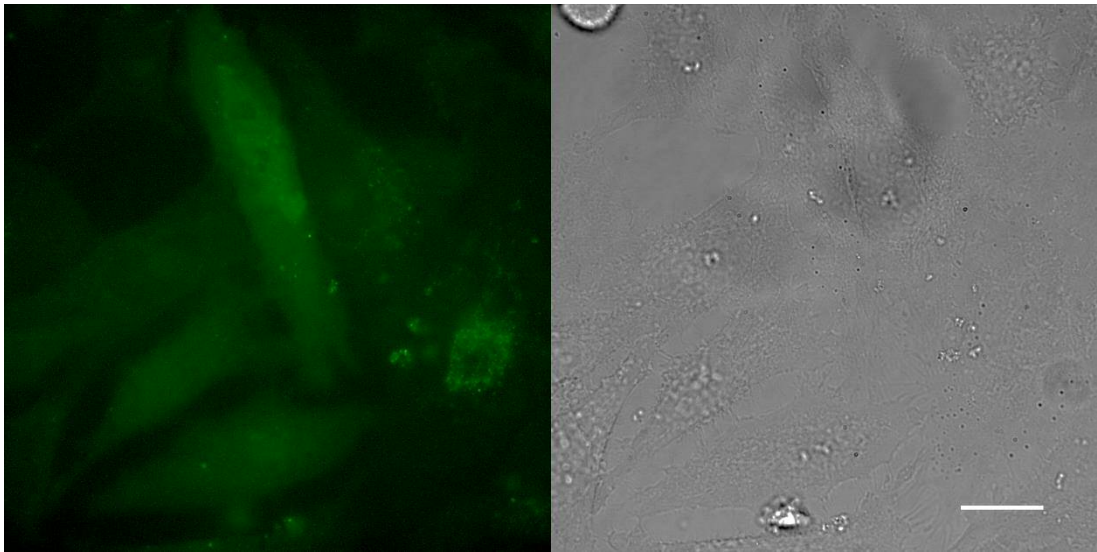
Figure 3-18 Movie of GFP complementation in live cells over time.
HeLa cells transiently expressing GFP1-10 were washed once in serum free media which was replaced with serum free and phenol red free RPMI containing R8-M3 peptide at 20 μM. GFP complementation was monitored every minute for 67 min. Sclae bar: 20 μm
Movie is available at https://youtu.be/pm969otSftA

A
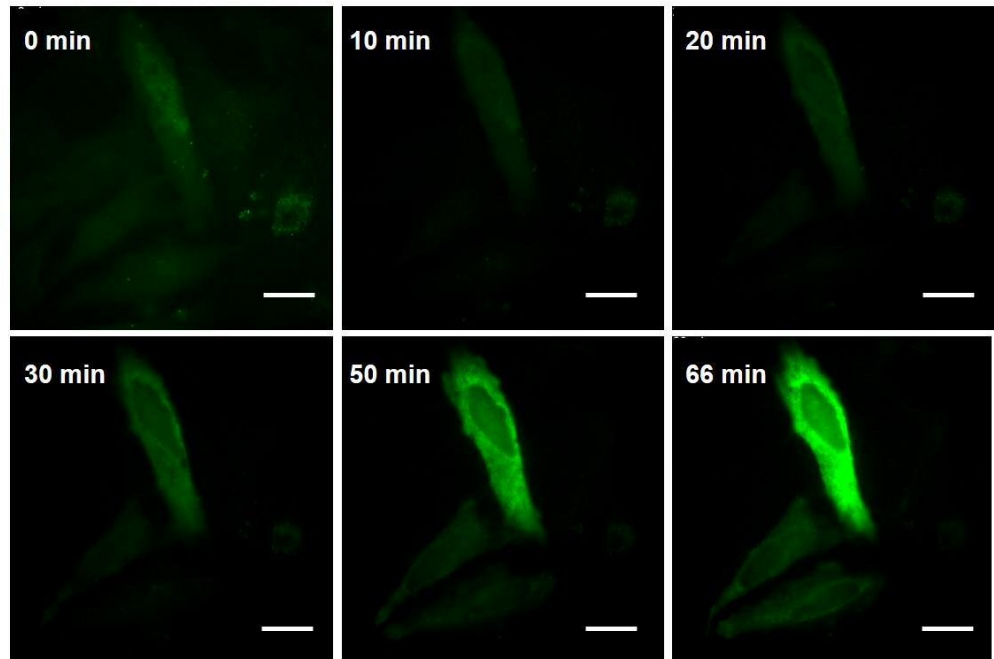
B
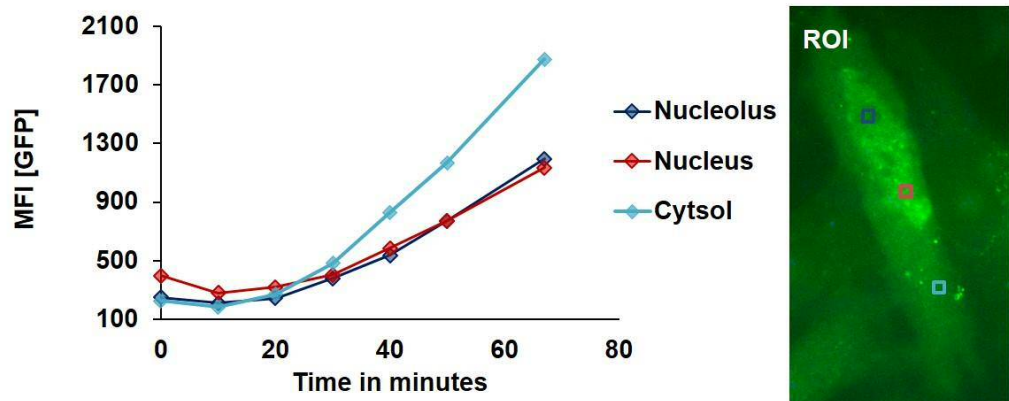
Figure 3-19 GFP complementation in live cells over time.
HeLa cells transiently expressing GFP1-10 were washed once in serum free media which was replaced with serum free media containing R8-M3 peptide at 20 µM. GFP complementation was monitored every minute for 67 min. (A) Single images from movie shown, captured at 0 min, 10 min, 20 min, 30 min, 40 min, 50 min and 67 min. Scale bar: 20µm. (B, right) Regions of interest (ROI) were placed in the nucleolus (dark blue), the nucleus (red) and the cytosol (light blue). (B, left) Mean fluorescent intensity shown for ROIs between 0 and 66 minutes. Data from a single cell from one experiment shown.

3.4 Discussion

Despite the great potential of peptides to act as therapeutic cargos, it is a challenge to facilitate their delivery to the cytosol of cells where they can carry out their function at their intracellular target. Drug delivery vectors such as cell penetrating peptides hold great potential to act as DDSs and facilitate their uptake (Copolovici *et al.* 2014). A major hurdle to evaluate the efficiency of these DDS to deliver their peptide cargo is to assess delivery into the cytosol and to asses if the peptide is intact to carry out its biological function.

In this chapter an assay was introduced that can serve as a solution to investigate delivery of a peptide to the cytosol facilitated by drug delivery systems and importantly also allows a direct correlation with its function. This assay allows the evaluation of DDS and their ability to functionally deliver peptides. This assay is based on split GFP (Cabantous *et al.* 2005) where GFP1-10 is expressed in the cytosol of a target cell and the M3 peptide serves as the model peptide cargo that is delivered by a DDS.

It was described previously that short amphipathic peptide carrier, Pep-1 can be used deliver M3 across the membrane by co-incubation to complement with its intracellular target (Pinaud and Dahan 2011). However, the intracellular GFP1-10 target protein was fused to Caveolin-1. Caveolin-1 is a protein involved in various processes within the cell. It is expressed at the cytoplasmic face of the plasma membrane and involved in endocytic uptake of cargo, membrane recycling back to the plasma membrane as well as trafficking to the Golgi apparatus (Rothberg *et al.* 1992; Conrad *et al.* 1995). These are mechanisms that can be involved in uptake and trafficking of a cargo molecule and overexpression of proteins can lead to mis-localisation to other cellular compartments. Hence, we excluded this protein as an intracellular GFP1-10 target to avoid the possibility of GFP complementation prior to

the M3 peptide reaching the cytosol. For this reason, the split GFP method in this project was developed to ensure cytosolic expression of the GFP1-10 target protein.

In this chapter it was shown that methods have been developed to prove that HeLa cells can express the intracellular GFP1-10 target when its green fluorescence is lost. GFP1-10 is missing the 11th beta sheet in its structure, nevertheless, it was possible to prove its presence in the cytosol using immunofluorescent staining as well as western blot analysis of cell lysate using an anti-GFP antibody.

An important finding that led towards the development of the split GFP assay was that GFP1-10 and M3 are able to complement in the cytosol to form full length GFP and GFP fluorescence is rescued. This was demonstrated using a co-transfection assay where GFP1-10 and mCherry-H6-Xa-R8-M3 were expressed in cells which served as a reliable method to test GFP complementation in the cytosol. Importantly, it was possible to detect the GFP signal arising from complemented GFP on a microscope which was crucial in order to develop the split GFP assay as a live cell imaging technique.

The M3 expression construct included various modifications resulting in expression of mCherry-H6-Xa-R8-M3. It was ruled out that mCherry can serve as a proton acceptor for GFP1-10 to rescue GFP expression. Thus, fusion of mCherry had the great advantage of being able to investigate H6-Xa-R8-M3 expression in live cells. Complementation of GFP1-10 with mCherry-H6-Xa-R8-M3 also confirmed that the drug delivery system R8 did not inhibit the complementation. This is an important finding leading towards a live assay where R8 is covalently conjugated to M3 to facilitate its delivery into the cytosol.

Proof of complementation of the split GFP fragments was not possible when cells were co-transfected with GFP1-10 and H6-Xa-R8-M3. This could have been due to expression and subsequent rapid degradation of the short peptide. It is important that

133

expressed proteins fold correctly inside the cell since there are pathways to degrade misfolded or damaged proteins to protect the cell. This mechanism, targeting proteins to the proteasome for degradation ensures quality of proteins and protects the cell from non-functional and potentially toxic proteins (reviewed in (Goldberg 2003)). H6-Xa-R8-M3 is a short peptide and with multiple repetitive, charged amino acids, consisting of mainly Histidine and Arginine, it is possible that it does not exhibit an ordered three dimensional structure. Hence, the cell could have detected it as a misfolded protein and targeted it for proteasomal degradation. One way to confirm this hypothesis would be to investigate GFP complementation when both fragments are co-expressed and cells are treated with a proteasome inhibitor to maintain H6-Xa-R8-M3 in the cell. Another possibility to prove H6-Xa-R8-M3 expression inside the cell could have been to detect the N-terminal His tag of the peptide using immunofluorescent staining with a His-tag antibody.

The development of an *in vitro* assay to assess complementation of GFP1-10 with pure synthetic peptides that will be evaluated and compared regarding their delivery efficiency of M3 is crucial. The proposed 'fix and stain experiment' was able to give information as to if the M3 peptide will complement with GFP1-10 but suggested that R8-M3 complements to a higher degree with GFP1-10 then M3 or L-M3. However, the success of GFP complementation with M3 and L-M3 was dependent on intracellular localisation of GFP1-10 in the cytosol or the Golgi apparatus. Due to the influence of PFA fixation and Triton-X100 permeabilisation on subcellular localisation of a cytosolic protein (Schnell *et al.* 2012) it is suggested that the lack of GFP complementation of M3 and L-M3 with cytosolic GFP1-10 was an artefact of the fixation method rather than inability of the two fragments to complement.

Hence, investigation of *in vitro* split GFP complementation should not involve fixation and permeabilisation protocols where protein could relocate to a different localisation inside the cell.

A better system to investigate GFP complementation of GFP1-10 with M3 peptides without the need for the peptides to cross the plasma membrane barrier is microinjection of M3 into the cytosol of cells expressing GFP1-10. This method would give a detailed insight of complementation dynamics of GFP1-10 with M3 peptides in the cytosol of live cells. However, microinjection is a time consuming process. Moreover, transient expression of GFP1-10 will introduce varying levels of expressed GFP1-10 which will require microinjection of a high amount of cells in order to gain information about complementation dynamics across a transient transfected cell population.

For this reason a true *in vitro* system would be beneficial where pure GFP1-10 protein can be mixed with M3 containing peptides. An even better estimation of complementation dynamics would be if M3 peptides are mixed with GFP1-10 originated from expression by HeLa cells. Thus, a cell lysate from HeLa cells expressing GFP1-10 could be obtained and used to investigate complementation with M3 containing peptides. This improvement of the split GFP *in vitro* assay will further be explored in Chapter 4.

When the live cell assay was performed to investigate M3 delivery by the drug delivery system R8 it was seen that GFP complementation took place and green fluorescence was increased when cells expressing GFP1-10 were incubated with 20 µM R8-M3 for 2 hours compared to L-M3 or DMSO. This data clearly showed that the split GFP assay can be used to investigate delivery of the M3 cargo peptide across the plasma membrane. Incubation of 20 µM L-M3 resulted in the same green fluorescent levels as detected in the DMSO control. No penetration ability of the M3 peptide or the flexible Serine-Glycine linker has been reported and Glycine rich linkers

are common in the CPP field to connect protein domains without interfering with the function of each domain (Sayers *et al.* 2014; Reddy Chichili *et al.* 2017). Hence, it is suggested that L-M3 cannot pass the plasma membrane. However, due to the lack of *in vitro* data about the L-M3 peptide to complement with cytosolic GFP1-10 it is also possible that L-M3 might have crossed the plasma membrane but was not able to complement with GFP1-10 in the live cell assay. Hence it is of high importance to assess complementation of GFP1-10 and L-M3 with the improved *in vitro* system to be able to correlate this data with the information gained from the live cell assay.

It was demonstrated that incubation time of 2 hours was sufficient in order to allow M3 delivery to the cytosol by R8 and complementation with GFP1-10. When delivering peptide cargo to the cytosol it is critical to consider uptake dynamics into the cytosol. The proposed uptake mechanism for R8 at low concentrations (< 10 µM) is endocytosis and labelled R8 was shown to be found in endocytic vesicles after 1 hour of incubation of Alex-488 labelled R8 with acute myeloid leukemic KG1a cells and HeLa cells (Jones and Sayers 2012; Sayers *et al.* 2014). Furthermore it was shown that defined endocytic labelling is lost in HeLa cells when incubated with increasing concentration of the fluorescein labelled Polyarginine peptide nonargginine (R9). From 10 µM, labelled peptide was found distributed in the cytosol with clear cytosolic labelling at 20 µM after 30 min which was suggested to be direct transcytosis across the plasma membrane (Duchardt *et al.* 2007; Jones and Sayers 2012). Based on that knowledge is was suggested that R8-M3 when applied at 20 µM crosses the plasma membrane through direct transcytosis in 30 min-1h. The movie of live delivery of M3 by R8 at 20 µM revealed that GFP complementation starts as fast as 20 min after R8-M3 has been applied onto the cells. This supports that hypothesis that R8-M3 crosses the plasma membrane through direct transcytosis.

Utilising the split GFP system to evaluate different drug delivery systems and their ability to deliver M3 has shown that differences in deliver efficiency can be

detected when R8-M3 is compared to RhR8-M3 at 20 μM. The Rhodamine peptide was originally purchased to be able to track the uptake of R8-M3 into the cell using a microscope. In order to explore the uptake mechanism of cell penetrating peptides using a microscope the attachment of a fluorophore is required. However, it has been reported that the attachment of fluorophores can lead be the reason of changed uptake dynamics into the cell (Jones and Sayers 2012). Rhodamine was shown to interact with arginine rich peptides like TAT and R9 which can enhance photo-induced release through endosomolytic activity and it can also be used as a photosensitiser. This was demonstrated when it was attached to the CPP Tat. Tetramethylrhodamine produced reactive oxygen species upon irradiation that can cause membrane damage when in close proximity to the plasma membrane through attachment to a CPP, thereby facilitating uptake (Meerovich *et al.* 2014). However, its photo-induced release through endosomolytic activity was also accompanied with phototoxicity and loss of plasma membrane integrity (Srinivasan *et al.* 2011). Furthermore, when it was conjugated to the CPP Penetratin an increase of the hydrodynamic radius of the CPP as well as a significant cellular uptake into cells was observed (Hyrup Moller *et al.* 2015). For these reasons Rhodamine might have not been the best choice to label R8-M3.

Nevertheless, it was an important finding that the uptake of 20 μM RhR8-M3 in GFP1-10 transfected cells was not significantly different compared to untransfected HeLa cells. This shows that Fugene6 transfection of cells did not alter plasma membrane characteristics and did not affect M3 delivery by Rh-R8-M3. Another important finding was that it was possible to show that RhR8-M3 increases delivery of M3 into the cytosol of cells compared to R8-M3. This outcome is a great example that differences of delivery efficiency can be evaluated using this split GFP assay when two different DDSs are used to deliver M3.

Detailed investigation of M3 delivery using a microscope revealed that complemented GFP was strongly localised to the nucleolus when GFP1-10 expressing cells were incubated with 20 μM RhR8-M3 and R8-M3. When GFP1-10 expression was investigated using immunofluorescence, GFP1-10 was expressed throughout the cytosol and was not concentrated in the nucleus. Hence, when complemented GFP can be found concentrated at the nucleolar region it was likely to be an effect of re-association with RhR8-M3 or R8-M3. This nucleolar localisation was shown before in co-expression experiments when GFP1-10 had complemented with mCherry-H6-Xa-R8-M3. R8 and other arginine rich peptides are well known to localise at the RNA in the nucleolus of cells (Vives *et al.* 1997; Gustafson *et al.* 1998; Martin *et al.* 2007) which could explain that complemented GFP was found at that location when GFP1-10 was expressed with R8 containing mCherry-H6-Xa-R8-M3 or in the live experiments when incubated with R8-M3 or RhR8-M3. This suggests that R8 was able to target M3 peptides (3.6 – 4 kDa) or even the whole fusion protein mCherry-H6-Xa-R8-M3 (~35kDa) through the nuclear pore to the nucleolus resulting in the nucleolar labelling once complemented with GFP1-10, if GFP1-10 was present in the nucleus through passive diffusion through the nuclear pore. Another scenario could have involved GFP complementation of GFP1-10 and mCherry-H6-Xa-R8-M3/R8-M3/RhR8-M3 in the cytosol and relocalisation of a complex of ~ 50kDa (for mCherry-H6-Xa-R8-M3) by R8 post complementation. With a size of ~ 50kDa it is a very large complex but it was found that proteins as large as 60 kDa are able to pass through the nuclear pore (Wang and Brattain 2007). It was also striking in the movie of live R8-M3 delivery that GFP complementation mainly took place in the cytosol and GFP fluorescence increased more at the nucleolar region compared to the surrounding nuclear region.

This is an important finding when characterising drug delivery systems because it shows what influence a DDS can have on the subcellular localisation of its cargo.

The movie of real time delivery as well as visualisation of the localisation of M3 delivery was only possible by detection of GFP complementation using a microscope. Results of previous studies using the split GFP complementation assay have only shown concentration depnendent peptide delivery by flow cytometry (Milech *et al.* 2015; Schmidt *et al.* 2015b). Further, more detailed microscopic analysis of the localisation of comoplemented GFP will be shown in Chapter 6.

In order to develop a method to evaluate drug delivery systems and their ability to functionally deliver the M3 peptide, it is of importance that this method is robust and reproducible. However, most importantly, the seen effect (e.g. increasing GFP fluorescence through GFP complementation) has to be solely dependent on the delivery efficacy of the drug delivery system itself.

A result of transient transfection of cells is that the expression levels of the protein vary hugely between single cells. This high variation in expression levels can be seen when GFP1-10 is expressed in HeLa cells. M3 will only complement to form full length GFP when GFP1-10 is available in the cytosol of the target cell. When cells express GFP1-10, it is non-fluorescent and it is not possible to determine if and how much GFP1-10 is expressed in a live cell experiment. For this reason it is not possible to differentiate between cells where the M3 peptide has been delivered to the cytosol but the cells were not expressing GFP1-10, and cells that were expressing GFP1-10 but delivery of M3 was not successful. The amount of expressed GFP1-10 will also determine the maximal degree of GFP complementation, regardless if more M3 was delivered into that cell. Hence, GFP1-10 is a limiting factor in this assay and represents a variable in this assay.

Furthermore, the uptake of RhR8-M3 into cells largely varied between single cells. This finding suggests that another mechanism is involved that determines how much peptide is taken up into cells. This variation of uptake was only possible to

determine by adding rhodamine as a fluorescent tag to the drug delivery system. Hence, if this is a Rhodamine specific effect or holds true for R8-M3 is unknown. However, the aim of this assay is to determine DDS specific delivery of the M3 peptide to be able to characterise the DDS. An assay with a cell population that expresses varying amounts of GFP1-10 and drug delivery systems that might enter the single cells unevenly across a cell population does not supply sufficient information to be able to determine a DDS specific effect on delivery. Hence, as novel DDSs will be characterised using this system they have to be the only variable in the assay. For this reason levels of GFP1-10 expression across the cell population have to be known.

There are two models proposed to achieve this. Firstly, generating a clonal stable cell line that expresses even amounts of GFP1-10 across the cell population. Secondly, a fluorescent expression marker of GFP1-10 can be introduced which would allow to track which cells express GFP1-10 and how much protein is expressed inside the cell. Generation of a stable cell line that expresses mCherry-GFP1-10 would even be more beneficial for the assay development because it would eliminate the chances of a cell not expressing the intracellular GFP1-10 at all, therefore making the assay even more robust. This system would then allow us to investigate concentration dependent functional M3 delivery by DDSs, and make a direct comparison of DDSs.

The improvement of the split GFP system by generating stable cell lines as well as an improved *in vitro* assay are further shown in Chapter 4.

4   Generation of stable cell lines for the improvement of the split GFP assay.

4.1   Introduction

In chapter 3 it was demonstrated that the split GFP system can be utilised to show that drug delivery systems are able to functionally deliver M3 peptide cargo to the cytosol when GFP1-10 is expressed transiently. Transient transfection, however, introduces high variability in GFP1-10 expression levels and makes it difficult to prove that a seen effect can solely be attributed to the delivery efficiency of the drug delivery system. In order to improve the split GFP system and be able to specifically evaluate the delivery efficiency of DDSs to deliver M3 peptide, two solutions are hypothesised. Firstly, to decrease the variation levels of GFP1-10 expression and ensure even GFP1-10 expression levels across the cell population. This will allow the full characterisation of M3 delivery systems because the degree of GFP complementation is only dependent on M3 delivery and not influenced by GFP1-10 expression. This can be achieved by the generation of a stable cell line that expresses GFP1-10 in its cytosol.

A second solution is to create a system where the variation of GFP1-10 expression levels can be quantified. This can be achieved by introducing a fluorescent expression partner that labels GFP1-10 expression. Previously it was shown that the fluorescent protein mCherry did not interfere with GFP complementation when GFP1-10 was expressed with mCherry-H6-Xa-R8-M3. Hence, mCherry is used in this Chapter to act as a fluorescent expression partner for GFP1-10 and its fluorescence can be correlated with the amount of expressed GFP1-10.

The aim of this chapter is to improve the split GFP system as hypothesised above, and the characterisation of these systems. The first focus of this chapter lies on the generation of the stable cell line that expresses GFP1-10. The second part of

this chapter will describe the full characterisation of the split GFP system when mCherry-GFP1-10 is utilised to obtain an expression marker for GFP1-10 expression.

4.2 Generation of a stable cell line that expresses GFP1-10: S̲table C̲ell L̲ine 1 (SCL1)

In order to generate a stable cell line that evenly expresses GFP1-10 across its cell population, HeLa cells were transfected with DNA coding for GFP1-10. GFP1-10 is cloned into the background vector EGFP-N1 which also carries the neomycin resistance gene (For vector map see Figure 9-1). Thus, cells that had stably integrated this expression construct into their genome were selected using selection media containing 400 mg/mL Geneticin (G418). To obtain a clonal cell line, limiting dilution was performed (for detailed stable cell line generation see (2.8.2). Because cells expressing GFP1-10 are not fluorescent, cells could not be sorted by fluorescent activated cell sorting (FACS). For this reason colonies that were obtained from limiting dilution were screened by immunofluorescence using an anti GFP antibody to detect cytosolic expression levels of GFP1-10. From over 1000 microwells that were screened, 56 wells contained cell colonies that expressed GFP1-10. The other wells did either not contain cells at all or cells did not express GFP1-10. From 56 cell colonies, the two most promising colonies were selected. The main criteria for selection was to identify a population in which every single cell was expressing GFP1-10, levels of GFP1-10 expression were equal between cells. From those two colonies the one expressing the highest amount of GFP1-10 in the cytosol was chosen. This cell line was named S̲plit C̲ell L̲ine 1̲ (SCL1) and underwent detailed characterisation using techniques developed previously to ensure a stable expression of GFP-10 while retaining compatibility of reassembly with M3.

4.2.1 Proof of even GFP1-10 expression levels in SCL1 cells

In order to confirm that SCL1 cells express even levels of GFP1-10 across the cell population compared to cells transiently transfected with GP1-10, immunofluorescent staining against GFP was performed (Figure 4-1). Microscopy

images demonstrate that there was a high variation in GFP1-10 expression levels in the cytosol of cells that were transiently expressing GFP1-10 (Figure 4-1 A IV). The GFP antibody detected very high expression levels in the cytosol of some cells and no expression at all in other cells. In comparison, GFP1-10 expression in SCL1 cells can be detected evenly across the cell population (Figure 4-1 A IX). The amount of expressed GFP1-10 appears to be considerably lower than when the protein is expressed transiently, hence, the staining detected for the anti-GFP stain is also displayed as a fire table which enhances low signals over the black background (Figure 4-1 A X). Importantly, Mock transfected cells did not show any staining against GFP (Figure 4-1 A XIV, XV) confirming that the low anti-GFP signal detected in SCL1 cells is a result of GFP1-10 detection rather than non-specific antibody staining that would also be visible in mock transfected cells. The microscopy images also reveal that GFP1-10 is not green fluorescent when transiently expressed in the cytosol (Figure 4-1 A III) as shown before when this system was characterised (see chapter 3 xy). This absence of green fluorescence is maintained when GFP1-10 is stably expressed in SCL1 cells (Figure 4-1 A VIII). This is of high importance for the assay in order to obtain a green fluorescent signal when M3 peptide is delivered to cytosolic GFP1-10 by a DDS.

Quantification of the corrected total cell fluorescence (CTCF) of anti GFP staining in the cytosol of these cells confirms what can be seen on the images. Because of the very high range of expression levels that is seen in transient transfections, this data is displayed on a logarithmic scale (Figure 4-1 B). Mock transfected cells show fluorescence in a range between 0.08 and 0.6 with a mean CTCF of 0.27. In comparison, SCL1 cells display a CTCF n a range between 1.1 and 21.2. When HeLa cells transiently express GFP1-10, expression levels range from 0.1 to 75.9 which is a 759 fold difference across the cell population. These data points include cells not expressing GFP1-10 as well as cells highly overexpressing GFP1-10 in their cytosol. Cells transiently expressing GFP1-10 and SCL1 cells show a mean CTCF of 7.7 and

5.1, respectively. Furthermore, the coefficient of variation is shown (Figure 4-1 C) that describes the variability of the data points to the mean and is was calculated by dividing the standard deviation of all data points by the mean value of all the data points. This means that if the mean value equals the standard deviation a value of 1 is obtained. The smaller the standard deviation is compared to the mean, the smaller the number appears with a minimum value of zero if a standard deviation of the value zero had been obtained.

The coefficient of variation was found to be 0.4 for mock transfected cells, showing the natural variation of fluorescence of the antibody stain, 0.7 for SCL1 cells and 1.4 for cell transiently expressing GFP1-10. Hence, even though the mean fluorescent intensity between cells transiently expressing GFP1-10 and SCL1 cells was found to be similar, the variation of fluorescence between the cells was decreased in SCL1 cells.

This data demonstrates that the stable cell line SCL1 expresses even amounts of GFP1-10 across the cell population. More importantly, every single cell is expressing GFP1-10, with the data of CTCF of anti GFP staining clearly separating from the fluorescent levels obtained from mock transfected cells (Figure 4-1 B). The amount of expressed protein is low (mean value of 5.1) compared to the maximum expression that can be achieved when cells are transiently transfected with GFP1-10 (maximum value > 60). In summary, SCL1 cells express even but low levels of GFP1-10.
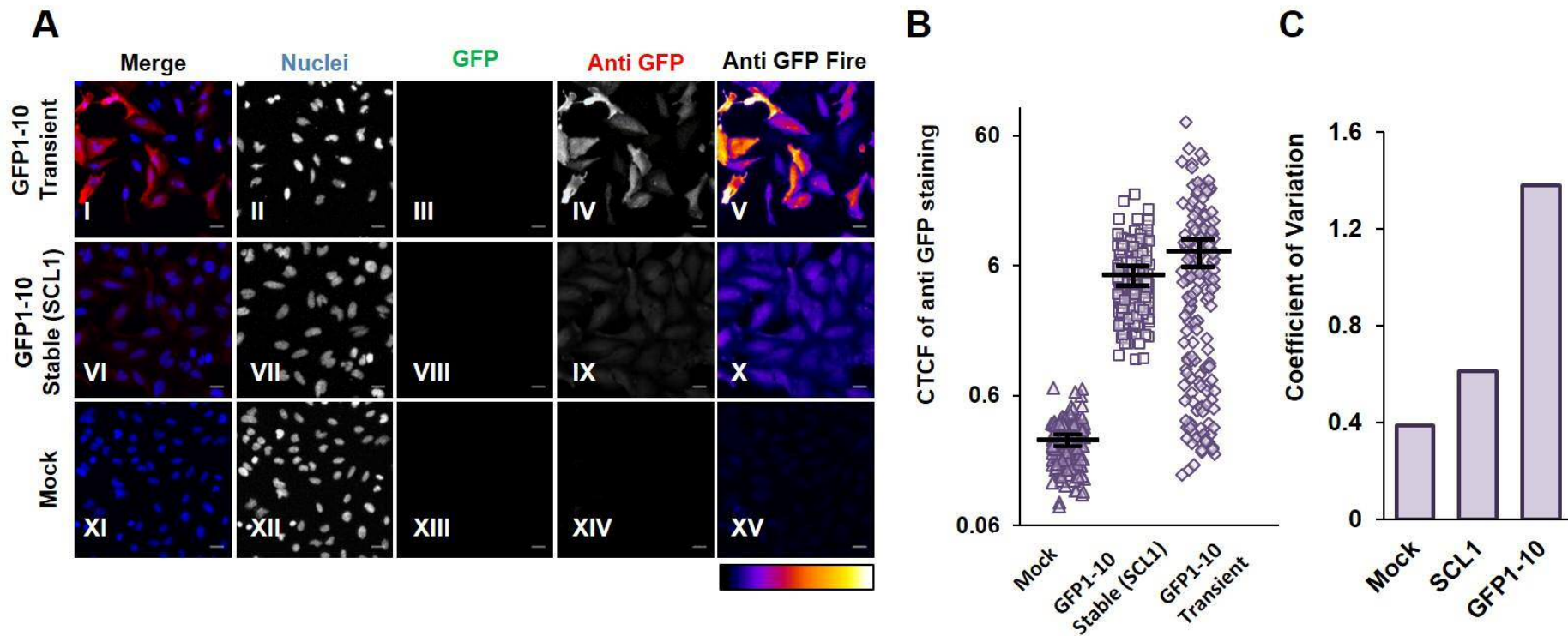
Figure 4-1 Comparison of GFP1-10 expression levels of SCL1 cells and cells transiently expressing GFP1-10 using immunofluorescence.
HeLa cells transiently expressing GFP1-10, SCL1 cells stably expressing GFP1-10 or mock transfected cells were PFA fixed and the plasma membrane was permeabilised with 0.1 % Triton-X-100. GFP1-10 expression was detected using a primary anti-GFP antibody raised in goat. A secondary anti-goat antibody conjugated to Alexa-647 was used to be able to visualise GFP expression. Nuclei were counterstained with DAPI. (A) Representative images of the immunofluorescent stain shown. Grey levels displayed on fire table range between 110-9487. Scale bars represent 30 µm. (B) Quantification of the CTCF of the anti GFP staining. Single data points represent the fluorescence in the cytosol of single cells. Bar displays the average CTCF of three experiments. Error bars show standard error of the mean between experiments. 46 to 68 cells were analysed per condition per experiment.(C) Coefficient of variation was calculated by dividing the standard deviation of the CTCF of all data points by the value of the mean CTCF. n=3.

4.2.2 GFP complementation in SCL1 cells using transfection

Next, it was tested if the expressed GFP1-10 in SCL1 cells is able to complement to full length GFP when DNA coding for the M3 fragment is transiently expressed in this cell line. It was found that GFP fluorescence can be detected with a microscope when mCherry-H6-Xa-R8-M3 is expressed in SCL1 cells (Figure 4-2 A III). No GFP fluorescence could be seen in mock transfected SCL1 cells (Figure 4-2 A VII). Transfection of a DNA construct coding for mCherry-H6-Xa-R8-M3 has the advantage that it is possible to identify which cells express the M3 fragment by its mCherry fluorescence (Figure 4-2 A IV). Every single cell that was transfected with mCherry-H6-Xa-R8-M3 was positive for GFP complementation which confirms that each of those cells was also expressing GFP1-10. The GFP fluorescence was detected in the nucleus or the cytosol consistent with what was found in transient co-expression experiments (3.2.2). GFP complementation through co-expression was also compared between SCL1 cells and HeLa cells transiently expressing GFP1-10 and mCherry-H6-Xa-R8-M3 (Figure 4-2 B) which was detected on a microplate reader (2.4.3.2). When HeLa cells were transfected with single DNA constructs coding for GFP1-10 and mCherry-M3 only very low signal of 1000 – 1500 RFU was detected when GFP fluorescence was measured. When these DNA constructs were co-expressed, GFP complementation occurred in transfected cells and high levels of 12,000 RFU were detected. GFP complementation was also detected when mCherry-H6-Xa-R8-M3 in SCL1 cells which confirmed what was seen before when co-expression was analysed using microscopy. GFP fluorescence was detected at 6400 RFU, hence, the brightness of GFP fluorescence when GFP complemented in SCL1 cells was half as bright as when both fragments were expressed in HeLa cells. This drop in fluorescence can be explained by the lower expression levels of GFP1-10 in SCL1 cells. The degree of GFP complementation is limited by the amount of GFP1-10 that is express in the cytosol and in previous studies it was shown that higher GFP1-10 expression can be achieved when cells transiently express this protein,

compared to the stable cell line (Figure 4-1). In previous experiments it was also shown that the fluorescent protein mCherry has no ability to complement GFP1-10 that is transiently expressed in HeLa cells (3.2.2). This also held true when mCherry alone was expressed in SCL1 cells. Levels of GFP fluorescence were not higher than in mock transfected SCL1 cells (Figure 4-2 B).

This data shows that M3 can complement with GFP1-10 expressed in the stable cell line SCL1 but to a lower degree as it can be achieved with transient transfection of GFP1-10 and mCherry-M3.
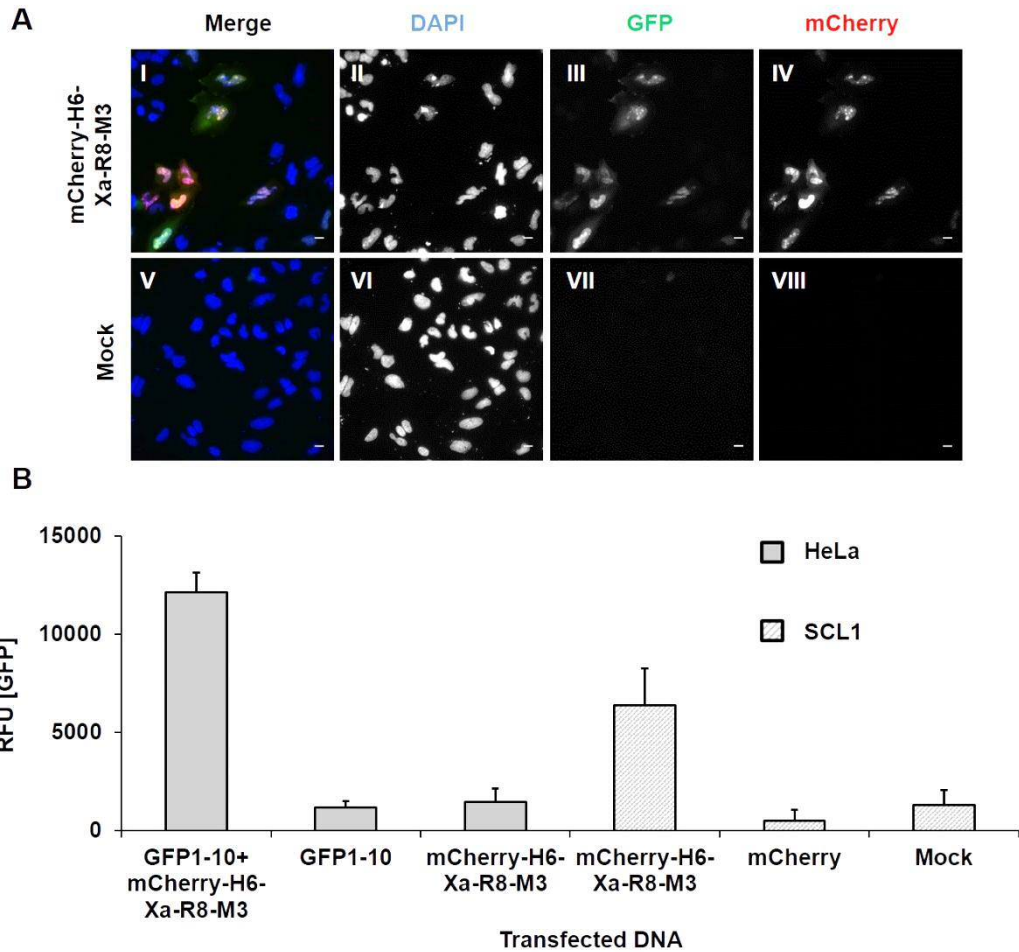
Figure 4-2 GFP complementation in SCL1 cells using transfection of mCherry-H6-Xa-R8-M3.
(A) Representative images of SCL1 cells transfected with mCherry-H6-Xa-R8-M3 or mock transfected. Cells were PFA fixed and imaged on a widefield microscope. Scale bar represent 30 μm. n=3 (B) Hela cells (solid grey) or SCL1 cells (grey pattern) were transfected with the indicated DNA constructs coding for GFP1-10, mCherry-H6-Xa-R8-M3, mCherry or no DNA (Mock). Green fluorescence of ~ 0.8 x 10^5 live cells was detected in triplicates on a microplate reader. Background subtraction of mock transfected HeLa cells was performed. n=2. Error bars show SEM.

4.2.4 *In vitro* GFP complementation of M3 peptides with SCL1 cells

Before a live cell assay could be performed on SCL1 cells, it was of importance to ensure that GFP1-10 expressed in the stable cell line is able to complement with the M3 and DDS-M3 peptides *in vitro*. The developed method in order to test this involved PFA fixation and Triton-X100 permeabilisation of the cells transiently expressing GFP1-10 followed by an incubation with 20 µM of the different peptides (3.2.4). However, it was shown in previous experiments that this method was not suitable when GFP1-10 was expressed in the cytosol (3.2.4). Hence, this method had to be improved in order to determine if GFP1-10, stably expressed in the cytosol of SCL1 cells can complement with the synthetic M3 peptides *in vitro*.

An undergraduate student in our lab had investigated the improvement of this assay under my supervision and had found that M3 peptides will complement with GFP1-10 in the presence of 0.1 % Triton-X-100 leading to the development of an improved *in vitro* assay including cell lysates obtained by Triton-X-100 permeabilisation of the plasma membrane. For the new *in vitro* assay, SCL1 cells stably expressing GFP1-10 were detached from the cell culture dish, cells were pelleted and resuspended in PBS containing 0.1% Triton-X-100 and left at room temperature for 4 min to allow permeabilisation of the plasma membrane. The obtained cell lysate containing GFP1-10 was then mixed in a 1:1 ratio with 80 µM or 20 µM of M3 containing peptides in PBS (Table 3-1). Thus, the final mixture contained 40 µM or 10 µM M3 containing peptide in a 0.05% Triton-X-100 in PBS solution and the GFP1-10 content of 0.8×10^5 SCL1 cells. The SCL1 cell lysate and M3 peptide mix was transferred into a 96 well plate which was kept under constant agitation at 4°C and GFP complementation was monitored over time. The incubation temperature of 4°C was chosen to avoid degradation of the proteins by proteases.

When the SCL1 cell lysate was incubated with the different peptides, no GFP complementation was detected with 10 µM (Figure 4-3 A) or 40 µM (Figure 4-3 B) R8 showing that the drug delivery system R8 by itself cannot replace the proton acceptor

located within the M3 peptide and rescue GFP fluorescence. A time dependent GFP complementation was seen when GFP1-10 lysate contained 10 µM or 40 µM M3, L-M3 or R8-M3. When GFP1-10 lysate was incubated with 10 µM peptides, first appearance of green fluorescence can be seen after 60 minutes for M3 and R8-M3. In comparison, GFP complementation was detected as fast as 5 min after the start of incubation of GFP1-10 with 40 µM M3 containing peptides. The fluorescent intensity of GFP is similar between M3 and R8-M3 throughout the experiment at 10 µM and 40 µM which suggest that M3 and R8-M3 complement with GFP1-10 at the same rate and they have the same ability for complementation *in vitro*. This is an important finding and an improvement to the 'fix-and stain' *in vitro* assay where GFP complementation of M3 could not be detected at the same rate and degree as it was seen for R8-M3 (Table 3-1). Importantly, the detected fluorescence was lower throughout the time course of the experiment when 10 µM peptides were mixed with the cell lysate compared to 40 µM. This confirms that utilising this *in vitro* assay a dose response of GFP complementation with varying amounts of M3 peptide can be seen.

Interestingly, when the cell lysate was incubated with the L-M3 peptide, fluorescence of GFP was increased at both concentrations and throughout the time course of the experiment compared to M3 and R8-M3. If fluorescence of complemented GFP was significantly different was tested at two time points; at the beginning of incubation after 2 hours and at the end of the incubation after 7 hours. It was found that there was no significant difference of GFP complementation between the M3 and the R8-M3 peptide. The fluorescence of L-M3 was found to be significantly different compared to either sample after 2 h ($p<0.001$) and 7 h ($p<0.01$). The significance was only determined between M3 containing peptides.
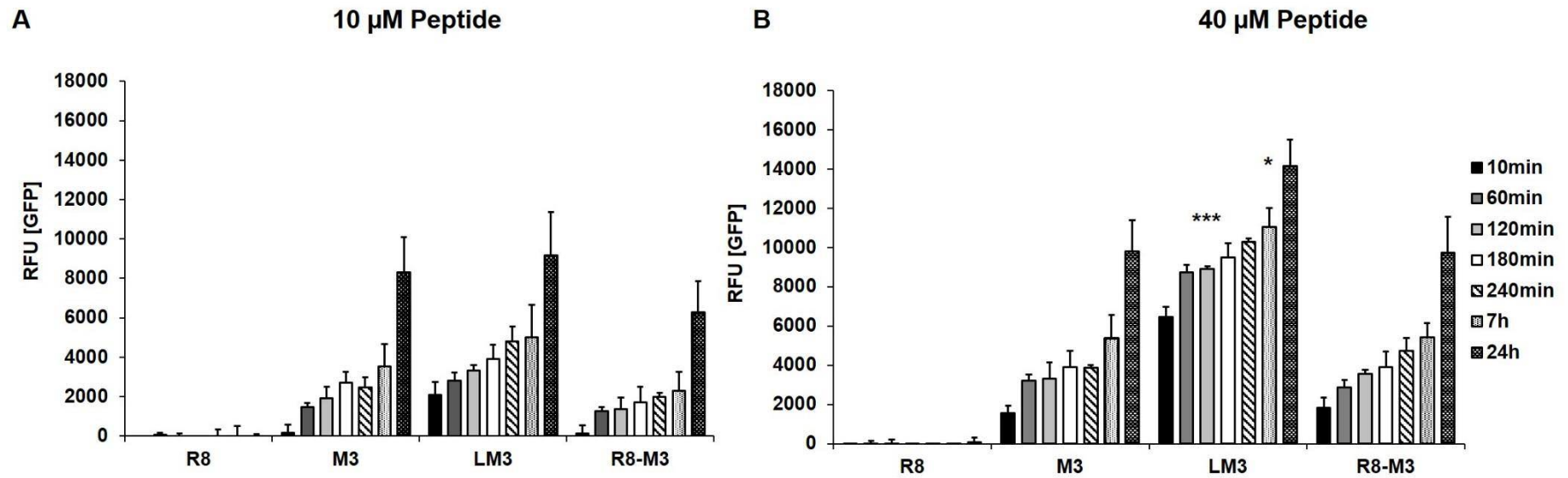
Figure 4-3 *In vitro* GFP complementation of SCL1 cell lysate with peptides.
SCL1 cells expressing GFP1-10 were trypsinised and lysed using 0.1% Triton-X100 in PBS. Cell lysate of 0.8×10^5 cells was mixed with (A) 20 µM M3 and CPP-M3 peptides to obtain a final concentration of 10 µM in 0.05% Triton-X-100/PBS or (B) 80 µM M3 and CPP-M3 peptides to obtain a final concentration of 40 µM in 0.05% Triton-X-100/PBS. Lysate mixture was left under constant agitation at 4 °C. The fluorescent signal resulting from GFP complementation was minored over 24 h using a microplate reader. DMSO only control was subtracted as sample background. n=3. Error bars present standard error of the mean. For statistical analysis data was tested using a One way Annova followed by multiple comparison using a Turkey HSD (honest significant difference) test. Data was tested at two time points, 120min and 7h. Significance is shown compared M3 and R8-M3. *: $p < 0.05$, **: $p < 0.01$, ***: $p < 0.001$, n.s.: not significant.

This increased fluorescence seen for the L-M3 peptide could be due to enhanced complementation of M3 with GFP1-10 achieved by the linker or an increased fluorescence of the peptide itself compared to other peptides.

The autofluorescence of the L-M3 peptide was also noticed during microscopy experiments compared to DMSO or R8-M3 when peptides were applied to the cells at a concentration of 30 µM. Increased green fluorescence was mainly localised to between the cells, indicating that it was not green fluorescence derived from GFP complementation and suggesting that this fluorescence is an effect caused by the peptide itself (Figure 4-4 A I, IV). Quantification of the background fluorescence detected in the GFP channel in this experiment also suggested that the green background fluorescence could be increased when L-M3 was incubated on cells compared to DMSO or R8-M3 (Figure 4-4 B).

Furthermore fluorescence derived from pure M3 containing peptides was investigated on a microplate reader. To compare the green autofluorescence of M3 containing peptides utilised in the *in vitro* assay, peptides at a final concentration of 40 µM and 10 µM diluted in 0.05% Triton-X-100/PBS were measured (Figure 4-4 C). Fluorescence of 10 µM peptide detected on the microplate reader did not show a difference between the fluorescence of the peptides themselves. When 40 µM of peptides were measured, fluorescence of the L-M3 peptide showed a low increased compared to other peptides. This data could indicate that the increased fluorescence of the L-M3 peptide could be due to the autofluorescence of the peptide itself rather than a different ability to complement with GFP in the *in vitro* assay, however this would need to be confirmed in further experiments.

In summary, the *in vitro* system using cell lysate is a major improvement to the characterisation of the split GFP assay. GFP complementation can be measured in a time and concentration dependent manner and this method also allows direct

comparison of the ability to complement with GFP between M3 and DDS-M3 peptides. It was shown that M3 and R8-M3 have the same complementation dynamics with GFP1-10 *in vitro*. Hence, addition of the DDS R8 does not interfere with GFP complementation. Moreover, R8 by itself cannot rescue GFP fluorescence.
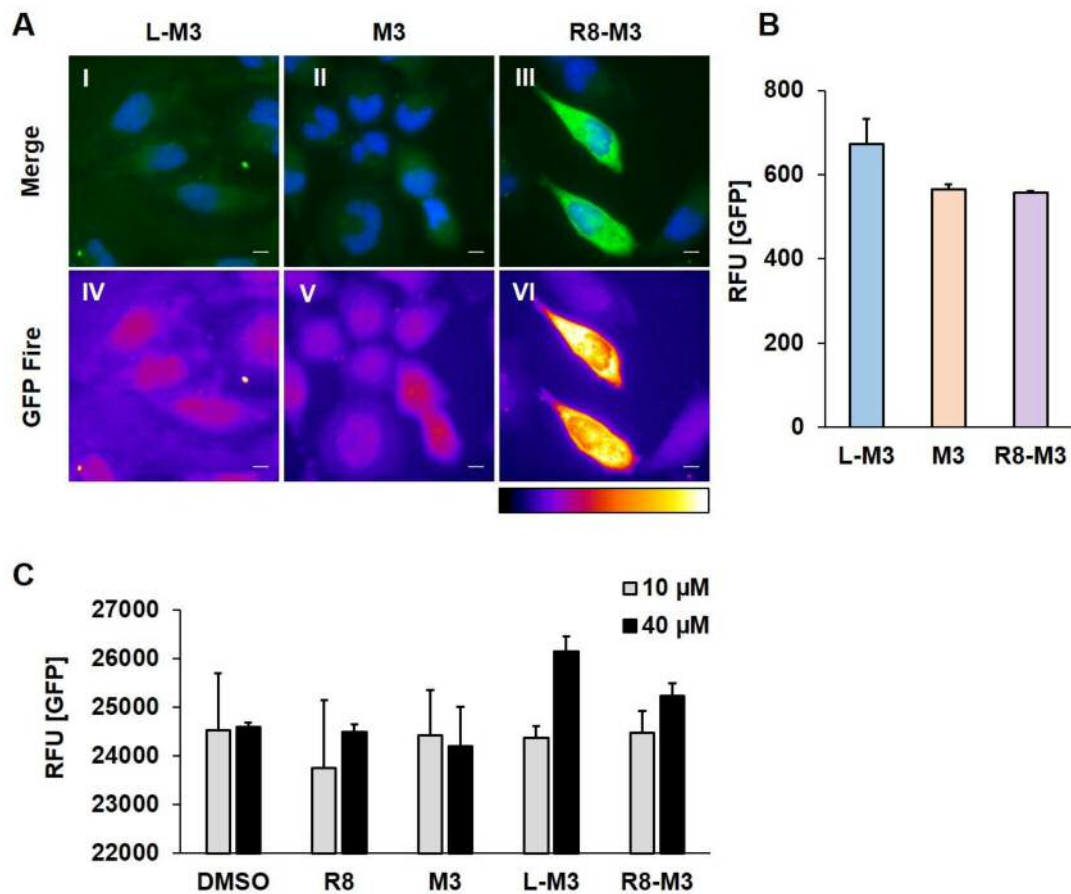
Figure 4-4 Autofluorescent background of the L-M3 peptide.
SCL1 cells were incubated with 30 μM L-M3, R8-M3 or DMSO for 2h at 37°C. (A) Representative images of fluorescent background in the different conditions. GFP channel was converted into a Fire table. Scale bar: 10 μm. (B) Quantification of green fluorescent intensity of background located between single cells. N=1, 3 images analysed per condition with 4 background measurements each. Error bar shows standard deviation of the mean between 3 images of the same condition. (C) M3 and CPP-M3 peptides were diluted in 0.05% Triton-X-100/PBS to a final concentration of 40 μM and 10μM. Green fluorescence of the peptides was monitored using a microplate reader. n=2. Error bars present standard deviation of the mean.

4.2.5 Live cell assay investigating functional delivery of M3 into SCL1

Next, it was tested if SCL1 cells can be used to show the delivery of M3 peptide into the cytosol. To investigate this, a live cell assay was performed where 30 µM L-M3, R8-M3 or DMSO was incubated with SCL1 cells for 2 hours, and cells were then analysed with a widefield microscope. No GFP complementation was detected when SCL1 cells were incubated with DMSO cells at 30 µM (Figure 4-5 C) or L-M3 (Figure 4-5 G). For cells incubated with 30 µM R8-M3, the M3 peptide was functionally delivered into the cytosol and complemented with GFP1-10 to form full length GFP (Figure 4-5K). Complemented GFP was again mainly localised in the cytosol and excluded from the nucleus (Figure 4-5K).

Interestingly, even though it was shown that cells of the SCL1 cell line expresses similar amounts of GFP1-10 in their cytosol, GFP fluorescence was not detected in every cell (Figure 4-5K). This means that M3 was delivered functionally in some cells but not in every cell, indicating there might be another cellular mechanism involved that determines functional delivery into cells.
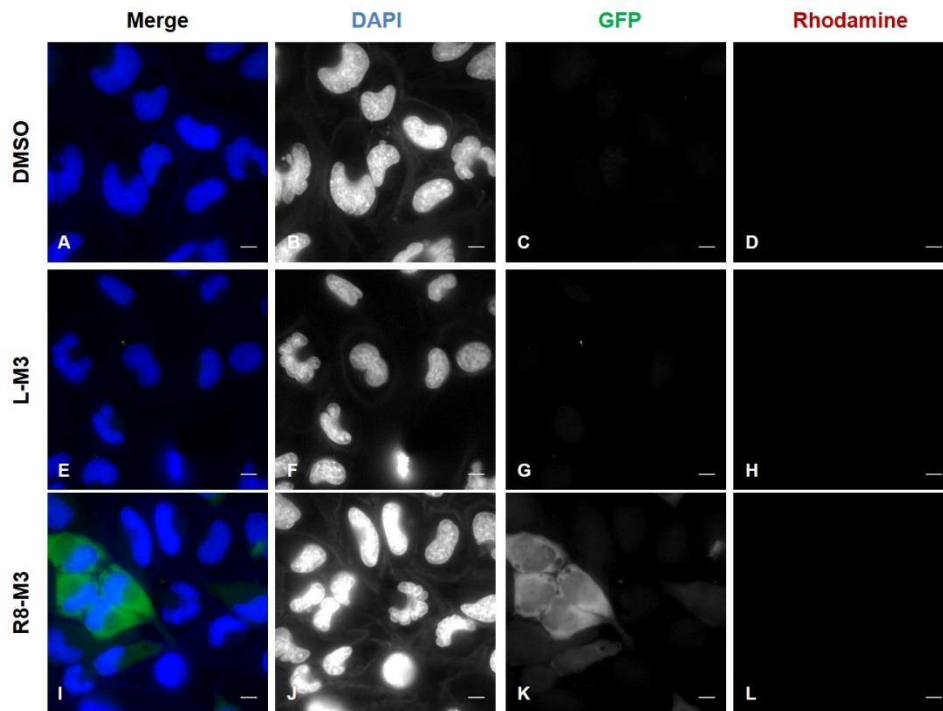
Figure 4-5 Live split GFP assay using SCL1 cells.
SCL1 cells were washed once in serum free media and incubated with L-M3, R8-M3 or DMSO at 30 µM for 2h at 37ºC. Cells were washed with phenol red free RPMI and counterstained with Hoechst nuclear dye. Live cells were images at 37˚C and 5% CO_2 in phenol red free RPMI. Representative images are shown for each condition. n=3. Scale bar: 10 µm.

4.2.6 Visualisation of real time delivery of M3 into SCL1 cells

In order to confirm that SCL1 cells can be utilised to explore real time delivery of the M3 peptide into the cytosol, GFP complementation was investigated over time when 40 µM R8-M3 peptide was applied on the cells in serum free and phenol red free RPMI. GFP complementation was investigated every two minutes using a fluorescent widefield microscope. Cells were first imaged 10 minutes after R8-M3 was incubated with the cells which when, surprisingly, GFP complementation had already taken place (Movie Figure 4-6). Increasing GFP fluorescence was clearly observed over 128 min and can be seen in single images extracted from the movie at time point 2 – 128 min (Figure 4-7 A). To investigate the increase in GFP fluorescence in one area of the cell, a region of interest (ROI) was selected (Figure 4-7 A white square). The increase of GFP fluorescence within this ROI over time is shown in Figure 4-7 B. M3 delivery and GFP complementation in this ROI mainly occurred within the first 20 min when the curve shows a rapid increase in fluorescence. This is followed by a decrease in fluorescence because the RIO was located closely to the nucleus and due to cell movement the fluorescence within the nucleus was detected which was lower compared to the cytosol. Overall, the fluorescence in the cytosol only increased slightly after 20 min and maintained this fluorescence until the end of the movie.
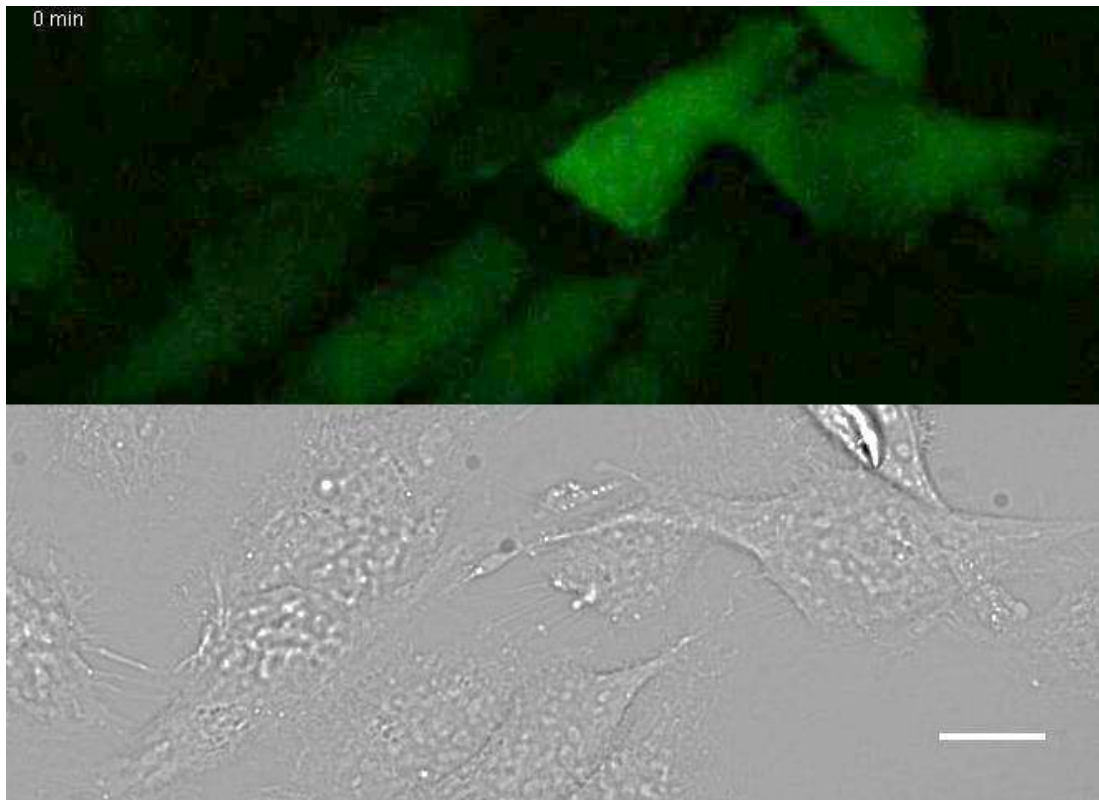
Figure 4-6 Movie of real time delivery of M3 using SCL1 cells
SCL1 cells were washed once in serum free media which was replaced with serum free and phenol red free RPMI containing R8-M3 peptide at 40 µM. GFP complementation was monitored every two minutes for 128 min. Scale bar: 20µm.
Video is available at https://youtu.be/YDNJjmhePIE

A
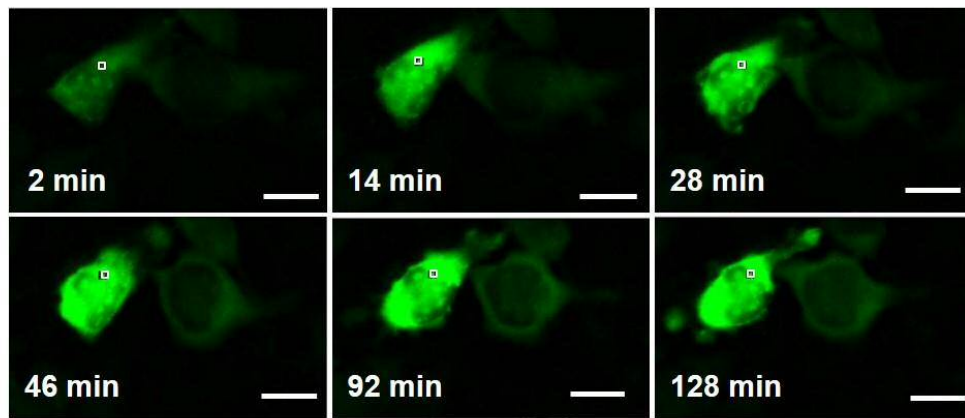
B
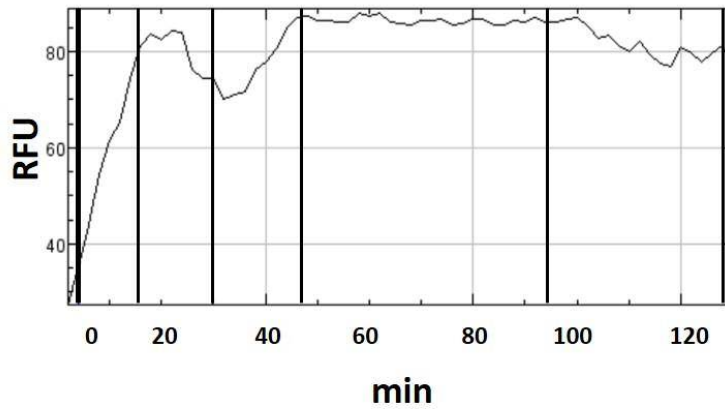
Figure 4-7 Real time delivery of M3 using SCL1 cells

SCL1 cells were washed once in serum free media which was replaced with serum free and phenol red free RPMI containing R8-M3 peptide at 40 µM. GFP complementation was monitored every two minutes for 128 min. (A) Single images from movie shown, captured at 2 min, 14 min, 28 min, 46 min, 92 min and 128 min. White square is RIO. Scale bar: 20µm. (B) RFU of GFP fluorescence shown over time at ROI. Black lines indicate time points of images shown in (A). Data from a single cell from one experiment shown.

4.2.7   Autofluorescence of SCL1 cells

During microscopy experiments it was noticed that untreated SCL1 cells exhibit green fluorescence above that of control cells when excited with 488 nm wavelength light. In order to fully characterise the SCL1 cell line, this fluorescence was investigated further. Figure 4-8 shows a comparison of green fluorescence found in mock transfected Hela cells, cells transiently expressing GFP1-10 and SCL1 cells. Mock transfected HeLa cells show a faint green fluorescence localised around the nucleus in the cell (Figure 4-8 A I). SCL1 cells show increased green fluorescence in the cytosol and the nucleus (Figure 4-8 A V). The population of cells transiently expressing GFP1-10 is mixed with cells that have a faint fluorescence around the nucleus which is similar to the fluorescence detected in mock transfected HeLa cells (marked with a star) and cells where green fluorescence is increased like in SCL1 cells (marked with an arrow) (Figure 4-8 A III). When microscopy images of three independent experiments are quantified it can be clearly seen that the green fluorescence in mock transfected HeLa cells is consistently low in HeLa cells (Figure 4-8 B). SCL1 cells have an increased fluorescence but fluorescence can vary by 5 fold within the cell population. Cells transiently expressing GFP1-10 have single cells with fluorescence as low as mock transfected HeLa cells as well as cells with a high range of green fluorescent levels like SCL1 cells. Resulting from that, the mean green fluorescent intensity across the cell population is the highest in SCL1 cells, decreased for cells transiently expressing GFP1-10 and the lowest for mock transfected HeLa cells (Figure 4-8 C). Furthermore, the green fluorescence was significantly different ($p < 0.001$) in cells transiently expressing GFP1-10 as well as SCL1 cells compared to HeLa cells. HeLa cells are known to contain natural components that exhibit green autofluorescence. However, because the increased green fluorescence in live cells appears in addition to the expression of GFP1-10 in SCL1 or cells transiently expressing GFP1-10, it was hypothesised that this fluorescence might not be increased autofluorescence of the cell but actual GFP fluorescence.
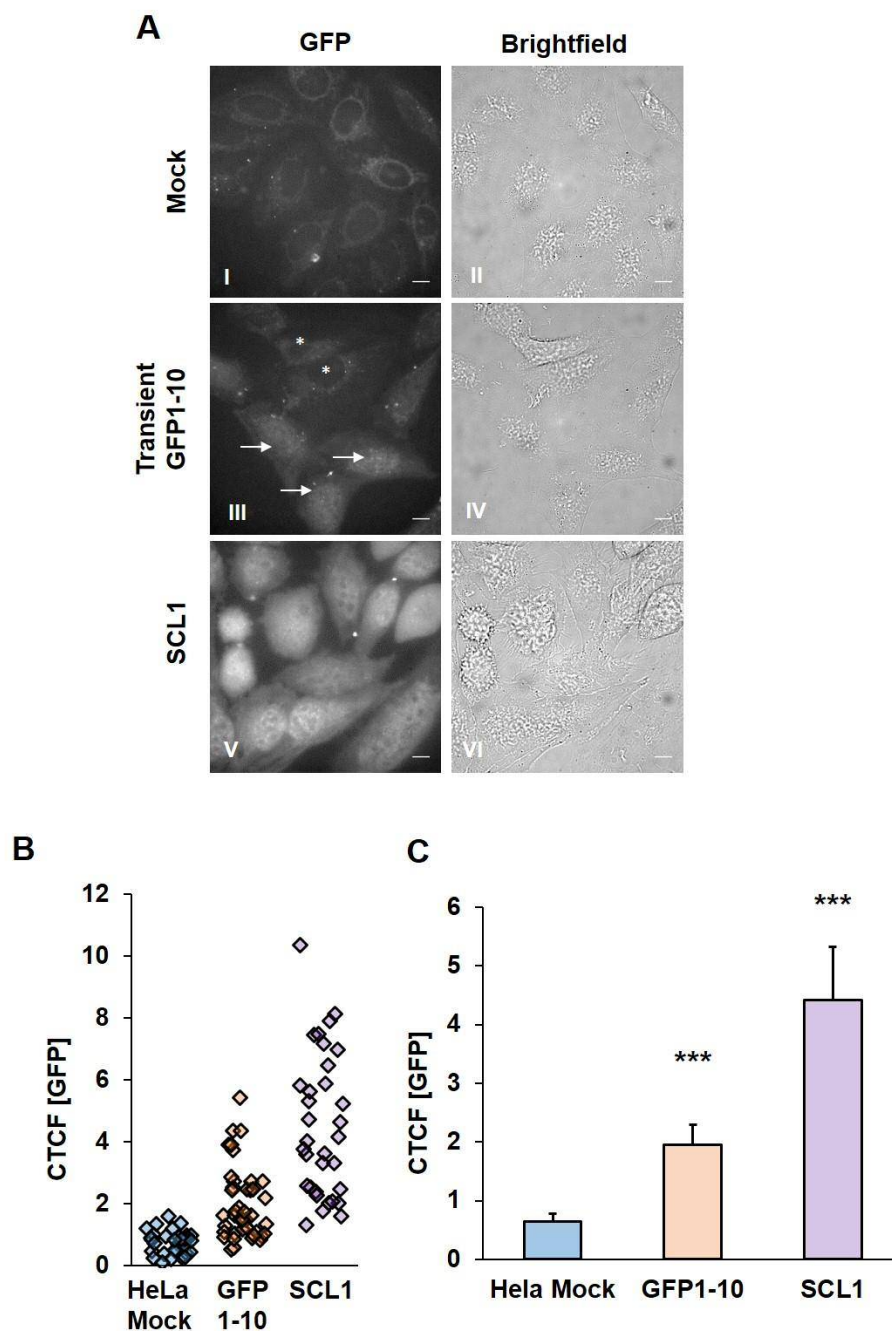
Figure 4-8 Green fluorescence in untreated cells.
Green fluorescence was detected in Mock transfected Hela cells, HeLa cells transiently expressing GFP1-10 and SCL1 cells. To ensure sufficient signal from the faint fluorescence, exposure time was set to 5.0 sec. (A) Representative images for each condition. Cells with high green fluorescence marked with arrow, cells with low green fluorescence marked with star. Scale bar: 10 μm. (B) Quantification of the corrected total cell fluorescence in single cells. (C) Mean fluorescent intensity of green fluorescence. 10-16 cells quantified per condition per experiment. For statistical analysis data was tested using a Kruskal-Wallis test. Significance of is shown compared to HeLa Mock. *: p<0.05, **: p<0.01, ***: p<0.001, n.s.: not significant. Error bar: standard error of the mean. n=3. Two of three experiments performed by Alexander Dudziak under my supervision.

In order to explore if the green fluorescence detected is originated from GFP fluorescence or autofluorescence, mock transfected cells, cells transiently expressing GFP1-10 and SCL1 cells were further analysed using spectral detection on a confocal microscope in a single experiment. This technique allows the detailed analysis of emission spectra that were collected from a sample excited with a 488 nm wavelength laser. The emission spectrum is divided regarding its wavelength between 496 nm and 682 nm wavelength light and collected on different detectors. This spectrum can then be analysed regarding the intensity of fluorescence collected on each detector. Figure 4-9 A shows examples images of each condition and the ROI selected in those cells. To obtain a positive control of the emission spectrum of EGFP, data from cells expressing EGFP was collected (no image shown). When the EGFP spectrum was analysed a peak was detected at 513 nm wavelength light (Figure 4-9 B black curve). In comparison, the green autofluorescence in mock transfected HeLa cells peaked at 539 nm wavelength light. This peak can be shown clearer when data is normalised so that the peak value of each spectrum is set to the value 1 (Figure 4-9 C grey curve). This result suggests that the green fluorescence derived from EGFP expression or autofluorescence of HeLa cells could be differentiated by the peak of their emission spectrum at 513 nm and 539 nm wavelength light, respectively when using the spectral detection method.

In comparison to these emission spectra, cells transiently expressing GFP1-10 were analysed. It was shown before that cells transiently expressing GFP1-10 consist of a divided cell population with cells showing low fluorescence like mock transfected HeLa cells and cells with higher fluorescence. When the emission spectrum of cells with low fluorescence was analysed, it peaked at 539 nm wavelength light (Figure 4-9 B, C orange curve). This aligns with the wavelength of light which was suggested to describe the autofluorescence in HeLa cells and could therefore be derived from the autofluorescence of these cells.

The emission spectrum of cells with high green fluorescence peaked at 513 nm wavelength light (Figure 4-9 B, C purple curve) which was suggested describe the wavelength of the emission peak for cells expressing EGFP. This could imply that the fluorescence of cells found with high green fluorescence is derived from GFP1-10 expression.

The same is suggested for the green fluorescence detected in SCL1 cells as the emission spectrum showed a peak at 513 nm aligning with the suggested EGFP emission spectrum (Figure 4-9 B, C blue curve). The fluorescent spectrum of cells transiently expressing GFP1-10 containing high green fluorescence as well as SCL1 could be a superposition of the spectra obtained when cells are expressing EGFP or autofluorescent control cells. This can be seen in more detail in Figure 4-9 B where the peaks of the emission spectra align with the emission spectrum of EGFP at 513 nm and an addition small peak can be seen at 539 nm and the shape of the emission spectrum curve is more similar to shape of the spectrum obtained for mock transfected control cells.

This data suggests that the green fluorescence seen in live SCL1 cells or cells transiently expressing GFP1-10 is derived from both, autofluorescence as well as GFP fluorescence derived from GFP1-10 expression.
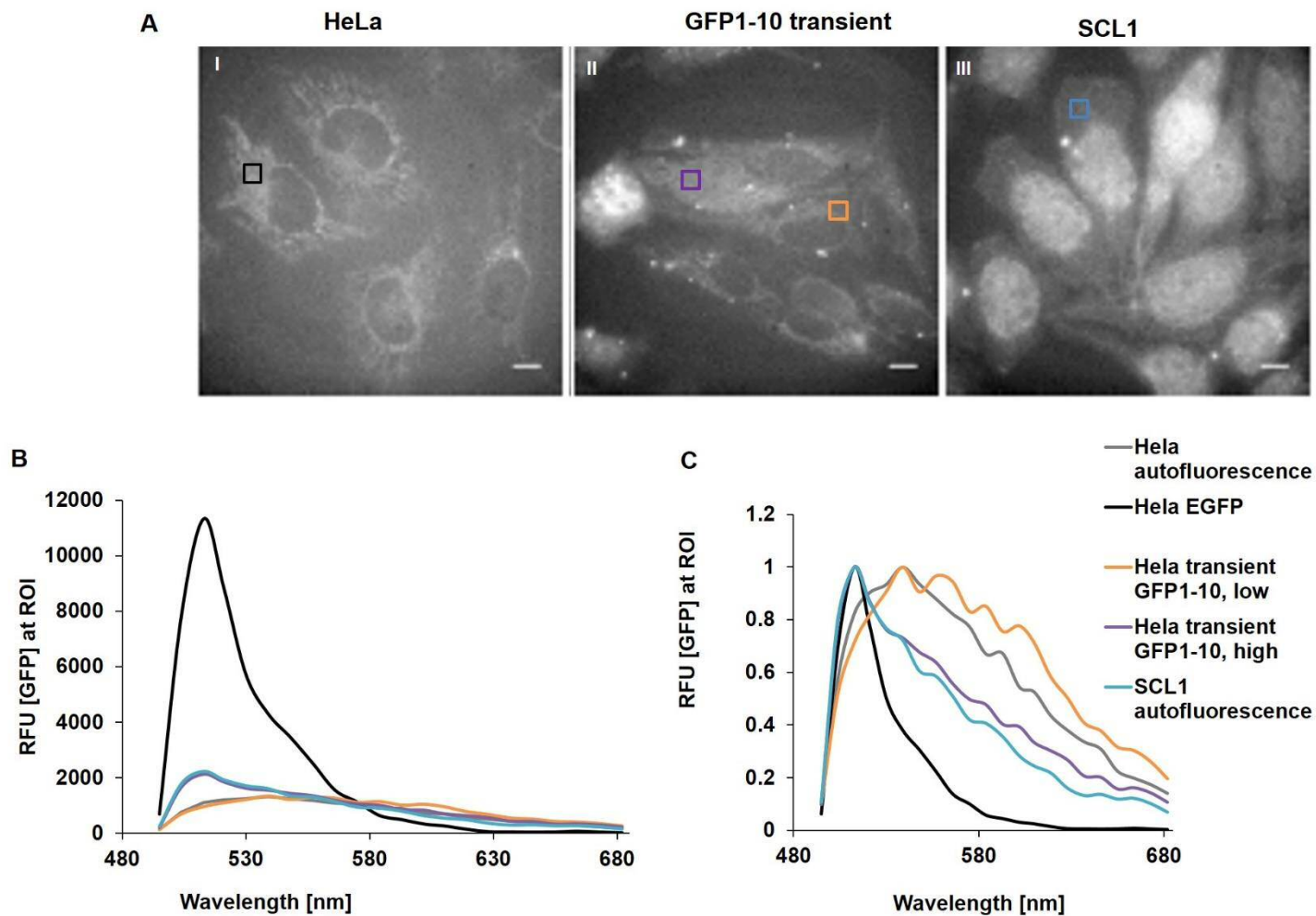
Figure 4-9 Spectral analysis of green fluorescence in SCL1 cells.
HeLa cells or SCL1 cells were grown on coverslips. HeLa cells were mock transfected or transfected with the plasmid coding for GFP1-10 or EGFP expression. (A) Example images of green fluorescence found in HeLa cells (I), GFP1-10 expressing HeLa cells (II) or SCL1 cells (III) no image for EGFP expression shown. ROI marked with coloured square. Scale bar: 10 µM. Images taken on a widefield microscope. (B) Spectral analysis of ROI on a confocal microscope. Untransfected HeLa cells (grey), HeLa cells expressing EGFP (black), HeLa cells expressing GFP1-10 with low fluorescence (orange), HeLa cells expressing GFP1-10 with high fluorescence (purple) and SCL1 cells (blue). Colours correspond to ROIs shown in (A). The data displayed is was collected and analysed by Alexander Dudziak under my supervision. n=1

4.3   Characterisation of mCherry-GFP1-10 expression

The main concern of a split GFP system where cells transiently express GFP1-10 was that expression levels between single cells vary. Hence it is difficult to determine if lack of GFP complementation is due to failure to deliver the M3 peptide or cells were not expressing the GFP1-10 target protein.

A first improvement was to create a stable cell line that expresses even amounts of GFP1-10 across the cell population (see 4.2). It was hypothesised that a second method to improve the split GFP assay is to introduce the fluorescent expression partner mCherry to express mCherry-GFP1-10. This fluorescently labels the presence of GFP1-10 expression and allows correlation of mCherry fluorescence with GFP1-10 expression levels in a live experiment. In order to pursue this strategy, two new expression constructs were generated: pcDNA3.1mCherry-GFP1-10 which codes for cytosolic mCherry-GFP1-10 expression and pcDNA3.1mCherry-GFP which served as a control construct coding for cytosolic mCherry-EGFP expression (see 2.11.6, 2.11.7). The generated mCherry-GFP1-10 expression construct was first tested regarding its expression in HeLa cells as well as its ability to complement with M3 using DNA co-expression and *in vitro* complementation with synthetic M3 peptides.

4.3.1 Immunofluorescent staining of cells expressing mCherry-GFP1-10

Immunofluorescent staining using an anti GFP antibody revealed that mCherry-GFP1-10 can be expressed in the cytosol of HeLa cells. GFP1-10 is non-fluorescent (Figure 4-10 H) while mCherry fluorescence serves as a marker of its expression and co-localises with the anti GFP staining detected by the antibody (Figure 4-10 I, J). Expression of full length mCherry-EGFP showed that the pattern of EGFP expression colocalised with mCherry expression and the anti-GFP staining.

Due to the structural similarity of the fluorescent proteins mCherry and GFP it was further tested that the anti GFP antibody would not cross react to detect mCherry expression. It was seen that fluorescence was detected in the Alexa647 channel on the microscope (Anti GFP) only when cells expressed high amounts of mCherry (Figure 4-10 O). This fluorescence could be due to cross reaction of the antibody or an effect of bleed through from mCherry which was excited with the excitation wavelength used in the Alexa647 channel. In order to fully investigate this, the bleed through into the Alexa647 channel of cells expressing mCherry but not treated with antibodies has to be investigated.

However the fluorescence seen in the Alexa647 channel for cells expressing mCherry is weak compared to the fluorescence seen when mCherry-EGFP and mCherry-GFP1-10 were expressed in the cytosol (Figure 4-10 E, J). Thus, the majority of the anti GFP antibody staining was still specific to EGFP or GFP1-10 expression.
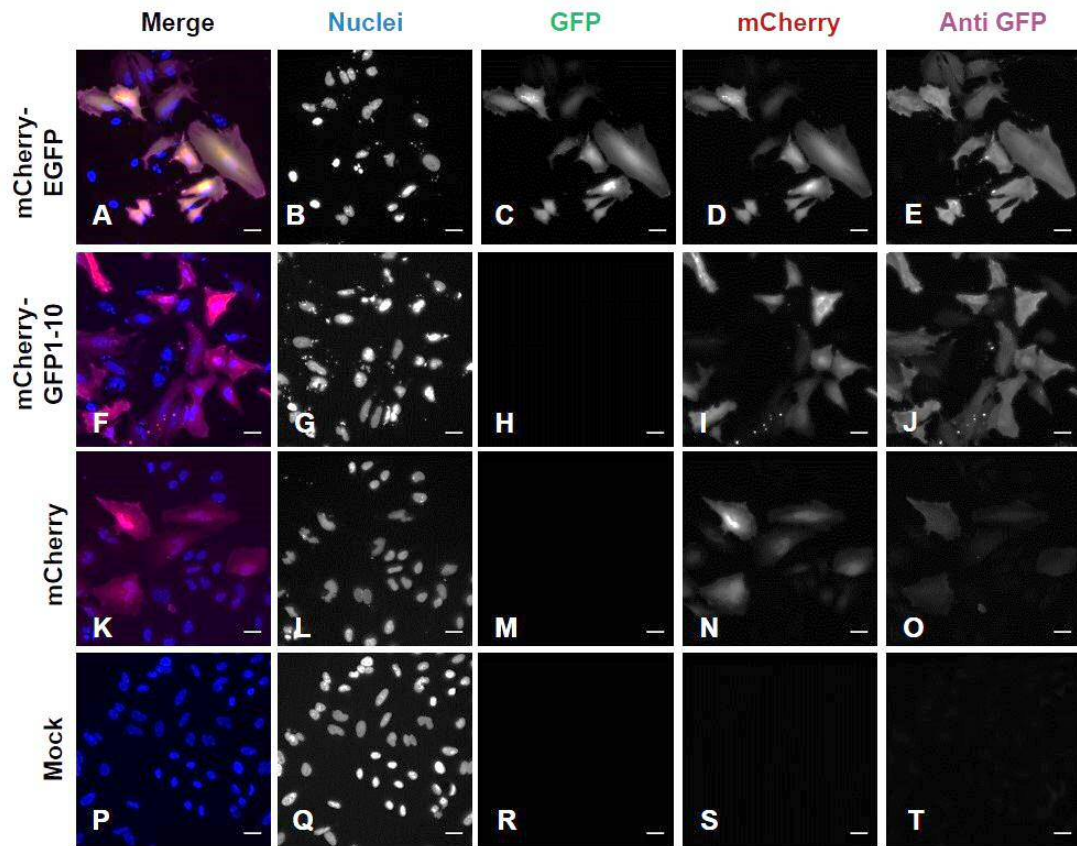
Figure 4-10 Detection of mCherry-GFP1-10 expression in HeLa cells using immunofluorescence.
HeLa cells were transiently transfected with DNA constructs coding for mCherry-GFP1-10 or full length mCherry-EGFP. The transfection mix of mock transfected cells did not contain DNA. Cells were incubated in transfection mix overnight and PFA fixed the next day. The plasma membrane was permeabilised with 0.1 % Triton-X-100 and GFP or GFP1-10 expression was detected using a primary anti-GFP antibody raised in goat. A secondary anti-goat antibody conjugated to Alexa-647 was used to visualise GFP expression. Nuclei were counterstained with DAPI. Representative images shown for each condition. Scale bars: 30 µm. n=3, mCherry n=2.

4.3.2   GFP complementation using co-expression of GFP fragments

Next, GFP complementation of M3 with mCherry-GFP1-10 was investigated using co-transfection of DNA coding for mCherry-H6-Xa-R8-M3 and mCherry-GFP1-10. GFP complementation was detected using a microscope (Figure 4-11 A). Complementation only occurred when both split GFP fragments were co-expressed inside the cell (Figure 4-11 XII); no GFP fluorescence was detected when the single fragments were expressed alone (Figure 4-11 III, VII). Furthermore, the localisation of complemented GFP was found in the cytosol and localised at the nucleolus (Figure 4-11 XII).

Detection of GFP complementation was also confirmed using detection of green fluorescence in trypsinsed cells on the microplate reader (Figure 4-11 B). Single split GFP fragments did not fluoresce in green; when both fragments were co-expressed, GFP complementation occurred and was detected as GFP fluorescence that was significantly different (p<0.001) from when single GFP fragments were expressed in in HeLa cells.
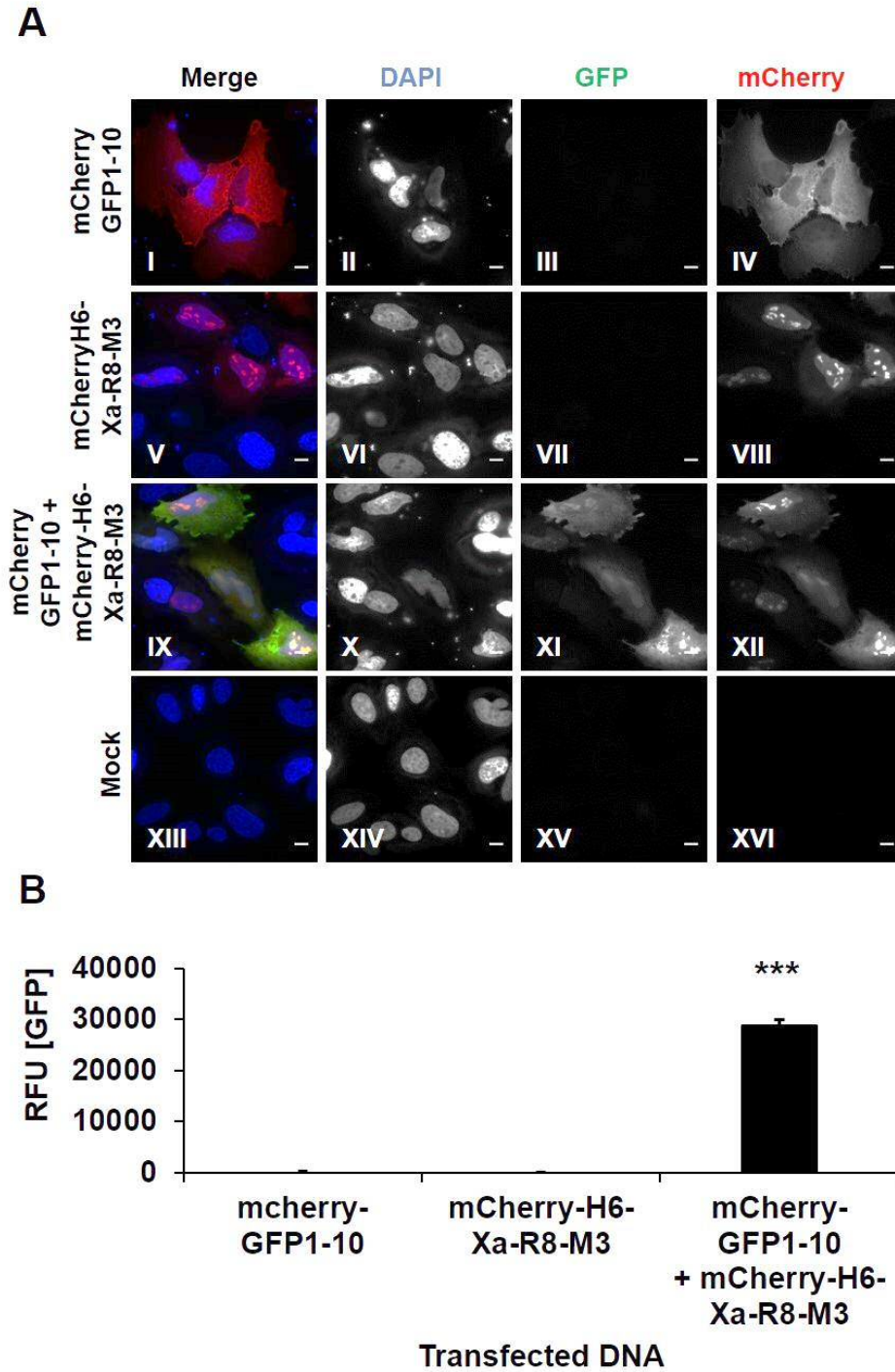
Figure 4-11 Co-transfection of GFP1-10 and mCherry-H6-Xa-R8-M3.
Transfections or co-transfections of HeLa cells were performed with DNA encoding for split GFP fragments. The transfection mix of mock transfected cells did not contain DNA. (A) Cells were left in transfection mix overnight and PFA fixed on the next day. Nuclei were counterstained with DAPI. Representative images for each condition shown. Scale bars: 10 μm. N=1. (B) Detection of co-expression on a microplate reader. RFU=Relative Fluorescent Units. Fluorescent background of mock transfected cells was subtracted from sample values. For statistical analysis data was tested using a One way Annova followed by multiple comparison using a Turkey HSD (honest significant difference) test. Significance is shown compared to mCherry-GFP1-10 and mCherry-H6-Xa-R8-M3. *: $p < 0.05$, **: $p < 0.01$, ***: $p < 0.001$, n.s.: not significant. Error bars present standard error of the mean. n=3.

4.3.3 *In vitro* complementation of M3 peptides with transient mCherry-GFP1-10

It was also investigated in a single experiment if cell lysate containing mCherry-GFP1-10 was able to complement with synthetic M3 peptides *in vitro* at 40 μM (Figure 4-12 A) using the improved *in vitro* assay. *In vitro* complementation of cell lysate derived from cells transiently expressing mCherry-GFP1-10 with M3 containing peptides was monitored for 2 hours. The data suggests that lysate of mCherry-GFP1-10 complemented with M3, L-M3 and R8-M3 resulting in GFP fluorescence that increased 2-3 fold between 15 min to 2 hours. The green fluorescence of L-M3 was slightly increased as it was shown in previous experiments. Interestingly, R8 itself shows a slight increase in GFP fluorescence over 2 hours. However, it was shown before that R8 itself cannot complement with GFP1-10 which suggests that this increase could be due to fluctuations of the measurements on the plate reader.

It is further shown on microscopy images that cell lysate incubated with R8 did not fluoresce in green (Figure 4-12 B) which could support the suggestion that the measured fluorescence on the microplate reader is due to plate reader variability.

Microscopy images further show that all samples contained cell lysate of mCherry-GFP1-10 indicated by its red fluorescence (Figure 4-12 B II, V, VIII, XII, XIV). However, GFP complementation only occurred when the cell lysate was incubated with M3 containing peptides L-M3, M3 and R8-M3 (Figure 4-12 B XI, XII, XV). No complementation was detected with the microscope when DMSO or R8 were incubated with the lysate (Figure 4-12 B III, VI). Interestingly, the cell lysate mixture looked like a homogenous solution when incubated with M3 and L-M3 but contained particles when incubated with R8-M3 (Figure 4-12 XV).
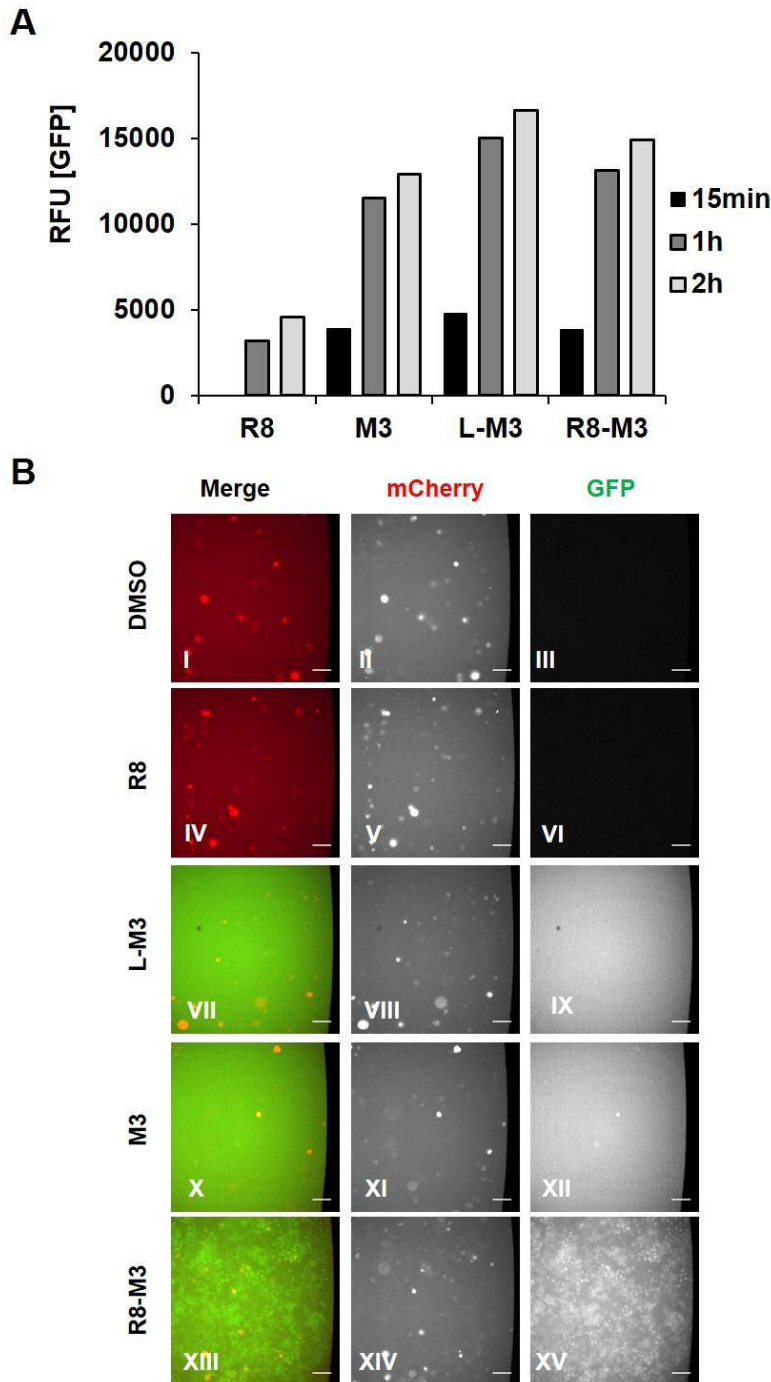
Figure 4-12 *In vitro* GFP complementation of transient mCherry-GFP1-10 cell lysate with peptides.

HeLa cells expressing mCherry-GFP1-10 were trypsinised and lysed using 0.1% Triton-X100 in PBS. Cell lysate of 0.8X105 cells was mixed with 80 µM M3 and CPP-M3 peptides to obtain a final concentration of 40 µM in 0.05% Triton-X-100/PBS. Lysate mixture was left under constant agitation at 4 ºC. (A) The fluorescent signal resulting from GFP complementation was monitored over 2 h using a microplate reader. DMSO only control was subtracted as sample background. (B) Microscopy images of cell lysates after two hours of incubation. Left edge of well was taken as a reference point in each well to image the same focal plane between conditions. Scale bar: 150 µM. n=1.

4.3.4 Live delivery of M3 by R8 to the cytosol of cells transiently expressing mCherry-GFP1-10

Next M3 delivery by R8 was tested in cells transiently expressing mCherry-GFP1-10. When DMSO and M3 at 20 µM were incubated with the cells, no GFP complementation was detectable after 2h (Figure 4-13 C, G). However, weak green fluorescence in cells was seen in both samples, the DMSO control as well in the cells incubated with M3. This weak fluorescence has been detected before when GFP1-10 was expressed in cells which could suggest that the weak fluorescence is derived from mCherry-GFP1-10 expression. An observation that could confirm this hypothesis is that only cells that were expressing mCherry-GFP1-10 (Figure 4-13 D, H) showed this weak fluorescence in the green channel.

Because this fluorescence was found in DMSO control cells it is suggested that it cannot derive from GFP complementation with the M3 peptide. Green fluorescence was also found previously in cells expressing GFP1-10, hence it is possible that this GFP fluorescence is also present when cells transiently express mCherry-GFP1-10. When 20 µM R8-M3 were incubated with cells transiently expressing mCherry-GFP1-10 for 2 h, GFP fluorescence is detectable in one cell and suggests that R8 mediated M3 delivery may have occurred in that cell (Figure 4-13 K). It can also be seen that GFP complementation occurred in cells expressing mCherry-GFP1-10 (Figure 4-13 L, K).

Taken together, this data presented suggests that cells transiently expressing mCherry-GFP1-10 could also be utilised to investigate M3 delivery by the DDS R8. mCherry can serve as an expression marker for GFP1-10 expression that enables us to track which cell expresses GFP1-10 and how much is expressed. This is an improvement to the assay and allows transient expression of mCherry-GFP1-10. However, it was seen that R8-M3 does not deliver M3 evenly across the cell population when it was incubated with the stable cell line SCL1 and another

mechanism was proposed to determine in which cells M3 cargo delivery is successful. Thus, utilising an assay where mCherry-GFP1-10 is expressed transiently will result in a diverse cell population where some cells do not express the protein at all. In order to be able to investigate the underlying mechanism of heterogeneous delivery across a cell population in the future, it is necessary to have a homogenous population of cells. Thus, a stable cell line was generated to express mCherry-GFP1-10. Another advantage to create a stable cell line was that experimental conditions are constant between experiments and not affected by transfection efficiency.
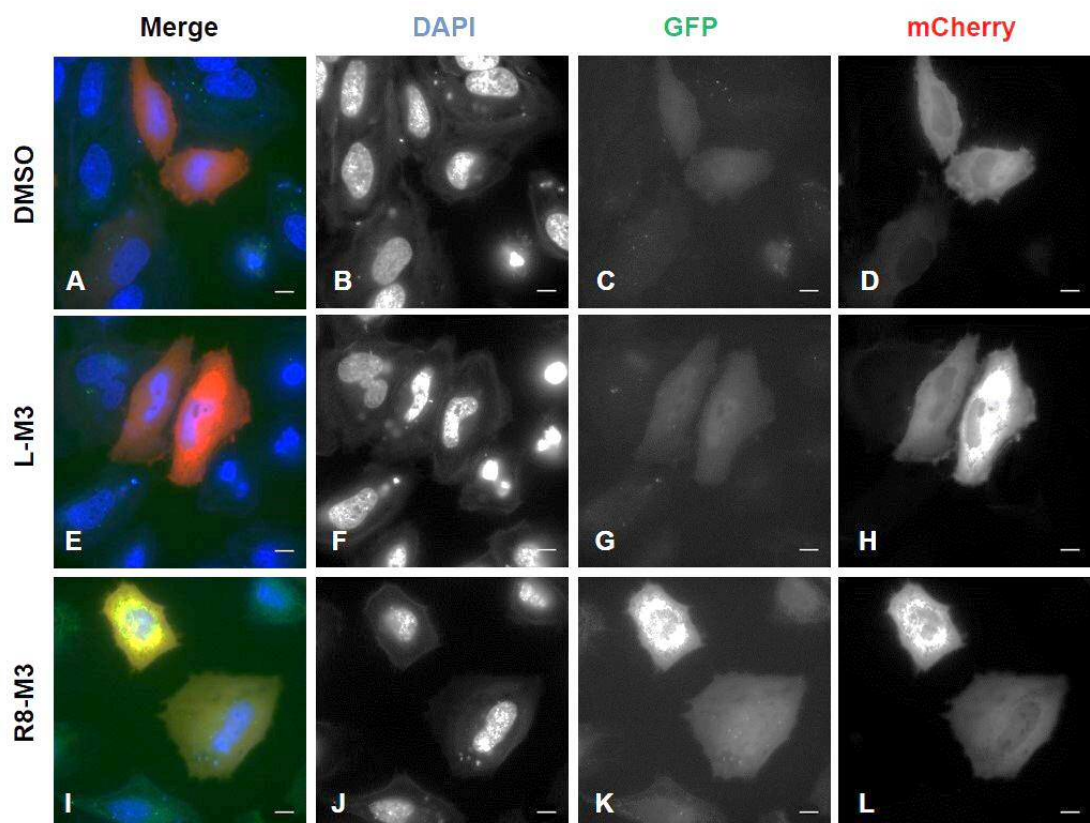
Figure 4-13 Delivery of M3 by R8 and GFP complementation in live cells transiently expressing mCherry-GFP1-10.
Cells transiently expressing mCherry-GFP1-10 were washed once in serum free media and incubated with DMSO, M3 or R8-M3 at 20µM in serum free media for 2 hours at 37˚C. Cells were washed with phenol red free RPMI and counterstained with Hoechst nuclear dye. Live cells were images at 37˚C and 5% CO_2 in phenol red free RPMI. Representative images shown for each condition. n=1. Scale bar: 10µm.

4.4   Generation of mCherry-SCL51

In order to generate a stable cell line that expresses mCherry-GFP1-10, HeLa cells were transfected with one DNA plasmid coding for mCherry-GFP1-10 and neomycin resistance. Thus, cells that had stably integrated this expression construct into their genome were selected using selection media containing 400 mg/mL Geneticin (G418). To obtain a clonal cell line, limiting dilution was performed (for detailed stable cell line generation see 2.8). mCherry as an expression marker for GFP1-10 had the great advantage that colonies could be screen by live microscopy. Single colonies were screened to obtain colonies with high and even fluorescent expression levels of mCherry-GFP1-10 throughout the cell population. In the first round of screening, mCherry-GFP1-10 expression was determined by mCherry fluorescence of live cells. In total 864 wells were screened using limiting dilution, 38 wells contained cells that showed mCherry fluorescence. From these cells the most promising cell colony with highest mCherry-GFP1-10 expression levels was mCherry Split Cell Line 34 (mCherry-SCL34). However, mCherry-SCL34 was a polyclonal cell line with a high number of cells not expressing mCherry-GFP1-10 at all (Appendix 9.4, Figure 9-6). For this reason, this cell line was expanded and another round of limiting dilution was performed. 96 cell colonies were screened in the second round of limiting dilution and 17 more colonies of cells were obtained. Of these cell lines the cell line which expressed highest amounts of mCherry-GFP1-10 and showed most even expression levels across the cell population was named mCherry Split Cell Line 51 (mCherrySCL51) and underwent detailed characterisation using techniques developed previously to ensure stable expression of mCherryGFP-10 while retaining compatibility of reassembly with M3.

4.4.1 Immunofluorescent staining of mCherry-SCL51

Immunofluorescent staining against GFP was performed to confirm that not only mcherry is expressed evenly across the cell population but also GFP1-10 as a fusion to mCherry. Staining against GFP revealed that the obtained cell line mCherry-SCL51 expressed even levels of mCherry-GFP1-10 compared to cells transiently expressing mCherry-GFP1-10 where expression levels vary highly between cells (Figure 4-14 A VI, XII). However, despite two rounds of limiting dilution in order to obtain a clonal cell line where every cell expresses mCherry-GFP1-10, the cell population of mCherry-SCL51 was not clonal and cells either expressed the same amount of mCherry-GFP1-10 or did not express the protein at all (Figure 4-14 A, XII). This finding was confirmed by quantification of the anti GFP stain of microscopy images (Figure 4-14 B). Mock transfected cells displayed a very low anti GFP staining. When mCherry-GFP1-10 was transiently expressed in HeLa cells, anti GFP staining ranged by 100 fold between the cells with cells not expressing the protein at all or cells highly expressing the protein. The quantification of the anti GFP staining for the mCherry-SCL51 cell line confirms that this cell line is split into two populations: cells not expressing mCherry-GFP1-10 showing the same fluorescent values as mock transfected cells and cells expressing mCherry-GFP1-10 in their cytosol with values located in the medium expression range of cells transiently expressing the protein. Calculation of the coefficient of variation confirmed that the variation of expression levels of GFP1-10 in single cells is reduced in the stable cell line mCherry-SCL51 (0.64) compared to cell transiently expressing mCherry-GFP1-10 (1.45) (Figure 4-14 C). Even though mCherry-SCL51 was found to be a polyclonal cell line containing cells not expressing mCherry-GFP1-10 at all, there was little difference of the coefficient of variation between mock transfected cells (0.56) and the stable cell line (0.64).
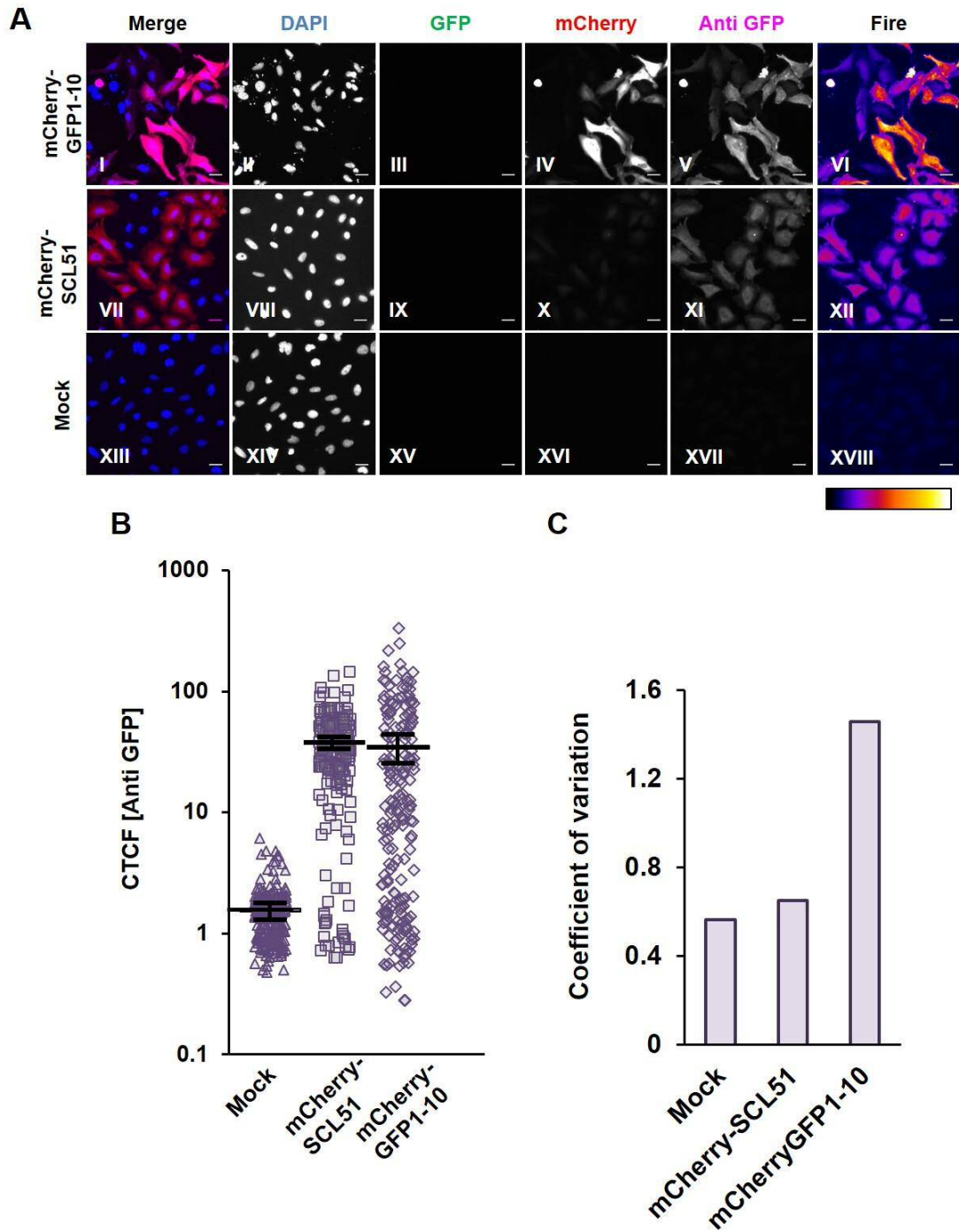
Figure 4-14 Comparison of mCherry-GFP1-10 expression levels of mCherry-SCL51 cells and cells transiently expressing mCherry-GFP1-10 using immunofluorescence. HeLa cells transiently expressing mCherry-GFP1-10, mCherry-SCL51 cells or mock transfected cells were PFA fixed and the plasma membrane was permeabilised with 0.1 % Triton-X-100. GFP1-10 expression was detected using a primary anti-GFP antibody raised in goat. A secondary anti-goat antibody conjugated to Alexa-647 was used to be able to visualise GFP expression. Nuclei were counterstained with DAPI. (A) Representative images of the immunofluorescent stain. Grey levels displayed on fire table range from 38 to 4368. Scale bars represent 30 µm. (B) Quantification of the CTCF of the anti GFP staining. (C) Coefficient of variation was calculated by dividing the standard deviation of the CTCF of all data points by the value of the mean CTCF. Error bars show SEM between experiments. 72 to 85 cells were analysed per condition per experiment. n=3.

4.4.2 Correlation of mCherry fluorescence and GFP1-10 expression

In order to use mCherry as a fluorescent expression marker for GFP1-10 expression it was next observed if there if the mCherry fluorescence can be correlated with the fluorescence obtained from the immunofluorescent staining against GFP1-10. For this reason the corrected total cell fluorescence (CTCF) of mCherry was determined in the same cells where the CTCF of the anti GFP stain was detected (Figure 4-15 A, B). When comparing the fluorescence of the antibody stain (Figure 4-15 A) with the mCherry fluorescence (Figure 4-15 B), it can be seen that the distribution of the single data points correlate. There is a high variation of mCherry and anti GFP fluorescence for cells transiently expressing mCherry-GFP1-10 and a divided cell population of mCherry-SCL51 cells, expressing even amounts of mCherryGFP1-10 or non-expressing cells with low values as low as mock transfected cells. These observations confirm that mCherry-SCL51 is a polyclonal cell line but cells expressing mCherry-GFP1-10 express similar amounts that are in the medium range of the expression that can be achieved using transient transfection. Furthermore, it is shown that the fluorescence of the antibody stain detecting GFP1-10 expression and mCherry fluorescence comparable when the same cells are measured suggesting that mCherry fluorescence can be correlated with GFP1-10 expression.

Next it was tested if mCherry fluorescence can be correlated with GFP1-10 expression in mCherry-SCL51 cells. Figure 4-15 C shows a graph correlation the mean fluorescence of mCherry of a single cell with the mean fluorescence of the anti GFP stain measured in the same cell representing GFP1-10 expression. A correlation coefficient of 0.79 was found which presents a correlation between mCherry fluorescence and anti GFP staining. The variation of data leading to a 0.79 correlation could have been due to the antibody detection of the GFP1-10 expression and the variability of antibody staining of GFP1-10 between single cells.
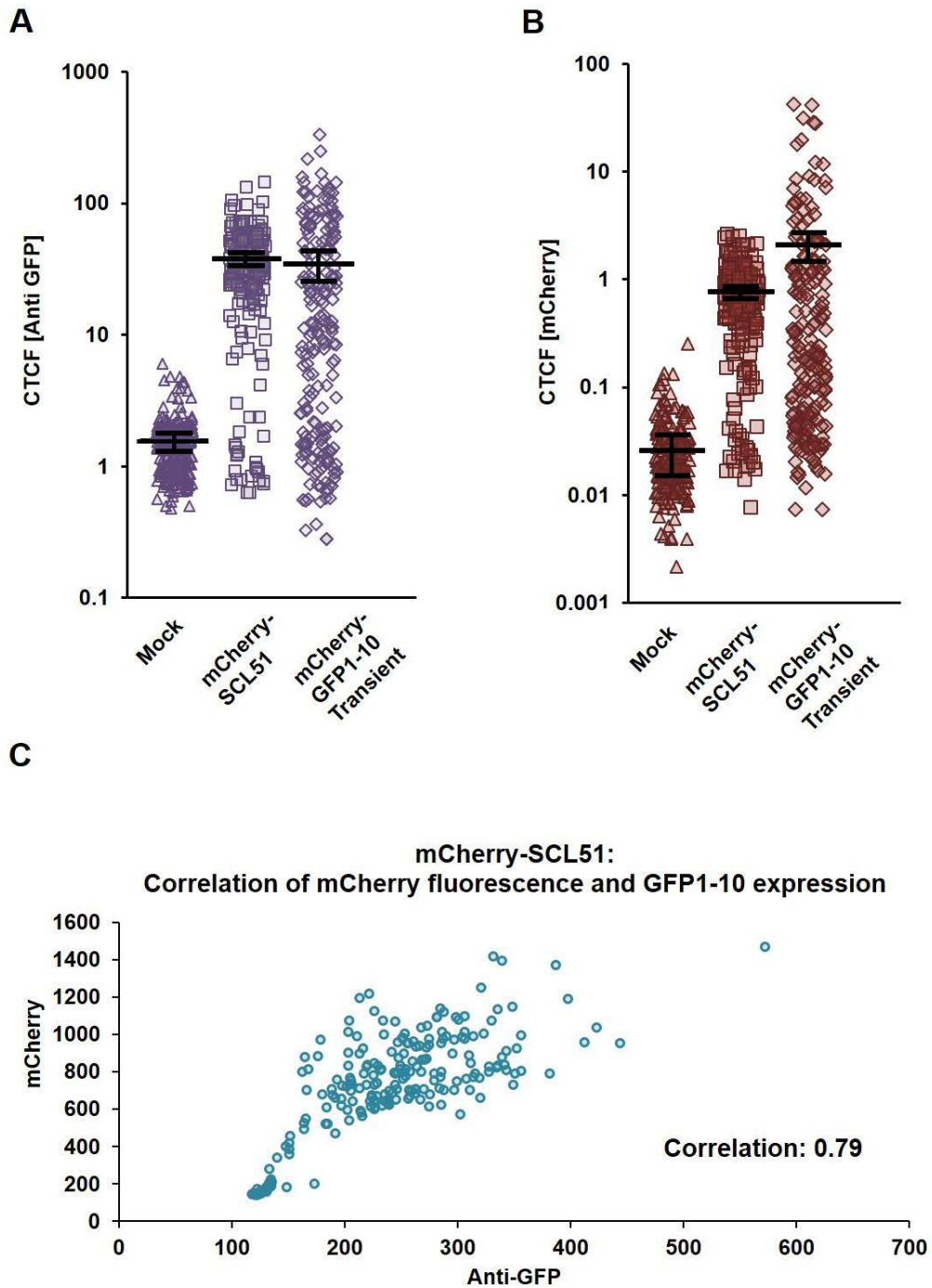
Figure 4-15 Correlation of GFP1-10 and mCherry expression
(A) Quantification of the CTCF of the anti GFP staining (B) Quantification of the CTCF of mCherry fluorescence. Single data point represent the fluorescence in the cytosol of single cells. Fluorescent intensities were measured within the same cells. Error bars show standard error of the mean between experiments. (C) Correlation of mean fluorescence of mCherry and anti-GFP staining in Mcherry-SCL51 cells. Fluorescence was measured within the same cell. 72 to 85 cells were analysed per condition per experiment. n=3.

4.4.3 Co-expression of mCherry-H6-Xa-R8-M3 in mCherry-SCL51

Next GFP complementation was tested using expression of the small split GFP fragment, mCherry-H6-Xa-R8-M3 in the stable cell line. When fluorescence of transfected cells was investigated using a microplate reader, it was seen that GFP complementation occured when mCherry-GFP1-10 and mCherry-H6-Xa-R8-M3 are co-expressed in the cytosol of HeLa cells (Figure 4-16). This fluorescence was significantly defferent compared to the fluorescence that was detected when single GFP fragments were expressed alone. When mCherry-H6-Xa-R8-M3 was expressed in the stable cell line mCherry-SCL51, GFP complementation occurred showing that the stable cell line expressing mCherry-GFP1-10 is abe to complement with the M3 fragment encoded in mCherry-H6-Xa-R8-M3. Importantly, this fluorescence was significantly different compared to fluorescence detected when mCherry was expressed in the stable cell line or when cell were mock transfected. This means expression of mCherry alone did not rescue GFP fluorescence confirming that mCherry does not have the ability to complement with GFP1-10 to form full length GFP. Fluorescence seen when mCherry was transfected into mCheryy-SCL51 was equal to the fluorescence on mock transfected cells.

It can also be seen that GFP fluorescence resulting from complementation with mCherry-H6-Xa-R8-M3 was five times lower in the stable cell line then in cells transiently expressing both split GFP fragements. This could have been due to one part of the cell population not expressing mCherry-GFP1-10 at all as well as lower expression levels of mCherry-GFP1-10 of the remaining cells compared to cells transiently expressing mCherry GFP1-10.
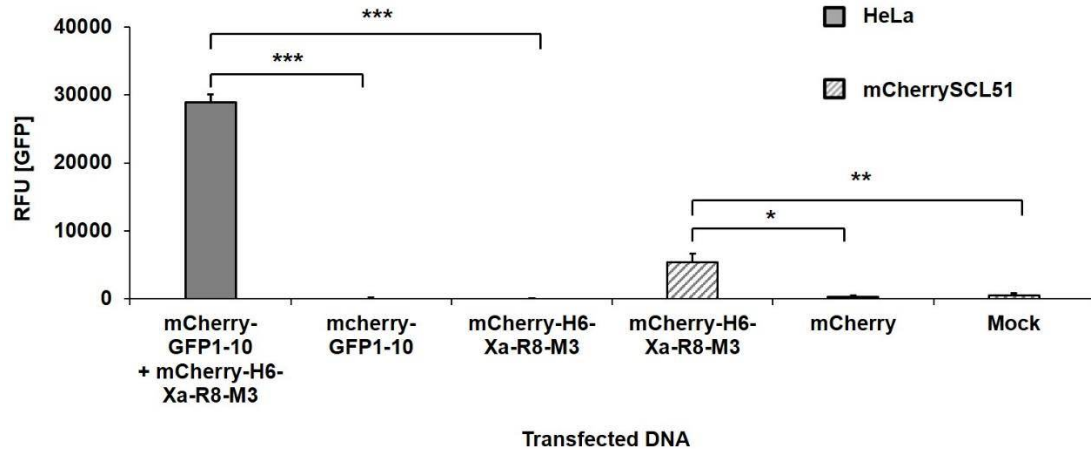
Figure 4-16 GFP complementation in mCherry-SCL51 cells using transfection of mCherry-H6-Xa-R8-M3.
HeLa cells (solid grey) or mCherry-SCL51 cells (striped) were transfected with DNA coding for with single or both split GFP fragments. Green fluorescence derived from GFP complementation was detected on a microplate reader. Value of mock transfected HeLa was subtracted to correct for background fluorescence. For statistical analysis data was tested using a One way Annova followed by multiple comparison using a Turkey HSD (honest significant difference) test. *: $p<0.05$, **: $p<0.01$, ***: $p<0.001$, n.s.: not significant. Error bars present standard error of the mean. n=3.

4.4.4 *In vitro* GFP complementation of M3 peptides with mCherry-SCL51

Next mCherry-SCL51 was tested regarding its ability to complement with synthetic M3 peptides *in vitro*. It was also of interest if the *in vitro* assay using cell lysate could be further improved by allowing GFP complementation at room temperature compared to 4°C. For this reason cell lysate of mCherry-SCL51 was incubated with M3 containing peptides in 0.05%Triton-X-100/PBS at a final concentration of 40 µM. Then the same cell lysate-peptide mix was incubated at either 4°C (Figure 4-17 A) or room temperature (Figure 4-17 B) under constant agitation, and GFP fluorescence was monitored on a microplate reader over 7h. In both samples R8 itself did not rescue GFP fluorescence. Moreover, the green fluorescence of lysate incubated with L-M3 was increased in samples incubated at 4°C as well as at room temperature throughout the experiment, as found earlier. Furthermore, the data from this single experiment suggested that GFP complementation was faster at room temperature compared to 4°C. This could be due to the increased motion of the

GFP fragments in solution which results in an increased rate of fragments complementing. When incubated at 4°C (Figure 4-17 A) green fluorescent levels reached 2100 and 1600 RFU after 5 min of incubation with M3 and R-M3, respectively. Green fluorescence peaked after 5 hours when GFP levels had reached 8600 RFU for M3 and 6900 RFU for R8-M3. Over the next two hours there was a slight decrease detected which resulted in 5800 RFU for M3 and 5700 RFU for R8-M3 after 7 h. Compared to that, GFP complementation constantly increased over time when the cell lysate was incubated with the peptides at room temperature (Figure 4-17 B). After 5 min green fluorescence was comparable with samples that were incubated at 4°C with 2500 RFU of M3 of and 1200 RFU for R8-M3. However, due to preparation of the samples at room temperature, samples had not been incubated at 4°C at that time. GFP fluorescence increase to 28,000 RFU for R8-M3 and M3 after 7 h which is a 10 fold increase compared to the fluorescence measured after 5 min. The increase of fluorescence of samples incubated at 4°C was only 3 fold. The data from this single experiment suggested that GFP complementation occurs faster, and time dependent complementation was more consistent at room temperature. Hence, *in vitro* complementation of peptides was continued to be investigated at room temperature in further experiments (Figure 4-17 C). The data from three independent *in vitro* experiments performed at room temperature confirmed that GFP complementation increased constantly over time and complementation only occurred when the M3 peptide was present.
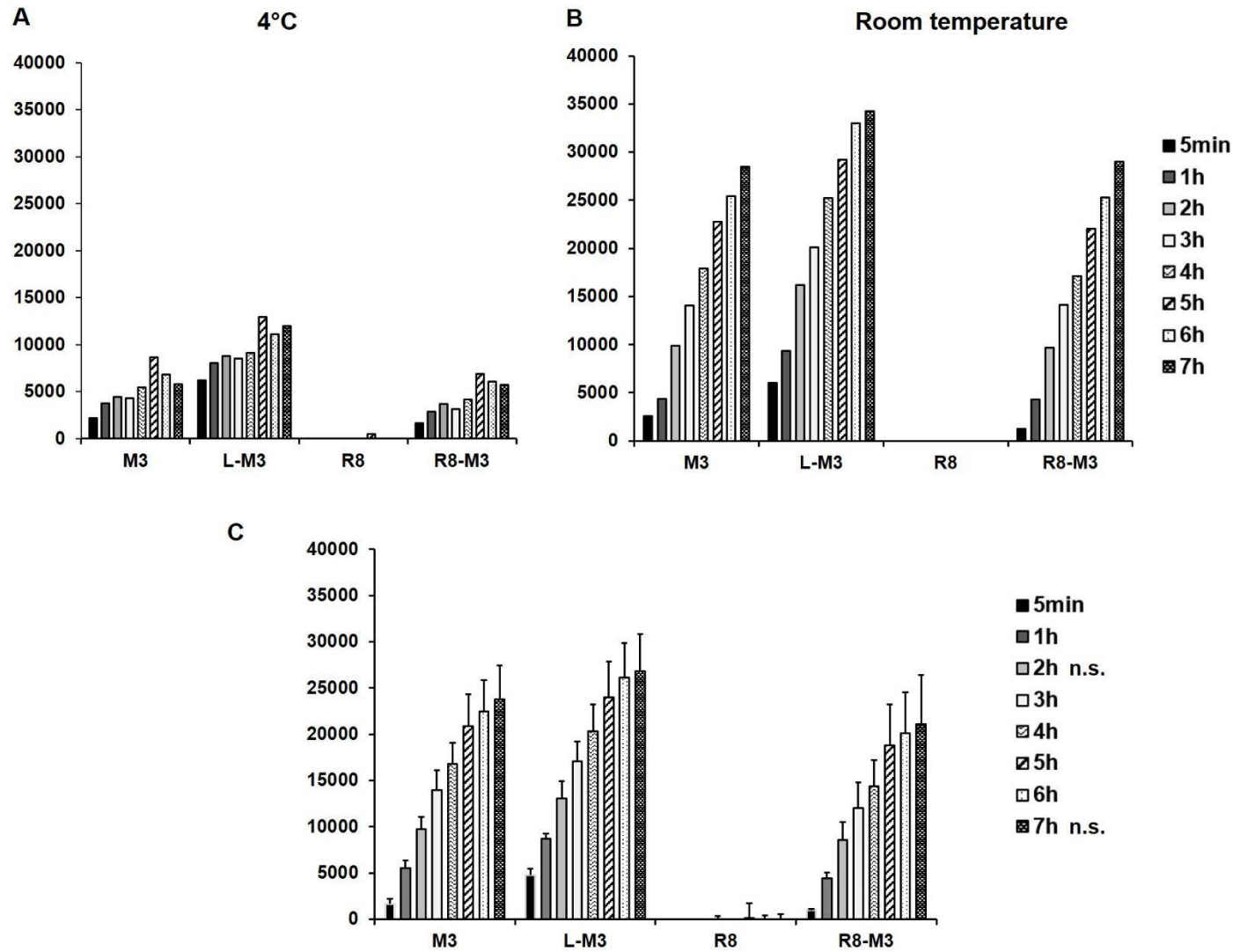
Figure 4-17 *In vitro* GFP complementation of mCherry-SCL51 cell lysate with M3 peptides.

mCherry-SCL51 cells were trypsinised and lysed using 0.1% Triton-X100 in PBS. Cell lysate of $0.8X10^5$ cells was mixed with 80 µM M3 and CPP-M3 peptides to obtain a final concentration of 40 µM in 0.05% Triton-X-100/PBS. GFP complementation was monitored over 7 h using microplate reader. (A) GFP complementation at 4°C. (B) The same samples were incubated at room temperature. n=1. (C) GFP complementation at room temperature. DMSO only control was subtracted as sample background. n=3. Error bars present standard error of the mean. For statistical analysis data was tested using a One way Annova followed by multiple comparison using a Turkey HSD (honest significant difference) test. Data was tested at two time points, 120min and 7h. No significant differences were detected between M3 containing peptides at time points 2h and 7h. n.s.: not significant.

4.4.5 Live cell assay mCherry-SCL51

Finally, it was investigated if M3 delivery by the DDS R8 can be monitored using the mCherry-SCL51 cell line. When DMSO and M3 were incubated with the cells at 40 μM, a high green fluorescent background in all cells was detected in the cytosol with a higher fluorescence in the nucleus (Figure 4-18 C, G). Incubation of 40 μM R8-M3 with mCherry-SCL51 resulted in clear GFP complementation in the cytosol of one cell in the field of view, other cells showed the same amount of fluorescent background like cells incubated with DMSO and M3 (Figure 4-18 K). This experiment suggests R8 dependent delivery at 40 μM as well as a heterogeneous M3 delivery across the cell population where every cell was expressing the mCherry-GFP1-10 target but GFP complementation was only successful in one cell. Furthermore, complemented GFP was localised in the cytosol, no GFP fluorescence was detected in the nucleus (Figure 4-18 K).
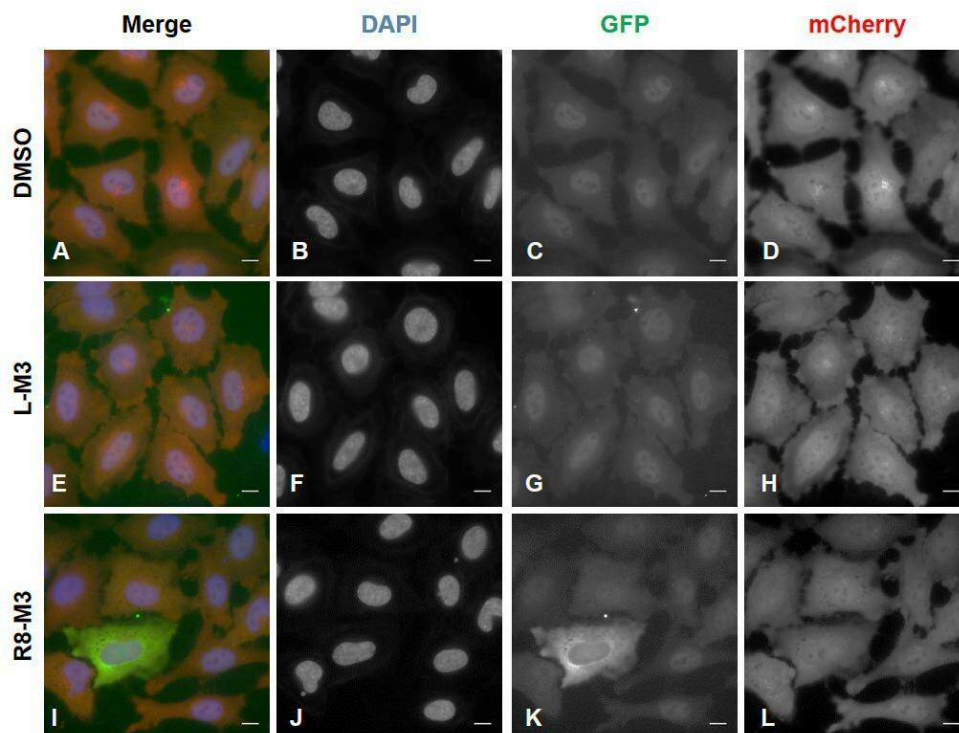
Figure 4-18 Live delivery of M3 into mCherry-SCL51 cells.
mCherry-SCL51 cells were washed once in serum free media and incubated with DMSO, L-M3 or R8-M3 at 40μM in serum free media for 2 hours at 37˚C. Cells were washed with phenol red free RPMI and counterstained with Hoechst nuclear dye. Live cells were images at 37˚C and 5% CO_2 in phenol red free RPMI. Representative images shown for each condition. n=1. Scale bar: 10μm.

4.4.6 Autofluorescence of mCherry-GFP1-10

The high green fluorescence that was seen in the stable cell line during live cell experiments, was further investigated to examine if this fluorescence can be attributed to the expression of GFP1-10 within the mCherry-GFP1-10 expression construct. It was found that green fluorescence located in the nucleus and the cytosol of cells is present when mCherry-GFP1-10 is expressed transiently in HeLa cells (Figure 4-19 C) as well as in the stable cell line mCherry-SCL51 (Figure 4-19 G). Mock transfected HeLa cells had a decreased green fluorescence and if fluorescence was found, it was localised in the perinuclear region (Figure 4-19 O). Cell transiently expressing mCherry also showed a decreased green fluorescence compare to the stable cell line or cells transiently expressing mCherry-GFP1-10 (Figure 4-19 K). For cells transiently expressing mCherry-GFP1-10 it was clearly visible that increased green fluorescence is only present in cells that express mCherry-GFP1-10, indicated by mCherry fluorescence (Figure 4-19 D). Compared to this no increase in green fluorescence can be seen in cells expressing mCherry transiently. The cell population of cells transiently expressing mCherry showed similar green fluorescence in the cytosol of cells (Figure 4-19 K) independent if they were expressing mCherry (Figure 4-19 L). Hence, the increased green fluorescence is not source of the mCherry fluorophore. This data suggests that increased green fluorescence is derived from GFP1-10 that is expressed as a fusion protein to mCherry. This green fluorescence was seen before when GFP1-10 was expressed in HeLa cells and spectral analysis suggested that this fluorescence is low GFP fluorescence. Hence, it is possible that this phenomenon is also present in cells expressing mCherry-GFP1-10 and this could be confirmed by spectral analysis of the emitted GFP fluorescence.
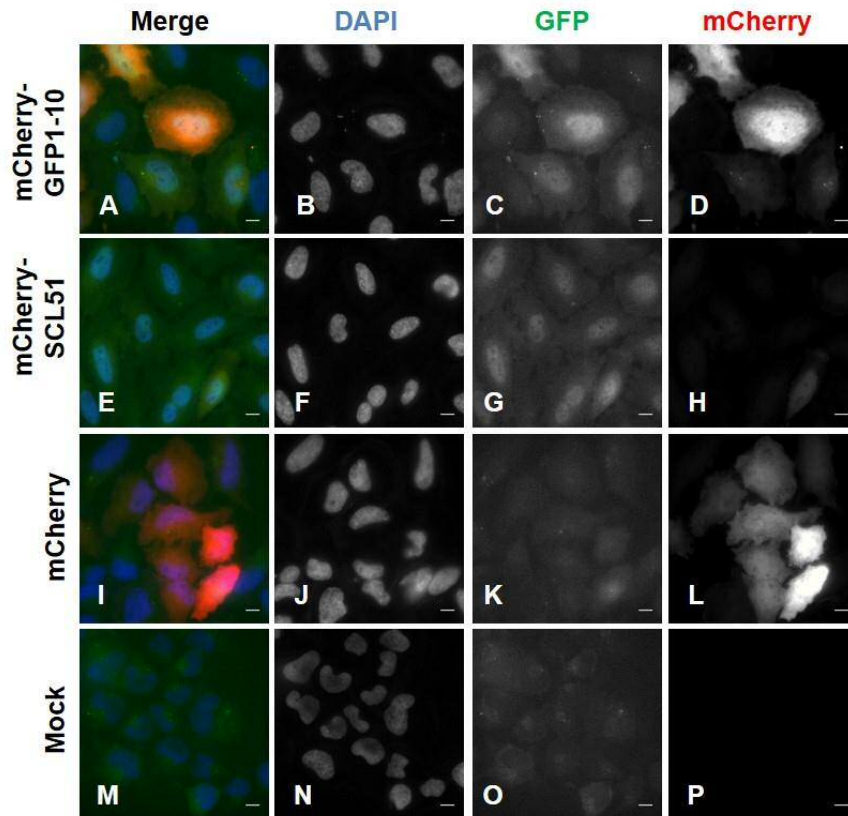
Figure 4-19 Autofluorescence in mCherry-SCL51
Green fluorescence in live cells was detected in Mock transfected Hela cells, HeLa cells transiently expressing mCherry-GFP1-10 or mCherry, and mCherry-SCL51 cells. Representative images for each condition. Nuclei of live cells were counterstained with Hoechst nuclear dye. Scale bar: 10 μm. n=1.

4.5　Discussion

In this Chapter it was shown that a stable cell line was successfully generated that expresses the large fragment of split GFP, GFP1-10, in the cytosol. The stably expressed protein was able to complement with the small fragment of GFP, M3, using co-expression and *in vitro* with chemically synthesised M3 peptides. Furthermore, an R8 dependent M3 delivery could be shown using this cell line.

The second stable cell line that was generated is mCherry-SCL51 expressing mCherry-GFP1-10 in its cytosol. mCherry as an expression marker of GFP1-10 had the advantage of marking cells that express GFP1-10. In a transient transfection model, as well as in the stable cell line it was shown that mCherry can serve as a fluorescent expression marker of GFP1-10 without interfering with its ability to complement with M3 using co-expression, *in vitro* complementation or in a live cells assay to show R8 dependent, functional M3 delivery.

While SCL1 expresses GFP1-10 evenly across its cell population, the generation of a clonal cell line that expresses even amounts of mCherry-GFP1-10 was not successful. The technique utilised to generate both cell lines was chosen to be limiting dilution where a cell line is aimed to be grown up from a single clone. This method was chosen to guarantee sterile culture conditions throughout the selection process. In order to further improve this cell line in the future to obtain a clonal cell line where cells express even amounts of mCherry, fluorescent activated cell sorting could be utilised where single cells can be separated according to their fluorescence.

Up until this stage, the split GFP system to investigate functional delivery of the M3 peptide by DDSs was extensively characterised in transient as well as stable cell models. Moreover it was shown that these models allow a DDS dependent evaluation of M3 delivery.

In studies by other groups, split GFP systems were utilised with transient transfection of mCherry-GFP1-10 into HEK293T cells as well as stable cell lines expressing GFP1-10 (HeLa, CHO-K1 and HCC827). (Schmidt *et al* and Kim *et al*) or S11 ((Milech *et al.* 2015)). The amino acid sequence of GFP11 is consistent with the M3 sequence used in this study and as it was first designed by Cabantous *et al*. (Cabantous *et al.* 2005). The S11 sequence utilised by Milech *et al* consists of an additional Glycine residue at its N-terminus.

The validation of split GFP complementation prior to live cell experiments in other studies was performed using co-transfection of the DNA of split GFP fragments (Kim *et al.* 2015; Milech *et al.* 2015). The split GFP assay of Milech *et al* included delivery of a cargo in addition to S11 (Milech *et al.* 2015).

The same group used a flexible GSSG linker to connect the cargo with S11. They validated the optimal linker size between the cargo and S11 for complementation with GFP1-10 and found that the linker [GSSG]x4 showed best results. In comparison, in this study a linker is used consisting of the amino acid sequence GSGGGSTS which is half the length of [GSSG]x4. It would be interesting to investigate if GFP complementation can be increased when this linker size is increased in size. Compared to this, Schmidt *et al*., used a very short linker (GSTS) to connect R9 to the M3 sequence and Kim *et al* connected GFP11 via a linker consisting of [GGGS]x3 to their cell penetrating antibody.

Techniques to investigate GFP complementation of DDS-GFP11 peptides without the plasma membrane as a barrier included electroporation of live cells expressing GFP1-10 to induce M3 or DDS-GFP11 peptides followed by flow cytometry analysis of GFP complementation (Schmidt *et al.* 2015a). Using this technique, Schmidt *et al* were able to show a concentration dependent increase of GFP complementation with M3 after 2 h. In this chapter an improved *in vitro* method was introduced where M3 peptides can be mixed with cell lysate of cells expressing

GFP1-10 and GFP complementation can be monitored using a microplate reader. Comparing these two methods, electroporation of live cells is advantageous because it assesses GFP complementation in the cellular environment of a live cell. However, when cells are electroporated, the total amount of GFP11 that enters the cell is unknown.

Milech *et al.* have developed an *in vitro* system where GFP1-10 and CPP_TRX_S11 peptides can be investigated when both fragments are sourced from bacterial expression and purification (Milech *et al.* 2015). A dose response was shown when 12.5 µM GFP1-10 was mixed with 0.375 – 3.0 µM CPP_TRX_S11 peptides at a single time point which is stated as overnight incubation and GFP fluorescence was measured on a microplate reader. This *in vitro* assay can be compared to the *in vitro* assay developed in this chapter. Milech *et al.* incubate split GFP fragments at room temperature. When GFP complementation was investigated here, incubation of split GFP fragments at room temperature and 4°C was compared and it was found that more GFP complementation had occurred when incubated at room temperature. However, Milech *et al.* utilises purified proteins for this assay compared to cell lysate containing GFP1-10 in the assay introduced in this chapter. With increasing temperature, cellular proteases can be more active. Hence, it would be interesting to investigate if the *in vitro* assay introduced in this chapter can be further improved by adding protease inhibitor to the cell lysate mix.

With help of the improved *in vitro* assay it was shown in this chapter that *in vitro* GFP complementation is time and concentration dependent. Furthermore, R8-M3 and M3 had a comparable amount of complemented GFP at each time point. L-M3 consistently showed a slight increase in GFP fluorescence. This was attributed to the increased green fluorescence of the peptide itself that was noticed during microscopy experiments and which also could be detected on the plate reader when green fluorescence of pure peptides was measured. Importantly, in this study it was shown

that the DDS R8 did not have an effect on GFP complementation compared to the pure M3 peptide.

In contrast, Milech *et al*., showed very different GFP complementation between the pure M3 peptide (S11) or CPP conjugated S11. In their study, pure TXR_S11 complementation with GFP1-10 was set to 100%. When the fluorescence achieved with the same concentration of R9_TXR_S11 was compared to this, it only reached approximately 30%. Moreover, other CPP_TXR_S11 fusions also showed decreased GFP complementation compared to the pure TXR_S11 peptide control. However, it was not further explored what the source of this difference is which could be due to difference in autofluorescence of the peptides or difference of the actual concentrations of the peptides even though they were believed to be used at the same concentrations. Nevertheless, their *in vitro* assay clearly shows that CPP_TXR_S11 peptides were able to achieve >100% GFP complementation compared to the TXR_S11 control meaning they are functional for GFP complementation *in vitro* but they did not deliver TXR_S11 in the live assay and no GFP complementation was detected.

This is also key to the improvement that was made to the *in vitro* assay here. In the fix and stain method in chapter 3 it was not possible to show that M3, L-M3 and R8-M3 have the same ability to complement with GFP1-10 when cells were fixed and permeabilised, therefore missing complementation for the M3 or L-M3 peptide in the live cell assay could not certainly be attributed to the inability for those peptides to cross the plasma membrane. Knowing that L-M3 and M3 complement with GFP1-10 and complementation is not significantly different to R8-M3 complementation with GFP1-10 *in vitro*, allows us to state that the absence of GFP fluorescence in the live assay when cells are incubated with 30 µM L-M3 means that L-M3 had not been delivered functionally into the cytosol of these cells. This also confirms that M3 delivery in the split GFP system is R8 dependent.

The *in vitro* GFP complementation system showed time dependent increase of GFP fluorescence over 24h. This can only be seen as an approximation of GFP complementation dynamics as they could occur in the cytosol of a living cell at 37°C. Nevertheless, the *in vitro* system shows a big increase between GFP fluorescence measured after 2 h and 24h. This raises the question if assessment of M3 delivery after 2h in live cells is too early and longer incubation time could achieve higher GFP complementation signals.

The live cell assay of Milech *et al.*, is performed when peptides were incubated with cells for 24 hours. It is not stated if peptides are added in serum free or serum containing media (Milech *et al.* 2015). In the paper of Schmidt *et al*, a comparative study is shown when GFP complementation is assessed after 2h and 24h of incubation with CPP-GFP11 peptides (Schmidt *et al.* 2015a). They identified 2h incubation as the better time point to assess GFP complementation because there was no increase in fluorescence detected after 24h incubation. However it is also important to mention that 10% FCS was added to the cell culture media when peptides were incubated for 24h which could affect peptide stability (Kosuge *et al.* 2008). Peptide stability is not only a factor to consider when peptides are incubated with cells but also once they have entered the cells. In this study presented here, L-amino acids were used to synthesize DDS-M3 peptides. It was demonstrated CPPs composed of the D-isoform were more stable in HeLa cells than CPPs composed of L-amino acids (Derek S. Youngblood *et al.* 2006) but this is also associated with decreased uptake compared to L-CPPs (Verdurmen *et al*. 2011). For this reason it is preferred use L-CPPs compared to D-CPPs even though the stability is decreased.

Strategies to prevent peptide degradation in the cytosol were shown to be through C-terminal attachment of a polyethylene glycol (PEG) moiety or amino acid substitution in order to prevent proteolytic degradation (Schmidt *et al.* 2015a).

Live assessment of M3 peptide delivery by DDSs was developed to be a microscopy technique in this study. Using a widefield fluorescent microscope it was possible to show delivery of M3 by R8 at concentrations ranging from 20-40 µM in single experiments. Due to the faint green fluorescence of complemented GFP, imaging had to be performed in glass bottom microscopy dishes on the highest magnification (100x, oil). This was associated with low throughput.

In other studies using GFP complementation to assess concertation dependent delivery of M3 peptide by DDSs, success of delivery was measured using flow cytometry (Milech *et al.* 2015; Schmidt *et al.* 2015a). This allowed the measurement of multiple peptides at a range of concentrations within one experiment. Nevertheless, it does not allow investigation of peptide uptake in real time.

Another important information when investigating drug delivery into cells is to determine how much cargo has been delivered to its intracellular target. Utilising mCherry as an expression marker for GFP1-10 expression could help us to investigate this. In this chapter it has been shown that mCherry-GFP1-10 can be expressed transiently or stably in cells and that GFP complementation upon M3 delivery can be determined. However, direct correlation between the amount of expressed mCherry and complemented GFP fluorescence has not been investigated further. For future experiments it would be beneficial to investigate if mCherry fluorescence and complemented GFP fluorescence can be correlated so that it will allow us to gain information about the amount of delivered M3 peptide. Quantitative assessment of delivered cargo using the split GFP system has been investigated by (Kim *et al.* 2015) where the complemented GFP fluorescence was compared to the fluorescence obtained from a standard curve obtained from intact GFP.

In summary, comparison of the split GFP systems utilised by other groups and the system presented in this study has shown that the similar techniques have been

utilised in order to characterise the split GFP system such as co-transfection of the split GFP fragments as well as *in vitro* complementation using pure split GFP fragments. The main difference is that the split GFP assay to determine functional delivery of a peptide presented here was characterised using microscopy. Already during the characterisation phase of the split GFP system in Chapter 3 it was emphasised that microscopy can add valuable information compared to techniques where only green fluorescent intensity is measured. One example is the co-expression experiment. Utilising the expression plasmid mCherry-H6-R8-M3 to express the small M3 fragment of GFP led to accumulation of complemented GFP to the nucleolus due to the presence of R8. Hence, using a microscope to assess the success of GFP complementation not only determined if the two fragments complement but also where they localise inside the cell.

This localisation change was also noticed in live experiments when M3 delivery by R8 across the plasma membrane was assessed using microscopy. When peptide delivery by a DDS was assessed in live cells by *Milech et al.* and *Schmidt el al.*, GFP fluorescence was only detected by flow cytometry measurement. Localisation changes of complemented GFP inside the cell remained due to conjugation to CPPs remains unknown in their experiments.

Split GFP to determine functional peptide delivery by DDSs is a powerful technique that should be utilised to its full potential. This includes to determine if a peptide is delivered by detection of green fluorescence but also when the peptide is delivered and where it is delivered to inside the cell. When and where the M3 peptide is delivered inside the cell is clearly shown in study during the extensive characterisation of the split GFP system using a microscope presented in Chapter 3 and 4. This demonstrates that data generated in this study help to characterise DDSs more detailed than it has been shown by *Milech et al.* and *Schmidt el al.*.

Another finding when characterising the stable cell lines live on a microscope was the increased green fluorescence in cells that expressed GFP1-10 or mCherry-GFP1-10 transiently as well as in stable cell lines. When compared to mock transfected HeLa cells this fluorescence differed in brightness as well as localisation. While autofluorescence in HeLa cells was mostly localised in the cytosol in the perinuclear region, increased fluorescence upon expression of GFP1-10 or mCherry-GFP1-10 was found throughout the cytosol as well as in the nucleus. This increased green fluorescence was also noticed in single cells during previous experiments when cells transiently expressed GFP1-10.

This fluorescence was also described by other groups working with split GFP. In a study by Kent and his colleagues it was mentioned that once GFP fragments had reassembled and the chromophore maturated, they can be separated by denaturation and GFP1-10 contains a mature chromophore (GFP1-10^{mat}). They stated that only weak fluorescence is observed for GFP1-10^{mat} (Kent *et al.* 2008). That statement could be indicative that the GFP fluorescence seen in cells expressing GFP1-10 and mCherry-GFP1-10 is due to the matured chromophore that is located on the central alpha helix of the GFP1-10 fragment. Furthermore, when stable cell lines expressing GFP1-10 were generated in other studies, low fluorescent background signal from the marginal fluorescent capability of GFP1-10 was observed (Milech *et al.* 2015).

NADH and FAD are autofluorescent cofactors in the 500 – 600 nm spectral region located in the mitochondrial electron transport chain (Aubin 1979; Benson *et al.* 1979). FAD with its emission spectrum of 535 nm lies within the spectral range that is collected when GFP emission is measured (GFP emission filter setting: 525/36 nm). For this reason it is likely that the autofluorescence seen in Hela cells, located in the perinuclear region is derived from FAD. Its localisation within the mitochondria also correlates with the phenotype of the autofluorescence in located around the nucleus. The change of the localisation of green fluorescence to the cytosol and the

nucleus, seen when GFP1-10 or mCherry-GFP1-10 were expressed was a first indication that this is a different phenomenon than simple autofluorescence.

Using spectral detection it was suggested that the green fluorescence seen when GFP1-10 is expressed is a combination of real GFP fluorescence as well as autofluorescence of the cell. The emission spectra of full length GFP and the spectrum detected in cells expressing GFP1-10 aligned and peaked at 513 nm wavelength light. Two scenarios could explain the emission of GFP fluorescence GFP fluorescence. The function of the M3 peptide to rescue GFP fluorescence is dependent in the proton acceptor Glutamic acid 222. It could be possible that GFP1-10 may have found another proton acceptor in the cytosol and GFP fluorescence in partly rescued. Another possibility is that the chromophore that is contained in GFP1-10 emits GFP fluorescence. Kent *et al.* 2008 have stated that weak fluorescence is observed for GFP1-10 when complemented GFP is denatured into two fragments and GFP1-10 contains a matured chromophore (Kent *et al.* 2008).

In summary, in this chapter it was shown that two stable cell lines were generated and functional M3 delivery can be assessed using these cell lines. The methods to validate GFP complementation in these cell lines were also used by other groups in the field utilizing the same assay. Furthermore, it was demonstrated that the developed split GFP assay can be utilised using a microscope to show real time delivery of the M3 peptide as well as its localisation adding valuable information beyond what has been published by other groups.

It is now of interest if the delivery efficiency of different DDSs can be evaluated in a concentration dependent manner using this system as well as the detailed analysis of subcellular localisation of the delivered M3 peptide.

5 Evaluation of the delivery efficiency of different DDSs using the split GFP assay

5.1 Introduction

In previous chapters, it was demonstrated that the split GFP assay can be utilised to investigate the delivery of the M3 peptide by the CPP R8 to the cytosol of cells expressing GFP1-10 or mCherry-GFP1-10. The same method has been utilised by other research groups in order to evaluate concentration dependent delivery of the M3 peptide by DDSs (Milech *et al.* 2015; Schmidt *et al.* 2015b).

In order to fully characterise the split GFP assay developed in this study, it was of interest to investigate if delivery efficiency can also be detected in a concentration dependent manner. Until now, functional delivery of M3 was only investigated using fluorescent widefield microscopy. The faint fluorescence of complemented GFP does not allow high throughput analysis of cells in a 96 well format at low magnification, yet. Due to this reason, data collection is a time consuming process and imaging can only be performed in single microscopy dishes at high magnification. Hence, analysis of multiple conditions within the same experiment is challenging. Moreover high magnification imaging only allows us to analyse a small subset of cell that might not represent the whole cell population.

Other research groups have used flow cytometry to determine M3 delivery by DDSs (Milech *et al.* 2015; Schmidt *et al.* 2015a). Flow cytometry can determine the fluorescence of 10,000 cells in only 1 minute which allows us to gain information on the fluorescence of multiple cell populations treated with different concentrations and different peptide formulations in a short amount of time. Importantly this data can be collected within the same experiment which allows accurate comparison of different conditions. For this reason, it was of interest to examine if the split GFP complementation assay developed utilising stable cell line SCL1 and mcherry-SCL51 can be performed, and GFP complementation detected using flow cytometry.

Hence, the primary focus of this chapter is to characterise stable cell lines by flow cytometry and then investigate if concentration dependent delivery of M3 by R8 into the cytosol of the stable cell lines SCL1 or mCherry-SCL51 can be detected.

Furthermore it is of interest to examine if the delivery efficiency of different DDSs can be investigated to allow the evaluation of DDSs to act as a peptide delivery vector. Other research groups have already investigated a wide range of well-known CPPs to deliver peptides using the split GFP assay (Milech *et al.* 2015; Schmidt *et al.* 2015a).

For this reason the peptide delivery performance of R8 based peptides with single amino acid additions will be examined here. It has been shown by our group that a single <u>residue change</u> from Glycine to Phenylalanine in the linker sequence <u>G</u>SGSGSGSG, N-terminally attached to cell penetrating peptides had a striking effect on the uptake of fluorophores into HeLa cells (Sayers *et al.* 2014). Two of the CPPs that were investigated in this study were R8 and TP10. N-terminal exchange of Glycine to Phenylalanine in the linker sequence attached to TP10 had the most enhancing effect on its uptake into HeLa cells at 2 µM and 5 µM. Single amino acid exchange of the linker attached to R8 showed a significant increase of its uptake in KG1a cells at 2 µM and 5 µM. In HeLa cells a significant increase was only observed at 5 µM and not at 2 µM. In this previous study, uptake of CPPs and enhancement of their uptake was investigated using fluorophore conjugated CPPs.

However, uptake does not equal cytosolic delivery and using fluorophores to track the uptake into cells did not assess cytosolic delivery which is of high interest when using CPPs as drug delivery systems. Furthermore fluorophores can change the uptake of CPPs into cells (Jones and Sayers 2012). For this reason it was of interest to utilise the split GFP system to elucidate if N-terminal phenylalanine can not only enhance cellular uptake, but also enhance functional delivery of a peptide cargo into the cytosol.

Thus, as a second focus of this chapter, delivery efficiency of R8 will be compared to R8 with N-terminal addition of Glycine or Phenylalanine residues. This will shed light on the influence of Phenylalanine substitution on R8 to enhance functional delivery of a peptide as well as further explore the potential of the split GFP assay to evaluate and compare different DDSs for peptide delivery.

5.2 Characterisation of stable cell lines using Flow cytometry

5.2.1 Cell morphology and viability

Before performing a split GFP complementation assay and measurement of green fluorescence by flow cytometry, the characteristics of the different cell lines and appropriate filter settings of the flow cytometer were examined. Schmidt *et al*., have published the split GFP complementation assay based on flow cytometry where GFP signal was measured from morphological intact cells based on forward scatter (FSC) and sideward scatter (SSC) measurements (Schmidt *et al.* 2015a). FSC and SSC measure cell size and cellular granularity (e.g. number and size of vesicles and mitochondria or the nucleus structure), respectively. In order to explore which FSC and SSC measurements correlate with morphological intact cells, HeLa, SCL1 and mCherry-SCL51 cells were analysed regarding their viability and morphology. Untreated cells were detached from the cell culture dish using trypsination and prepared for flow cytometry. After washing the cells with PBS twice, cells were treated with LIVE/DEAD™ Violet Stain and left on ice for 30min. Cells were washed again, resuspdended in PBS, transferred into a FACS tube and left on ice until flow cytometry measurements.

First, the cell morphology was explored using FSC and SSC measurements (Figure 5-1). On the dot plots obtained from the measurement it can be clearly seen that the variety of cell morphology was very similar between HeLa cells (Figure 5-1 I) and the stable cell line mCherry-SCL51 (Figure 5-1 III). The cells of the cell line SCL1 were bigger in size as well as more granular and the whole cell population was shifted towards the centre of the FACS plot (Figure 5-1 II). This difference in granularity could be due to the different shape of the nucleus between SCL1 cell and HeLa cells that was observed by Alexander Dudziak during his placement in our lab (Appendix 9.5, Figure 9-7). He further performed morphological analysis of SCL1 cells compared to HeLa cells and demonstrated that the morphology of the cell membrane of SCL1

stained with Concanavalin-A did not differ from HeLa cells (Appendix 9.5, Figure 9-8). Furthermore, he analysed the actin (Appendix 9.5, Figure 9-9) and tubulin (Appendix 9.5, Figure 9-10) cytoskeleton in HeLa and SCL1 cells using immunofluorescence and found that the morphology was not different between then.

To investigate the viability of these cells, the fluorescence of the LIVE/DEAD™ Violet Stain (excitation/emission: 405/451) was measured using the violet laser (407 nm excitation) Pacific Blue filter setting (collection of 425 - 475 nm wavelength light) (Figure 5-2). The stain reacts with free amines and when cells are intact it is restricted to the cell surface which results in weak fluorescent staining. When the plasma membrane is compromised the dye has access to amines on the cell surface and the interior of the cell which results in more intense staining. The cells were gated into two populations to describe morphologically intact cells (live cell gate) and cells where the plasma membrane was not intact (dead cells). The live cell gate was drawn around the centre in which cells where highly concentrated which included 92.5% cells, 86.5% cells and 93.8% cells of the population for the cell lines HeLa, SCL1 and mCherry-SCL51, respectively (Figure 5-2 I, IV, VII) . Detection of the live/dead cell staining within this gate showed one clear peak for each cell line with the same fluorescent intensity between the cell lines (Figure 5-2 II, V, VIII). The dead cell gate was located around cells that were smaller and less granular than intact cells and only included 2.31%, 4.16% and 1.08% cells of the population for the cell lines HeLa, SCL1 and mCherry-SCL51, respectively (Figure 5-2 I, IV, VII). When measuring the live/dead cell stain within this gate all cell lines showed one peak in the same position as the live cell gate and another peak shifted to the right indicating more intense staining of the dye (Figure 5-2 III, VI, IX).

This data suggests that the cells measured in the live cell gate were morphologically intact and the dye did not enter the cells because only one clear peak

with weak fluorescence of the dye was seen. The cells within the dead cell gate consisted of cells that were morphologically intact as well as cells with a compromised plasma membrane. This was visible by the separation of cells into two peaks, one that was positive for the live/dead cell dye and one with only weak fluorescence of the dye.

A clearer result could have been obtained with an experimental control that contained cells with a compromised plasma membrane (e.g. Triton-X-100 treatment). However this control was absent in this experiment but measurements should be confirmed in the future.

For further experiments morphologically intact cells were gated according to the position of the live cell population dependent on FCS and SSC measurements shown in this experiment.
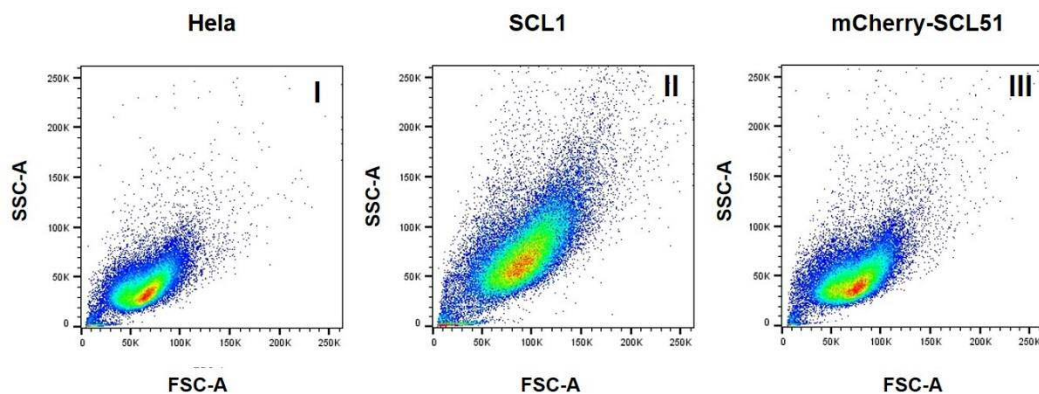
Figure 5-1 Morphology of HeLa cells and stable cell lines
Hela cells, SCL1 cells or mCherry-SCL51 cells were detached from a cell culture dish using trypsinisation and prepared for flow cytometry measurement including LIVE/DEAD™ Violet Stain treatment. Cell morphology was assessed using forward scatter (FSC-A) and sideward scatter (SSC-A) measurement. Assessment of morphology of 50,000 cells. Samples were measured in duplicates. n=1.
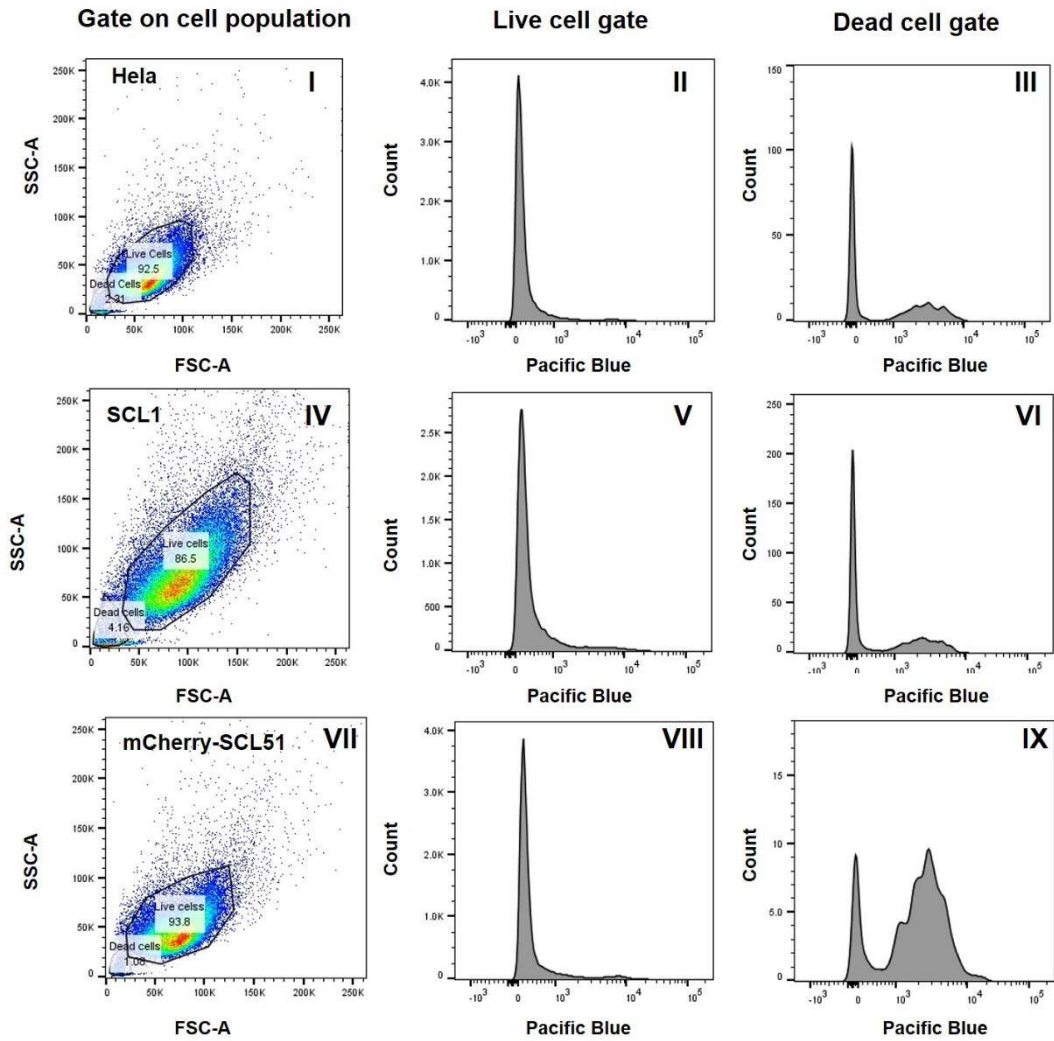
Figure 5-2 Gating for morphologically intact cells.
Hela cells, SCL1 cells or mCherry-SCL51 cells were detached from a cell culture dish using trypsinisation and prepared for flow cytometry measurement including LIVE/DEAD™ Violet Stain treatment. Cell morphology was assessed using forward scatter (FSC-A) and sideward scatter (SSC-A) measurement. Assessment of morphology of 50,000 cells. (I, IV, VII). LIVE/DEAD™ Violet Stain (excitation/emission: 405/451) was excited using the violet laser (405 nm) and collected using the Pacific blue filter setting (425 - 475 nm). Live cell gate was drawn around cells that were assumed to be morphologically intact. Dead cell gate was drawn around smaller and less granular cells that were assumed to be dead. LIVE/DEAD™ cell stain signal is shown for cells included in the live cell gate (II, V, VIII) and the dead cell gate (III, VI, XI). Samples were measured in duplicates. n=1.

5.2.2 Cell fluorescence

Next, green fluorescence was measured in morphologically intact cells shown in Figure 5-2. HeLa, SCL1 and mCherry-SCL51 cells were excited using the 488 nm wavelength light laser and green fluorescence was collected using the FITC filter (515 - 545 nm) (Figure 5-3). The geometric mean of FITC fluorescence was measured in duplicates for the different cell types. Figure 5-3 A demonstrates that the stable cell lines had increased green fluorescence compared to HeLa cells. HeLa cells showed a fluorescence of 274 RFU; For SCL1 cells and mCherry-SCL51 cells a value of 1395 RFU and 1226 RFU was measured, respectively. This shows that the green fluorescence in SCL1 cells is 5 times higher compared to HeLa cells and 4.5 times increased in mCherry-SCL51 cells.

Comparison of the histograms shows that the cell population of HeLa cells (Figure 5-3 B I, IV) and SCL1 (Figure 5-3 B II) cells had a single peak and even distribution of green fluorescence across the cell population. When comparing this green fluorescence between HeLa cells and SCL1 cells (Figure 5-3 B II), it is visible that the green fluorescence of SCL1 cells is shifted to the right which means that these cells are more fluorescent than HeLa cells.

mCherry-SCL51 cells showed 2 peaks when green fluorescence was measured in this cell line (Figure 5-3 B V). When this fluorescence is compared to HeLa cells (Figure 5-3 B VI) the smaller peak did align with the fluorescence measured in HeLa cells and the larger peak was shifted to the right indicating higher green fluorescence similar to that observed for the SCL1 cell line.

These findings are consistent with the observation made using fluorescent microscopy, that stable cell lines were found to be more fluorescent in the GFP channel compared to HeLa cells. mCherry-SCL51 was characterised to be a polyclonal cell line. Hence, the two cell populations when green florescence was measured could represent this separation of the cell population.
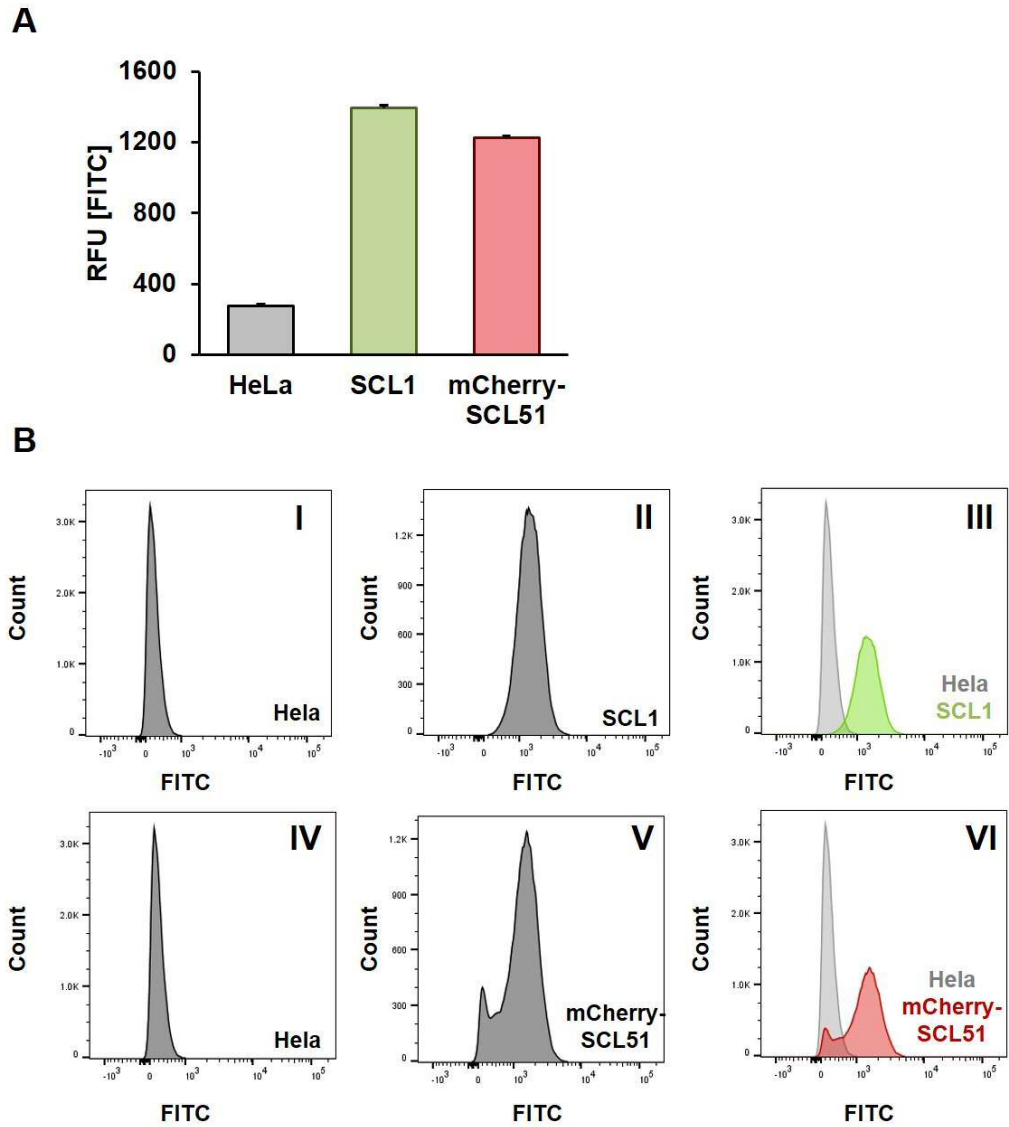
Figure 5-3 Green fluorescence of stable cell lines measured by flow cytometry.
Hela cells, SCL1 cells or mCherry-SCL51 cells were detached from a cell culture dish using trypsinisation and prepared for flow cytometry measurement including LIVE/DEAD™ Violet Stain treatment. Green fluorescence of morphologically intact cells was measured using the 488 nm excitation laser and the FITC filter (515 - 545 nm). (A) Geometric mean of cell fluorescence is shown. Cell types were measured in duplicates. Error bar shows standard deviation. (B) Histograms of green fluorescence of single cell populations shown in I,II,IV and V. Green fluorescence of stable cell lines with respect to the fluorescence of HeLa cells shown in III, VI. 50,000 cells were measured in total. n=1.

Due to the fact that mCherry-SCL51 is a polyclonal cell line it is necessary that GFP complementation in live cells is only measured in mCherry positive cells (e.g. only cells that express mCherry-GFP1-10). For this reason it is important that mCherry fluorescence can be measured with the flow cytometer in order to allow appropriate gating for a mCherry positive cell population. The excitation maximum of mCherry is at 587 nm wavelength light, which would require a yellow laser (560 nm excitation wavelength) to excite the fluorescent protein mCherry at its excitation maximum. The flow cytometer that was used in this study was not equipped with a yellow laser. Due to the absence of this laser it was tested if mCherry fluorescence in these cells can be determined using excitation of the fluorescent protein with the 488nm wavelength light laser. This wavelength does not correspond with the excitation optimum of mCherry, but it lies within the wavelength range which can excite mCherry (Figure 5-4). However, excitation with 488nm wavelength light will also excite GFP which has its excitation maximum at 488nm wavelength light. Thus, to clearly separate the emission of the fluorophores and to only collect signal that is emitted following mCherry excitation, it was important to choose an emission filter that lies outside the emission range of GFP. The chosen filter for that measurement was the PerCP-Cy5-5 filter collecting 670 – 753nm wavelength light.
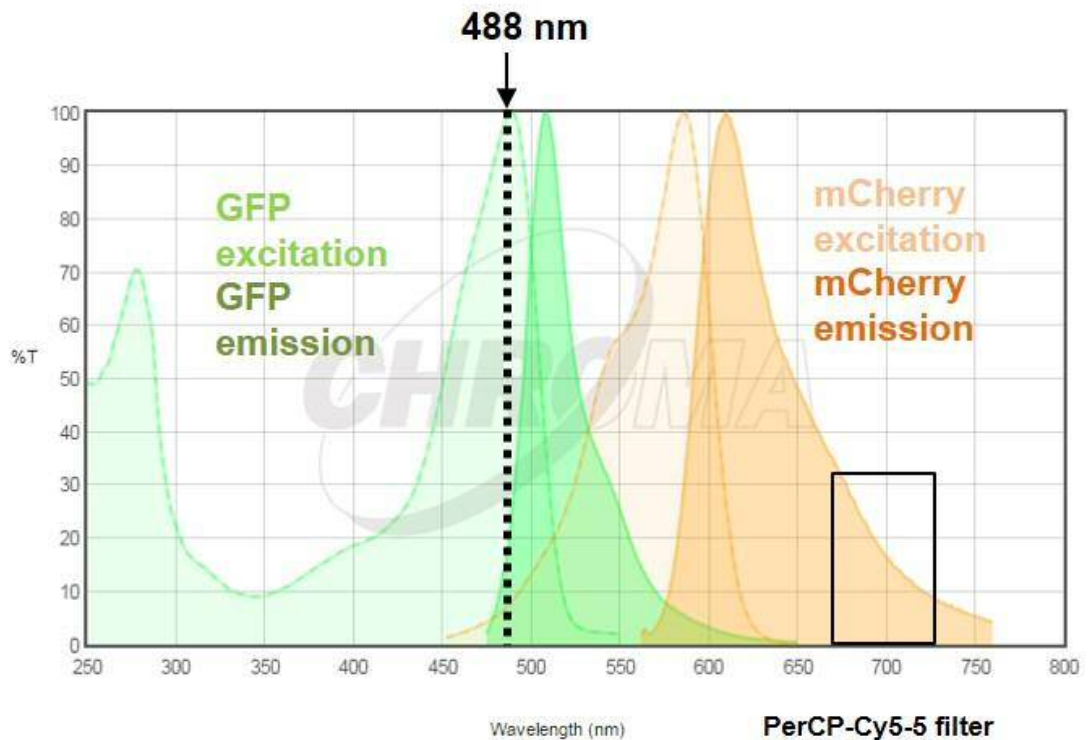
Figure 5-4 Excitation and emission spectrum of mCherry and GFP with regard to flow cytometer laser excitation and emission filter setting.
The graph shows GFP excitation (light green) and emission (dark green) spectrum and mCherry excitation (light orange) ad emission (dark orange) spectrum. Spectra were obtained from the Chroma website. Black dotted line indicates excitation wavelength 488 nm. Solid black box indicates wavelengths 670-753 nm collected by the PerCP-Cy5-5 emission filter.

When mCherry fluorescence was measured using the described filter settings, it was seen that it was possible to measure the emission of mCherry fluorescence in the stable cell line mCherry-SCL51. The stable cell line showed high red fluorescence (2757 RFU) compared to HeLa cells (246 RFU) (Figure 5-5 A). Furthermore, the percentage of mCherry positive cells was analysed in duplicate samples. It revealed that 86% of the cell population of mCherry-SCL51 is positive for mCherry fluorescence, therefore expressing mCherry-GFP1-10 (Figure 5-5 B).

When the histograms of these samples were analysed, a single emission peak was seen in HeLa cells (Figure 5-5 C I). mCherry-SCL51 cells showed two peaks indicating varying mCherry fluorescence across the cell population (Figure 5-5 C II). When both histograms where superimposed, the two peaks of mCherry-SCL51 cells were clearly separate from each other and the lower peak aligned with the mCherry

fluorescence detected in untreated HeLa cells(Figure 5-5 C II). The second peak was shifted to the right indicating higher fluorescent signal.

This data is another conformation that mCherry-SCL51 is a polyclonal cell line and that there are cells within the cell population that do not express mCherry-GFP1-10, aligning with the emission spectrum obtained from HeLa cells. Furthermore, it confirmed that mCherry fluorescence can be measured on the flow cytometer which will allow the investigation M3 delivery and GFP complementation in mCherry-GFP1-10 positive cells.
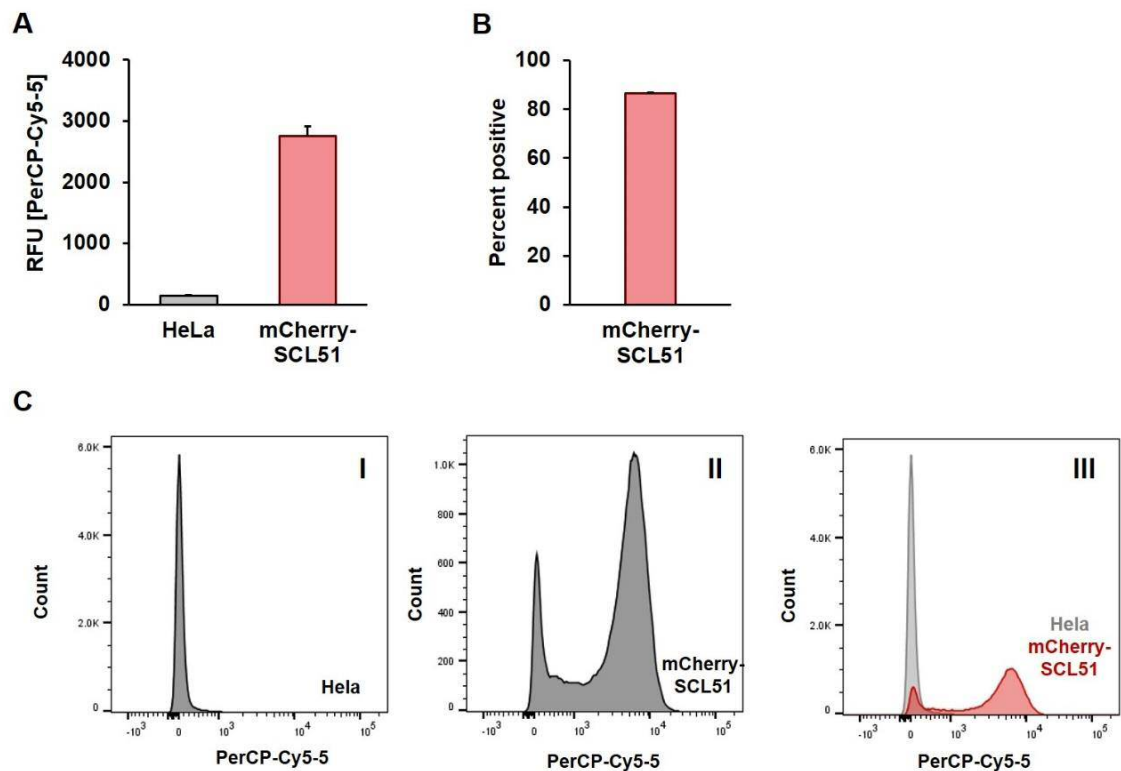
Figure 5-5 Detection of mCherry fluorescence using flow cytometry.
Hela cells or mCherry-SCL51 cells were detached from a cell culture dish using trypsinisation and prepared for flow cytometry measurement including LIVE/DEAD™ Violet Stain treatment. mCherry fluorescence of morphologically intact cells was measured using the 488 nm excitation laser and the PerCP-Cy5-5 emission filter (670 – 753 nm). (A) Geometric mean of cell fluorescence is shown. Cell types were measured in duplicates. Error bar shows standard deviation. (B) Percentage of mCherry positive cells within the cell population of mCherry-SCL51. (C) Histograms of red fluorescence of single cell populations shown in I and II. Green fluorescence of stable cell line mCherry-SCL51 with respect to the fluorescence of HeLa cells shown in III. Samples were measured in duplicates. 50,000 cells were measured in total. n=1.

5.3 Design of different R8 based peptides

In order to investigate if the split GFP assay allows us to evaluate the delivery efficiency of different DDSs, new R8 based peptides were designed. Based on previous studies that showed that a switch from a N-terminal Glycine to Phenylalanine attached to CPPs can enhance their uptake into cells (Sayers *et al.* 2014), it was of interest to examine if this exchange of amino acids can also facilitate enhancement of the functional delivery of M3 cargo peptide. The enhancing effect on uptake due to a Glycine to Phenylalanine exchange was investigated when the Glycine (G) or Phenylalanine (F) residue were attached N-terminally via an 8 amino acid linker (SGSGSGSG). Enhancement of uptake using this amino acid change was less effective for R8 than other CPPs tested in this study. Hence, for the design of new R8 based peptides to deliver M3, the linker sequence was removed and Phenylalanine or Glycine were directly attached to the N-terminus of R8 to obtain the new peptides FR8-M3 and GR8-M3 (Table 5-1). Direct attachment of the amino acid addition to R8 was hoped to achieve enhanced delivery characteristics. Along with these peptides, two more R8 based peptides were purchased with the addition of two N-terminal Phenylalanine (FFR8-M3) or Glycine (GGR8-M3) residues to investigate if delivery can be further enhanced when two Phenylalanine residues are attached to R8.

Table 5-1 R8 based peptides with Glycine or Phenylalanine modifications

DDS	Cargo	Peptide name	Sequence DDS-linker-M3	Modifications		Number of amino acids	Molecular weight [kDa]
				N-terminal acetylation	C-terminal amidation		
FR8	M3	FR8-M3	FRRRRRRRRGSGGGSTSRDHMVLHEYVNAAGIT	-	-	33	3.79
GR8	M3	GR8-M3	GRRRRRRRRGSGGGSTSRDHMVLHEYVNAAGIT	-	-	33	3.70
FFR8	M3	FFR8-M3	FFRRRRRRRRGSGGGSTSRDHMVLHEYVNAAGIT	-	-	34	3.94
GGR8	M3	GGR8-M3	GGRRRRRRRRGSGGGSTSRDHMVLHEYVNAAGIT	-	-	34	3.76

Table displays sequences, modification and characteristics of DDS-M3 peptides used in this chapter. All peptides use L-amino acids, blue letters denote the sequence of the cell penetrating peptide R8 (octaarginine) containing Glycine (G) or Phenylalanine (F) modifications; M3 sequence is coloured in green. R8 is conjugated to M3 via a linker (grey).

5.4 Delivery of M3 by different R8 based peptides in SCL1 cells

5.4.1 Concentration dependent delivery of M3 by R8

Using flow cytometry measurement it was first explored if a concentration dependent increase of functional M3 delivery by R8 can be detected using the stable cell line SCL1. To test this, SCL1 cells were washed once in serum free media and incubated with DMSO, M3, L-M3 or R8-M3 at a concentration range of 10-40 µM for 2h at 37ºC. Then cells were washed in 0.5 mg/ml Heparin 3 times in order to remove membrane bound CPP-M3 peptide. Cells were detached from the cell culture dish using trypsin and washed with PBS twice. Cells were then transferred into a FACS tube in a volume of 500 µl of PBS and kept on ice until flow cytometry measurements. GFP fluorescence of 20,000 cells were detected using flow cytometry and cells were gated for morphologically intact cells using FSC and SSC measurements. Green fluorescence was measured and the geometric mean of samples was taken to compare GFP complementation. The geometric mean of all samples was normalised to the DMSO control that was set to a value of 1 to display a fold change in GFP fluorescence. The results are shown in Figure 5-6.

Incubation of the cells with M3 or L-M3 at a concentration range of 10-40 µM did not result in functional delivery of M3. This is shown by green fluorescence levels that were lower or the same as the DMSO control. M3 delivery using R8 did result in M3 delivery and green fluorescence of cells increased in a concentration dependent manner. Even at a low concentration of 10 µM, M3 was successfully delivered to the cytosol of GFP1-10 expressing cells and resulted in a 1.06 fold change of GFP fluorescence. Delivery was linear to the concentration for 10 µM (1.06 fold), 20 µM (1.11 fold) and 30 µM (1.18 fold) and increased to 1.36 fold when cells were incubated with 40 µM R8-M3. This was significantly different compared to the fluorescence detected when 40 µM M3, L-M3 or DMSO were incubated with the cells.

This experiment shows a concentration dependent increase of M3 delivery and GFP complementation when R8-M3 was applied on SCL1 cells. Importantly, M3 as well as L-M3 were not able to cross the plasma membrane at concentrations of 10-40 µM. This data also reveals that SCL1 cells can be utilised to determine a DDS dependent M3 delivery into cells. Furthermore, flow cytometry can be utilised as a method to detect concentration dependent delivery of M3 by a DDS.
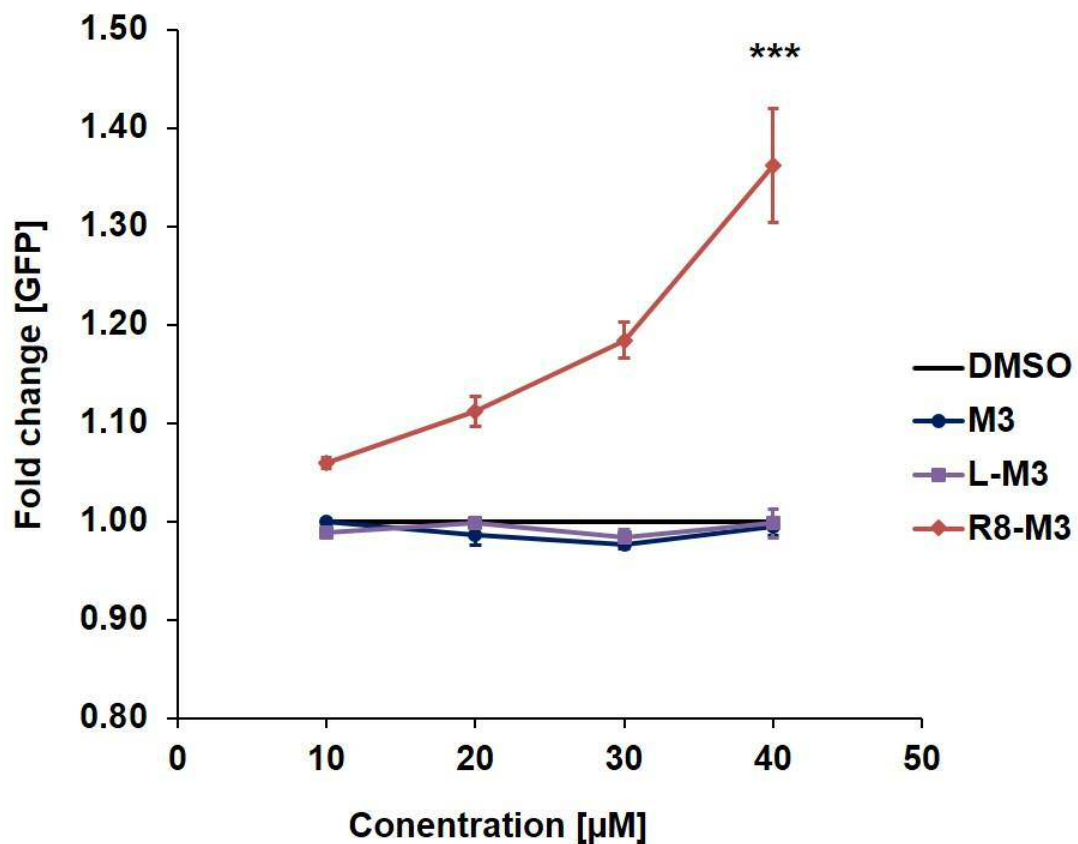
Figure 5-6 Concentration dependent delivery of M3 by R8 using SCL1 cells.
SCL1 cells were washed once in serum free media and incubated with DMSO, M3, L-M3 or R8-M3 at 10-40 µM for 2h at 37ºC. Cells were washed in 0.5 mg/ml Heparin 3 times and detached from the cell culture dish using trypsin. Cells were washed with PBS twice, transferred into a FACS tube in a volume of 500 µl of PBS and kept on ice until flow cytometry measurements. In total 20,000 cells were measured. Cells were gated for morphologically intact cells using SSC and FSC measurements and green fluorescence within this cell population was measured using the 488 nm excitation laser and the FITC emission filter. Fold change is shown compared to the DMSO control which was set to the value 1. Error bars show standard error of the mean. For statistical analysis data was tested using a One way Annova followed by multiple comparison using a Turkey HSD (honest significant difference) test. Significance is shown compared to treatment with 40 µM M3, L-M3 or DMSO. *: $p<0.05$, **: $p<0.01$, ***: $p<0.001$, n.s.: not significant. n=3.

5.4.2 Effect of Phenylalanine or Glycine substitution to R8 on the efficiency to deliver M3 to the cytosol of SCL1 cells

Next it was tested if an N-terminal addition of one or two Phenylalanine (FR8-M3/FFR8-M3) or Glycine (GR8-M3/GGR8-M3) residues changes the efficiency to functionally deliver M3 to its cytosolic GFP1-10 target expressed in SCL1 cells. In order to test the compatibility of these peptides to complement with GFP1-10, complementation was first investigated using the improved *in vitro* assay where peptides are mixed with cell lysate of SCL1 cells containing GFP1-10. 80 µM of M3 containing peptide was mixed with cell lysate of 0.8×10^5 SCL1 cells expressing GFP1-10 and GFP complementation was monitored on a microplate reader over 24 h at 4ºC. Figure 5-7 shows the time dependent increase of GFP fluorescence of M3 containing peptides with GFP1-10. R8 itself did not have the ability to rescue GFP fluorescence. GFP complementation of R8-M3 was slightly increase at each time point compared to FR8M3, FFR8-M3, GR8-M3 and GGR8-M3. Complementation of FFR8-M3, GR8-M3 and GGR8-M3 was similar between the samples. Only complementation of FR8-M3 was decreased until the 4 h time point compared to other samples. All samples showed a time dependent complementation of GFP1-10 that was contained in the SCL1 cell lysate and the CPP-M3 peptides. Importantly, there was no significant difference found when peptides containing M3 were compared regarding their ability to complement with SCL1 cell lysate *in vitro* at time points 120 min or 7h. Overall, Phenylalanine or Glycine additions to R8-M3 did not alter the ability to complement with M3 significantly.
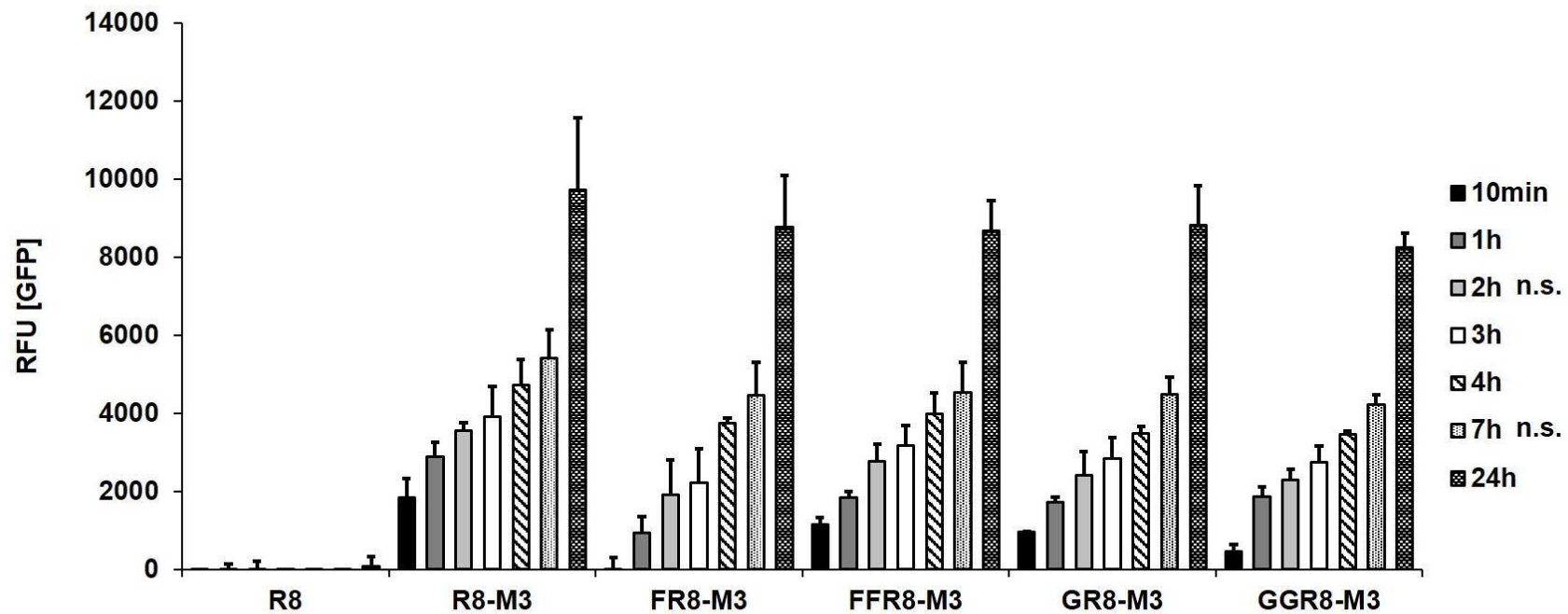
Figure 5-7 *In vitro* **complementation of R8-M3 peptides with a Phenylalanine or Glycine residue addition with SCL1 cells.**
(A) *In vitro* complementation of lysed SCL1 cells with peptides. SCL1 cells were trypsinised and lysed using 0.1% Triton-X100 in PBS. Cell lysate of 0.8×10^5 cells was mixed with 80 µM M3 and CPP-M3 peptides to obtain a final concentration of 40 µM in 0.05% Triton-X-100/PBS. Lysate mixture was left under constant agitation at 4°C. The fluorescent signal resulting from GFP complementation was monitored over 24 h using a microplate reader. DMSO only control was subtracted as the sample background. n=3. Error bars present SEM. For statistical analysis data was tested using a One way Annova followed by multiple comparison using a Turkey HSD (honest significant difference) test. Data was tested at two time points, 120min and 7h. No significant difference of fluorescence was found between peptides containing M3. n.s.: not significant.

After the ability of R8 containing M3 peptides to complement with GFP1-10 was confirmed *in vitro*, the different R8 derived peptides were evaluated regarding their ability to deliver M3 in a live experiment. To explore this, SCL1 cells were washed once in serum free media and incubated with DMSO, R8-M3 or Phenylalanine/Glycine added versions of R8-M3 at concentration range of 10-40 µM for 2h at 37ºC. Then cells were washed in 0.5 mg/ml Heparin for 3 times in order to remove membrane bound CPP-M3 peptide. Cells were detached from the cell culture dish using trypsin and washed with PBS twice. Cells were then transferred into a FACS tube in a volume of 500 µl of PBS and kept on ice until flow cytometry measurements. GFP fluorescence of 20,000 cells were detected using flow cytometry and cells were gated for morphologically intact cells and green fluorescence of the population was measured using the geometric mean of samples. The geometric mean of all samples was normalised to the DMSO control that was set to a value of 1 to display a fold change in GFP fluorescence.

Single addition of Phenylalanine (FR8-M3) or Glycine (GR8-M3) residues to R8-M3 did not result in an increased delivery of M3 into SCL1 cells compared to R8-M3 (Figure 5-8 A). Nevertheless, FR8-M3 and GR8-M3 did show peptide delivery activity in a concentration dependent manner. GR8-M3 delivered M3 half as effective as R8-M3 and followed the same trend seen for R8-M3 that delivery increased linear when used at 10 µM, 20 µM or 30 µM (1.02, 1.04, 1.07 fold respectively) and a higher increase was seen at 40 µM when delivery increased by 1.2 fold compared to the DMSO control (1 fold). The delivery efficiency of FR8-M3 was decreased compared to GR8-M3 and R8-M3 and only reached a 1.11 fold change when applied at 40 µM compared to R8-M3 (1.36 fold) or GR8-M3 (1.2 fold). No significant difference was seen between functional delivery of M3 by R8, FR8 or GR8.

However, when two Phenylalanine residues were added to R8-M3 (FFR8-M3), M3 delivery dramatically increased (Figure 5-8 B) compared to R8-M3. M3 delivery

was concentration dependent and rapidly increased from 1.1 fold at 10 µM to 1.86 fold at 20 µM, 2.54 fold at 30 µM and reached 3.13 fold at 40 µM. Hence, M3 delivery using FFR8-M3 was 6 times higher at a 40 µM than R8-M3. In contrast, addition of two Glycine residues (GGR8-M3) decreased M3 delivery compared to R8-M3 and M3 delivery was similar to the peptide with a substitution of a single Glycine (GR8-M3) and did not decrease M3 delivery further.

This increase in M3 delivery when FFR8-M3 is used as a drug delivery vector was further shown to be significantly different to R8-M3 and GGR8-M3 at concentrations of 30 µM and 40 µM.

In addition to the fold change of GFP fluorescence within the SCL1 cell population, the percentage of GFP positive cells was calculated using histograms obtained from flow cytometry measurement. Figure 5-9 A shows an example of a histogram that describe the green fluorescence of the cell population when SCL1 cells were incubated with 40 µM of the different peptides. Figure 5-9 B displays the same histogram with a staggered offset so that every condition is clearly visible. It can be seen that the cell population of SCL1 cells treated with M3 or L-M3 did have the same distribution of green fluorescence as the DMSO control across the cell population and the histograms are overlayed. When cells were treated with R8-M3, GR8-M3 or GGR8-M3, the peaks of the histograms were shifted to the right, meaning that M3 was delivered to these cells and increased green fluorescence was detected. The histogram of F-R8-M3 was only slightly shifted to the right, indicating a small change of green fluorescence and M3 delivery by FR8. In contrast, when FFR8-M3 was incubated with SCL1 cells at 40 µM, there is a clear shift of the cell population towards higher green fluorescence.
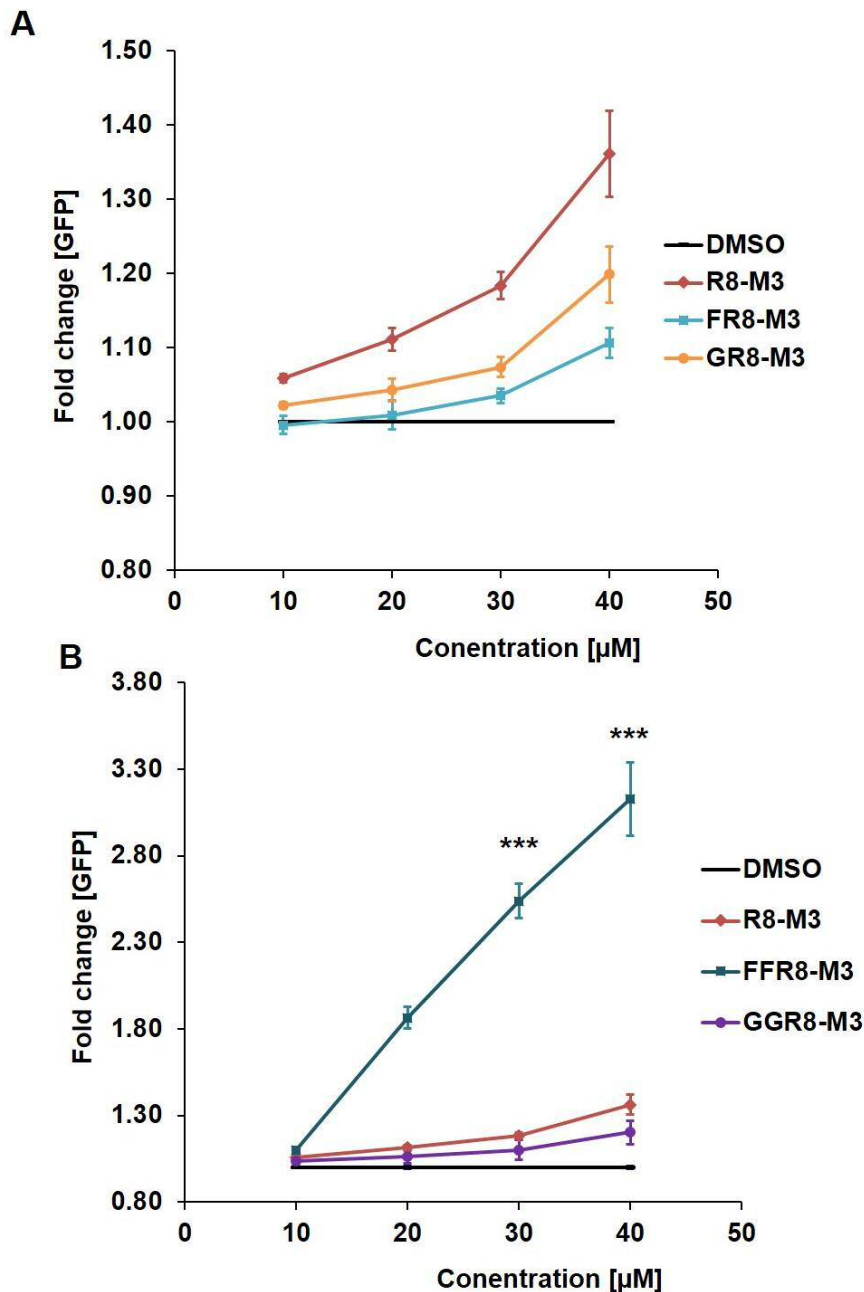
Figure 5-8 Effect of Phenylalanine or Glycine residue addition to R8-M3 on functional delivery of M3

Live split GFP complementation assay to monitor M3 delivery. SCL1 cells were washed once in serum free media and incubated with DMSO, R8-M3, FR8-M3, GR8-M3, FFR8-M3 or GGR8-M3 at 10-40 µM for 2h at 37°C. Cells were prepared for flow cytometry measurement. In total 20,000 cells were measured. Cells were gated for morphologically intact cells using SSC and FSC measurements and green fluorescence within this cell population was measured using the 488 nm excitation laser and the FITC emission filter. Fold change is shown compared to the DMSO control which was set to the value 1. (A) Comparison of single amino acid additions to R8-M3. For statistical analysis data was tested using a One way Annova followed by multiple comparison using a Turkey HSD (honest significant difference) test. No significant difference was seen for M3 delivery by FR8-M3 or GR8-M3 compared to R8-M3. (B) Comparison of addition of two amino acid additions to R8-M3.For statistical analysis data was tested using a One way Annova followed by multiple comparison using a Turkey HSD (honest significant difference) test. Significance is shown for FFR8-M3 compared to the corresponding concentrations of GGR8-M3 and R8-M3. *: $p<0.05$, **: $p<0.01$, ***: $p<0.001$, n.s.: not significant. Error bars: standard error of the mean n=3.

This change of green fluorescence within the cell population was further calculated to display the percentage of GFP positive cells (Figure 5-9 C). It can be seen that SCL1 cells were not positive for GFP complementation when they were incubated with M-3 or L-M3 at concentrations ranging from 10-40 μM. Treatment of SCL1 cells with R8-M3 showed a concentration dependent increase of cells that were positive for M3 delivery ranging from 5% at 10 μM to 28% at 40 μM. When cells were incubated with FR8-M3 no change was seen at 10 μM and the cell population was 11% positive at 40 μM. The highest increase of positive cells was seen for FFR8-M3. At 10 μM, 10% of the cell population were detected as GFP positive. This rapidly increased to 51% when 20 μM were applied and further increased to 65% and 72% for when incubated with 30 μM and 40 μM, respectively. Substitution of one or two Glycine residues had a similar effect on delivery efficiency of M3 into SCL1 cells. For both conditions the percentage of GFP positive cells was decreased at each concentration compared to R8-M3 and both peptides achieved a 17% GFP positive SCL1 cell population at the maximum concentration of 40 μM.

This shift in percentage positive cells correlates with the fold change of GFP fluorescence seen for the different peptides when incubated with SCL1 cells. This data demonstrated that functional cytosolic M3 delivery is most efficient using FFR8 as a drug delivery vector. The second efficient delivery vector was shown to be R8 followed by GR8-M3 and GGR8-M3. The least effective drug delivery vector in this study was FR8-M3.

This experiment clearly shows that the SCL1 cell line can be utilised to evaluate different CPPs regarding their ability to deliver M3 peptide cargo into cells.
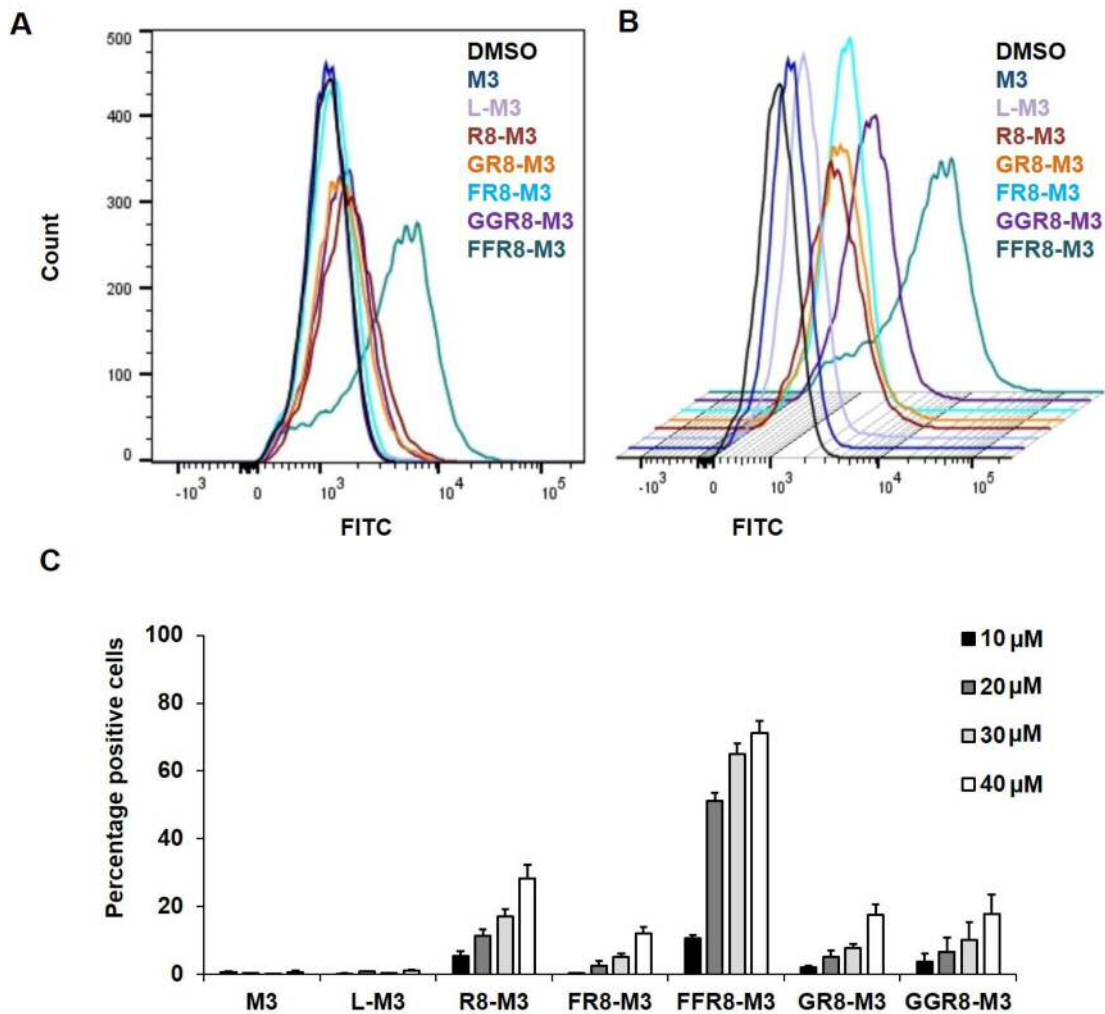
Figure 5-9 Shift of green fluorescence in SCL1 cell population when treated with different peptides.

Live split GFP complementation assay to monitor M3 delivery. SCL1 cells were washed once in serum free media and incubated with DMSO, M3, L-M3, R8-M3, FR8-M3, GR8-M3, FFR8-M3 or GGR8-M3 at 10-40 µM for 2h at 37ºC. Cells were washed in 0.5 mg/ml Heparin 3 times and detached from the cell culture dish using trypsin and prepared for flow cytometry measurement. In total 20,000 cells were measured. Cells were gated for morphologically intact cells using SSC and FSC measurements and green fluorescence within this cell population was measured using the 488 nm excitation laser and the FITC emission filter. (A) Example histogram shown when SCL1 cells were incubated with 40 µM of peptide. (B) Histogram with a staggered offset to emphasize shift of populations. (C) Percentage positive cells were determined using the population comparison tool in the FlowJo software. DMSO control samples were used for the corresponding concentration to compare populations. Error bars: SEM. n=3.

5.5 Delivery of M3 by different DDSs using mCherry-SCL51 cells

After it was seen that two phenylalanine residues can significantly increase M3 delivery into cells, the different M3 containing peptide formulations were further tested using the stable cell line mCherry-SCL51.

However, before M3 delivery by R8 containing drug delivery systems was investigated in a live cell assay, the compatibility of the M3 containing peptides to complement to full length GFP with mCherry-GFP1-10 expressed by mCherry-SCL51 cells was first tested in an *in vitro* assay.

5.5.1 *In vitro* complementation of peptides with mCherry-SCL51 lysate

To investigate GFP complementation *in vitro*, mCherry-SCL51 cells were trypsinised and pelleted. The cell pellet was resuspended in 0.1% Triton-X-100 and left to lyse the plasma membrane for 4 min. 80 µM of M3 containing peptides in PBS were then mixed with cell lysate of mCherry-SCL51 cell expressing mCherry-GFP1-10 to a obtain a final mix of lysate in 0.05% Triton-X100 in PBS with 40 µM of M3 containing peptides. mCherry-GFP1-10 lysate with the peptides was then left at room temperature under constant agitation and GFP complementation was monitored using a microplate reader every hour for 7 h (Figure 5-10). The *in vitro* complementation assay revealed that cell lysate from mCherry-SCL51 only complemented to form full length GFP when M3 was present. The drug delivery system R8 alone did not rescue GFP fluorescence. *In vitro* complementation using 40 µM R8-M3 showed a time dependent increase of GFP complementation with mCherry-GFP1-10. An N-terminal addition of Phenylalanine (F) or Glycine (G) residue to R8-M3 did not alter complementation dynamics, nor did an addition of two Phenylalanine (FF) or Glycine (GG) residues.

For all peptides a similar amount of GFP fluorescence was detected at each time point and the GFP complementation was not significantly different between the M3

containing peptides at time points 2h and 7h. This shows that addition of Phenylalanine or Glycine residues to R8-M3 did not inhibit or enhance the ability to complement with mCherry-GFP1-10 *in vitro* as it was seen before when peptides were tested with SCL1 cell lysate *in vitro*.
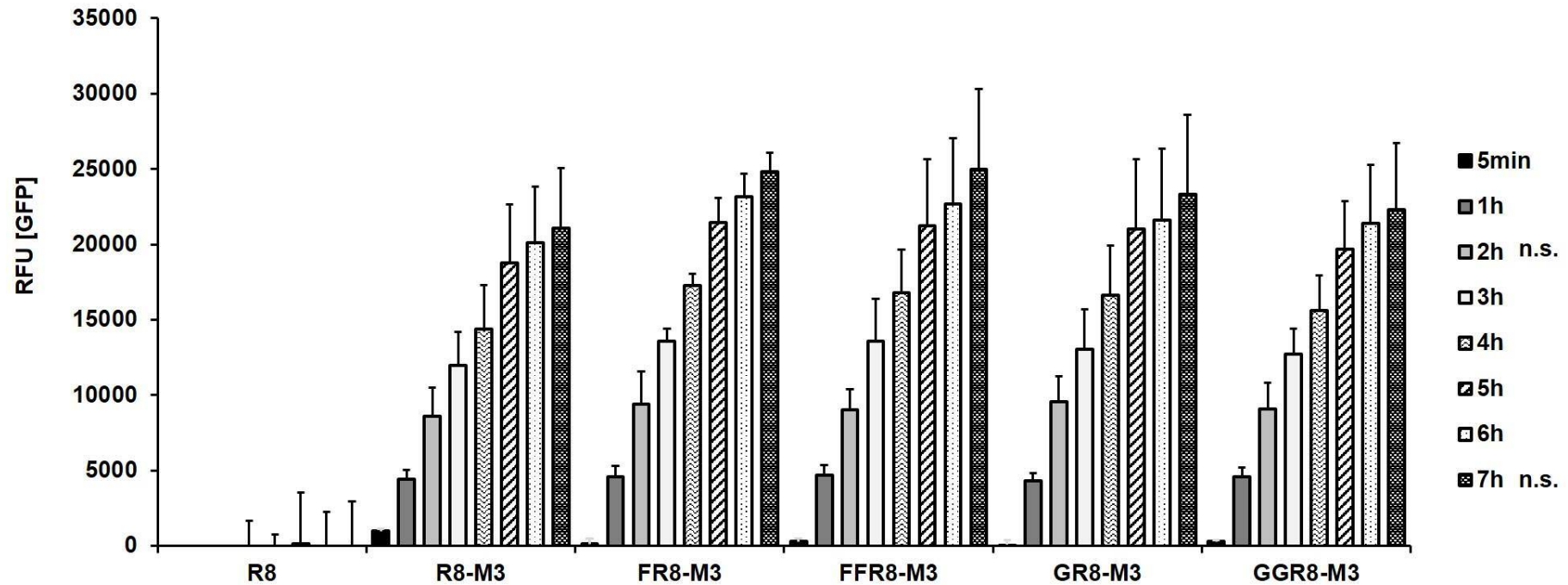
Figure 5-10 *In vitro* complementation of peptides with mCherry-SCL51.

In vitro complementation of lysed mCherry-SCL51 cells with peptides. Cells were trypsinised and lysed using 0.1% Triton-X100 in PBS. Cell lysate of 0.8×10^5 cells was mixed with 80 µM M3 and CPP-M3 peptides to obtain a final concentration of 40 µM in 0.05% Triton-X-100/PBS. Lysate mixture was left under constant agitation at room temperature. The fluorescent signal resulting from GFP complementation was minored over 24 h using a microplate reader. DMSO only control was subtracted as the sample background. n=3. Error bars present SEM. For statistical analysis data was tested using a One way Annova followed by multiple comparison using a Turkey HSD (honest significant difference) test. Data was tested at two time points, 120min and 7h. No significant differences were detected between M3 containing peptides at time points 2h and 7h. n.s.: not significant.

5.5.2 Effect of Phenylalanine or Glycine substitution to R8 on the efficiency to deliver M3 to the cytosol

It was next explored if a concentration dependent as well as DDS dependent delivery of M3 by different R8 based peptides can be observed in a live split GFP complementation assay using mCherry-SCL51 by flow cytometry. To test this, mCherry-SCL51 cells were washed once in serum free media and incubated with DMSO, M3, L-M3, R8-M3 or Glycine/ Phenylalanine added versions of R8-M3 (G/GG/F/FF) at a concentration range of 10-40 µM for 2h at 37ºC. The cells were then washed in 0.5 mg/ml Heparin for 3 times in order to remove membrane bound CPP-M3 peptide. Cells were detached from the cell culture dish using trypsin and washed with PBS twice. Cells were then resuspended in PBS and transferred into a FACS tube and kept on ice until flow cytometry measurements. GFP fluorescence of 10,000 cells was detected using flow cytometry and cells were gated for morphologically intact cells using FSC and SSC measurements. (For the 40 µM R8-M3 sample, GFP fluorescence of 20,000 cells were accidently collected.) The geometric mean of all samples was normalised to the DMSO control that was set to a value of 1 to display a fold change in GFP fluorescence. Figure 5-12 A displays the concentration dependent delivery of M3 by R8 compared to mCherry-SCL51 cells that were incubated with M3 or L-M3 only. M3 and L-M3 were not able to access the cytosol when incubated at concentrations of 10-40 µM. When mCherry-SCL51 cells were incubated with 10 µM R8-M3, GFP fluorescence was increased to 1.02 fold compared to the DMSO control (1 fold) indicating functional delivery of the M3 peptide to the cytosol. GFP fluorescence increased to 1.05 fold at 20 µM and remained at that fluorescence when incubated at 30 µM. Incubation with 40 µM R8-M3 resulted in 1.08 fold change compared to the DMSO control (1.0 fold). Hence, R8 was able to delivery M3 to the cytosol of SCL1 cells at each concentration but a concentration dependent increase was not observed when mCherry-SCL51 cells were incubated with 30 µM

R8-M3. In contrast, when single amino acids F or G were added to the N-terminus of R8-M3, a concentration dependent delivery was observed for both of the peptides (Figure 5-11 B). GR8-M3 showed no functional delivery of M3 at 10 µM but increased to 1.14 fold at 40 µM and was therefore more efficient to deliver M3 than R8-M3. Compared to that, FR8-M3 delivered M3 to an even greater extend, starting at the same efficiency like R8-M3 at 10 µM (1.03 fold) and achieving a 1.19 fold change at 30 µM and a 1.3 fold change of GFP fluorescence at 40 µM.

Figure 5-11 C displays the M3 delivery efficiency of peptides with addition of two amino acid residues, FFR8-M3 and GGR8-M3. N-terminal substitution of FF to R8-M3 had a great effect on functional delivery of M3 and achieved a 1.06 fold change in GFP fluorescence at 10 µM and 1.5 fold and 2.5 fold at 20 µM 30 µM, respectively. When cell were incubated with 40 µM, GFP fluorescence even changed by 3.1 fold. In contrast, substitution of GG to R8-M3 did not result in the same enhancement for M3 delivery. M3 delivery using GGR8-M3 increased compared to GR8-M3 and R8-M3 and fold change in GFP fluorescence was comparable to FR8-M3 at every concentration.

A

B

C
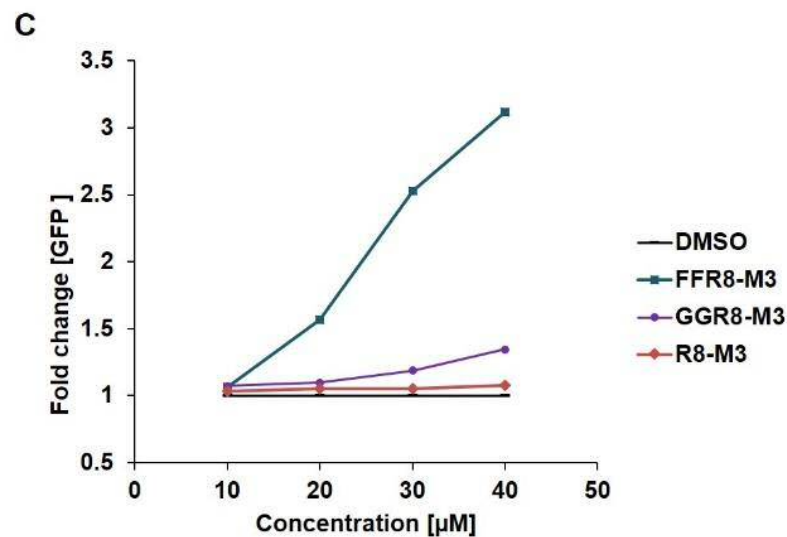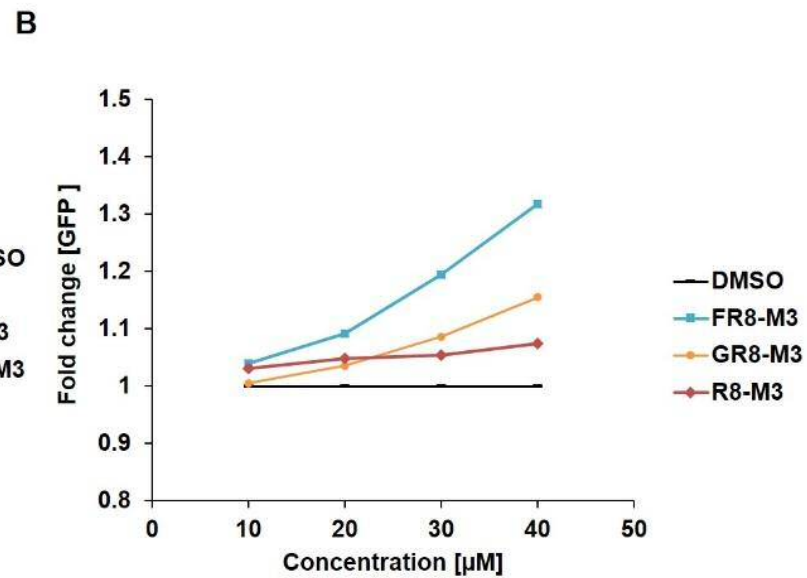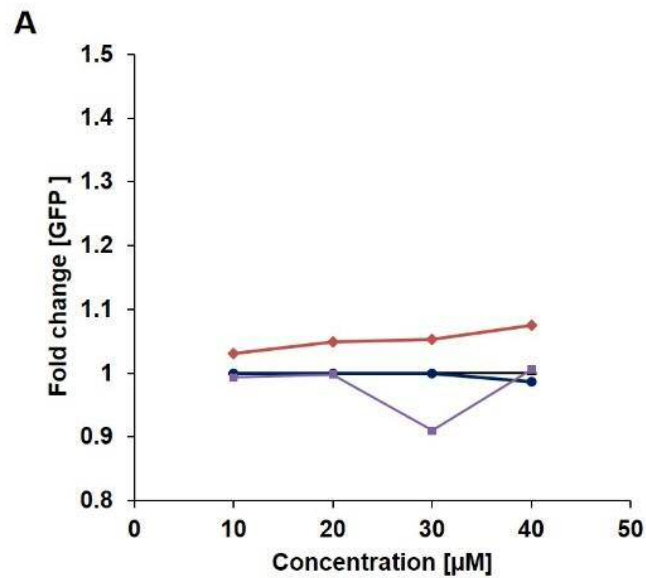
Figure 5-11 Effect of Phenylalanine or Glycine substitution to R8 on M3 delivery using mCherry-SCL51.

mCherry-SCL51 cells were washed once in serum free media and incubated with DMSO, M3, L-M3, R8-M3, FR8-M3, GR8-M3, FFR8-M3 or GGR8-M3 at 10-40 µM for 2h at 37ºC. Cells were washed in 0.5 mg/ml Heparin for 3 times and detached from the cell culture dish using trypsin and prepared for flow cytometry measurement. In total 10,000 cells were measured (20,000 cells for 40 µM R8-M3 treated cells). Cells were gated for morphologically intact cells using SSC and FSC and then for mCherry positive cells using the red signal detected through the PerCP-Cy5-5 filter. Within that population, green fluorescence was measured using the 488 nm excitation laser and the FITC emission filter. Fold change is shown compared to the DMSO control which was set to the value 1. n=1.

223

The efficiency of the different peptides to deliver M3 was also reflected in the histograms of the fluorescence of the whole population. Figure 5-12 A shows an example histogram that resulted when mCherry-SCL51 cells were incubated with 40 µM peptides. The same histogram is shown using a staggered offset in Figure 5-12 B. It can be seen that histograms of M3 and L-M3 were overlaid with the histogram obtained from the DMSO sample and histograms of GR8-M3, FR-M3, GGR8-M3 and FFR8-M3 were shifted to the right, indicating higher green fluorescence of cell populations demonstrating M3 delivery. The peak obtained from R8-M3 was higher compared to others because 20,000 cells were measured compared to 10,000 for other samples.

When the shift of histograms was calculated as percentage positive cells compared to the DMSO control, the same trend as when fold change of GFP fluorescence was calculated was seen. Cell populations of M3 and L-M3 were negative for GFP complementation and M3 delivery. A small change can be detected for R8-M3 at all concentrations but the change of percentage positive cells is not concentration dependent between 20 µM and 30 µM but reaches 8.33% of GFP positive cells at 40 µM. F-R8-M3, GR8-M3 and GGR8-M3 all show a concentration dependent increase in percentage positive cells of M3 delivery reaching 29.43% 15.79% and 29.08% when incubated with 40 µM, respectively. FFR8-M3 delivers M3 most efficient and achieves a 67.58% positive cell population when cells are incubated with 40 µM. The highest increase in percentage positive cells can be observed when FFR8-M3 concentration increases from 10 µM (8.58%) to 20 µM (39.37%).

This data obtained using mCherry-SCL51 cells indicates that FFR8-M3 delivered M3 most efficient followed by FR8-M3 and GGR8-M3. Substitution of one Glycine resulted in decreased efficiency to deliver M3 compare to GGR8-M3 but it was more efficient than R8-M3. R8-M3 did not show a concentration dependent increase in

delivery and the delivery efficiency was the least effective compared to all delivery systems that were investigated.

However, this data was obtained from a single experiment and should be repeated in order to confirm these results.
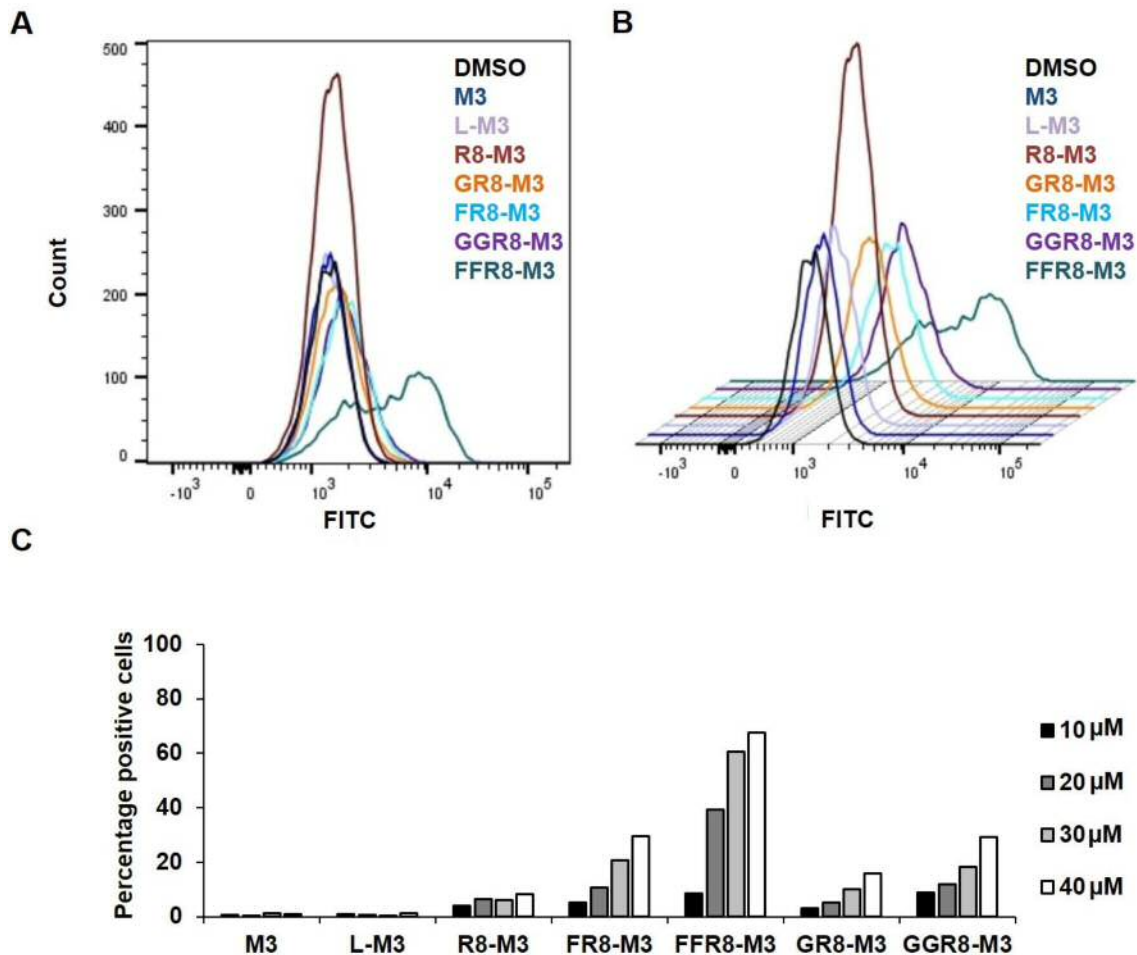
Figure 5-12 Shift of green fluorescence in mCherry-SCL51 cell population when treated with different peptides.
Live split GFP complementation assay to monitor M3 delivery. mCherry-SCL51 cells were washed once in serum free media and incubated with DMSO, M3, L-M3, R8-M3, FR8-M3, GR8-M3, FFR8-M3 or GGR8-M3 at 10-40 μM for 2h at 37ºC. Cells were washed in 0.5 mg/ml Heparin for 3 times and detached from the cell culture dish using trypsin and prepared for flow cytometry measurement. In total 10,000 cells were measured (20,000 cells for 40 μM R8-M3). Cells were gated for morphologically intact cells using SSC and FSC measurements and then for mCherry positive cells using the red signal detected through the PerCP-Cy5-5 filter. Within that population, green fluorescence was measured using the 488 nm excitation laser and the FITC emission filter. (A) Example histogram shown when mCherry-SCL51 cells were incubated with 40 μM of peptides. (B) Histogram with a staggered offset to emphasize shift of populations. (C) Percentage positive cells were determined using the population comparison tool in the FlowJo software. DMSO control samples were used for the corresponding concentration to compare populations. n=1.

5.6 Discussion

Split GFP has recently been utilised by several research groups in order to prove M3 peptide delivery and thereby evaluate the delivery efficiency of different peptide delivery vectors (Kim *et al.* 2015; Milech *et al.* 2015; Schmidt *et al.* 2015a; Lönn *et al.* 2016). In this Chapter it was demonstrated that the split GFP system that was developed here can also be utilised to determine a concentration dependent delivery of M3 by a DDS. Moreover it allows evaluation of DDSs and their efficiency to functionally deliver peptide cargo to an intracellular target.

Testing the delivery efficiency of functional M3 by different R8 derived peptides on two stable cell lines, SCL1 and mCherry-SCL51, showed a clear trend that a substitution of two Phenylalanine residues can enhance functional delivery of M3 peptide cargo compared to R8-M3. One Phenylalanine residues did not result in an enhancement of functional delivery compared to R8 on SCL1 cells. A single experiment on mCherry-SCL51 cells indicated that FR8-M3 could have an increased delivery compared to R8-M3. It was also demonstrated that this increased delivery is specific to the hydrophobic Phenylalanine residue because functional M3 delivery was not increased with GR8-M3 or GGR8-M3 in SCL1 cells.

Importantly, the effect of substitution of Phenylalanine residues on functional delivery in a live cell assay can be specifically shown by comparing the live cell assay data obtained from the *in vitro* assay. In the *in vitro* assay it was shown that every peptide has the same ability to complement with SCL1 expressed GFP1-10 to form full length GFP, with the complementation even being slightly increased for R8-M3 compared to FFR8-M3. In contrast, in the live cell assay FFR8-M3 delivered the M3 peptide highly increased compared to R8-M3. Because the two peptides complemented to the same degree with GFP1-10 *in vitro*, increase in GFP complementation in the live assay is specific to the delivery efficiency of the peptide. Hence, it was demonstrated that the improved *in vitro* system allows us to compare

complementation rates and degree of complementation of different peptides. This improvement is of high importance when different DDS-M3 peptides will be compared with each other to confirm that the effect seen in live uptake experiments is due to the DDS and not varying complementation ability of the peptides.

In other GFP complementation studies, the intracellular GFP1-10 target was either expressed stably (Milech *et al.* 2015; Lönn *et al.* 2016) or transiently as a fusion protein to the expression marker mCherry (Schmidt *et al.* 2015a). Here it was shown that the generated cell line SCL1 stably expressing GFP1-10 can be utilised to investigate concentration dependent and DDS dependent delivery of M3. One experiment also indicated that mCherry-SCL51 can be utilised to evaluate DDSs to deliver M3 is a dose dependent manner.

It was seen on both cell lines that FFR8-M3 delivered M3 to a higher degree than the other peptides that were tested. FR8-M3 delivered M3 less efficiently than R8-M3 on SCL1 cells but on the mCherry-SCL51 cell line it was indicated that FR8 could increase M3 delivery into cells. Results obtained from the mCherry-SCL51 cells should be confirmed, however, the reason for varying performance of the peptides on different cell lines can be hypothesised. The two factors that could influence the delivery performance in this assay are the peptides themselves as well as the two cell lines.

When the R8 based peptides were purchased they were received as 1.0 mg powder aliquots. EZBiolabs reassured that the accuracy of the measured weight is to the best of their performance. Different batches of peptides were consistently diluted with the same amount of DMSO to a final concentration of 10 mM. However, slight batch to batch variations are possible and factors like long term storage and freeze thaw cycles could have influenced peptide performance.

SCL1 cells and mCherry-SCL1 cells both stably express a protein in their cytosol. The site of integration of the DNA into the genome could be critical and uptake

mechanisms between the cell lines could be altered between the cell lines which could lead to different performance of the peptides on the cell lines.

In Chapter 4 it was shown that even though the GFP1-10 target is expressed in every cell in the SCL1 cell line, only selected cells showed M3 delivery. It was hypothesised that a cellular factor (e.g. mitotic cells, plasma membrane composition) could be responsible to determine in which cells delivery takes place. If that mechanism is revealed in the future, the mCherry-SCL51 and SCL1 cell line should be characterised regarding that factor.

Most importantly, the split GFP assay was not limited by the amount of intracellular expressed GFP1-10, even though it was demonstrated in Chapter 4 that the amount of expressed GFP1-10 was low compared to the levels that can be achieved using transient transfection. The expressed levels of GFP1-10 were sufficient to achieve a dose response for all R8 based delivery vectors used in this study.

R8 and its function as a peptide delivery vector has not been investigated before by other groups utilising the split GFP system. One Arginine rich peptide similar to R8 that has been characterised regarding its ability to deliver peptide cargo to the cytosol is nonaarginine (R9) (Milech *et al.* 2015; Schmidt *et al.* 2015a). Delivery efficiency of M3 by R9 was tested at a concentration range of 5-20 µM in both studies and in total three cell lines were investigated; CHO-K1 and HCC827 stably expressing GFP1-10 and HEK293Tcells transfected with mCherry-GFP1-10. In all cell lines, delivery of M3 was shown to be least efficient at concentrations of 5 and 10 µM. When the concentration was increased to 20 µM, a large increase in delivery efficiency was seen. In this chapter it was demonstrated that R8 efficiently acts as a drug delivery vector at concentrations of 10-40 µM and M3 was delivered to 28% of the cell population when incubated at 40 µM on SCL1 cells. R8 was able to deliver M3 at

concentrations as low as 10 µM. It would be interesting to investigate if delivery can also be detected down to 5 µM as it was shown in other studies for different CPPs.

Two mechanisms are proposed by which CPPs like R8 can enter cells: by direct translocation or uptake via endocytic pathways. It was shown that R8 enters the cell by endocytic pathways like clathrin-mediated endocytosis or micropinocytosis at concentrations below 10 µM (Kaplan *et al.* 2005; Ikuhiko Nakase *et al.* 2006(Kawaguchi *et al.* 2016). If they enter through endocytic mechanism it is critical for the peptide to escape the endosome to reach the cytosol and avoid degradation in the lysosome.

The direct transduction efficiency of fluorophore conjugated polyarginines has been assessed. For R8 and longer polyarginines it was shown that direct transduction of the cells started as low as 5 µM (Tunnemann *et al.* 2008). This study was based on a phenotypic analysis where endocytic uptake was scored when fluorescent signal was enclosed in vesicles and direct transduction was accounted for when both, completely cytosolic distribution of the fluorophore was seen as well as a combination of cytosolic fluorescent signal and endosome enclosed CPP. A study by (Tunnemann *et al.* 2006) also suggested that CPPs with smaller cargos like non globular peptides can enter the cell through direct penetration.

How uptake of R8-M3 is facilitated across the plasma membrane, through endocytic uptake followed by endosomal escape or direct translocation remains unknown. However, considering the high concentrations of R8 of 10-40 µM that have been used in this assay and the relatively small size of the M3 peptide cargo (1.8 kDa) could suggest that direct translocation across the plasma membrane is possible.

Lönn *et al*., 2016 have shown that the limiting factor for cargo delivery is endosomal escape and have shown that M3 delivery by Tat upon treatment with the endosomolytic agent chloroquine was greatly enhanced (Lönn *et al.* 2016). It would be interesting to investigate if treatment of chloroquine could enhance R8-M3

delivery. This could lead to the model that R8-M3 can cross the plasma membrane directly as well as via endocytosis. The direct entry is seen in 28% of the cell population, in other cells R8-M3 remains entrapped in endosomes.

This would also explain the heterogeneous delivery of M3 across the cell population. It was seen that M3 was not functionally delivered into every cell of the SCL1 cell population. This cannot be attributed to the lack of expression of the intracellular GFP1-10 target protein because it was shown that SCL1 cells express even amounts of GFP1-10 across the cell population. Hence, another cellular mechanism is suggested that could be underlying that favours direct translocation or endocytic uptake. Interaction with the plasma membrane is critical for the uptake of CPPs and Schmidt *et al*., 2015 have shown that treatment of the plasma membrane with bacterial sphingomyelinase which leads to conversion from sphingomyelin into ceramide, increases M3 cargo delivery into cells by R9. Lipid composition and localisation is also changed during mitosis (Atilla-Gokcumen *et al.* 2014). It would be interesting to investigate the change of lipid composition throughout the cell cycle and test if direct M3 delivery by R8 is dependent of the stage of the cell cycle of the target cell.

Popular strategies to enhance uptake of CPPs are the substitution or modification of single amino acids to enhance cell penetration. Especially hydrophobic residues like Phenylalanine or Tryptophan have been used to increase uptake of CPPs (Takayama *et al.* 2009; Rydberg *et al.* 2012; Takayama *et al.* 2012; Sayers *et al.* 2014; Lönn *et al.* 2016). A study by the group of Shiroh Futaki identified a penetration acceleration sequence (pas) consisting of the amino acid sequence FFLIPKG. N-terminal conjugation of that sequence to Alexa 488 labelled R8 highly increased its uptake in HeLa cells (Takayama *et al.* 2012). In that study, uptake of Alexa 488 labelled R8 with the N-terminal addition of two Phenylalanine residues via a Glycine residue (FFGR8) was investigated. Uptake of FFGR8 was examined at 1

µM and 15 min incubation time but was not of further interest because in only yielded a low increase of uptake compared to R8 and substitution of four Phenylalanine residues achieved even more increased uptake.

However in that study Alexa 488 labelled FFGR8 was investigated using flow cytometry. Hence, the uptake of the peptide was investigated, not the ability of functional delivery of a cargo. In this chapter it was clearly shown that substitution of two phenylalanine residues to R8 (FFR8) enhances the functional delivery of the M3 cargo peptide compared to R8 at concentrations between 10 and 40 µM. This effect is specific to the hydrophobic Phenylalanine residues and was not achieved when conjugating two Glycine residues to the CPP R8. Conjugation of one Phenylalanine did not result in an enhancing effect compared to R8-M3 when investigated on SCL1 cells. Based on the previous study that FFFFGR8 uptake was more enhanced that FFGR8 (Takayama *et al.* 2012), it would be interesting to test if the addition of four phenylalanine residues to R8-M3 could have an even more enhancing effect on delivery than FFR8-M3.

Steven Dowdy's group has utilised the split GFP assay to determine endosomal escape domains (EEDs) attached to the CPP TAT to enhance the functional delivery of GFP11 to intracellular GFP1-10 by enhancing endosomal escape (Lönn *et al.* 2016). EEDs consisted of either Phenylalanine or Tryptophan residues were investigated in his study. The EEDs which was identified to increase cytosolic delivery of the cargo peptide was a residue consisting of two Phenylalanine residues with a central Tryptophan residue (FWF). An EED consisting of four Phenylalanine residues was shown to increase delivery but was also associated with severe cytotoxic effects. When Shiroh Futaki's group tested the enhanced uptake of FFFFGR8 it was reported that this peptide was not accompanied by sever cytotoxicity monitored by the live cell impermeable stain propidium iodide (PI) (Takayama *et al.* 2012).

Membrane integrity and cytotoxicity is an important factor to consider when evaluating drug delivery vectors because in addition to their ability to deliver cargo into cells, they should not affect the viability of the target cell. Especially when working with CPPs this is critical because they have the ability to penetrate the plasma membrane. Hence, it will be critical to evaluate the cytotoxic effects of FFR8-M3 in order to fully characterise this peptide as a delivery vector for peptides.

In a study by Gisela Tuennemann the penetration ability of polyarginines with respect to their cytotoxicity was tested (Tunnemann *et al.* 2008). For R8 it was seen that cells where direct translocation of the fluorophore tagged R8 took place were stained for PI from a concentration of 10 µM. However concentration up to 50 µM only showed a PI staining of under 10% of the cell population. In this study a concentration range of 10-40 µM was used. However R8 was also conjugated to a 2.4 kDa cargo peptide (including the linker between cargo and R8) which could have an influence on membrane integrity when this cargo is delivered across the plasma membrane.

The selection of morphologically intact cells was aimed to be achieved by flow cytometry measurements. Gating of morphologically intact cells by flow cytometry and measurement of green fluorescence of viable cells was based on the Split GFP study published by Schmidt and his colleagues (Schmidt *et al.* 2015a). Using a Live/Dead cell stain, data collected from a single experiment suggested which FSC and SSC measurements correlate with morphologically intact cells. It was shown that cells that small and less granular included cells that were positive for the cells stain. However this experiment should be repeated including an experimental control with cells where the plasma membrane has been permeabilised.

A different method to assess the integrity of the plasma membrane includes the treatment of cells with the nuclear counterstain propidium iodide (PI). This a popular stain to determine membrane damage by CPPs (Tunnemann *et al.* 2008; Takayama

et al. 2012). The stain is not permeable to live cells and only stains cells with a non-intact plasma membrane. However, PI (excitation/emission: 535 m/617nm) has similar fluorescent characteristics like mCherry and it would not have been possible to distinguish the fluorescent signal from cells that were expressing mCherry-GFP1-10 or cells that were permeable for the PI stain. In order to perform the flow cytometry experiments consistently between cell lines SCL1 and mCherry-SCL51, this method was not followed up on further.

Milech and colleagues have included the violet Live/Dead cell stain within their M3 delivery studies by CPPs (Milech *et al.* 2015). However, this cell stain requires incubation of 30 min according to the manufactures instructions which delays flow cytometry measurements additional to the time that is needed for the sample preparation. Because this method is supposed to be a real time assessment of M3 delivery so that the time between the end of incubation of the DDS-M3 peptide until flow cytometry measurements should be kept minimal.

Retrospective, it would have been beneficial to add the cell stain PI to assess membrane integrity of SCL1 cells when treated with different CPP-M3 compounds. This would have given valuable information about the influence on membrane integrity depended on the type of CPP as well as on the concentration dependent influence on membrane integrity. For this reason it is inevitable to assess the cytotoxicity of the peptides used in this study to be able to correlate cytotoxicity data with the ability to delivery M3 cargo into cells.

In summary, in this chapter it was shown that the generated cell line SCL1 can be utilised to investigate DDS dependent as well as concentration dependent delivery of the M3 peptide and allows characterisation of the DDSs. To obtain the full picture of the performance of the DDS this should be correlated with cytotoxicity studies.

Moreover it was shown that the substitution of two Phenylalanine residues to R8-M3 can significantly increase delivery of the M3 peptide and this effect can be specifically attributed to the Phenylalanine residue.

6 Microscopic analysis of M3 delivery by R8 based peptides

6.1 Introduction

Thus far, it is has been established that the split GFP assay developed within this study can be utilised to evaluate the M3 peptide delivery efficiency of different R8 based peptides. In order to gain information of delivery in a large number of cells and to be able to assess multiple conditions within the same experiment, flow cytometry measurement was chosen as a detection method. This detection method was also utilised by other research groups that have developed the split GFP assay as a method to characterise novel DDSs to functionally deliver M3 peptide (Milech *et al.* 2015; Schmidt *et al.* 2015b; Lönn *et al.* 2016).

One aim of this project was utilise the split GFP as a microscopy based technique to not only show if the M3 peptide has been functionally delivered to its cellular target but also to investigate its subcellular localisation. This will help to examine if DDSs have an influence on the localisation of their cargo.

Detailed microscopic analysis of M3 peptide delivery by DDSs has not been shown by other research groups so far. One figure including microscopy images was published by the group of Roland Brock to confirm GFP complementation using R9 as a delivery vector is increased in bacterial sphingomyelinase treated cells (Schmidt *et al.* 2015a). However, those images did not add any further information to the assay other than confirming that the M3 peptide had been delivered and GFP complementation had occurred.

Microscopic analysis has the potential to add more valuable information in order to characterise DDSs than just answering the question if a cargo has reached the cytosol of a cell. Utilising widefield microscopy, it was shown in Chapter 3 and Chapter 4 that real time delivery of M3 peptide by a DDS can be observed in live cells which allows us to image an effect of cargo and target interaction in real time. Furthermore,

it was seen that complemented GFP localises to the nucleolus when R8 is used as a DDS to deliver the peptide. In a study by Giesela Tuennemann, fluorophore conjugated R8 has been characterised to be able to act as a nucleolar live cell marker for imaging (Martin *et al.* 2007).

Subcellular localisation of a delivered peptide cargo is critical when it has to function at a specific site of action. For this reason it is important to not only be able to monitor <u>if</u> and <u>when</u> the peptide is delivered into the intracellular target but also <u>where</u> the target-cargo complex is localised inside the cell and what influence a drug delivery system has on subcellular localisation of a peptide cargo and its associated target.

The aim of this chapter is to analyse and characterise the localisation of M3 delivery by R8 based peptides with Glycine and Phenylalanine residue addition using microscopy as the detection method for split GFP complementation. It is hypothesised that microscopy can add further information as to where complemented GFP localises inside the cell and what influence a drug delivery vector can have on the peptide-cargo complex localisation.

6.2 Localisation of complemented GFP

6.2.1 Localisation of complemented GFP using R8-M3 as a DDS

In chapter 3 and 4, complemented GFP was noticed to be localised to the nucleolus when cells were treated with R8-M3. In order to confirm the subcellular localisation of complemented GFP when R8 is utilised as a DDS to deliver M3, SCL1 cells were washed once with serum free media, incubated with 40 µM R8-M3 for 2h at 37ºC and the nucleus was stained with Hoechst. In chapter 5 it was shown that green fluorescence from GFP complementation was highest when SCL1 cells were incubated with 40 µM peptide. Furthermore, it was previously shown that untreated SCL1 cells are green fluorescent as a result of GFP1-10 expression. Hence, a concentration of 40 µM was chosen to achieve the highest GFP complementation signal in order to visualize the subcellular localisation of GFP and obtain a sufficient signal over the green fluorescent background of SCL1 cells.

Figure 6-1 shows a typical image of cells where GFP has complemented as a result of M3 delivery to the cytosol by R8. It can be seen that the GFP fluorescence is mainly localised in two compartments: the cytosol and the nucleus (Figure 6-1 C). Enlargement of a cell that exhibits GFP fluorescence reveals that fluorescence is not distributed in the entire nucleus but concentrated as round structures at specific localisations that remind of nucleolar labelling (red arrow heads).
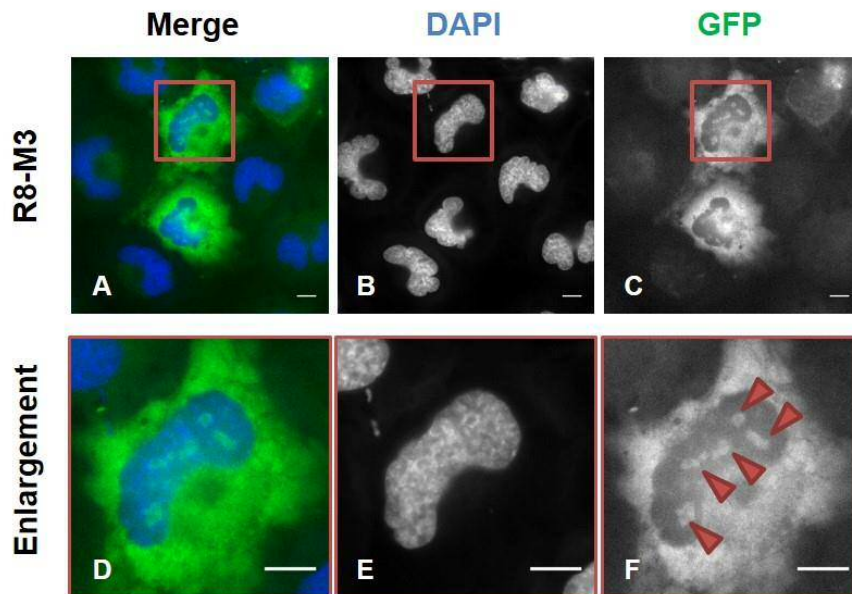
Figure 6-1 Localisation of complemented GFP using R8-M3.
SCL1 cells were incubated with R8-M3 at 40 μM in serum free media for 2 hours at 37˚C. Cells were counterstained with Hoechst nuclear dye and kept in phenol red free RPMI for imaging. GFP fluorescence was detected using a widefield fluorescent microscope. (A-C) Representative image that shows GFP complementation achieved by M3 delivery by R8. Cell in red square is enlarged in images D-E. (F) Red arrow heads point out nucleolar localisation of GFP. Scale bar: 10μm.n=3.
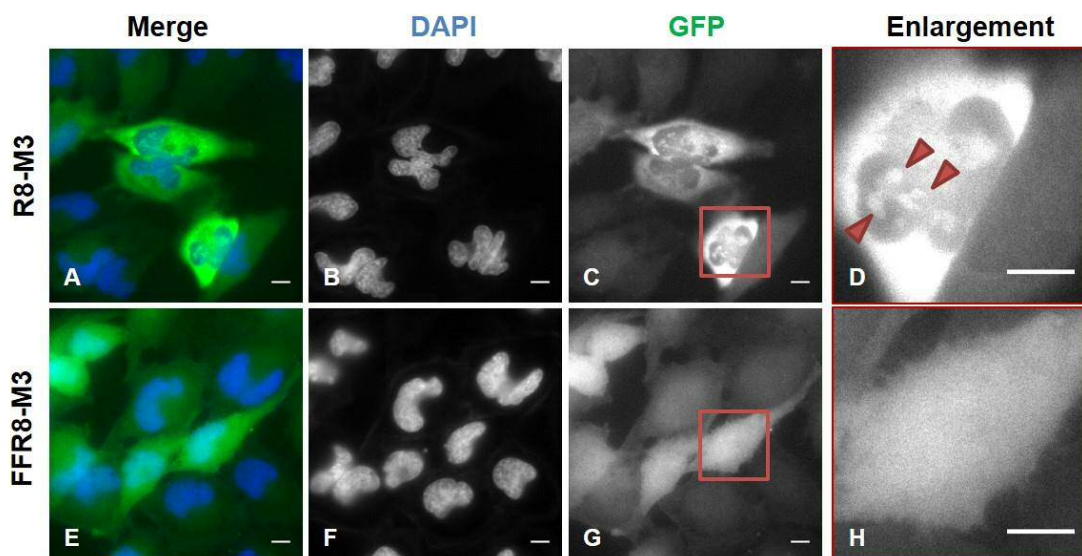
Figure 6-2 Comparison of localisation of complemented GFP using R8 or FFR8 to deliver M3.
SCL1 cells were incubated with R8-M3 or FFR8-M3 at 40 μM in serum free media for 2 hours at 37˚C. Cells were counterstained with Hoechst nuclear dye and kept in phenol red free RPMI for imaging. GFP fluorescence was detected using a widefield fluorescent microscope. Representative images show GFP complementation achieved by M3 delivery by R8 (A-D) or FFR8 (E-H). Cells in red squares are enlarged in images D and H. (D) Red arrow heads point out nucleolar localisation of GFP. Scale bar: 10μm.n=3.

238

6.2.2 Localisation of complemented GFP using FFR8-M3 as a DDS

It was next investigated if the N-terminal addition of Glycine or Phenylalanine residues to R8-M3 influences the subcellular localisation of complemented GFP compared to R8-M3. We have previously shown that substitution of two Phenylalanine residues (FFR8-M3) had the most dramatic effect to increase M3 delivery to the cytosol of SCL1 cells. Hence, it was first compared if a difference in complemented GFP localisation can be seen when cells are incubated with R8-M3 of FFR8-M3. To investigate this, SCL1 cells were washed once with serum free media, incubated with 40 µM R8-M3 or FFR8-M3 for 2h at 37ºC and the nucleus was stained with Hoechst.

Comparison of the localisation of complemented GFP using R8-M3 or FFR8-M3 to deliver M3 cargo to the cytosol reveals that complemented GFP is distributed differently inside the cells (Figure 6-2). Complemented GFP is again localised in the cytosol and concentrated as punctate structures in the nucleus (red arrow heads) when R8-M3 served as a delivery vector for M3 (Figure 6-2 C, D). When FFR8-M3 was utilised for delivery, complemented GFP signal is evenly distributed throughout the entire cell (Figure 6-2 G). When the image is enlarged in the area where the nucleus is localised, no distinct nuclear structure can be seen and even distribution of GFP signal between the nuclear area and the cytosol is observed (Figure 6-2 H). When comparing the two samples, it is striking that the exact localisation of the nucleus can be determined on the basis of complemented GFP distribution when incubated with R8-M3. There is a clear separation of the GFP signal between the cytosol and the nucleus which emphasizes the outline of the nucleus within the cell. Complemented GFP signal is excluded from the nucleus and only localises to the nucleolus inside the cell.

6.2.3 Influence of N-terminal amino acid substitutions to R8-M3 on the localisation of complemented GFP

It was next explored if the change of localisation of complemented GFP that is seen between R8-M3 and FFR8-M3 is specific to the addition of two Phenylalanine residues or whether this is an effect of N-terminally 'capping' of R8. To investigate this, cytosolic localisation of complemented GFP was investigated when cells were treated with either R8-M3 or the amino acid substituted versions of R8-M3, FR8-M3, FFR8-M3, GR8-M3 or GGR3-M3. This experiment was carried out using cells transiently expressing GFP1-10 because it was previously shown that stable GFP1-10 expression in SCL1 cells results in a high amount of green fluorescence.

Moreover, delivery efficiency of M3 by peptides with one addition of a Phenylalanine or Glycine residue the amino acid was not as great as seen with FFR8-M3. Hence, green fluorescence in SCL1 cells could be confused with low signal of GFP complementation resulting from treatment with non-efficient peptide when localisation is visually analysed. In order to ensure that the green fluorescence that is seen in localisation experiments can be certainly attributed to the fluorescence of complemented GFP further localisation experiments were performed using HeLa cells transiently expressing GFP1-10.

To explore the intracellular localisation of complemented GFP when cells were treated with different peptides, cells transiently expressing GFP1-10 were washed once with serum free media and incubated with 40 µM R8-M3 or amino acid substituted versions, FR8-M3, FFR8-M3, GR8-M3 or GGR3-M3 for 2h at 37ºC. After incubation the nucleus was stained with Hoechst. Figure 6-3 shows representative images obtained from analysing cells using a widefield microscope. It is again visible that cells incubated with R8-M3 show a distribution of complemented GFP in the cytosol as well as localised to the nucleolus (Figure 6-3 G, H). Only weak green fluorescence can be seen for the DMSO control that is likely to be a source of GFP fluorescence resulting from transient GFP1-10 expression (Figure 6-3 C, D). Addition

of one or two Glycine residues to R8-M3 (GR8-M3/GGR8-M3) showed the same distribution of complemented GFP as it was seen when cell were incubated with R8-M3. When cells were treated with 40 µM GR8-M3 and GGR8-M3, the GFP signal was localised at the nucleolus or the cytosol (Figure 6-3 L, P). For cells treated with R8-M3, GR8-M3 and GGR8-M3, a clear separation of GFP fluorescence can be seen between the nucleus and the cytosol and almost no green fluorescence is detected at the nucleus apart from GFP localised at the nucleolus (red arrow heads). Addition of Phenylalanine residues changed the localisation of complemented GFP and this effect is seen for a single substitution (FR8-M3) or a double substitution (FFR8-M3). Incubation of 40 µM FR8-M3 or FFR8-M3 resulted in an even distribution of GFP signal throughout the cell and no separation can be seen between the cytosol and the nucleus (Figure 6-3 T,X).

This data shows that complemented GFP is localised at different places inside the cell depending on which drug delivery vector was chosen. Furthermore, N-terminal 'capping' of R8-M3 with one or two Glycine residues did not have an influence on subcellular localisation compared to R8-M3. Thus, relocalisation of complemented GFP to be distributed evenly throughout the cell is an effect that can be specifically attributed to the addition of Phenylalanine residues. The main difference between Phenylalanine substituted R8-M3 and R8-M3 or Glycine substituted versions was this distinct separation of complemented GFP signal from the nucleus and the cytosol for R8-M3 and Glycine substituted R8-M3. However, these images were taken with a widefield microscope. In order to confirm that there is a localisation difference seen within the plane of the nucleus inside the cell, this experiment was repeated on a confocal microscope.
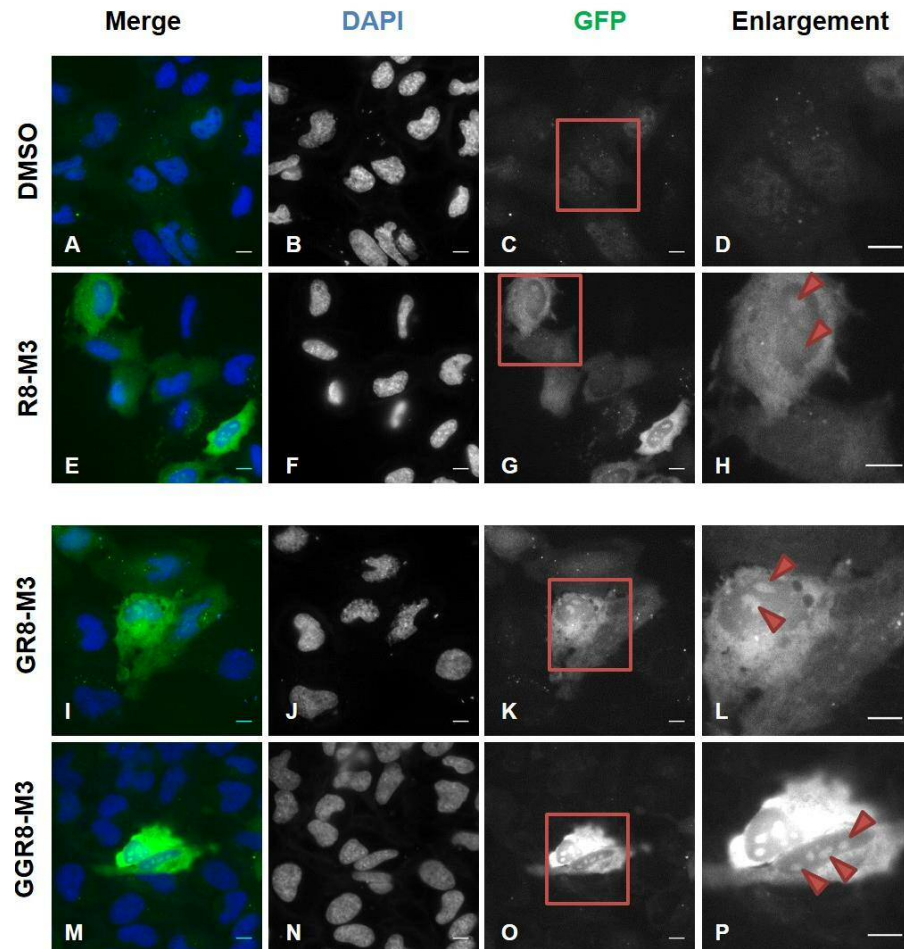
Figure 6-3 Influence of substitution of Glycine or Phenylalanine residues to R8-M3 on complemented GFP localisation.

HeLa cells transiently expressing GFP1-10 were incubated with DMSO, R8-M3, FR8-M3, FFR8-M3, GR8-M3 or GGR8-M3 at 40 µM in serum free media for 2 hours at 37˚C. Cells were counterstained with Hoechst nuclear dye and kept in phenol red free RPMI for imaging. GFP fluorescence was detected using a widefield fluorescent microscope. Representative images show GFP complementation achieved by M3 delivery. Cells in red squares are enlarged in images D, H, L, P, T and X. Red arrow heads point out nucleolar localisation of GFP. Scale bar: 10µm.n=2.
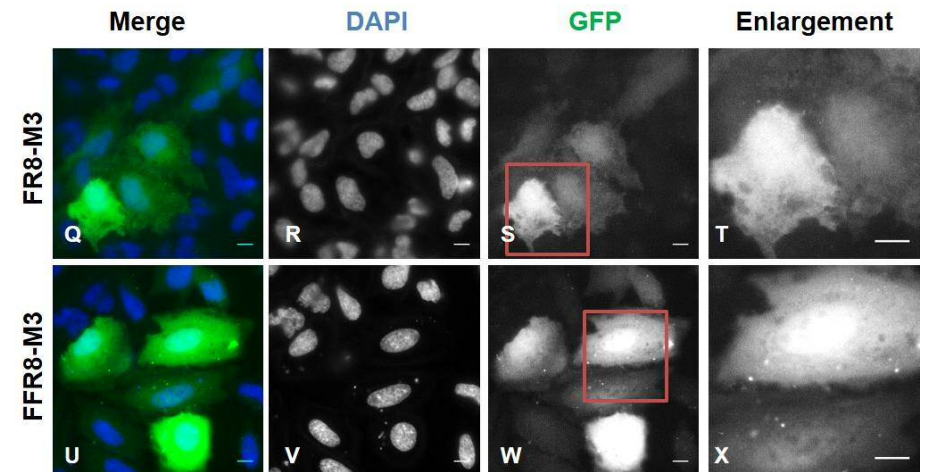
6.2.4 Confocal analysis of complemented GFP localisation

For confocal analysis of complemented GFP distribution inside the cell, HeLa cells transiently expressing GFP1-10 were washed once with serum free media and incubated with 40 µM R8-M3 or amino acid substituted versions, FR8-M3, FFR8-M3, GR8-M3 or GGR3-M3 for 2h at 37ºC. The nucleus was stained with Hoechst and cells were imaged on a confocal microscope. Images of single planes through the cells were taken. The nucleus served as an orientation point to visualize different samples at comparable z localisation within the cell. Representative images for each condition are shown in Figure 6-4 A. The exact localisation of complemented GFP can be seen in Figure 6-4 B where images obtained from the GFP channel are enlarged. These images confirm the results observed with a widefield microscope and show that complemented GFP is localised in the cytosol and at the nucleolus when incubated with R8-M3, GR8-M3 or GGR8-M3 (Figure 6-4 B). For all three conditions a clear separation of complemented GFP from the nucleus can be seen. Compared to these samples, the complemented GFP fluorescence is evenly distributed within the cells when cells were incubated with F8-M3 or FFR8-M3; and this observation is independent on the amount of complemented GFP (brightness of the cell). Observation of the GFP channel of the samples incubated with F8-M3 or FFR8-M3 does not give a hint of where the nucleus or nucleolus could be localised within the cell (Figure 6-4 B). Even though the GFP intensity is not highly increased compared to the DMSO control, a difference between these samples can be seen suggesting that fluorescence is indeed derived from GFP complementation. The DMSO sample shows two cells with increased fluorescence compared to other cells in the field of view (marked with red stars). This fluorescence is suggested to be derived from GFP1-10 expression in cells as it was previously shown to occur when GFP1-10 is expressed in HeLa cells. Green fluorescence in those cells is localised in the cytosol and the nucleus but not at the nucleolus which can be seen as punctate structures without GFP fluorescence. Compared to that green fluorescence, GFP fluorescence

derived from complementation for cells treated with 40 µM FR8-M3 and FFR8-M3 is increased and no nucleolar structures can be seen.

The data obtained from confocal microscopy confirms that distribution of complemented GFP is altered depending on the type of drug delivery vector used to deliver M3 into the cell.
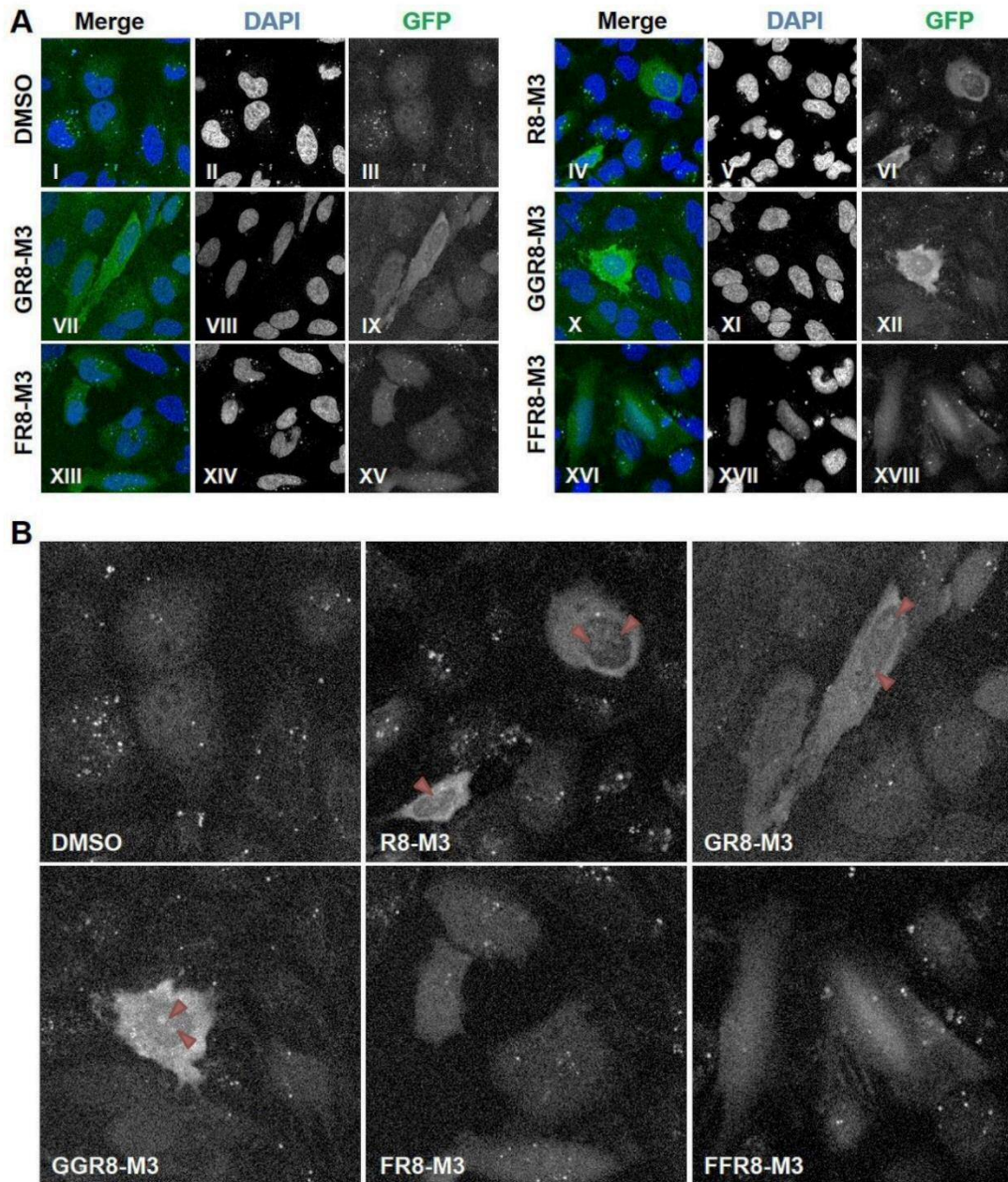
Figure 6-4 Confocal analysis of complemented GFP localisation.
HeLa cells transiently expressing GFP1-10 were incubated with DMSO, R8-M3, FR8-M3, FFR8-M3, GR8-M3 or GGR8-M3 at 40 µM in serum free media for 2 hours at 37˚C. Cells were counterstained with Hoechst nuclear dye and kept in phenol red free RPMI for imaging. GFP fluorescence was detected a confocal microscope. (A) Representative images for each condition show GFP complementation achieved by M3 delivery. (B) GFP channels shown for each condition. Red arrows point out nucleolar localisation of GFP. n=1.

6.3 GFP complementation at the Golgi membrane

In Chapter 3 it was mentioned that the expression construct GRASP65-GFP1-10 had been generated to obtain GFP1-10 expression that is retained at the Golgi membrane.

Using the GRASP65-GFP1-10 expression construct, it was investigated in a final experiment if the M3 peptide can be delivered to the outside of the Golgi membrane (cytosolic access) to complement with GFP1-10. To test this, Hela cells were transiently transfected with 125 ng DNA coding for GRASP65-GFP1-10. The next day, cells were incubated with 40 µM of M3 peptides for 2h at 37ºC. The peptides that were chosen to be investigated were M3, as a non-DDS conjugated version; R8-M3, representing the peptides that localised complemented GFP to in the cytosol and the nucleolus and FF-R8M3, a peptide highly efficient at delivering M3 to the cytosol and locating complemented GFP in the cytosol. Figure 6-5 shows the result of the experiment suggesting that M3, not conjugated to a DDS was not able to enter the cells (Figure 6-5 III). R8-M3 did deliver M3 to the cytosol of cells, however only cells were found where the whole cytosol was found to be positive for GFP complementation (Figure 6-5 VI). No cell was found where complemented GFP was localised to the Golgi apparatus. When FFR8-M3 was incubated with the cells, clear complementation of Golgi retained GRASP65-GFP1-10 with M3 was seen (Figure 6-5 IX).

This was an interesting finding which could indicate that, even though R8-M3 and FFR8-M3 both deliver the M3 peptide to the cytosol, the delivery vector however can influence cargo localisation and delivery to cytosolic targets of intracellular organelles.

However, more work has to been done to confirm these findings and elucidate if the delivery of the M3 peptide to the Golgi apparatus can be enhanced by attachment

of a Phenylalanine residues to R8-M3 and if this effect is specific to the Phenylalanine substitution.
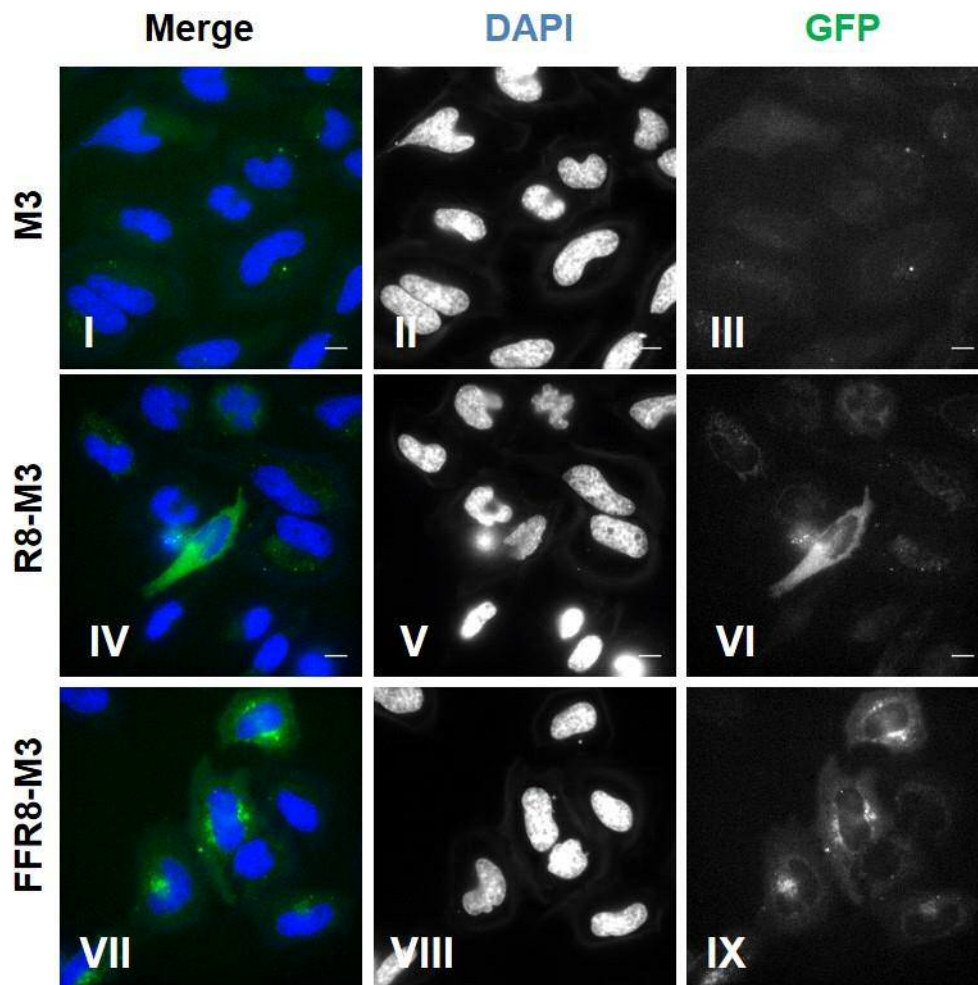
Figure 6-5 M3 delivery to the Golgi apparatus.
HeLa cells transiently expressing GRASP65-GFP1-10 were incubated with M3, R8-M3 or FFR8-M3 at 40 µM in serum free media for 2 hours at 37˚C. Cells were counterstained with Hoechst nuclear dye and kept in phenol red free RPMI for imaging. GFP fluorescence was detected using a widefield fluorescent microscope. Representative images show GFP complementation achieved by M3 delivery. Scale bar: 10µm.n=1.

6.4   Discussion

Cytosolic delivery of macromolecules bears the huge potential for these drugs to act at specific intracellular targets. Their high specificity has the potential to result in increased therapeutic efficacy and reduced toxicity (Panyam and Labhasetwar 2004). Hence, it is not only important to deliver the macromolecule to the cytosol of a cell but also ensure that it reaches its site of action within the cell. Intracellular targets include the cytosol to target kinases or other enzymes, apoptotic factors residing in the mitochondria or modulators of gene expression (e.g. transcription factors) within the nucleus (Panyam and Labhasetwar 2004; Mitragotri *et al.* 2014). For this reason drug delivery vectors are designed to not only overcome the plasma membrane barrier but to also enter intracellular organelles like the mitochondria or the nucleus (Jensen *et al.* 2003; Cardarelli *et al.* 2008; Horton *et al.* 2008; Horton *et al.* 2012; Cerrato *et al.* 2015).

For penetrating peptides it was shown that their intracellular localisation can be changed when altering amino acid residues or substitutions of additional amino acid residues. Modification with Phenylalanine residues is a popular choice to impart lipophilicity and to target conjugated CPPs for mitochondrial delivery. Targeting of penetrating peptides was monitored by conjugation with fluorophores like thiazole orange or 5(6)-carboxyfluorescein (Horton *et al.* 2008; Cerrato *et al.* 2015). These studies are important to characterise CPPs and shed light on their intracellular localisation. However, these utilise fluorophore conjugated peptides to visualize intracellular localisation. Conjugated fluorophores can alter uptake dynamics and could also have an effect on the intracellular localisation (Jones and Sayers 2012). Furthermore, these studies do not give information about cargo delivery, e.g. subcellular localisation of a delivered cargo and its activity once it has reached its site of action.

Split GFP enables us to investigate the localisation of the delivered M3 peptide and there is huge potential to investigate intra-organelle delivery by the expression of GFP1-10 inside an organelle to detect GFP complementation once M3 has reached the same location. This investigation would not necessarily require microscopy and flow cytometry measurement would be sufficient to detect green fluorescence of complemented GFP in order to determine if M3 had been delivered to the organelle.

However, in this chapter it was shown that even though the intracellular GFP1-10 target was expressed in the same localisation (cytosol), two different DDSs localised complemented GFP to different places inside the cell after delivery into the cytosol. When R8-M3 and Glycine added versions GR8-M3 or GGR8-M3 were utilised to deliver the M3 peptide, localisation of complemented GFP was found to be localised in the cytosol and the nucleolus. There was a clear separation of complemented GFP from the nucleus. When FR8-M3 or FFR8-M3 served as delivery vectors for the M3 peptide, complemented GFP was evenly localised throughout the cell. This important information would have been missed if GFP complementation had only been measured using flow cytometry.

Hence, using microscopic analysis of the split GFP assay developed within this project allows us to visualize the intracellular localisation of a peptide cargo delivered by DDSs once it has complemented with its intracellular GFP1-10 target.

Whether the preferential recruitment of R8-M3 into the cytosol or nucleus takes place before or after complementation with GFP1-10 remains unknown. GFP1-10 was generated as a cytosolic expression construct meaning it was not fused to a protein or a sequence that specifically targets GFP1-10 to a subcellular location within the cell. It was shown that transient expression of non-targeted EGFP in HeLa cells is located at in the cytosol as well as the nucleus. It reaches the nucleus via diffusion through the nuclear pore and it was shown that even a fusion proteins consisting of

four GFPs (110 kDa) can enter the nucleus through the nuclear pore (Wang and Brattain 2007). Hence, it is suggested that GFP1-10 that is expressed in the cytosol diffuses through the nuclear pore and is also present in the nucleus, therefore being present in both compartments. Nucleolar and cytosolic localisation of complemented GFP when R8-M3 is used as a drug delivery vector can thought to be achieved in different scenarios. Once R8-M3 crosses the plasma membrane it complements with cytosolic GFP1-10 which diffuses into the nucleus and localises to the nucleolus. R8-M3 could also diffuse into the nucleus and localise at the nucleolus where it complements with GFP1-10 already located in the nucleus through diffusion. It is also possible that a combination of both scenarios takes place in a live cell.

Independent of one or the other, one important question is: why does R8 localise to the nucleolus and the cytosol but not to the rest of the nucleus?

The nucleolus is the site of ribosomal biogenesis where the ribosomal RNA (rRNA) is generated which is the building block of ribosomes (Scheer and Hock 1999). Furthermore, it is known that RNA binding proteins are enriched with arginine residues (Bayer *et al.* 2005) and Arginine residues strongly interact with negatively charged phosphate groups of the RNA (Treger and Westhof 2001; Woods and Ferré 2005).

The laboratory of Christina Cardoso has first published in 2006 that FITC labelled Decaarginine (FITC-R10) can act as a nucleolar marker in living cells such as HeLa cells, mouse fibroblasts or rat cardiomyocytes (Martin *et al.* 2007). In 2016 their protocol to stain the nucleolus with FITC-R10 was published in the Springer series The Nucleus Methods and Protocols (Martin *et al.* 2016). Furthermore, they investigated the principle of protein targeting to the nucleolus (Martin *et al.* 2015). They identified that Polyarginines labelled with FITC (R6 – R12) localised to the nucleolus while Polylysines of the same length did not specifically localise to the

nucleolus but were distributed within the whole nucleus. It was found that the nucleolar environment is more acidic compared to the surrounding nucleoplasm providing an ideal environment to bind poly-arginine containing proteins. Hence, it is likely that interaction between highly positively charged Arginine residues and the nucleolus where negatively charged rRNA resides is via electrochemical interaction (Martin *et al.* 2015).

N-terminal addition of one or two Phenylalanine residues to R8-M3 can change the intracellular distribution of the delivered cargo peptide and its intracellular target GFP1-10 when they have reassembled to GFP. When Phenylalanine was attached to R8-M3, there was no separation of complemented GFP from the nucleus. Confocal analysis confirmed that it was distributed evenly throughout the cell.

Phenylalanine is a basic amino acid and is added to peptides to increase the lipophilicity. It has been reported to be associated with targeting mitochondrial membranes (Horton *et al.* 2008; Cerrato *et al.* 2015). The data in this chapter does not show specific localisation of complemented GFP to mitochondria, however it remains unknown if FFR8-M3 enters the mitochondrial membrane. It would be interesting to test this, in fact, there are GFP1-10 DNA constructs available that ensure GFP1-10 expression localised to the outer mitochondrial membrane (accessible in the cytosol) as well as GFP1-10 expression in the mitochondrial matrix where translocation of M3 into the mitochondria would be necessary (Cali *et al.* 2014).

Furthermore, GFP does not enter the mitochondria and these are seen as dark structures within cytosolic expressed GFP. Further experiments could investigate if these dark structures are still visible when R8-GFP or FFR8-GFP is expressed in the cytosol (both of which expression constructs are available in our lab).

The general increase in lipophilicity when Phenylalanine residues are attached to R8-M3 could enhance its interaction with intracellular membranes which could be

an explanation why FFR8-M3 complemented with GFP1-10 localised at the Golgi membrane.

This Chapter highlights the influence that a chosen DDS can have on subcellular localisation of the cargo peptide (and its target). This can be disadvantageous when the cargo-target complex needs to act in the cytosol but a large portion is located at the nucleolus. Microscopic analysis of the split GFP complementation will help to gain information about this and indicate whether intracellular cleavage mechanisms that separate the cargo from the DDS have to be incorporated. A popular tool to achieve this is the linkage of DDS and cargo via a disulfide bond that can be cleaved in the reducing environment of the cytosol (reviewed in (Saito *et al.* 2003)) and it was shown that gene silencing by delivered siRNA can be increased using this strategy (Kam *et al.* 2005; Breunig *et al.* 2008). Another strategy that has been utilised is the co-incubation of cell penetrating peptides with the cargo that also led to the uptake of the co-incubated cargo molecule (Lee *et al.* 2010; Pinaud and Dahan 2011).

However, targeting a cargo-target complex to a specific subcellular localisation also bears opportunities. R8 as a drug delivery system would be of interest if a peptide-target complex that assembled in the cytosol should be located to a specific subcellular localisation (e.g. nucleolus) to carry out their function. CPPs could then not only act as Trojan horses in order to guide cargo into the cytosol but also to locate cargo-target complex to a subcellular localisation.

In fact, this has very recently been achieved and published (Herce *et al.* 2017). In this publication nanobodies against GFP (13-14 kDa) were delivered by tetramethylrhodamine labelled cyclic R10 (cR10) into cell expressing full length GFP. When full length GFP is expressed in the cytosol it is not found at the nucleolus. However, the nanobody against GFP was able to bind to GFP upon cytosolic delivery by cR10 and was able to target it to the nucleolus. Utlising this strategy they have

further shown that the polymerase clamp PCNA (proliferating cell nuclear antigen) and tumour suppressor p53 were located to the nucleolus.

In summary, this data shows that microscopic analysis of GFP complementation by M3 delivery can add additional information about the localisation of complemented GFP. This is valuable information when characterising a drug delivery system and should be included in addition to flow cytometry measurements when analysing delivery efficiency of M3 peptides by DDSs using the split GFP system.

7 General Discussion

7.1 Summary of findings

In this thesis a method has been established to investigate cytosolic delivery of a functional peptide cargo to its intracellular target by different drug delivery systems. Peptides require drug delivery vectors for their intracellular delivery, hence, it is critical to be able to evaluate their ability to functionally deliver their peptide cargo to its intracellular target in order to select the most efficient drug delivery systems. Our method utilising the split GFP system allows us to investigate real time peptide delivery and to assess if the peptide cargo is still functional and whether it interacts with its intracellular target. Furthermore subcellular localisation of the peptide cargo and its target can be investigated using this method.

7.1.1 Development of the Split GFP complementation assay

Chapter 3 describes the development of the split GFP system in HeLa cells to investigate M3 peptide delivery to its intracellular GFP1-10 target by a drug delivery system. It was shown that the expression of the intracellular GFP1-10 target protein can be detected using immunofluorescence with an anti GFP antibody. Not every anti-GFP antibody was able to detect GFP1-10 expression, possibly due to their epitope specificity and the fact that GFP1-10 misses its 11th beta sheet from its structure. However, an anti GFP antibody has been identified that can prove that GFP1-10 is expressed in the cytosol of a target cell and this can be observed using immunofluorescent staining or western blot analysis.

Initial testing of split GFP complementation can be performed using co-expression of the DNA coding for the M3 peptide and GFP1-10 within the same cell. The GFP complementation can be monitored in fixed cells using a widefield fluorescent microscope or in live cells using a microplate reader.

Most importantly, a method has been developed that proves the *in vitro* complementation of GFP1-10 originated from cellular expression and M3 peptide conjugated to its drug delivery vector. By mixing cell lysate of cells expressing GFP1-10 and with DDS-M3 peptide, it was possible to show concentration dependent as well as time dependent complementation of the two fragments. This is a critical step because the *in vitro* complementation can give insight if conjugation of the DDS to the M3 peptide influences ability to complement with GFP1-10. Furthermore, when comparing two DDSs, the *in vitro* assays can give information if GFP complementation is impaired or enhanced *in vitro* which allows correlation to the data obtained from live experiments to define if delivery efficiency is more or less efficient compared to the other DDS.

7.1.2   The transient GFP1-10 expression system

It was shown that the developed techniques can be utilised to characterise the split GFP assay and allowed the successful development of a transient expression systems to determine delivery of M3 by a drug delivery system. Functional and cytosolic M3 delivery was shown to be achieved using the drug delivery vectors R8 as well as RhodamineR8 (Rh-R8).

Labelling of R8 with the fluorescent tag Rhodamine showed that uptake of the RhR8-M3 peptide is heterogeneous across the cell population. It was also demonstrated that functional delivery of M3 was not observed in every cell, even though cells had taken up similar amounts of RhR8-M3 peptide shown by the fluorescence of rhodamine. However, the attachment of rhodamine to R8-M3 not only labelled the peptide but also increased uptake into the cells. It has been reported that the attachment of fluorophores can to changed uptake dynamics of CPPs into the cell (Jones and Sayers 2012) and especially for rhodamine it was recently shown that it increases the hydrodynamic radius of the CPPs significantly enhances cellular uptake into cells (Hyrup Moller *et al.* 2015).

Hence, attachment of rhodamine did not give a detailed insight of how the unlabelled peptide R8-M3 enters the cell. However, it gave important detail about the heterogeneous uptake of peptide across the cell population and that a transient expression system was not sufficient in order to show drug delivery system specific effect on M3 delivery.

This highlighted the need to improve the split GFP method so that DDS specific effects can be seen on functional M3 delivery and the method is not dependent on intracellular expression levels of the GFP1-10 target protein. These findings led to the generation of two stable cell lines; one expressing GFP1-10 (SCL1) and a second cell line including the fluorescent expression marker mCherry to express mCherry-GFP1-10 (mCherry-SCL51).

7.1.3 Stable cell line SCL1

The stable cell line SCL1, expressing GFP1-10, has been fully characterised utilising the methods developed in order to characterise the split GFP system. This included the detection of GFP1-10 expression using immunofluorescence, expression of the DNA of the M3 fragment (H6-Xa-R8-M3) in SCL1 as well as *in vitro* complementation with M3 containing peptides. It was revealed that the cell line SCL1 expresses even amounts of GFP1-10 across the cell population that can complement with the M3 fragment when expressed in the cell or *in vitro* when incubated with synthetic M3 peptides.

Stable cell lines expressing GFP1-10 have been utilised by two other research groups who developed the split GFP method to determine functional delivery of the M3 peptide by DDSs (Milech *et al.* 2015; Lönn *et al.* 2016). These groups have only used flow cytometry as a detection method for GFP complementation. In our study we have utilised flow cytometry as well as microscopy. Utilising both techniques it was shown that the stable cell line SCL was more fluorescent than HeLa cells that did not express GFP1-10. This enhanced green fluorescence was examined by

spectral analysis of the emission spectrum and it is suggested that this fluorescence originates from autofluorescence of the cell as well as GFP fluorescence. This hypothesis was further confirmed when this enhanced green fluorescence was also detected in cells transiently expressing GFP1-10. Furthermore, this green fluorescence in stable cell lines was also described by (Milech *et al.* 2015) and was also attributed to the expression of GFP1-10.

Moreover, the morphology of SCL1 cells was changed compared to HeLa cells which was seen by flow cytometry analysis of the cell line. The cells were bigger and more granular compared to HeLa cells. The granularity can be influenced by the shape of the nucleus and it was found by Alexander Dudziak that the shape of the nuclei were changed in SCL1 cell compared to HeLa cell which would be an explanation for this finding. Importantly, no morphological changes to the actin or tubulin skeleton were detected which is critical when the delivery M3 by the CPP R8 is investigated that may deliver the M3 cargo by micropinocytosis which is dependent on the actin skeleton.

In summary, the SCL1 cell line can be utilised to investigate functional M3 delivery by DDSs. However, the high green fluorescent background in this cell line in combination with weak signal of GFP complementation (due to insufficient delivery) make it challenging to obtain a sufficient fluorescent signal on the microscope. Flow cytometry measurement is more representative of GFP complementation across the cell population. It would be a major improvement to the assay if a cell line could be obtained that emits less green fluorescence whilst maintaining sufficient expression levels of GFP1-10.

7.1.4   Stable cell line mCherry-SCL51

Introducing an expression marker for GFP1-10 expression improves the split GFP method, so that it can be visualised which cells are expressing the GFP1-10 target protein in their cytosol when transient expression is used. This approach has

also been utilised by Schmidt and his colleagues in order to investigate M3 delivery by the CPP R9. (Schmidt *et al.* 2015a). Utlising this technique using transient transfection will give insight if the M3 peptide has been delivered to the cytosol. Howerver, it has been previousely shown that uptake of CPPs is dependent on the peptide to cell ratio rather than the absolute peptide concentration (Hallbrink *et al*. 2004). As a results of transient expression of mCherry-GFP1-10, some cells will not express the mcherry-GFP1-10 target protein. This will result in a number of cells that are investigated in the split GFP assay and will take up peptide but they cannot give a readout about functional peptide delivery.

Hence, the generation of a stable cell line expressing mCherry-GFP1-10 was advantageous when investigating functional delivery of the M3 peptide. The generated stable cell line, mCherry-SCL51 was found to be a polyclonal cell line with 86% of the cells expressing mCherry-GFP1-10 which was confirmed by immunofluorescent staining to detect GFP1-10 expression. mCherry-SCL51 was further found to be able to complement with M3 by transfection of DNA coding for M3 or *in vitro* when mCherry-SCL51 cell lysate was used to complement with synthetic M3 containing peptides.

Cytosolic green fluorescence was also found to be increased in mCherry-SCL51 cells compared to HeLa cells, as seen in the SCL1 cell line. No spectral analysis of emitted green fluorescence was perfromed on this cell line. However, it is suggested that this green fluorescence is derived from GFP1-10 expression like it was shown for SCL1 cells.

In summary, it was shown that a stable cell line has been created expressing mCherry-GFP1-10 and this cell line can be utilised to determine M3 delivery by different DDS. Resulting GFP complementation can be monitored by flow cytometry as well as microscopy. The stable cell line can further be improved in order to obtain a clonal cell line where all cells expressing even amounts of mCherry-GFP1-10 across the cell population.

The expression marker mCherry that labels GFP1-10 expression also has the potential to allow us to obtain a quantitative readout of how much M3 peptide is delivered in the cytosol of target cells and correlate mCherry and GFP fluorescence.

7.1.5 Octaarginine and its performance as a peptide delivery vector

In this study octaarginine (R8) was utilised as a drug delivery vector to facilitate functionally delivery of the M3 peptide cargo. It was shown that R8-M3 enhances GFP fluorescence compared to L-M and M3 when incubated at 10-40 µM with SCL1 for 2 h. This demonstrated that R8 is able to act as a drug delivery vector to functionally deliver M3 peptide cargo which leads to GFP complementation and increase of GFP fluorescence compare to M3 peptides that are not conjugated to drug delivery systems. M3 delivery was shown to be significantly different ($p<0.001$) at 40 µM and M3 was delivered to 28% of the SCL1 cell population. When the split GFP assay was utilised by other research groups, functional delivery of M3 by arginine rich peptides like R9 and Tat was shown at concentrations between at 5-20 µM and 5-60 µM, respectively (Milech *et al.* 2015; Schmidt *et al.* 2015a; Lönn *et al.* 2016). The mode of uptake of R8-M3 through direct penetration or endocytosis followed by endosomal escape remains unknown and is subject to future studies.

In this study, we have also shown that M3 delivery by R8 can be enhanced by the N-terminal addition of two Phenylalanine residues. M3 delivery using FFR8-M3 was significantly enhanced compared to R8-M3 at concentrations of 30 µM and 40 µM ($p<0.001$). Addition of two Glycine residues (GGR8-M3) did not result in enhanced M3 delivery, nor did the addition of one Phenylalanine residue (FR8-M3).

Moreover, it was found that an addition of Phenylalanine residues to R8-M3 not only enhanced the functional delivery of the M3 peptide but also influenced the localisation of complemented GFP in the cytosol. When M3 was delivered using 40 µM R8-M3, complemented GFP was localised in the cytosol as well as located at the

nucleolus. The addition of one or two Phenylalanine residues to R8-M3 resulted in an even distribution of complemented GFP thought the cell. This effect was also specific to Phenylalanine residues and was not seen for the addition of one or two Glycine residues.

Other research groups have also demonstrated enhanced uptake of M3 by modified CPPs to increase intracellular stability or enhance endosomal escape (Schmidt *et al.* 2015a; Lönn *et al.* 2016). However, the influence of the CPP or modified CPP on the intracellular localisation of the cargo has not been shown before utilising GFP. The importance of this effect and the chances of targeted re-localisation of intracellular protein to compartments (e.g. the nucleolus) has recently been demonstrated (Herce *et al.* 2017) and is of high importance when characterising DDSs.

Importantly, in this study compared to other split GFP systems that have been developed, it is shown that functional M3 delivery can be captured in real time using a widefield fluorescent microscope and functional delivery and GFP complementation was seen to be as fast as 5 minutes. Visualisation of real time delivery using a microscope can give important information about M3 peptide delivery and allows us to investigate live dynamics of functional M3 delivery within the same cell over time which is not possible using flow cytometry.

Key to a perfect DDS is the ability to efficiently deliver cargo with minimal cytotoxicity. Much effort has been put into identifying new CPPs or modify existing CPPs so that a maximal delivery of cargo is achieved with decreased cytotoxicity (Lönn *et al.* 2016; Schmidt *et al.* 2017). In this study, the cytotoxicity or the effect on membrane integrity of R8-M3 or Phenylalanine or Glycine modified versions of R8-M3 has not been investigated. This data will be critical in order to characterise these

DDSs and their ability to functionally deliver cargo into <u>live</u> cells and will be investigated in the future.

7.1.6 Limitations of the Split GFP system

The developed methods and resources are an important advance in order to investigate functional M3 peptide delivery by novel DDSs and assess their ability to functionally deliver peptide cargo. However, this method can further be improved. Complemented GFP fluorescence was only weak to be detected on the microscope. This is likely to be due to insufficient delivery of the M3 peptide to the cytosol. The weak green fluorescence could also be due to limited GFP1-10 expression in the cytosol of the stable cell line. However, when concentration dependent delivery of the M3 peptide by different CPPs was investigated no saturation of complemented GFP1-10 was seen. If the weak fluorescence is due to insufficient delivery of the M3 peptide to the cytosol it would be advantageous to increase the sensitivity of this method by an intracellular enhancing cascade resulting in increased fluorescence.

Kim and colleagues have introduced an enhanced split GFP system (Kim *et al.* 2015). In their method, the short M3 fragment was delivered by a penetrating antibody to cells expressing GFP1-10 in order to prove the cytosolic delivery of the antibody. They utilised an enhanced split GFP system where GFP1-10 is expressed as a fusion to streptavidin (SA) which naturally forms tetramers connecting GFP1-10 in the cell. The penetrating antibody-M3 peptide complex was fused to an SBP2 peptide. One tetramer of streptavidin bind two molecules of SBP2 peptide which leads to enhanced GFP complementation through SBP2-SA interaction. In their publication they state that it was possible to measure GFP fluorescence in a 96 well format on a spectrofluorometer which suggests high fluorescent signal of complemented GFP in these cells (which could be due to the enhanced split GFP assay or the great penetrating ability of the antibody utilised in this study).

It is also known that the size of a cargo attached to DDS like CPPs changes the mode of uptake into the cell (Maiolo *et al.* 2005; Tunnemann *et al.* 2006). Using the split GFP system it is possible to investigate the functional delivery of a peptide cargo of the size of 1.8 kDa. However, once a DDS is selected to functionally delivery peptides, the conjugation of a different peptide cargo could lead to unpredicted change in delivery of that cargo to its intracellular target.

7.2   Future directions

7.2.1   Use of split GFP assay to determine peptide delivery into organelles

The use of the split GFP assay to investigate functional delivery of the M3 peptide has the great potential to be utilised to not only characterise DDSs and their ability to delivery functional cargo into the cytosol, but also determine the ability to functionally deliver the peptide into organelles. Recently Split GFP has developed into a popular tool, not only regarding DDS characterisation but also to determine orientation or localisation of proteins (Cali *et al.* 2014; Hyun *et al.* 2015). Thus a range of subcellular split GFP expression constructs have been generated and published (Cali *et al.* 2014; Hyun *et al.* 2015). Utilising split GFP in a co-expression study with an endoplasmatic reticulum (ER) based membrane protein it was shown that the orientation of the membrane protein can be determined by co-expression with cytosolic GFP1-10 or luminal GFP1-10 (Hyun *et al.* 2015). Luminal localisation of GFP1-10 was ensured by attachment of an ER retention sequence. Furthermore, GFP1-10 can be expressed at the outer membrane of mitochondria (cytosolic access) and the mitochondrial matrix (Cali *et al.* 2014). It would be interesting to investigate M3 peptide delivery to these organelles using novel drug delivery vectors and this would open up new possibilities for macromolecular therapeutics to not only gain access to cytosolic targets but to targets located in specific organelles which could help to cure disease with even higher specificity and less side effects.

7.2.2 Colour variants

GFP is a fluorescent protein that can easily be genetically manipulated to exhibit changed excitation and emission characteristics. Point mutations in the fluorophore allows us to utilise it as a yellow (T203Y) or cyan (Y66W) fluorescent probe named YFP (yellow fluorescent protein) and CFP (cyan fluorescent protein), respectively (Heim *et al.* 1994; Heim and Tsien 1996; Ormo *et al.* 1996). All mutations that result in a shift of fluorescence spectra are located within the amino acid sequence of the GFP1-10 fragment. Hence it has been possible to introduce these mutations to obtain YFP1-10 and CFP1-10 (Kamiyama *et al.* 2016). This has great potential because the same M3 peptide (GFP11) can rescue the fluorescence of GFP1-10, YFP1-10 or CFP1-10. This opens up new opportunities in the field of drug delivery. Different colour variants could be expressed in different subcellular localisation within the same cell and functional delivery to a certain position would be indicated by which colour fluorescence is rescued.

In addition to that another split fluorescent colour variant is available: split Cherry (sfCherry1-10). mCherry has a different precursor than GFP and is derived from a tetrameric protein found in reef corals, DsRed (Matz *et al.* 1999). In a stepwise process a monomeric protein was created and a range of red colour fluorescent variants were developed by mutation of critical residues. mCherry has excitation/emission peaks at 587nm/610nm wavelength (Campbell *et al.* 2002; Shaner *et al.* 2004) and the development of super-folder Cherry (sfCherry) has led to creation of split mCherry. sfCherry1-10 requires a different small peptide fragment compared to the M3 peptide that rescues its fluorescence and is called sfCherry11. Its fluorescence is not yet rescued as efficiently as seen for split GFP but once this issue is overcome, a second split peptide cargo is available to test functional delivery of peptides into cells.

7.2.3 Split GFP as a high throughput imaging technique

The split GFP as a microscopy based technique has the potential to be utilised as a fully automated high throughput screening platform to determine novel DDSs to functionally deliver peptide cargo into cells. In order to pursue this goal sensitivity issued have to be overcome. Thus far, the split GFP system developed in this thesis lacks brightness so that imaging in a 96 well format at low magnification is challenging. However, the lack of brightness could also be attributed to poor delivery of the M3 peptide into the cytosol and therefore GFP fluorescence is low. In order to utilise the split GFP system as a high throughput imaging technique it is probably necessary to improve both, the efficiency of M3 delivery by vectors and a cell line that expresses maximal amounts of GFP1-10 in the cytosol. Multiple stable cell lines expressing GFP1-10 have been generated by different research groups investigating M3 delivery by DDSs (Milech *et al.* 2015; Schmidt *et al.* 2015b; Lönn *et al.* 2016). It would be interesting to compare the delivery of M3 by the same DDS utilising those different cell lines to gain information if there is a cell line available that is more promising to be utilised on a high throughput imaging platform.

7.2.4 Delivery into organoids and animal models

In this thesis, the split GFP complementation was developed using a two dimensional (2-D) tissue culture model in the cell line HeLa. Other groups have used different cell types to investigate M3 delivery to cells expressing GFP1-10, however, all of them were adherent 2-D cell models (Milech *et al.* 2015; Schmidt *et al.* 2015b; Lönn *et al.* 2016). The choice of a 2-D cell model was the best choice to develop the split GFP complementation assay because 2-D cell models like HeLa cells are well characterised and more importantly, easy to genetically modify their protein expression using transfection. However peptide drugs are designed to be administered in humans where cells grow in 3 dimensional structures. Hence, a better description of the cell barrier that a DDS with its peptide cargo has to overcome are

three dimensional (3-D) cell models like spheroids or organoids (reviewed in (Breslin and O'Driscoll 2013) (Fatehullah *et al.* 2016)). These cell models would have been challenging to develop the split GFP complementation assay because they can be hard to transfect and the cell models themselves are still being characterised. Nevertheless, it should be pursued to integrate the split GFP complementation assay into spheroid models and ultimately in organoid models. In the future, the split GFP system could even be utilised to investigate tissue specific delivery in a genetically modified mouse model.

7.3 Concluding remarks

An increased understanding of functional delivery of macromolecules such as peptides and their access to their intracellular targets is important and comes with the great opportunity to develop biopharmaceutical drugs with increased specificity and reduced side effects. In order ensure intracellular peptide delivery novel drug delivery vectors are needed. The successful development of novel drug delivery vectors relies on a technique that allows us to assess their ability to deliver functional peptide cargo to their intracellular targets.

Within this project, a method based on split GFP complementation has been developed that allows us to evaluate drug delivery vectors regarding their ability to functionally deliver peptide cargo into the cytosol. In this thesis it is highlighted that microscopy analysis can give insight as to when peptide cargo is delivered to its target as well as where it is delivered to. This adds valuable information to the characterisation of novel DDSs and has not been shown before by other groups utilising this assay to characterise peptide delivery vectors. Hence, the split GFP complementation system presented in this study is a great method to characterise DDSs regarding their ability to functionally deliver M3 peptide cargo and gives insight as to if, when and where peptide cargo is delivered to.

8   References

Akishiba, M., Takeuchi, T., Kawaguchi, Y., Sakamoto, K., Yu, H. H., Nakase, I., Takatani-Nakase, T. *et al.* (2017). Cytosolic antibody delivery by lipid-sensitive endosomolytic peptide. *Nat Chem* **9:**751-761.

Arthanari, Y., Pluen, A., Rajendran, R., Aojula, H. and Demonacos, C. (2010). Delivery of therapeutic shRNA and siRNA by Tat fusion peptide targeting BCR-ABL fusion gene in Chronic Myeloid Leukemia cells. *J Control Release* **145:**272-280.

Atilla-Gokcumen, G. E., Muro, E., Relat-Goberna, J., Sasse, S., Bedigian, A., Coughlin, M. L., Garcia-Manyes, S. *et al.* (2014). Dividing cells regulate their lipid composition and localization. *Cell* **156:**428-439.

Aubin, J. E. (1979). Autofluorescence of viable cultured mammalian cells. *J Histochem Cytochem* **27:**36-43.

Bayer, T. S., Booth, L. N., Knudsen, S. M. and Ellington, A. D. (2005). Arginine-rich motifs present multiple interfaces for specific binding by RNA. *RNA* **11:**1848-1857.

Bednarkiewicz, A., Rodrigues, R. M. and Whelan, M. P. (2011). Non-invasive monitoring of cytotoxicity based on kinetic changes of cellular autofluorescence. *Toxicol In Vitro* **25:**2088-2094.

Benson, R. C., Meyer, R. A., Zaruba, M. E. and McKhann, G. M. (1979). Cellular autofluorescence--is it due to flavins? *J Histochem Cytochem* **27:**44-48.

Brejc, K., Sixma, T. K., Kitts, P. A., Kain, S. R., Tsien, R. Y., Ormö, M. and Remington, S. J. (1997). Structural basis for dual excitation and photoisomerization of the Aequorea victoria green fluorescent protein. *Proc Natl Acad Sci U S A* **94:**2306-2311.

Breslin, S. and O'Driscoll, L. (2013). Three-dimensional cell culture: the missing link in drug discovery. *Drug Discov Today* **18:**240-249.

Breunig, M., Hozsa, C., Lungwitz, U., Watanabe, K., Umeda, I., Kato, H. and Goepferich, A. (2008). Mechanistic investigation of poly(ethylene imine)-based siRNA delivery: disulfide bonds boost intracellular release of the cargo. *J Control Release* **130:**57-63.

Burlina, F., Sagan, S., Bolbach, G. and Chassaing, G. (2005). Quantification of the cellular uptake of cell-penetrating peptides by MALDI-TOF mass spectrometry. *Angew Chem Int Ed Engl* **44:**4244-4247.

Cabantous, S., Terwilliger, T. C. and Waldo, G. S. (2005). Protein tagging and detection with engineered self-assembling fragments of green fluorescent protein. *Nat Biotechnol* **23:**102-107.

Cabantous, S. and Waldo, G. S. (2006). In vivo and in vitro protein solubility assays using split GFP. *Nat Methods* **3:**845-854.

Cali, T., Ottolini, D., Soriano, M. E. and Brini, M. (2014). A new split-GFP-based probe reveals DJ-1 translocation into the mitochondrial matrix to sustain ATP synthesis upon nutrient deprivation. *Hum Mol Genet*.

Campbell, R. E., Tour, O., Palmer, A. E., Steinbach, P. A., Baird, G. S., Zacharias, D. A. and Tsien, R. Y. (2002). A monomeric red fluorescent protein. *Proc Natl Acad Sci U S A* **99:**7877-7882.

Cardarelli, F., Serresi, M., Bizzarri, R. and Beltram, F. (2008). Tuning the transport properties of HIV-1 Tat arginine-rich motif in living cells. *Traffic* **9:**528-539.

Cerrato, C. P., Pirisinu, M., Vlachos, E. N. and Langel, Ü. (2015). Novel cell-penetrating peptide targeting mitochondria. *FASEB J* **29:**4589-4599.

Chalfie, M., Tu, Y., Euskirchen, G., Ward, W. W. and Prasher, D. C. (1994). Green fluorescent protein as a marker for gene expression. *Science* **263:**802-805.

Chang, X., Keller, D., Bjorn, S., Led, J.J. (2001). Structure and folding of glucagon like peptide 1 (7–36) amide in aqueous trifluoroethanol studied by NMR spectroscopy. *Magnetic Resonance in Chemistry* **39:**477-483.

Chudakov, D. M., Matz, M. V., Lukyanov, S. and Lukyanov, K. A. (2010). Fluorescent proteins and their applications in imaging living cells and tissues. *Physiol Rev* **90:**1103-1163.

Chudakov, D. M., Verkhusha, V. V., Staroverov, D. B., Souslova, E. A., Lukyanov, S. and Lukyanov, K. A. (2004). Photoswitchable cyan fluorescent protein for protein tracking. *Nat Biotechnol* **22:**1435-1439.

Cody, C. W., Prasher, D. C., Westler, W. M., Prendergast, F. G. and Ward, W. W. (1993). Chemical structure of the hexapeptide chromophore of the Aequorea green-fluorescent protein. *Biochemistry* **32:**1212-1218.

Conrad, P. A., Smart, E. J., Ying, Y. S., Anderson, R. G. and Bloom, G. S. (1995). Caveolin cycles between plasma membrane caveolae and the Golgi complex by microtubule-dependent and microtubule-independent steps. *J Cell Biol* **131:**1421-1433.

Copolovici, D. M., Langel, K., Eriste, E. and Langel, Ü. (2014). Cell-Penetrating Peptides: Design, Synthesis, and Applications.

Cormack, B. P., Valdivia, R. H. and Falkow, S. (1996). FACS-optimized mutants of the green fluorescent protein (GFP). *Gene* **173:**33-38.

Crameri, A., Whitehorn, E. A., Tate, E. and Stemmer, W. P. (1996). Improved green fluorescent protein by molecular evolution using DNA shuffling. *Nat Biotechnol* **14:**315-319.

D'Astolfo, D. S., Pagliero, R. J., Pras, A., Karthaus, W. R., Clevers, H., Prasad, V., Lebbink, R. J. *et al.* (2015). Efficient intracellular delivery of native proteins. *Cell* **161:**674-690.

Dautry-Varsat, A., Ciechanover, A. and Lodish, H. F. (1983). pH and the recycling of transferrin during receptor-mediated endocytosis. *Proc Natl Acad Sci U S A* **80:**2258-2262.

Davenport, D. and Nicol, J. A. C. (1955). Luminescence in Hydromedusae. *Proceedings of the Royal Society Series B-Biological Sciences* **144:**399-411.

Derek S. Youngblood, Susie A. Hatlevig, Jed N. Hassinger, Patrick L. Iversen, a. and Moulton*, H. M. (2006). Stability of Cell-Penetrating Peptide−Morpholino Oligomer Conjugates in Human Serum and in Cells.

Derossi, D., Joliot, A. H., Chassaing, G. and Prochiantz, A. (1994). The third helix of the Antennapedia homeodomain translocates through biological membranes. *J Biol Chem* **269:**10444-10450.

Devi, G. R. (2006). siRNA-based approaches in cancer therapy. *Cancer Gene Ther* **13:**819-829.

Doak, B. C., Zheng, J., Dobritzsch, D. and Kihlberg, J. (2016). How Beyond Rule of 5 Drugs and Clinical Candidates Bind to Their Targets. *J Med Chem* **59:**2312-2327.

Doherty, G. J. and McMahon, H. T. (2009). Mechanisms of endocytosis. *Annu Rev Biochem* **78:**857-902.

Doig Alfred, E. D., Ransohoff Thomas. (2015). Monoclonal Antibody Targets and Indications. *American Pharmaceutical Review*.

Dom, G., Shaw-Jackson, C., Matis, C., Bouffioux, O., Picard, J. J., Prochiantz, A., Mingeot-Leclercq, M. P. *et al.* (2003). Cellular uptake of Antennapedia Penetratin peptides is a two-step process in which phase transfer precedes a tryptophan-dependent translocation. *Nucleic Acids Res* **31:**556-561.

Duchardt, F., Fotin-Mleczek, M., Schwarz, H., Fischer, R. and Brock, R. (2007). A comprehensive model for the cellular uptake of cationic cell-penetrating peptides. *Traffic* **8:**848-866.

El-Sayed, A., Futaki, S. and Harashima, H. (2009). Delivery of macromolecules using arginine-rich cell-penetrating peptides: ways to overcome endosomal entrapment. *AAPS J* **11:**13-22.

Erazo-Oliveras, A., Muthukrishnan, N., Baker, R., Wang, T. Y. and Pellois, J. P. (2012). Improving the endosomal escape of cell-penetrating peptides and their cargos: strategies and challenges. *Pharmaceuticals (Basel)* **5:**1177-1209.

Erazo-Oliveras, A., Najjar, K., La Dayani, L., Wang, T. Y., Johnson, G. A. and Pellois, J. P. (2014). Protein delivery into live cells by incubation with an endosomolytic agent. *Nature Methods* **11:**861-867.

Fatehullah, A., Tan, S. H. and Barker, N. (2016). Organoids as an in vitro model of human development and disease. *Nat Cell Biol* **18:**246-254.

Fawell, S., Seery, J., Daikh, Y., Moore, C., Chen, L. L., Pepinsky, B. and Barsoum, J. (1994). Tat-mediated delivery of heterologous proteins into cells. *Proc Natl Acad Sci U S A* **91:**664-668.

Foged, C. and Nielsen, H. M. (2008). Cell-penetrating peptides for drug delivery across membrane barriers. *Expert Opin Drug Deliv* **5:**105-117.

Fretz, M. M., Penning, N. A., Al-Taei, S., Futaki, S., Takeuchi, T., Nakase, I., Storm, G. *et al.* (2007). Temperature-, concentration- and cholesterol-dependent translocation of L- and D-octa-arginine across the plasma and nuclear membrane of CD34+ leukaemia cells. *Biochem J* **403:**335-342.

Futaki, S., Goto, S. and Sugiura, Y. (2003). Membrane permeability commonly shared among arginine-rich peptides. *J Mol Recognit* **16:**260-264.

Ghosh, I., Hamilton, A. D. and Regan, L. (2000). Antiparallel leucine zipper-directed protein reassembly: Application to the green fluorescent protein. *Journal of the American Chemical Society* **122:**5658-5659.

Goldberg, A. L. (2003). Protein degradation and protection against misfolded or damaged proteins. *Nature* **426:**895-899.

Gruenberg, J., Griffiths, G. and Howell, K. E. (1989). Characterization of the early endosome and putative endocytic carrier vesicles in vivo and with an assay of vesicle fusion in vitro. *J Cell Biol* **108:**1301-1316.

Gustafson, W. C., Taylor, C. W., Valdez, B. C., Henning, D., Phippard, A., Ren, Y., Busch, H. *et al.* (1998). Nucleolar protein p120 contains an arginine-rich domain that binds to ribosomal RNA. *Biochem J* **331 (Pt 2):**387-393.

Gutknecht, J. and Tosteson, D. C. (1973). Diffusion of weak acids across lipid bilayer membranes: effects of chemical reactions in the unstirred layers. *Science* **182:**1258-1261.

Hallbrink, M., Oehlke, J., Papsdorf, G. and Bienert, M. (2004). Uptake of cell-penetrating peptides is dependent on peptide-to-cell ratio rather than on peptide concentration. *Biochimica Et Biophysica Acta-Biomembranes* **1667:**222-228.

Harris, L. J., Larson, S. B., Hasel, K. W. and McPherson, A. (1997). Refined structure of an intact IgG2a monoclonal antibody. *Biochemistry* **36:**1581-1597.

Hassane, F. S., Abes, R., El Andaloussi, S., Lehto, T., Sillard, R., Langel, U. and Lebleu, B. (2011). Insights into the cellular trafficking of splice redirecting oligonucleotides complexed with chemically modified cell-penetrating peptides. *J Control Release* **153:**163-172.

Heim, R., Cubitt, A. B. and Tsien, R. Y. (1995). Improved green fluorescence. *Nature* **373:**663-664.

Heim, R., Prasher, D. C. and Tsien, R. Y. (1994). Wavelength mutations and posttranslational autoxidation of green fluorescent protein. *Proc Natl Acad Sci U S A* **91:**12501-12504.

Heim, R. and Tsien, R. Y. (1996). Engineering green fluorescent protein for improved brightness, longer wavelengths and fluorescence resonance energy transfer. *Curr Biol* **6:**178-182.

Herce, H. D., Schumacher, D., Schneider, A. F. L., Ludwig, A. K., Mann, F. A., Fillies, M., Kasper, M. A. *et al.* (2017). Cell-permeable nanobodies for targeted immunolabelling and antigen manipulation in living cells. *Nat Chem* **9:**762-771.

Hopkins, A. L. and Groom, C. R. (2002). The druggable genome. *Nat Rev Drug Discov* **1:**727-730.

Hopkins, C. R., Miller, K. and Beardmore, J. M. (1985). Receptor-mediated endocytosis of transferrin and epidermal growth factor receptors: a comparison of constitutive and ligand-induced uptake. *J Cell Sci Suppl* **3:**173-186.

Horton, K. L., Pereira, M. P., Stewart, K. M., Fonseca, S. B. and Kelley, S. O. (2012). Tuning the activity of mitochondria-penetrating peptides for delivery or disruption. *Chembiochem* **13:**476-485.

Horton, K. L., Stewart, K. M., Fonseca, S. B., Guo, Q. and Kelley, S. O. (2008). Mitochondria-penetrating peptides. *Chem Biol* **15:**375-382.

Hu, C. D., Chinenov, Y. and Kerppola, T. K. (2002). Visualization of interactions among bZIP and Rel family proteins in living cells using bimolecular fluorescence complementation. *Mol Cell* **9:**789-798.

Hu, C. D. and Kerppola, T. K. (2003). Simultaneous visualization of multiple protein interactions in living cells using multicolor fluorescence complementation analysis. *Nat Biotechnol* **21:**539-545.

Huotari, J. and Helenius, A. (2011). Endosome maturation. *EMBO J* **30:**3481-3500.

Hyrup Moller, L., Bahnsen, J. S., Nielsen, H. M., Ostergaard, J., Sturup, S. and Gammelgaard, B. (2015). Selenium as an alternative peptide label - comparison to fluorophore-labelled penetratin. *Eur J Pharm Sci* **67:**76-84.

Hyun, S. I., Maruri-Avidal, L. and Moss, B. (2015). Topology of Endoplasmic Reticulum-Associated Cellular and Viral Proteins Determined with Split-GFP. *Traffic* **16:**787-795.

Ikuhiko Nakase, §, Akiko Tadokoro, ∥, Noriko Kawabata, Toshihide Takeuchi, Hironori Katoh, Kiyo Hiramoto, Manabu Negishi *et al.* (2006). Interaction of Arginine-Rich Peptides with Membrane-Associated Proteoglycans Is Crucial for Induction of Actin Organization and Macropinocytosis†.

Jensen, K. D., Nori, A., Tijerina, M., Kopeckova, P. and Kopecek, J. (2003). Cytoplasmic delivery and nuclear targeting of synthetic macromolecules. *J Control Release* **87:**89-105.

Jones, A. T. (2007). Macropinocytosis: searching for an endocytic identity and role in the uptake of cell penetrating peptides. *J Cell Mol Med* **11:**670-684.

Jones, A. T. and Sayers, E. J. (2012). Cell entry of cell penetrating peptides: tales of tails wagging dogs. *J Control Release* **161:**582-591.

Kam, N. W., Liu, Z. and Dai, H. (2005). Functionalization of carbon nanotubes via cleavable disulfide bonds for efficient intracellular delivery of siRNA and potent gene silencing. *J Am Chem Soc* **127:**12492-12493.

Kamiyama, D., Sekine, S., Barsi-Rhyne, B., Hu, J., Chen, B., Gilbert, L. A., Ishikawa, H. *et al.* (2016). Versatile protein tagging in cells with split fluorescent protein. *Nat Commun* **7:**11046.

Kaplan, I. M., Wadia, J. S. and Dowdy, S. F. (2005). Cationic TAT peptide transduction domain enters cells by macropinocytosis. *J Control Release* **102:**247-253.

Kaspar, A. A. and Reichert, J. M. (2013). Future directions for peptide therapeutics development. *Drug Discov Today* **18:**807-817.

Kawaguchi, Y., Takeuchi, T., Kuwata, K., Chiba, J., Hatanaka, Y., Nakase, I. and Futaki, S. (2016). Syndecan-4 Is a Receptor for Clathrin-Mediated Endocytosis of Arginine-Rich Cell-Penetrating Peptides. *Bioconjug Chem* **27:**1119-1130.

Kent, K. P., Childs, W. and Boxer, S. G. (2008). Deconstructing green fluorescent protein. *J Am Chem Soc* **130:**9664-9665.

Kim, J. S., Choi, D. K., Park, S. W., Shin, S. M., Bae, J., Kim, D. M., Yoo, T. H. *et al.* (2015). Quantitative assessment of cellular uptake and cytosolic access of antibody in living cells by an enhanced split GFP complementation assay. *Biochem Biophys Res Commun* **467:**771-777.

Kim, S. H., Mok, H., Jeong, J. H., Kim, S. W. and Park, T. G. (2006). Comparative evaluation of target-specific GFP gene silencing efficiencies for antisense ODN, synthetic siRNA, and siRNA plasmid complexed with PEI-PEG-FOL conjugate. *Bioconjug Chem* **17:**241-244.

Kola, I. and Landis, J. (2004). Can the pharmaceutical industry reduce attrition rates? *Nature Reviews Drug Discovery* **3:**711-716.

Koren, E. and Torchilin, V. P. (2012). Cell-penetrating peptides: breaking through to the other side. *Trends Mol Med* **18:**385-393.

Kosuge, M., Takeuchi, T., Nakase, I., Jones, A. T. and Futaki, S. (2008). Cellular Internalization and Distribution of Arginine-Rich Peptides as a Function of Extracellular Peptide Concentration, Serum, and Plasma Membrane Associated Proteoglycans.

Ladner, R. C., Sato, A. K., Gorzelany, J. and de Souza, M. (2004). Phage display-derived peptides as therapeutic alternatives to antibodies. *Drug Discov Today* **9:**525-529.

Lane, J. D., Lucocq, J., Pryde, J., Barr, F. A., Woodman, P. G., Allan, V. J. and Lowe, M. (2002). Caspase-mediated cleavage of the stacking protein GRASP65 is required for Golgi fragmentation during apoptosis. *J Cell Biol* **156:**495-509.

Layek, B., Lipp, L. and Singh, J. (2015). Cell Penetrating Peptide Conjugated Chitosan for Enhanced Delivery of Nucleic Acid. *Int J Mol Sci* **16:**28912-28930.

Lazo, J. S. and Sharlow, E. R. (2016). Drugging Undruggable Molecular Cancer Targets. *Annu Rev Pharmacol Toxicol* **56:**23-40.

Lee, Y. J., Erazo-Oliveras, A. and Pellois, J. P. (2010). Delivery of macromolecules into live cells by simple co-incubation with a peptide. *Chembiochem* **11:**325-330.

Leeson, P. (2012). Drug discovery: Chemical beauty contest. *Nature* **481:**455-456.

Lewis, W. (1931). Pinocytosis. Johns Hopkins Hosp . Johns Hopkins Hosp . pp. 17–27.

Li, L., Vorobyov, I. and Allen, T. W. (2013). The different interactions of lysine and arginine side chains with lipid membranes. *J Phys Chem B* **117:**11906-11920.

Lipinski, C. A., Lombardo, F., Dominy, B. W. and Feeney, P. J. (1997). Experimental and computational approaches to estimate solubility and permeability in drug discovery and development settings. *Adv Drug Deliv Rev* **46:**3-26.

Lobato, M. N. and Rabbitts, T. H. (2003). Intracellular antibodies and challenges facing their use as therapeutic agents. *Trends Mol Med* **9:**390-396.

Lundberg, M. and Johansson, M. (2002). Positively charged DNA-binding proteins cause apparent cell membrane translocation. *Biochem Biophys Res Commun* **291:**367-371.

Lundberg, M., Wikström, S. and Johansson, M. (2003). Cell surface adherence and endocytosis of protein transduction domains. *Mol Ther* **8:**143-150.

Lundin, K. E., Gissberg, O. and Smith, C. I. (2015). Oligonucleotide Therapies: The Past and the Present. *Hum Gene Ther* **26:**475-485.

Lönn, P., Kacsinta, A. D., Cui, X.-S., Hamil, A. S., Kaulich, M., Gogoi, K. and Dowdy, S. F. (2016). Enhancing Endosomal Escape for Intracellular Delivery of Macromolecular Biologic Therapeutics. *Scientific Reports* **6**.

Madani, F., Lindberg, S., Langel, U., Futaki, S. and Graslund, A. (2011). Mechanisms of cellular uptake of cell-penetrating peptides. *J Biophys* **2011:**414729.

Maiolo, J. R., Ferrer, M. and Ottinger, E. A. (2005). Effects of cargo molecules on the cellular uptake of arginine-rich cell-penetrating peptides. *Biochim Biophys Acta* **1712:**161-172.

Martin, R. M., Herce, H. D., Ludwig, A. K. and Cardoso, M. C. (2016). Visualization of the Nucleolus in Living Cells with Cell-Penetrating Fluorescent Peptides. *Methods Mol Biol* **1455:**71-82.

Martin, R. M., Ter-Avetisyan, G., Herce, H. D., Ludwig, A. K., Lättig-Tünnemann, G. and Cardoso, M. C. (2015). Principles of protein targeting to the nucleolus. *Nucleus* **6:**314-325.

Martin, R. M., Tunnemann, G., Leonhardt, H. and Cardoso, M. C. (2007). Nucleolar marker for living cells. *Histochem Cell Biol* **127:**243-251.

Matz, M. V., Fradkov, A. F., Labas, Y. A., Savitsky, A. P., Zaraisky, A. G., Markelov, M. L. and Lukyanov, S. A. (1999). Fluorescent proteins from nonbioluminescent Anthozoa species. *Nature Biotechnology* **17:**969-973.

Maxfield, F. R. and Yamashiro, D. J. (1987). Endosome acidification and the pathways of receptor-mediated endocytosis. *Adv Exp Med Biol* **225:**189-198.

McFedries, A., Schwaid, A. and Saghatelian, A. (2013). Methods for the elucidation of protein-small molecule interactions. *Chem Biol* **20:**667-673.

McGregor, D. P. (2008). Discovering and improving novel peptide therapeutics. *Curr Opin Pharmacol* **8:**616-619.

Meerovich, I., Muthukrishnan, N., Johnson, G. A., Erazo-Oliveras, A. and Pellois, J. P. (2014). Photodamage of lipid bilayers by irradiation of a fluorescently labeled cell-penetrating peptide. *Biochimica Et Biophysica Acta-General Subjects* **1840:**507-515.

Michaelson, D. and Philips, M. (2006). The use of GFP to localize Rho GTPases in living cells. *Methods Enzymol* **406:**296-315.

Milech, N., Longville, B. A., Cunningham, P. T., Scobie, M. N., Bogdawa, H. M., Winslow, S., Anastasas, M. *et al.* (2015). GFP-complementation assay to detect functional CPP and protein delivery into living cells. *Sci Rep* **5:**18329.

Mitchell, D. J., Kim, D. T., Steinman, L., Fathman, C. G. and Rothbard, J. B. (2000). Polyarginine enters cells more efficiently than other polycationic homopolymers. *J Pept Res* **56:**318-325.

Mitragotri, S., Burke, P. A. and Langer, R. (2014). Overcoming the challenges in administering biopharmaceuticals: formulation and delivery strategies. *Nat Rev Drug Discov* **13:**655-672.

Motley, A., Bright, N. A., Seaman, M. N. and Robinson, M. S. (2003). Clathrin-mediated endocytosis in AP-2-depleted cells. *J Cell Biol* **162:**909-918.

Munyendo, W. L., Lv, H., Benza-Ingoula, H., Baraza, L. D. and Zhou, J. (2012). Cell penetrating peptides in the delivery of biopharmaceuticals. *Biomolecules* **2:**187-202.

Nakase, I., Niwa, M., Takeuchi, T., Sonomura, K., Kawabata, N., Koike, Y., Takehashi, M. *et al.* (2004). Cellular uptake of arginine-rich peptides: roles for macropinocytosis and actin rearrangement. *Mol Ther* **10:**1011-1022.

Nasu, Y., Asaoka, Y., Namae, M., Nishina, H., Yoshimura, H. and Ozawa, T. (2015). Genetically Encoded Fluorescent Probe for Imaging Apoptosis in Vivo with Spontaneous GFP Complementation. *Anal Chem*.

Naylor, M. R., Bockus, A. T., Blanco, M. J. and Lokey, R. S. (2017). Cyclic peptide natural products chart the frontier of oral bioavailability in the pursuit of undruggable targets. *Curr Opin Chem Biol* **38:**141-147.

Nevola, L. and Giralt, E. (2015). Modulating protein-protein interactions: the potential of peptides. *Chem Commun (Camb)* **51:**3302-3315.

Niikura, K., Horisawa, K. and Doi, N. (2015). A fusogenic peptide from a sea urchin fertilization protein promotes intracellular delivery of biomacromolecules by facilitating endosomal escape. *J Control Release* **212:**85-93.

Nobelprize.org. (Last accessed 07/2017). The Nobel Prize in Chemistry 2008 [Online]. <https://www.nobelprize.org/nobel_prizes/chemistry/laureates/2008/>: Nobel Media AB 2014. Available at: [Accessed.

Ormo, M., Cubitt, A. B., Kallio, K., Gross, L. A., Tsien, R. Y. and Remington, S. J. (1996). Crystal structure of the Aequorea victoria green fluorescent protein. *Science* **273:**1392-1395.

Orth, J. D., Krueger, E. W., Weller, S. G. and McNiven, M. A. (2006). A novel endocytic mechanism of epidermal growth factor receptor sequestration and internalization. *Cancer Res* **66:**3603-3610.

Palm-Apergi, C., Lorents, A., Padari, K., Pooga, M. and Hällbrink, M. (2009). The membrane repair response masks membrane disturbances caused by cell-penetrating peptide uptake. *FASEB J* **23:**214-223.

Palmer, E. and Freeman, T. (2004). Investigation into the use of C- and N-terminal GFP fusion proteins for subcellular localization studies using reverse transfection microarrays. *Comp Funct Genomics* **5:**342-353.

Panyam, J. and Labhasetwar, V. (2004). Targeting intracellular targets. *Curr Drug Deliv* **1:**235-247.

Patterson, G. H. and Lippincott-Schwartz, J. (2002). A photoactivatable GFP for selective photolabeling of proteins and cells. *Science* **297:**1873-1877.

Pearse, B. M. (1976). Clathrin: a unique protein associated with intracellular transfer of membrane by coated vesicles. *Proc Natl Acad Sci U S A* **73:**1255-1259.

Pedelacq, J. D., Cabantous, S., Tran, T., Terwilliger, T. C. and Waldo, G. S. (2006). Engineering and characterization of a superfolder green fluorescent protein. *Nat Biotechnol* **24:**79-88.

Pichereau, C. a. A., C. (2005). Therapeutic peptides under the spotlight. *Eur. Biopharm. Rev* 88–91.

Pinaud, F. and Dahan, M. (2011). Targeting and imaging single biomolecules in living cells by complementation-activated light microscopy with split-fluorescent proteins. *Proc Natl Acad Sci U S A* **108:**E201-210.

Prasher, D. C., Eckenrode, V. K., Ward, W. W., Prendergast, F. G. and Cormier, M. J. (1992). Primary structure of the Aequorea victoria green-fluorescent protein. *Gene* **111:**229-233.

Ramanujam, N., Mitchell, M. F., Mahadevan, A., Thomsen, S., Silva, E. and Richards-Kortum, R. (1994). Fluorescence spectroscopy: a diagnostic tool for cervical intraepithelial neoplasia (CIN). *Gynecol Oncol* **52:**31-38.

Reddy Chichili, V. P., Department of Biological Sciences, N. U. o. S., Singapore 117543, Singapore, Kumar, V., Department of Biological Sciences, N. U. o. S., Singapore 117543, Singapore, Sivaraman, J., Department of Biological Sciences, N. U. o. S., Singapore 117543, Singapore and Department of Biological Sciences, S. D., National University of Singapore, Singapore 117543, Singapore. (2017). Linkers in the structural biology of protein–protein interactions. *Protein Science* **22:**153-167.

Richard, J. P., Melikov, K., Brooks, H., Prevot, P., Lebleu, B. and Chernomordik, L. V. (2005). Cellular uptake of unconjugated TAT peptide involves clathrin-dependent endocytosis and heparan sulfate receptors. *J Biol Chem* **280:**15300-15306.

Richard, J. P., Melikov, K., Vives, E., Ramos, C., Verbeure, B., Gait, M. J., Chernomordik, L. V. *et al.* (2003). Cell-penetrating peptides. A reevaluation of the mechanism of cellular uptake. *J Biol Chem* **278:**585-590.

Rodrigues, R. M., Macko, P., Palosaari, T. and Whelan, M. P. (2011). Autofluorescence microscopy: a non-destructive tool to monitor mitochondrial toxicity. *Toxicol Lett* **206:**281-288.

Rosenow, M. A., Huffman, H. A., Phail, M. E. and Wachter, R. M. (2004). The crystal structure of the Y66L variant of green fluorescent protein supports a cyclization-oxidation-dehydration mechanism for chromophore maturation. *Biochemistry* **43:**4464-4472.

Rothberg, K. G., Heuser, J. E., Donzell, W. C., Ying, Y. S., Glenney, J. R. and Anderson, R. G. (1992). Caveolin, a protein component of caveolae membrane coats. *Cell* **68:**673-682.

Rydberg, H. A., Matson, M., Amand, H. L., Esbjörner, E. K. and Nordén, B. (2012). Effects of tryptophan content and backbone spacing on the uptake efficiency of cell-penetrating peptides. *Biochemistry* **51:**5531-5539.

Sahay, G., Querbes, W., Alabi, C., Eltoukhy, A., Sarkar, S., Zurenko, C., Karagiannis, E. *et al.* (2013). Efficiency of siRNA delivery by lipid nanoparticles is limited by endocytic recycling. *Nat Biotechnol* **31:**653-658.

Saito, G., Swanson, J. A. and Lee, K. D. (2003). Drug delivery strategy utilizing conjugation via reversible disulfide linkages: role and site of cellular reducing activities. *Adv Drug Deliv Rev* **55:**199-215.

Sayers, E. J., Cleal, K., Eissa, N. G., Watson, P. and Jones, A. T. (2014). Distal phenylalanine modification for enhancing cellular delivery of fluorophores, proteins and quantum dots by cell penetrating peptides. *J Control Release* **195:**55-62.

Scheer, U. and Hock, R. (1999). Structure and function of the nucleolus. *Curr Opin Cell Biol* **11:**385-390.

Schmidt, S., Adjobo-Hermans, M. J., Kohze, R., Enderle, T., Brock, R. and Milletti, F. (2017). Identification of Short Hydrophobic Cell-Penetrating Peptides for Cytosolic Peptide Delivery by Rational Design. *Bioconjug Chem* **28:**382-389.

Schmidt, S., Adjobo-Hermans, M. J., Wallbrecher, R., Verdurmen, W. P., Bovee-Geurts, P. H., van Oostrum, J., Milletti, F. *et al.* (2015a). Detecting Cytosolic Peptide Delivery with the GFP Complementation Assay in the Low Micromolar Range. *Angew Chem Int Ed Engl*.

Schmidt, S., Adjobo-Hermans, M. J., Wallbrecher, R., Verdurmen, W. P., Bovee-Geurts, P. H., van Oostrum, J., Milletti, F. *et al.* (2015b). Detecting Cytosolic Peptide Delivery with the GFP Complementation Assay in the Low Micromolar Range. *Angew Chem Int Ed Engl* **54:**15105-15108.

Schnell, U., Dijk, F., Sjollema, K. A. and Giepmans, B. N. (2012). Immunolabeling artifacts and the need for live-cell imaging. *Nat Methods* **9:**152-158.

Shaner, N. C., Campbell, R. E., Steinbach, P. A., Giepmans, B. N., Palmer, A. E. and Tsien, R. Y. (2004). Improved monomeric red, orange and yellow fluorescent proteins derived from Discosoma sp. red fluorescent protein. *Nat Biotechnol* **22:**1567-1572.

Shimomura, O. (2009). Discovery of green fluorescent protein (GFP) (Nobel Lecture). *Angew Chem Int Ed Engl* **48:**5590-5602.

Shimomura, O., Johnson, F. H. and Saiga, Y. (1962). Extraction, purification and properties of aequorin, a bioluminescent protein from the luminous hydromedusan, Aequorea. *J Cell Comp Physiol* **59:**223-239.

Sigismund, S., Argenzio, E., Tosoni, D., Cavallaro, E., Polo, S. and Di Fiore, P. P. (2008). Clathrin-mediated internalization is essential for sustained EGFR signaling but dispensable for degradation. *Dev Cell* **15:**209-219.

Skala, M. and Ramanujam, N. (2010). Multiphoton redox ratio imaging for metabolic monitoring in vivo. *Methods Mol Biol* **594:**155-162.

Smietana, K., Siatkowski, M. and Møller, M. (2016). Trends in clinical success rates. *Nat Rev Drug Discov* **15:**379-380.

Sniegowski, J. A., Lappe, J. W., Patel, H. N., Huffman, H. A. and Wachter, R. M. (2005). Base catalysis of chromophore formation in Arg96 and Glu222 variants of green fluorescent protein. *J Biol Chem* **280:**26248-26255.

Srinivasan, D., Muthukrishnan, N., Johnson, G. A., Erazo-Oliveras, A., Lim, J., Simanek, E. E. and Pellois, J. P. (2011). Conjugation to the cell-penetrating peptide TAT potentiates the photodynamic effect of carboxytetramethylrhodamine. *PLoS One* **6:**e17732.

Stadler, C., Rexhepaj, E., Singan, V. R., Murphy, R. F., Pepperkok, R., Uhlén, M., Simpson, J. C. *et al.* (2013). Immunofluorescence and fluorescent-protein tagging show high correlation for protein localization in mammalian cells. *Nat Methods* **10:**315-323.

Stadler, C., Skogs, M., Brismar, H., Uhlén, M. and Lundberg, E. (2010). A single fixation protocol for proteome-wide immunofluorescence localization studies. *J Proteomics* **73:**1067-1078.

Steinman, R. M., Mellman, I. S., Muller, W. A. and Cohn, Z. A. (1983). Endocytosis and the recycling of plasma membrane. *J Cell Biol* **96:**1-27.

Stockwin, L. H. and Holmes, S. (2003). Antibodies as therapeutic agents: vive la renaissance! *Expert Opin Biol Ther* **3:**1133-1152.

Takayama, K., Hirose, H., Tanaka, G., Pujals, S., Katayama, S., Nakase, I. and Futaki, S. (2012). Effect of the attachment of a penetration accelerating sequence and the influence of hydrophobicity on octaarginine-mediated intracellular delivery. *Mol Pharm* **9:**1222-1230.

Takayama, K., Nakase, I., Michiue, H., Takeuchi, T., Tomizawa, K., Matsui, H. and Futaki, S. (2009). Enhanced intracellular delivery using arginine-rich peptides by the addition of penetration accelerating sequences (Pas). *J Control Release* **138:**128-133.

Timofeev, V. I., Chuprov-Netochin, R. N., Samigina, V. R., Bezuglov, V. V., Miroshnikov, K. A. and Kuranova, I. P. (2010). X-ray investigation of gene-engineered human insulin crystallized from a solution containing polysialic acid. *Acta Crystallogr Sect F Struct Biol Cryst Commun* **66:**259-263.

Treger, M. and Westhof, E. (2001). Statistical analysis of atomic contacts at RNA-protein interfaces. *J Mol Recognit* **14:**199-214.

Tunnemann, G., Martin, R. M., Haupt, S., Patsch, C., Edenhofer, F. and Cardoso, M. C. (2006). Cargo-dependent mode of uptake and bioavailability of TAT-containing proteins and peptides in living cells. *FASEB J* **20:**1775-1784.

Tunnemann, G., Ter-Avetisyan, G., Martin, R. M., Stockl, M., Herrmann, A. and Cardoso, M. C. (2008). Live-cell analysis of cell penetration ability and toxicity of oligo-arginines. *J Pept Sci* **14:**469-476.

van IJzendoorn, S. C. and Hoekstra, D. (1999). The subapical compartment: a novel sorting centre? *Trends Cell Biol* **9:**144-149.

Venkatesan, K., Rual, J. F., Vazquez, A., Stelzl, U., Lemmens, I., Hirozane-Kishikawa, T., Hao, T. *et al.* (2009). An empirical framework for binary interactome mapping. *Nat Methods* **6:**83-90.

Verdurmen, W. P., Bovee-Geurts, P. H., Wadhwani, P., Ulrich, A. S., Hällbrink, M., van Kuppevelt, T. H. and Brock, R. (2011). Preferential uptake of L- versus D-amino acid cell-penetrating peptides in a cell type-dependent manner. *Chem Biol* **18:**1000-1010.

Vives, E., Brodin, P. and Lebleu, B. (1997). A truncated HIV-1 Tat protein basic domain rapidly translocates through the plasma membrane and accumulates in the cell nucleus. *J Biol Chem* **272:**16010-16017.

Vlieghe, P., Lisowski, V., Martinez, J. and Khrestchatisky, M. (2010). Synthetic therapeutic peptides: science and market. *Drug Discov Today* **15:**40-56.

Waldo, G. S., Standish, B. M., Berendzen, J. and Terwilliger, T. C. (1999). Rapid protein-folding assay using green fluorescent protein. *Nat Biotechnol* **17:**691-695.

Wang, R. and Brattain, M. G. (2007). The maximal size of protein to diffuse through the nuclear pore is larger than 60kDa. *FEBS Lett* **581:**3164-3170.

Wang, Y. Z., Satoh, A. and Warren, G. (2005). Mapping the functional domains of the Golgi stacking factor GRASP65. *Journal of Biological Chemistry* **280:**4921-4928.

Watts, J. K. and Corey, D. R. (2012). Silencing disease genes in the laboratory and the clinic. *J Pathol* **226:**365-379.

Woods, A. S. and Ferré, S. (2005). Amazing stability of the arginine-phosphate electrostatic interaction. *J Proteome Res* **4:**1397-1402.

Young, S. W., Stenzel, M. and Yang, J. L. (2016). Nanoparticle-siRNA: A potential cancer therapy? *Crit Rev Oncol Hematol* **98:**159-169.

Zhang, X. and Wang, Y. (2015). GRASPs in Golgi Structure and Function. *Front Cell Dev Biol* **3**.

Ziegler, A. (2008). Thermodynamic studies and binding mechanisms of cell-penetrating peptides with lipids and glycosaminoglycans. *Adv Drug Deliv Rev* **60:**580-597.

9 Appendices

9.1 Recipes and buffers

Mowiol

Mowiol 4-88 2.4 g
Glycerol 6 g
H2O 6 ml
0.2M Tris pH 8.5 12 ml

Non- denaturing lysis buffer

50mM Tris-Cl
150mM NaCl,
1%Triton-X-100,
Protease inhibitor (cOmplete™, EDTA-free)

Loading Buffer (gel electrophoresis)

Glycerol 30%(v/v)
Bromophenol Blue (0.25%)
In TE (10mM Tris, pH7.4, 1mM EDTA)
Final conc of 0.1mg/ml ethidium bromide

9.2 Vector map EGFP-N2
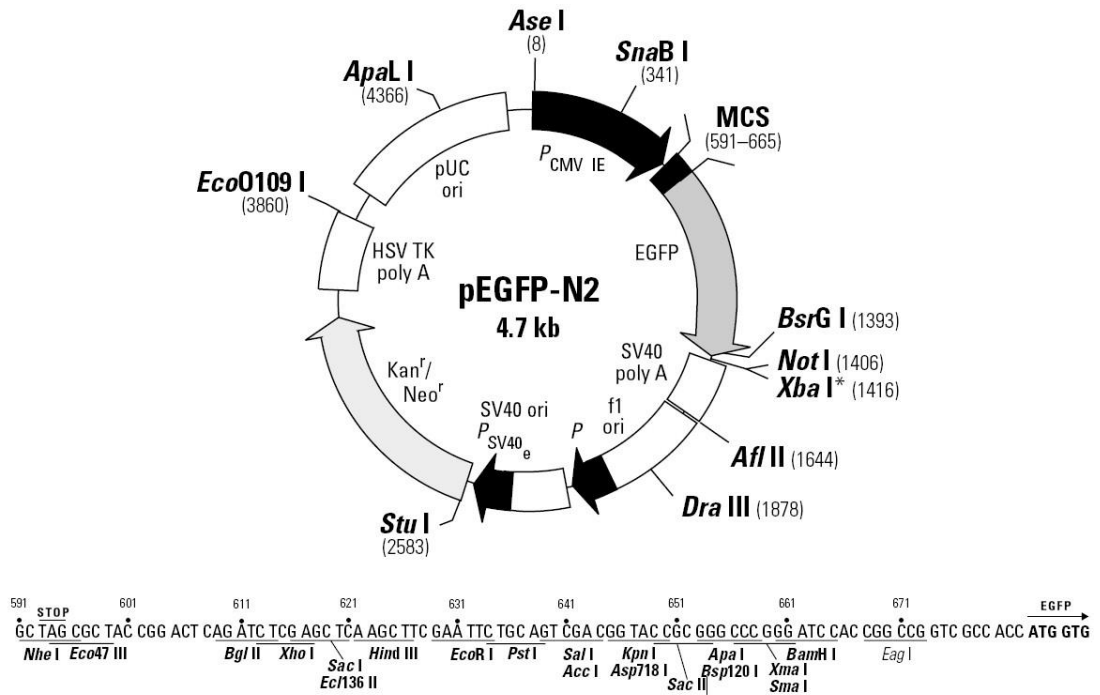
Restriction Map and Multiple Cloning Site (MCS) of pEGFP-N2 Unique restriction sites are in bold. The *Not* I site follows the EGFP stop codon. The *Nhe* I site cannot be used for fusions since it contains an in-frame stop codon. The *Xba* I site (*) is methylated in the DNA provided by BD Biosciences Clontech. If you wish to digest the vector with this enzyme, you will need to transform the vector into a *dam⁻* host and make fresh DNA.

Figure 9-1 Vector map of EGFP-N2.

9.3 Appendix Chapter 3

A Anti GFP (Roche)
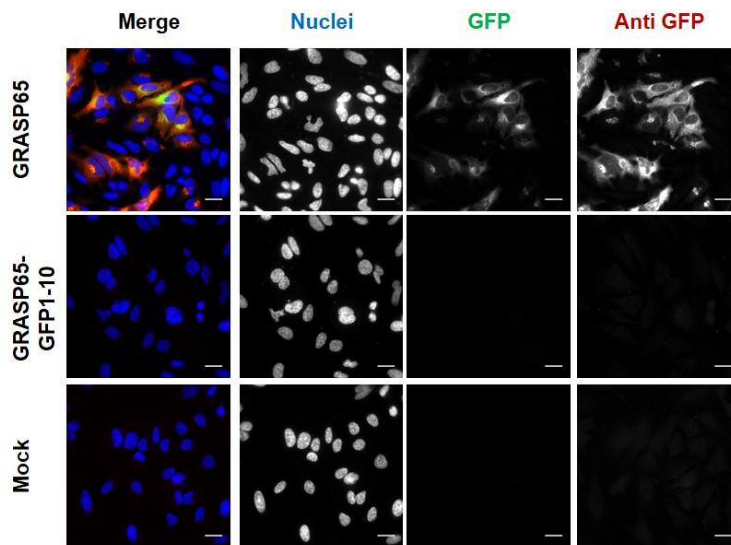
B Anti GFP (Vector Laboratories)
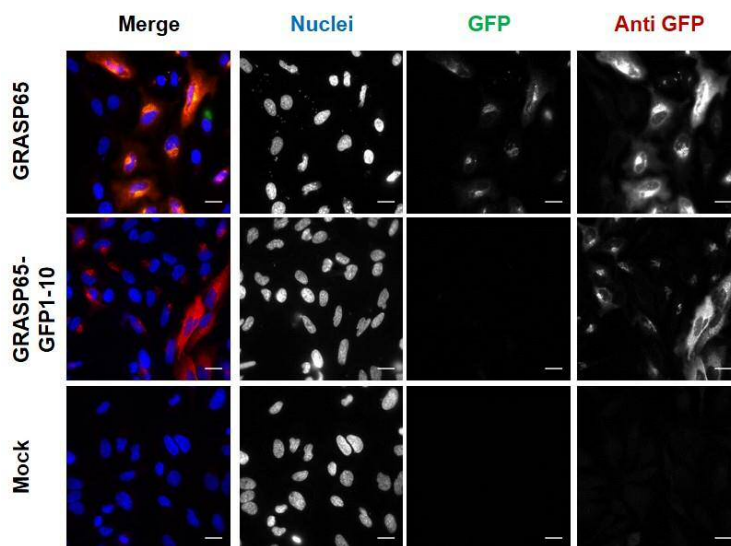
Figure 9-2 Comparison of two anti-GFP antibodies
HeLa cells were transiently transfected with DNA constructs coding for GRASP65-GFP or GRASP65-GFP1-10 expression. The transfection mix of mock transfected cells did not contain DNA. Cells were incubated in transfection mix overnight and PFA fixed the next day. The plasma membrane was permeabilised with 0.1 % Triton-X-100. (A) GRASP65-GFP or GRASP65-GFP1-10 expression was detected using a primary anti-GFP antibody (Roche) raised in mouse. A secondary anti-mouse antibody conjugated to Alexa-568 was used to visualise GFP expression (Anti GFP). (B) GRASP65-GFP or GRASP65-GFP1-10 expression was detected using a primary anti-GFP antibody (Vectorlaboratories) raised in goat. A secondary anti-goat antibody conjugated to Alexa-647 was used to visualise GFP expression (Anti GFP). Representative images shown for each condition. Nuclei were counterstained with DAPI. Scale bars: 30 µm. N=1.
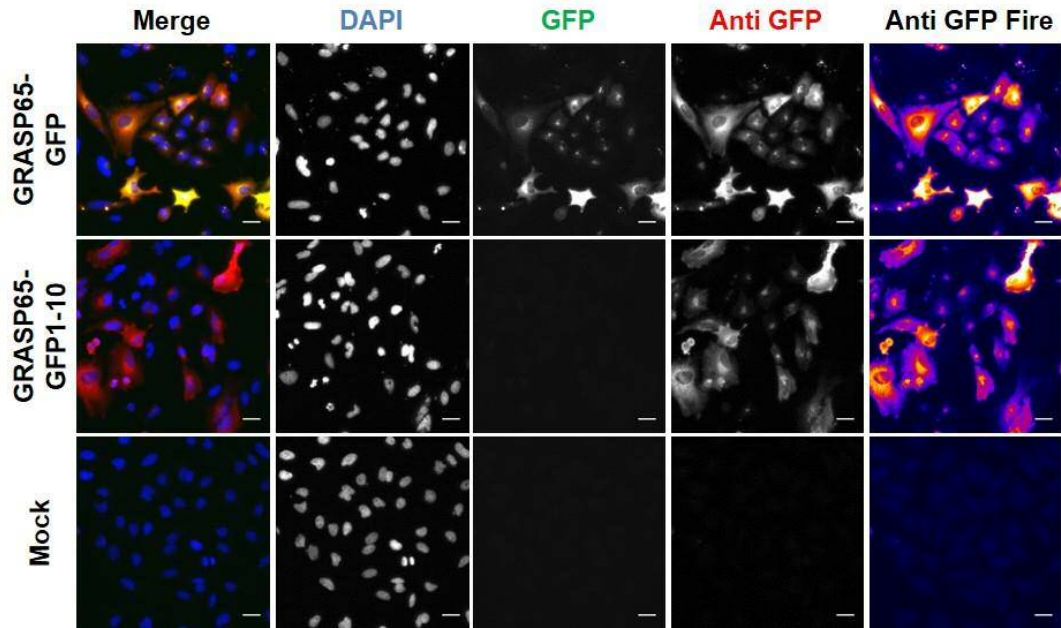
Figure 9-3 Detection of GRASP65-GFP1-10 expression in HeLa cells using immunofluorescence.
HeLa cells were transiently transfected with DNA constructs coding for GRASP65-GFP1-10 or full length GRASP65-GFP. The transfection mix of mock transfected cells did not contain DNA. Cells were incubated in transfection mix overnight and PFA fixed the next day. The plasma membrane was permeabilised with 0.1 % Triton-X-100 and GRASP65-GFP1-10 or full length GRASP65-GFP expression was detected using a primary anti-GFP antibody raised in goat. A secondary anti-goat antibody conjugated to Alexa-647 was used to visualise GFP expression (Anti GFP). Nuclei were counterstained with DAPI. Representative images are shown for each condition. Scale bars: 30 µm. n=3.
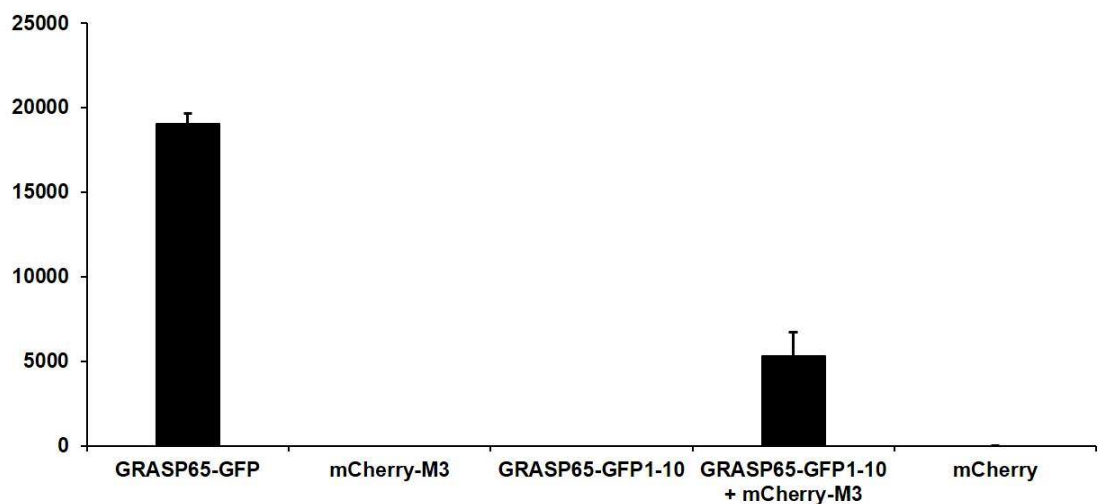
Figure 9-4 Detection of GRASP65-GFP complementation after co-tranfection using a microplate reader.
Single transfections or co-transfections of HeLa cells were performed with DNA encoding for GRASP65-GFP, GRASP65-GFP1-10, mCherry-H6-Xa-R8-M3 and mCherry. The transfection mix of mock transfected cells did not contain DNA. Cells were left in transfection mix overnight. The next day, cells were detached from their dish using trypsin, washed and transferred into a clear bottom, black walled microwell plate. Green fluorescence was monitored using a microplate reader. n=2.

D
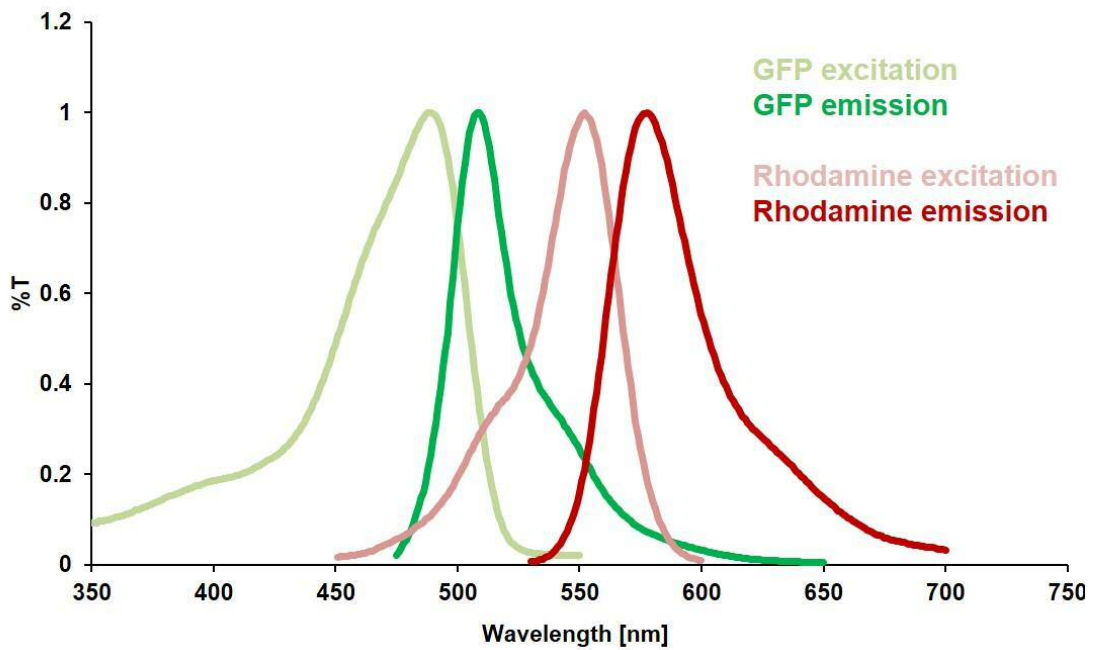
Figure 9-5 Excitation and emission spectrum of Rhodamine (TMR) and GFP.
The graph shows GFP excitation (light green) and emission (dark green) spectrum and TMR-Rhodamine excitation (light red) and emission (dark red) spectrum. Spectra were obtained from the Chroma website.

9.4 Appendix Chapter 4
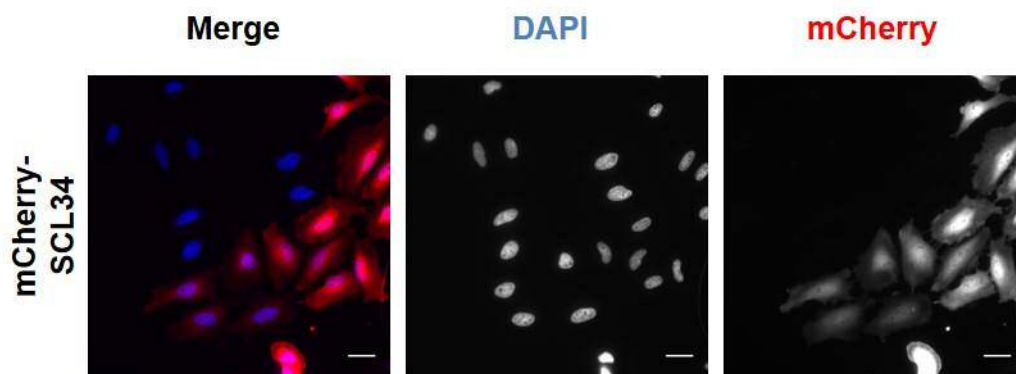
Figure 9-6 mCherry-SCL34
mCherry-SCL34 was obtained after the first round of limiting dilution was expanded and used for the second round of limiting dilution. Images show the polyclonal cell line before the second round of limiting dilution was performed.

9.5 Appendix Chapter 5
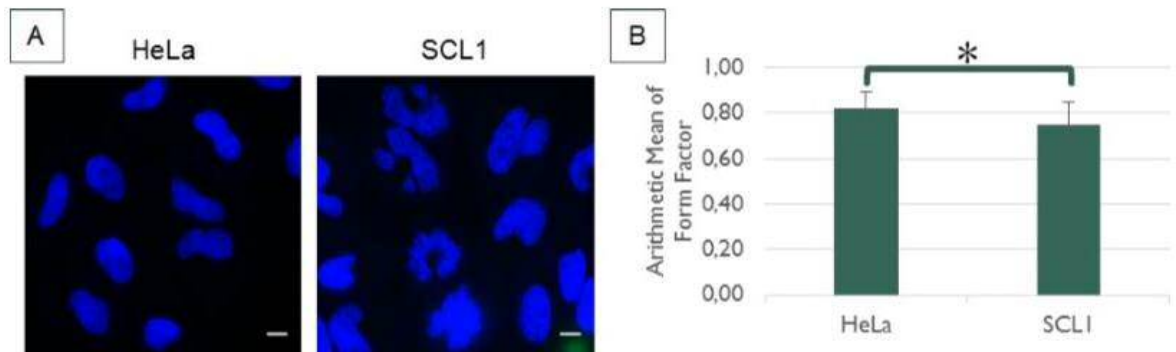
Figure 6: Analysis of the nuclear Form Factor of HeLa and SCL1 cells

A Exemplary widefield fluorescence microscopy images of HeLa and SCL1 cells. The cells were grown on coverslips, PFA fixed, stained with DAPI and mounted in Mowiol on microscopy slides. The images are taken from separate experiments performed on different days. Different settings regarding the contrast and brightness were applied for an optimal visualisation of the nuclear shape. Hence, the signal intensities are not comparable. Scale bar: 10 µm

B Statistical evaluation of the Form Factor of nuclei of HeLa and SCL1 cells. Living cells were stained with Hoechst, washed and images were taken on low magnification. The Form Factor of every single nucleus was calculated using the software CellProfiler. 444 HeLa cells and 450 SCL1 cells were analysed. The arithmetic mean and standard deviation are plotted. The data was tested for significance by a t-test. $p < 0.05$

Figure 9-7 Form factor of the nucleus of SCL1 and HeLa cells
This figure was copied from the report Characterisation of a stable cell line expressing the large component of a split GFP system by Alexander Dudziak, University of Duisburg-Essen, 2015. All experiments were performed under my supervision.
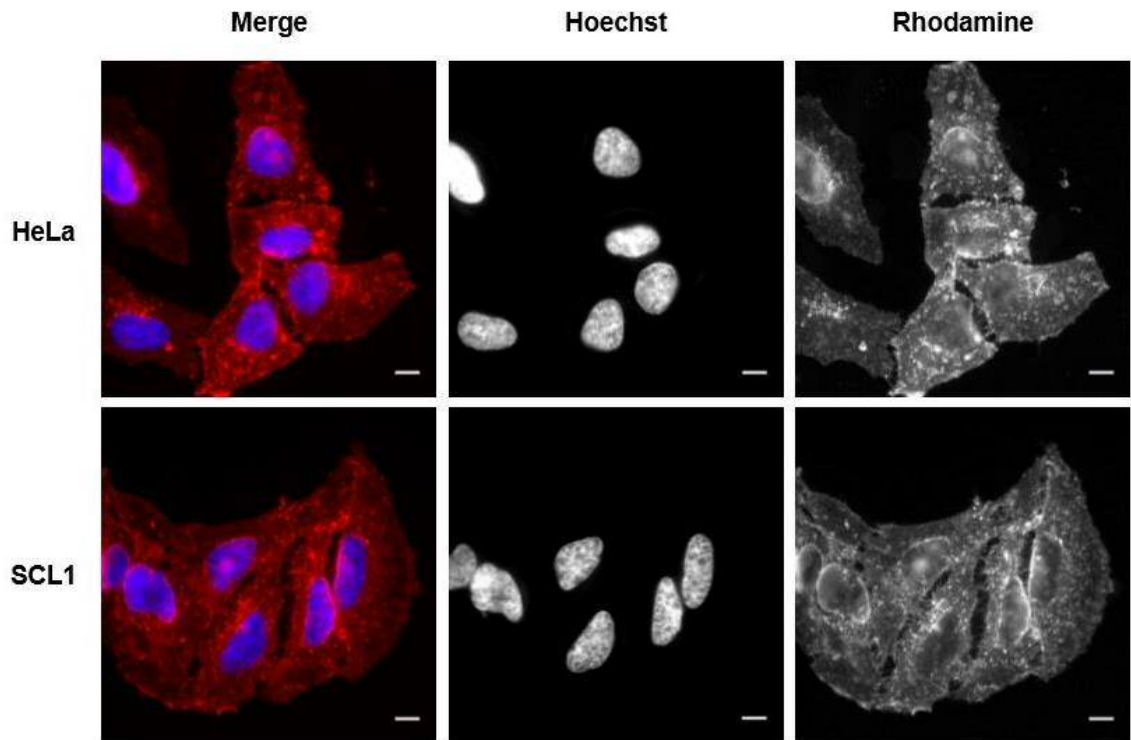
Figure 1: Widefield fluorescence microscopy images of fixed, unpermeabilised HeLa and SCL1 cells stained with Rhodamine labelled Concanavalin A

HeLa and SCL1 cells were grown on coverslips, PFA fixed, stained with Hoechst and rhodamine labelled concanavalin A, mounted on microscope slides and imaged. Scale bar: 10 µm

Figure 9-8 Labelling of the plasma membrane of SCL1 and HeLa cells.
This figure was copied from the report Characterisation of a stable cell line expressing the large component of a split GFP system by Alexander Dudziak, University of Duisburg-Essen, 2015. All experiments were performed under my supervision.
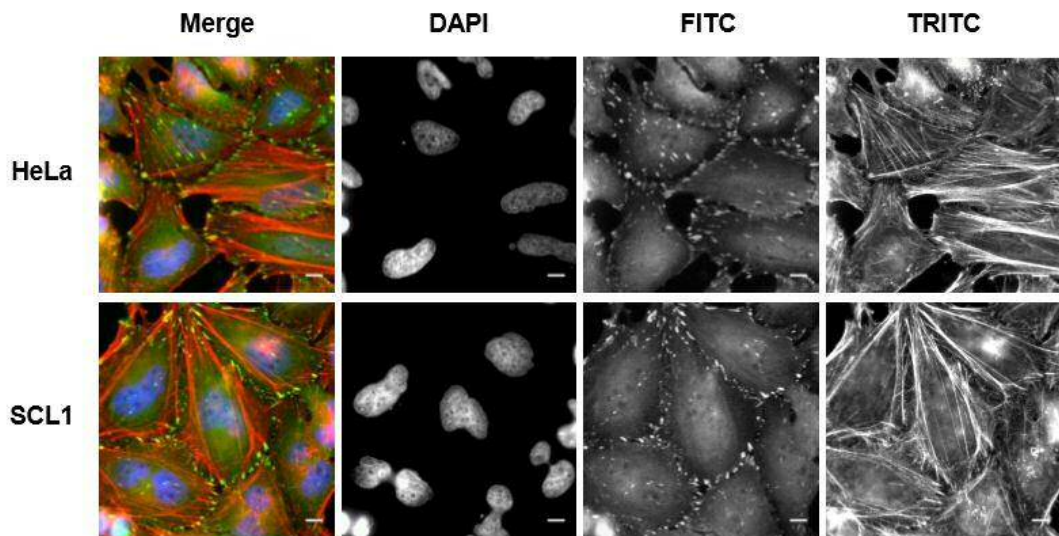
Figure 4: Widefiled fluorescence microscopy images of HeLa and SCL1 cells stained for vinculin and actin filaments

HeLa and SCL1 cells were grown on coverslips, fixed with PFA, incubated with FITC labelled anti-vinculin antibody, stained with DAPI and TRITC labelled phalloidin, mounted in Mowiol on microscope slides and imaged. Scale bar: 10 µm

Figure 9-9 Immunofluorescence of the actin cytoskeleton in HeLa and SCL1 cells.
This figure was copied from the report Characterisation of a stable cell line expressing the large component of a split GFP system by Alexander Dudziak, University of Duisburg-Essen, 2015. All experiments were performed under my supervision.
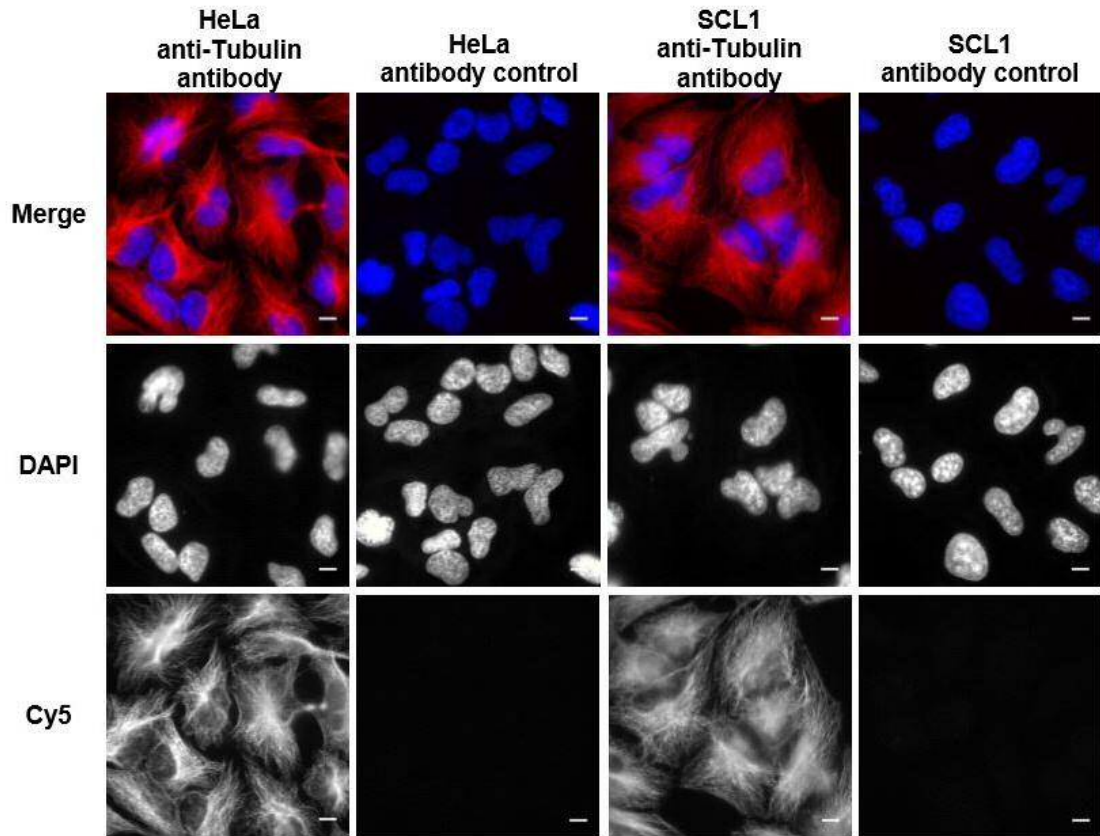
Figure 3: Widefield fluorescence microscopy images of microtubule antibody stain of HeLa and SCL1 cells

HeLa and SCL1 cells were grown on coverslips, fixed with methanol, incubated with anti-tubulin and secondary Cy5 labelled antibody, stained with DAPI, mounted in Mowiol on microscope slides and imaged. For antibody control the cells were incubated with 3 % BSA in PBS without the primary antibody. Scale bar: 10 µm

Figure 9-10 Immunofluorescence of tubulin in HeLa and SCL1 cells.
This figure was copied from the report Characterisation of a stable cell line expressing the large component of a split GFP system by Alexander Dudziak, University of Duisburg-Essen, 2015. All experiments were performed under my supervision.